

Distribution Agreement

In presenting this thesis or dissertation as a partial fulfillment of the requirements for an advanced degree from Emory University, I hereby grant to Emory University and its agents the non-exclusive license to archive, make accessible, and display my thesis or dissertation in whole or in part in all forms of media, now or hereafter known, including display on the world wide web. I understand that I may select some access restrictions as part of the online submission of this thesis or dissertation. I retain all ownership rights to the copyright of the thesis or dissertation. I also retain the right to use in future works (such as articles or books) all or part of this thesis or dissertation.

Signature:

Elizabeth Q. Littauer

Date

The Effect of Pregnancy on Immune Responses to H1N1 Influenza Virus Infection

By

Elizabeth Q. Littauer
Doctor of Philosophy

Graduate Division of Biological and Biomedical Science
Microbiology & Molecular Genetics

Richard W. Compans, Ph.D.
Advisor

Ioanna Skountzou, M.D./Ph.D.
Advisor

Joshy Jacob, Ph.D.
Committee Member

Brian P. Pollack, M.D./Ph.D.
Committee Member

David A. Steinhauer, Ph.D.
Committee Member

Mehul S. Suthar, Ph.D.
Committee Member

Accepted:

Lisa A. Tedesco, Ph.D.
Dean of the James T. Laney School of Graduate Studies

Date

The Effect of Pregnancy on Immune Responses to H1N1 Influenza Virus Infection

By

Elizabeth Q. Littauer
B.A., University of North Carolina at Chapel Hill, 2012

Advisors: Richard W. Compans, Ph.D.; Ioanna Skountzou, M.D./Ph.D.

An abstract of
A dissertation to the Faculty of the
James T. Laney School of Graduate Studies of Emory University
in partial fulfillment of the requirements for the degree of
Doctor of Philosophy
in Microbiology & Molecular Genetics
2018

Abstract

The Effect of Pregnancy on Immune Responses to H1N1 Influenza Virus Infection

By Elizabeth Q. Littauer

In 2009, the H1N1 swine flu pandemic highlighted the vulnerability of pregnant women to influenza viral infection. Pregnant women infected with influenza A virus were at increased risk of hospitalization due to severe acute respiratory distress syndrome (ARDS), and rates of morbidity and mortality among infected pregnant women were five-fold higher than the non-pregnant infected population. Moreover, newborns born to mothers infected mid-gestation had an increased risk of preterm birth or low birth weight. Pregnant women have a unique immunological profile modulated by the sex hormones required to maintain pregnancy, namely progesterone and estrogen. In this dissertation, I describe H1N1 influenza A viral pathogenesis during pregnancy, the crosstalk between innate immune signaling and hormonal regulation, and the role of pregnancy hormones in modulating cellular responses to virus infection mid- to late gestation. In a pregnant mouse model, I highlight the ways in which lung architecture and function is perturbed by pregnancy and demonstrated that infection with lethal doses of seasonal H1N1 A/Brisbane59/07 disrupts progesterone expression and upregulates cyclooxygenase-2 (COX-2) and prostaglandins, resulting in placental degradation, pre-term labor and spontaneous abortions.

I also investigate mechanisms by which pregnancy alters activation and maturation of cellular immune responses to pandemic H1N1 A/California/07/2009 influenza viral infection. Pregnant mice infected mid-gestation with sublethal doses of H1N1 A/California/07/09 exhibited reduced serum influenza-specific antibody avidity and HAI titers compared to infected non-pregnant controls despite equivalent activation of H1N1-specific antibody secreting cells up to 6 weeks post infection. While pregnancy reduced the frequency of lung-resident CD4+ T cells, virus-specific IFN- γ secreting and IgA-secreting cells were increased in the lungs 42 d.p.i. These data suggest that the condition of pregnancy enhances cellular responses to H1N1 infection within the mucosa following offspring delivery and maternal recovery while overall antibody quality is weakened due to immune suppression during gestation.

Finally, I highlight advancements in the field of reproductive immunology in response to viral infection and illustrate how that knowledge might be utilized to develop more effective post-infection therapies and vaccination strategies during pregnancy.

The Effect of Pregnancy on Immune Responses to H1N1 Influenza Virus Infection

By

Elizabeth Q. Littauer
B.A., University of North Carolina at Chapel Hill, 2012

Advisors: Richard W. Compans, Ph.D.; Ioanna Skountzou, M.D./Ph.D.

A dissertation to the Faculty of the
James T. Laney School of Graduate Studies of Emory University
in partial fulfillment of the requirements for the degree of
Doctor of Philosophy
in Microbiology & Molecular Genetics
2018

Table of Contents

CHAPTER I: Introduction	1
CHAPTER II: H1N1 influenza virus infection results in adverse pregnancy outcomes by disrupting tissue-specific hormonal regulation	13
Abstract	14
Author summary	15
Introduction	16
Results	20
Discussion	31
Materials and Methods	38
Acknowledgments	43
References	44
Figure 1. Influenza infection inhibits gestational development and offspring health.	61
Figure 2. Pregnancy results in increased inflammation in the lungs and enhanced viral growth in lungs but not detected in placenta.	63
Figure 3. Viral infection disproportionately reduces cytokine and hormone expression in the sera and lungs during pregnancy.	65
Figure 4. Pregnancy increases lung tissue expression of proinflammatory cytokines and chemokines while dampening the upregulation of progesterone and PGF2 α following infection.	67
Figure 5. Infection increases placental expression of contraction-inducing PGF2 α and reduces pregnancy-supportive progesterone.	68
Figure 6. Infection damages placental architecture and increases activation of structural protein degrading matrix metalloproteinases (MMPs).	70

Figure 7. Infection changes pregnancy-supportive PIBF expression in the placenta and lungs.	72
Figure 8. Infection and pregnancy increase COX-2 expression in the lungs.	73
Supplementary Figure 1. Viral titer in the lungs affects expression of progesterone and PGF2 α in a compartment-specific manner.	74
Supplementary Figure 2. Infection and pregnancy impact cytokine expression in a compartment-specific manner.	76
Supplementary Table 1. Serum chemokine and cytokine levels 4 days post-infection.	77
Supplementary Table 2. Lung chemokine and cytokine levels 4 days post-infection.	78
Supplementary Table 3. Placental and fetal chemokine and cytokine levels 4 days post-infection.	79
CHAPTER III: Pregnancy dysregulates innate immune responses to 2009 H1N1 influenza viral infection and the efficacy of long term anti-influenza antibodies	80
Abstract	81
Introduction	82
Materials and Methods	85
Results	89
Discussion	97
Acknowledgments	101
References	103
Figure 1. H1N1 influenza virus infection results in increased pathogenicity during pregnancy.	115

Figure 2. Hormone and cytokine expression in lung tissue 4 dpi and 7 dpi.	117
Figure 3. Hormone and cytokine expression in serum samples 4 dpi and 7 dpi.	119
Figure 4. Hormone and cytokine expression in placental tissue 4 dpi and 7 dpi.	121
Figure 5. Innate immune activation following H1N1 influenza virus infection.	123
Figure 6. Germinal center reactions and plasmablast activation.	124
Figure 7. Pregnancy increases virus-specific IgA-secreting cells in the lungs 6 weeks post infection.	125
Figure 8. Pregnancy induces increased IgG expression with reduced avidity and HAI titers.	126
Figure 9. Pregnancy increases virus-specific IFN- γ secreting cells in the lungs 6 weeks post infection.	127
Figure 10. Pregnancy induces an IgG2a-specific response to boost vaccination 42 d.p.p.	128
Figure 11. Activation of vaccine-specific B and T cells following vaccination during pregnancy and boost post-weaning.	129
Suppl Fig 1. Gating settings for flow cytometry.	130
Suppl Table 1. Lung cytokine expression.	132
Suppl Table 2. Sera cytokine expression.	134
Suppl Table 3. Placental cytokine expression.	136
CHAPTER IV: CONCLUSIONS	137
REFERENCES	144
APPENDIX I: Stable incorporation of GM-CSF into dissolvable microneedle patch improves skin vaccination against influenza	169
Abstract	170

Introduction	171
Materials and Methods	174
Results	182
Discussion	192
Conclusions	195
Acknowledgments	196
References	197
Figure 1. Adjuvantation with 100 ng GM-CSF in intradermal H1N1 A/California/07/09 subunit vaccination improves antibody responses and enhances protection to lethal virus challenge.	207
Figure 2. GM-CSF is an effective adjuvant at low doses in H3N2 vaccinations.	209
Figure 3. GM-CSF retains proliferative capacity in bone marrow cells following MN patch fabrication and dissolution.	211
Figure 4. GM-CSF retains bioactivity following fabrication with a range of MN excipients.	212
Figure 5. The inclusion of GM-CSF in MN patches in H1N1 influenza vaccination is dose-sparing and generates superior IgG expression against homologous and heterologous HAs compared to ID and IM vaccination	214
Figure 6. H1N1 subunit vaccination with GM-CSF improved protection of mice from lethal H1N1 influenza challenge	216
Figure 7. GM-CSF improved antibody responses and avidity when included in MN patch vaccination.	217
Figure 8. Inclusion of GM-CSF enhanced activation of B cells in spleen and bone marrow.	219
Fig 9. MN patch vaccination with GM-CSF increased CD8+ T cell responses in inguinal lymph nodes (ILN) and vaccine-specific IFN- γ responses in the spleen.	220

Fig. 10. GM-CSF adjuvanted MN patch immunization improved cross-reactive neutralization responses between homologous and heterologous viral strains.	222
Fig. 11. Th1 cytokine responses to viral infection were increased in GM-CSF-adjuvanted MN vaccinated mice.	223
Supplementary Figure 1. Gating strategies for flow cytometry.	224
Supplementary Figure 2. Activation of T cells in inguinal lymph nodes (ILN) and spleen.	225
Supplementary Figure 3. Cross-reactive antibody titers against H1N1 and H3N2 viruses	226

Chapter I: Introduction

Influenza viruses are segmented, negative-stranded enveloped viruses that cause respiratory infections, fever, malaise, coughing, and mucus production. Influenza viruses are divided into A, B, and C groups; while all three can be infectious in humans, influenza A viruses cause the most widespread disease [1, 2]. Influenza A viruses are further classified by the antigenicity of their surface proteins hemagglutinin (HA) and neuraminidase (NA), which are encoded on individual gene segments, and define the host range of each virus [1, 3]. Through a process unique to influenza and other segmented genome viruses, co-infection of different viral subtypes in a host can result in reassortment leading to antigenically unique novel viruses that may take advantage of an immunologically naïve host species [4]. This process of reassortment resulted in the rapid global infection and transmission of the 1918 Spanish influenza, 1957 Asian influenza, 1968 Hong Kong influenza, and 2009 swine influenza pandemics, that infected up to 50% of the global population and significant increased mortality [2, 3]. While infection can occur year-round, the epidemiology of influenza virus infection is seasonal, causing peak illness in November through March in the Northern Hemisphere and approximately 200,000 hospitalizations and 36,000 deaths annually in the United States [3]. Currently, the most common circulating subtypes, and thus the ones included in quadrivalent vaccines, are influenza A H1N1 and H3N2 and influenza B Yamagata and Victoria lineages [5]. Due to the wide variety of circulating viruses and the frequency of genetic reassortment between subtypes, vaccination is required annually to provide immune protection during each influenza season although it may not be complete if there is mismatch between predicted strains included in the vaccine and the resultant circulating strains in the following season.

While seasonal influenza infection routinely affects infants and the elderly at higher rates, the most recent pandemic H1N1 influenza virus outbreak in 2009 highlighted a particularly vulnerable subset of healthy adults: pregnant women and their fetuses [6, 7]. Clinical reports from around the globe reported that this group, when infected with H1N1 influenza A virus, was at an increased risk of cardiopulmonary complications, gestational abnormalities and increased rates of maternal and fetal morbidity and mortality[7]. While pregnant women typically represent 1% of the American population, they comprised 6.4% of all hospitalizations due to 2009 H1N1 influenza virus infection and 4.3% of all deaths [8, 9]. Over half of those hospitalized for H1N1 influenza virus infection had another pre-existing condition, such as asthma, high blood pressure, and diabetes; pregnant women with asthma represented 43.5% of deaths from influenza virus infection [9]. Additionally, influenza viral infection during pregnancy increased the incidence of pre-term birth from 7 per 1000 births to 39 per 1000 births and the incidence of stillbirth from 6 to 27 stillbirths per 1000 births [8, 10, 11]. Specifically, for the 2009 H1N1 pandemic influenza virus infection, pregnant women who tested positive for the virus were more likely to deliver low birthweight infants than pregnant women who delivered following influenza-like illness that was not caused by the pandemic strain [12]. There is historical evidence that the 1918 and 1957 pandemics produced similar clinical outcomes for pregnant women; however, modern diagnostic procedures employed during the 2009 H1N1 pandemic allow for more direct linkage between influenza viral infection of pregnant mothers and poor outcomes for maternal and neonate health [10].

These mortality rates to both women and their newborns led to initiatives by the Centers for Disease Control and Prevention (CDC) and the World Health Organization (WHO) to increase vaccination rates among women [5, 13]. However, while the conventional intramuscular

vaccination has been determined to be reasonably safe for routine use during pregnancy, clinical data is inconclusive that pregnant women respond as efficiently to trivalent influenza vaccination as non-pregnant women [13-15]. Moreover, there is concern about existing antiviral treatments disrupting fetal neurodevelopment or inducing preterm birth. Further studies into the molecular mechanisms of viral pathogenesis may reveal alternate pathways for effective antiviral therapy [7]. Research into the specific mechanisms by which H1N1 influenza virus infection causes pregnancy complications and how pregnancy hormones modulate the immune response to infection and vaccination may reveal improved routes of therapy for women infected with influenza A virus during pregnancy. This introduction will discuss how H1N1 influenza virus infection disrupts maternal lung and placental function as well as the role of pregnancy hormones in shaping the innate and cellular immune responses to H1N1 influenza virus infection.

The physiology of influenza A viral infection and immune responses

Human influenza A virus is typically transmitted through respiratory droplets and inhaled into the nasopharynx. Initial virus infection occurs when virus particles bind the hemagglutinin (HA) protein to α 2,6-linked sialic acids that are widely expressed on the surface of ciliated airway epithelial cells throughout the upper respiratory tract [16, 17]. Viruses are then endocytosed primarily via a clathrin-mediated pathway; upon acidification of the vesicle containing influenza virions, the HA protein is triggered to fuse viral and cellular membranes, releasing the viral genome into the cell [18-20]. These negative stranded genomes are then translocated to the nucleus, where they replicate and use host genomic replication and protein translation machinery in the cytoplasm to produce more virions which bud from the apical cellular membranes to infect nearby cells and result in viral amplification [19, 21]. Viruses shedding from the nasopharynx may

be inhaled further into the lower respiratory tract causing severe pulmonary infections or transmitted through respiratory droplets from the upper respiratory compartment to the next person. People infected with 2009 H1N1 influenza A virus can be contagious as early as 12 hours post-inoculation and typically begin experiencing symptoms approximately 2 days following infection [22].

The release of viral RNA within the cell activates innate immune signaling pathways, especially toll-like receptors (TLRs) and retinoic-acid-inducible gene 1 (RIG1), which induce the expression of the pro-inflammatory cytokines interferon- α (IFN- α) and interferon- β (IFN- β) [23, 24]. The secretion of these cytokines activates the surrounding epithelial cells to produce antiviral genes that hamper viral entry and replication and recruit innate immune cells to the site of infection. [23, 25, 26] Natural killer (NK) cells and neutrophils kill infected cells, and additional cytokines expressed by activated airway epithelium and innate immune cells induce fever and mucus production, which in turn results in coughing and rhinorrhea to shed the virus and cellular debris from the lungs and the nose [26, 27]. These physiological responses are the hallmark of influenza illness symptomatology, and in clinically vulnerable populations, chest congestion due to viral infection and the ensuing immune response can lead to bronchitis, pneumonia, and secondary bacterial infections [28-30]. Viral clearance finally occurs around 8 to 10 days post-symptom onset when the adaptive immune response mounts virus-specific clearing of infected tissue [26, 31]. Dendritic cells take up viral antigen, migrate to draining mediastinal lymph nodes, and prime naïve resident B and T cells to respond to the infection; ultimately, cytotoxic lymphocytes (CD8⁺ CTLs) with costimulatory help from CD4⁺ T cells and B cell-secreted virus-specific neutralizing antibodies will result in the eradication of virus from the lungs [26, 32, 33]. Upon resolution of disease, alveolar macrophages clear cellular debris, and basal stem cells

regenerate healthy airway epithelium to restore healthy tissue [34, 35]. Virus-specific CD103+ CD8+ T cells will become tissue resident memory (TRM) cells in the lungs to provide rapid response upon the next infection, and memory B cells will persist in the mediastinal lymph nodes to secrete virus-neutralizing antibody into the circulatory system [36-38].

Research into the specific mechanisms of H1N1 influenza A virus binding, entry, RNA replication, transmission, and induction of the host immune system has been extensive since the 1918 Spanish influenza pandemic; however, investigations into how these mechanisms manifest in disease in immunologically unique populations, such as infants, the elderly, HIV+ or asthmatic patients, and pregnant women are limited.

Hormonal regulation of pregnancy and immune signaling are delicately balanced to protect fetal development

Female reproduction is regulated predominately via estrogen, progesterone, luteinizing hormone (LH), and follicular stimulating hormone (FSH). Estrogen receptors (ERs) and progesterone receptors (PGRs) are typically expressed within the cytosol and translocated to the nucleus upon ligand binding to induce a suite of genes encoding immunomodulators, regulators for tissue remodeling, mammary gland development, metabolism, and importantly for the topic of this dissertation, lung physiology and function [39-41]. LH and FSH are synthesized in the anterior pituitary gland and coordinate the decidualization of the uterine endometrium and the release of oocytes from mature ovarian follicles into the uterus, where they may be fertilized by sperm introduced in the uterus by sexual intercourse [42]. A fertilized oocyte develops into a blastocyst and then a polarized structure called the trophoctoderm; a layer of these cells will then form the placental layer and secrete human chorionic gonadotropin (hCG) [43]. Placental hCG expression

signals the maternal corpus luteum to produce progesterone, which maintains the appropriate thickness and vascularization of the endometrium to support embryonic growth [42].

Insufficient progesterone expression has been associated with infertility and recurrent spontaneous abortions, indicating that variations in progesterone levels are not well tolerated by the maternal immune system [39]. Sex hormones play a crucial role in organizing endometrial granulated lymphocytes (EGLs) in the innermost layer of epithelial tissue in the uterus, and populations of uterine natural killer (NK) cells, dendritic cells, macrophages, and memory and regulatory T cells are tightly controlled throughout the first, second, and third trimesters of pregnancy [42, 44, 45]. Estrogen is expressed in several major forms, mainly estradiol (E2) and estriol (E3); each can have biphasic effects in stimulating pro-inflammatory signaling via mitogen-associated protein kinases (MAPKs) and NK activation at low concentrations or enhancing the expression of PD-L1 on T cells and the synthesis of TGF- β and IL-10 at high concentrations [45]. Progesterone receptors are expressed broadly on most immune cell subsets and are produced in higher levels in females [45-47]. In the uterus, progesterone induces naïve Th0 cells into antibody-inducing, IL-4, IL-5, and IL-6 secreting Th2 memory cells upon antigen recognition [44]. The expression of IL-4 and IL-6 then promotes hCG expression from the corpus luteum, which in turn releases more progesterone, creating a positive feedback loop for the amplification of hormone-mediated Th2 polarization [44]. This phenomenon has been shown to be important for maintaining immune tolerance, and recurrent miscarriage is associated with a predominance of Th1 memory cells in the endometrium [48]. Estrogen has also been implicated in inducing CD4⁺ CD25⁺ Tregs and is critical for maintaining tolerance within the maternal-fetal interface [49]. Progesterone also upregulates the activity of uterine Tregs, which act as suppressors of inflammatory immune subsets, particularly NK cells and macrophages resident to the endometrium [45, 47]. In this way,

estrogen and progesterone coordinate an environment in which both uterine epithelial cells and innate immune cells resident to uterine tissue will tolerate the implantation of a fertilized oocyte and the development of a placenta and fetus.

The structure and cellular composition of placenta is critical to maintaining fetal growth and development as well as protection from inflammation. Placenta develops from the cells in the implanted blastocyst as it transitions into a trophoblast; a layer of cells which transitions into a chorionic labyrinthine layer with intertwined villi composed of porous and highly specialized fetal syncytiotrophoblasts [43]. Here, maternal blood makes direct contact with fetal cells, allowing for gas, nutrient, and waste exchange but also providing a potential door for entry of bacteria, viruses, and parasites to a fetus with an undeveloped immune system [50]. Few pathogens can cross the placental barrier from the mother to the fetus. “TORCH pathogens,” defined as Toxoplasma gondii, other (which includes human immunodeficiency virus (HIV), varicella zoster virus (VZV), malaria-causing Plasmodium species, Listeria monocytogenes, Treponema pallidum, parvoviruses B19, enteroviruses, and recently, Zika virus), rubella virus, cytomegalovirus (CMV), and herpes simplex virus 1 and 2 (HSV), can cause serious fetal injury, including blindness, deafness, neurological impairment, premature birth, low birth weight and fetal demise [50, 51]. However, there is limited evidence that influenza A virus crosses the maternal-fetal barrier. The 2009 H1N1 influenza A pandemic was notable in that despite the widespread reports of increased risk of maternal and fetal mortality, development of chorionic villitis, and the demonstrated ability of the pandemic strains to infect fetal trophoblasts, there were few conclusive cases of vertical transmission via the placenta [52, 53]. Thus, pathogenesis during pregnancy is likely due to indirect exposure to maternal inflammatory cytokine expression and dysregulation of pregnancy-supportive hormones.

In addition to preventing pathogen entry into the fetal bloodstream, it is critical that cytokines that make it across the placental syncytiotrophoblast layer into the fetal circulatory system will not cause inflammation or immune cell activation that interrupts fetal growth and development; clinical reports of maternal inflammation and infection during pregnancy have been associated, although inconclusively, with the development of autism, bipolar disorders, and schizophrenia in children born to mothers infected with influenza A virus during pregnancy [54-56]. A shift away from inflammatory Th1 cytokines (TNF- α , IFN- γ , IL-2) can limit potential cytotoxic damage to the fetus and placenta [44, 45]. Thus, hormone-mediated suppression of inflammatory responses may benefit the fetus in the short-term by protecting the placenta from inflammation that could trigger pre-term birth or neurodevelopment damage; however, proper inflammatory signals must still be activated to recruit innate immune cells and CD8+ T cells in order to clear viruses.

The effect of hormonal expression during pregnancy on innate immune responses is complicated. Estrogen expression has been shown to reduce type I IFN signaling and impair CD8+T cell function, while 17 β -estradiol (E2 in mice) enhanced the recruitment of neutrophils and virus-specific T cells to promote viral clearance in H1N1 influenza A virus infected mice [57, 58]. Peripheral blood mononuclear cells (PBMCs) isolated from healthy pregnant women and co-cultured with 2009 H1N1 influenza virus or circulating rhinovirus strains (HRV43 and HRV1B) had significantly reduced IFN- α and IFN- γ responses, indicating increased susceptibility to severe outcomes of viral infection during pregnancy [59, 60]. In contrast, pregnant mice infected with 2009 H1N1 influenza expressed elevated levels of IL-1 α , IL-6, granulocyte-colony stimulating factor (G-CSF), monocyte chemotactic protein (MCP-1), CXCL1, and RANTES and experienced more severe pathology and mortality when compared to non-pregnant mice. These cytokines were highly expressed in humans who died as a result of 2009 H1N1 influenza A virus [61, 62].

Consequently, *ex vivo* modeling of a single subset of cells may not depict the entire story of hormonal, cytokine and immune cell signaling between lung, fetus, and placenta in an infected pregnant woman. While pre-term birth and low birth weight neonates have been well-documented outcomes of the 2009 H1N1 influenza virus infection in pregnant women, a mechanism for this phenotype is unclear, though placental transmission of inflammatory cytokines, dysregulated hormone signaling, and oxygen deprivation due to maternal respiratory distress have all been implicated [45, 63, 64]. This balance of fetal protection from inflammatory responses and stress hormone signaling while still mounting an effective immune response to influenza virus antigen is the focus of the second chapter of this dissertation.

Humoral immune responses following infection and vaccination during pregnancy

The natural outcome of infection is the development of immunological memory to prevent re-infection and future cellular damage. As discussed previously in this chapter, antigen-presenting cells from an influenza virus-infected lung process viral antigen and prime B cells in the draining lymph nodes near the lungs by binding to the B cell receptor (BCR), crosslinking several BCRs in the process and amplifying an activation signal [33, 65-67]. Additional co-stimulation by either activated toll-like receptors (TLRs) or CD4+ helper T cells responding to bound antigen on MHC is required to fully activate B cells and provides a second activation signal, resulting in clonal proliferation and amplification of antibodies specific for influenza viral antigens [68]. Selection for B cells with BCRs most tightly fitting viral antigen occurs in the germinal centers found in secondary lymphoid tissues such as the spleen where cells undergo somatic hypermutation, a process by which DNA encoding hypervariable Ig regions is broken by activation-induced deaminase (AID) and uracil-DNA glycosylase (UNG) and repaired by MSH2/6 and REV1 to

generate new combinations that may more tightly bind to viral antigen [68, 69]. Immunoglobulin class-switching increases the range of functions by recombining antibody variable regions encoding specificity for influenza viral proteins with constant regions encoding receptors for various innate immune cells and intercellular trafficking [69]. Ultimately, most antibody-secreting cells (ASCs) will undergo apoptosis following viral clearance, and a small percentage of these high-specificity B cell clones will become plasma cells that secrete low levels of antibody into the serum for up to months, or memory cells that take up residence in the bone marrow, where they can be reactivated to provide antibody responses to a subsequent infection [33, 70].

This system-wide coordination of B cell activation and survival in response to foreign antigen delicately balances the pregnant mother's serum antibody levels to both provide the benefits of transplacental immunity to the fetus and avoid the development of fetal-reactive antibodies. The competing priorities of fetal antigen tolerance and the production of antibodies that can be transplacentally conferred to the fetus to promote maternal immunity is tightly regulated by pregnancy hormone expression. Clinical evidence has long documented that the symptoms of autoimmune diseases arising from the generation of antibodies against self-antigen tend to recede during pregnancy and resurge after parturition and breastfeeding, indicating that pregnancy hormones play a role in coordinating immune tolerance at the local uterine and systemic level [45, 47]. In general, the development of autoimmune disorders such as multiple sclerosis, rheumatoid arthritis, and systemic lupus erythematosus (SLE), which are more prevalent in women, have been linked to the effects of estrogen on B cell activation and function [71]. Estrogen (E2) has been shown to upregulate Bcl-2, inducing survival of autoreactive B cells and changing signaling thresholds required to induce apoptosis [72, 73]. In contrast, progesterone has been established as negative regulator of B cell lymphopoiesis [74-76]. Reduced expansion of B cells within a

pregnant mother may help establish allotolerance to the fetus by preventing antibody recognition of fetal antigen, which might result in inflammation, lymphocyte cytotoxicity, and complement activation [46]. Healthy pregnancy has been shown to suppress B cell lymphopoiesis in BALB/c mice, which could be reversed by the exogenous addition of IL-7 [77-79]. These data suggest that pregnancy may reduce or redirect activated B cells during their migration to the lungs or bone marrow. Differential recruitment of IgA+ plasmablasts to the murine mammary glands after parturition and during nursing has been demonstrated, but specific homing receptors have not been identified, suggesting a role of local chemoattractants such as E-selectin [80, 81]. In this way, maintaining immunological tolerance of fetal antigen that reaches the maternal circulatory system may require that B cell activation and antibody expression be altered in order to prevent the proliferation of anti-fetal antibodies.

Understanding how pregnancy impacts the development of immune memory is of clinical significance. Trivalent and quadrivalent vaccination has been reported to reduce hospitalization and influenza-like illness of pregnant women and their newborns during the flu season with no record of increased adverse events due to vaccination between pregnant vaccinated and pregnant unvaccinated women [82-85]. Clinical trials of seasonal trivalent inactivated influenza vaccination (TIV) in Bangladesh showed improved transplacental transfer of influenza-specific antibodies from mother to child [86]. However, there are mixed results in how pregnancy affects serological immunity following vaccination. Schlaudecker et al reported that pregnant women seroconverted at the same rate as non-pregnant women following TIV but generated lower geometric mean titers (GMTs) against H1N1 (A/California) and H3N2 (A/Perth) viruses [13, 14]. Serological data from a cohort of healthy pregnant and non-pregnant women in California generated similar hemagglutinin inhibition (HAI) titers, and higher plasmablasts and HAI-fold changes in women

vaccinated during pregnancy [87]. Analysis of these two cohorts show that nearly all the pregnant women in the California study had been vaccinated in the years prior and suggested that pregnancy affected the serological recall to previous antigens [13]. Thus, while influenza vaccination during pregnancy has been demonstrated to be safe and to reduce the incidence of influenza-induced hospitalization and preterm birth, further research into antibody functionality and expression is still needed.

Introduction to Dissertation Research

In this dissertation, I investigate the mechanisms of viral pathogenesis during pregnancy and how the hormonal environment required to support healthy fetal development impacts the immune responses to infection and vaccination. In Chapter II, I provide evidence for how lung and placental structures are compromised by seasonal H1N1 influenza A infection and how infection disrupts hormonal and cytokine signaling throughout the pregnant mother's body. For my research, I utilized a mouse model due to its well-characterized immune cell subsets and cytokine responses to influenza A virus infection, the similarities between placental architecture between mice and humans, the ease of generating timed pregnancies, the short duration of pregnancy (21 days), and the reduced cost and facility requirements of mice compared to other rodents and non-human primates. In Chapter III, I profile how these signaling disruptions affect the development of cellular and serological memory to influenza antigen following infection and vaccination during pregnancy. In Chapter IV, I summarize these findings and place them in the larger context of maternal health and the immune response to respiratory viral infections and propose future avenues of research and potential for the development of more informed clinical treatment of pregnant women infected with influenza virus during pregnancy.

Chapter II: H1N1 influenza virus infection results in adverse pregnancy outcomes by disrupting tissue-specific hormonal regulation

Elizabeth Q. Littauer¹, E. Stein Esser¹, Olivia Q. Antao, Elena V. Vassilieva, Richard W.

Compans and Ioanna Skountzou*

Department of Microbiology & Immunology and Emory Vaccine Center,
Emory University School of Medicine, Atlanta, GA 30322, U.S.A.

¹: The authors contributed equally to this work

*Corresponding author

E-mail address: iskount@emory.edu

1518 Clifton Road, CNR 5015, Atlanta, GA 30322

Published in PLoS Pathogens, 2017, 13(11): e1006757.

Abstract

Increased susceptibility to influenza virus infection during pregnancy has been attributed to immunological changes occurring before and during gestation in order to “tolerate” the developing fetus. These systemic changes are most often characterized by a suppression of cell-mediated immunity and elevation of humoral immune responses referred to as the Th1-Th2 shift. However, the underlying mechanisms which increase pregnant mothers’ risk following influenza virus infection have not been fully elucidated. We used pregnant BALB/c mice during mid- to late gestation to determine the impact of a sub-lethal infection with A/Brisbane/59/07 H1N1 seasonal influenza virus on completion of gestation. Maternal and fetal health status was closely monitored and compared to infected non-pregnant mice. Severity of infection during pregnancy was correlated with premature rupture of amniotic membranes (PROM), fetal survival and body weight at birth, lung viral load and degree of systemic and tissue inflammation mediated by innate and adaptive immune responses. Here we report that influenza virus infection resulted in dysregulation of inflammatory responses that led to pre-term labor, impairment of fetal growth, increased fetal mortality and maternal morbidity. We observed significant compartment-specific immune responses correlated with changes in hormonal synthesis and regulation. Dysregulation of progesterone, COX-2, PGE2 and PGF2 α expression in infected pregnant mice was accompanied by significant remodeling of placental architecture and upregulation of MMP-9 early after infection. Collectively these findings demonstrate the potential of a seasonal influenza virus to initiate a powerful pro-abortive mechanism with adverse outcomes in fetal health.

Author summary

Maternal immunology is finely balanced to maintain a tolerant and supportive molecular environment for the developing fetus while continuing surveillance against foreign microbial threats. Influenza viral infection during pregnancy is a significant clinical risk for mothers and their newborns, increasing hospitalization, preterm birth, low birth weight, and maternal and neonatal deaths worldwide. In a mouse pregnancy model, we show how influenza virus infection disrupts the delicate and interconnected cytokine and hormonal signaling pathways that respond to respiratory pathogens. The health of mothers and offspring was impacted in our study, after pregnant mothers' lung and placental architecture was compromised by infection. Influenza virus infection increased the stress on the mother's body already present due to pregnancy, or reversed the hormonal environment required to establish and maintain healthy pregnancy. By dissecting the effects of inflammation post-infection throughout the mother's anatomy, we can tailor anti-inflammatory treatments for the pregnant population. Also, thorough knowledge of immune responses will assist in tailoring vaccine design and dosage for this delicate period of women's immunological and reproductive health.

Introduction

Influenza virus has been responsible for four pandemics in the past century, with an additional global health burden of seasonal influenza-related illness estimated at five million cases of severe illness and nearly 500,000 deaths annually [1].

Pregnant women are among the high-risk groups who are more susceptible to seasonal and pandemic influenza viral infections, with pronounced lung immunopathology [2] and increased incidence of complications, such as pre-eclampsia, pneumonia or heart failure during all 3 trimesters of gestation resulting in high hospitalization rates and mortality [1, 3-8]. Notably, during the 2009 H1N1 pandemic, pregnant women in the United States showed a disproportionately high mortality rate, accounting for 5% of deaths while representing only 1% of the total population [9]. The majority of pregnant women who died of influenza-related illness during the pandemic were infected in the second and third trimesters of pregnancy [10].

Both seasonal and pandemic influenza virus have a substantial impact on the developing fetus. Infection during late-second or third trimester of pregnancy is associated with significant increases in miscarriages, stillbirths, and early neonatal diseases and death [1, 11]. Several studies indicate that infants born to influenza virus-infected mothers have an increased risk of developing health problems later in life ranging from chronic immune diseases to schizophrenia [12, 13].

Though the mechanisms predisposing pregnant women and their fetuses to an increased rate and severity of influenza virus infection-related complications are not fully elucidated, it is generally accepted that the feto-placental tolerance developed during pregnancy to support life of a semi-allogeneic fetus is a contributing factor to adverse outcomes [6, 7, 14, 15]. Dynamic immunological processes that occur throughout pregnancy are regulated by pregnancy hormones, whose receptors are found on most immune cells [7, 16-20]. Researchers have demonstrated a shift

away from type Th1 cell-mediated responses toward enhanced type Th2 humoral-mediated responses during pregnancy, suggesting a protective role for the developing fetus, although these alterations could predispose to increased susceptibility to infections from respiratory viruses such as influenza [18, 21]. Inflammation plays a major role in tissue pathogenesis and it is more pronounced during the last 2 trimesters of pregnancy due to changes in cytokine levels that regulate fetal-placental tolerance, that suppress some cytokines (e.g. IFN- γ and VEGF), while elevating the levels of others (e.g. TNF- α and G-CSF) [14, 22, 23].

Presently there are very few studies that have examined the adverse effects of influenza virus infection in pregnancy mainly using the pregnant mouse model due to histological similarities of rodent to human placenta [24]. These reports demonstrated adverse effects of the 2009 pandemic influenza A (H1N1) virus on lung immunopathology [25-27], and more recently Kim et al reported severe pathogenesis of influenza B virus in the pregnant mouse model. However, the impact of seasonal H1N1 influenza A virus infection on maternal and fetal health during pregnancy, and the exact mechanisms leading to premature rupture of membranes (PROM) and preterm birth after influenza virus infection during pregnancy have not been fully elucidated [6, 11].

The objective of this study was to recapitulate the adverse outcomes of seasonal influenza virus infection in maternal, placental and fetal compartment using the mouse model. We aimed to correlate disease burden with progesterone and prostaglandin levels since their role is critical in lung and placental health; and assess the magnitude of endocrine and immunological changes that through tissue inflammation and pathology lead to maternal and fetal distress. To achieve this objective, we chose as a model influenza virus the seasonal H1N1 A/Brisbane/59/07 strain to sub-lethally infect BALB/c mice at the second third of gestation period and monitor maternal-fetal health. All correlations between progesterone and prostaglandins with compartment-specific

inflammation and immune responses as well as tissue remodeling took place at 4 days post-infection, when weight loss was first exhibited in our mouse model and at which time point pregnant women are most susceptible to ICU admission and death in previous pandemics [10].

Results

Influenza viral infection during pregnancy results in shorter gestation period. In order to assess the impact of seasonal influenza virus infection in maternal and fetal health, we first infected pregnant mice at day 12 of gestation and non-pregnant controls with a low dose of H1N1 A/Brisbane/59/07. With this approach we aimed to recapitulate human infection at the end of 2nd to 3^d trimester of pregnancy with a low pathogenicity seasonal influenza virus. Uninfected pregnant controls reached a peak bodyweight that was 56.2% greater than that of their pre-pregnancy bodyweight (Fig 1A). The infected pregnant animals reached a peak bodyweight of 34% of their original bodyweight and the average gestation period decreased by 6.7% to 19.6 days ($p < 0.001$) (Fig 1B). Additionally, pregnant mice infected during gestation dropped to 89 % of their initial body weight following pre-term delivery, while uninfected pregnant mice remained at 116% of their initial body weight following delivery. We found that infection with a low pathogenicity influenza virus interrupted the normal progression of pregnancy to completion inducing pre-term labor in our mouse model. The initial experiment recapitulated the clinical phenotype of pre-term birth observed in human women infected mid-gestation with seasonal influenza virus [28].

Mice born from influenza virus-infected mothers have an increased likelihood of stillbirth or being small for gestational age (SGA). Next, we examined the impact of infection on offspring viability and health status of pregnant mice. Numbers of viable and non-viable pups were recorded, bodyweights were taken at birth and classified as non-viable (≤ 1 g), SGA (1.1-1.25 g) and healthy (> 1.25 g) and monitored daily for growth curves. Litter size averaged 4.5 pups per uninfected healthy pregnant controls while infected mothers gave birth to an average of 2.7 pups per litter; however, because infected mothers often consume sick or stillborn offspring, these

results are not necessarily reflective of number of offspring carried to parturition. The average weight of offspring from uninfected pregnant mice was 1.46g. When mothers were infected with the virus, the body weight of newborns was 19% lower, averaging 1.18g ($p < 0.0001$) (Fig 1C). Pups born from infected mothers at days 18 and 19 of gestation had lower body weight compared to the pups born at day 20; however, 10 mice born on day 21 were all stillborn (Fig 1D). Thus, the length of pregnancy did not necessarily correlate with the health outcome of the offspring; that is, SGA condition was not dependent on the length of gestation. In uninfected pregnant mothers, 85% of pups were born with a healthy weight, while 13% were SGA pups and 2% were stillborn (Fig 1E). Infection with seasonal influenza virus reduced the number of healthy offspring to 25%; the remaining pups were 25% SGA, and 50% stillborn (Fig 1E). Overall, offspring born from infected mothers were approximately 20% smaller in terms of body weight compared to offspring of uninfected mothers. Infection nearly doubled the incidence of SGA pups from 13% to 25%, and the likelihood for stillbirth increased by 35-fold from 2% to 70% following infection (Fig 1C, 1D, 1E). Low birthweight or SGA offspring are a common outcome of pregnant mothers infected with pandemic H1N1 influenza virus during the second and third trimester and has been observed in cohorts of pregnant women infected with seasonal H1N1 influenza virus in Nova Scotia [6]. Thus our model replicates more serious clinical birth complications associated with influenza A viral infection during mid- to late-gestation pregnancy.

Pregnancy reduces viral clearance in the lungs of influenza virus-infected mice. The severity of viral infection in pregnancy was initially assessed by examination of various organs for systemic spread of pathogen, viral load and tissue inflammation at 4 d.p.i. The results from lungs of infected pregnant mice were compared to those of non-pregnant infected controls. Although both pregnant

and non-pregnant infected lungs were heavily infiltrated by neutrophils showing intense inflammation (Fig 2A), viral loads were 8-fold higher ($p < 0.05$) in pregnant animals compared to non-pregnant ones, suggesting hampered virus clearance during pregnancy (Fig 2B). Interestingly, lungs of mock-infected pregnant mice showed increased airway inflammation over mock-infected non-pregnant mice, indicating that there is increased physiological stress in the lungs during pregnancy (Fig 2a: a, d).

Viral titers were undetectable in the placentas and fetuses of infected mice. This was further confirmed with qPCR measuring viral RNA (M gene) levels (Fig 2C). Lack of detectable viral RNA in placental and fetal tissues indicates that transplacental transmission of influenza virus from mother to child is unlikely and that retardation in fetal development was not due to *in utero* infection. These findings correspond with clinical reports on pregnant mothers infected with influenza A virus during pregnancy; while several H1N1 strains can infect fetal trophoblast cells *in vitro*, clinical evidence of vertical transmission is uncommon and inconclusive [29-31]. Despite the presence of influenza virus receptors α -2,6 sialic acids on human placental membranes, only H5N1 viruses have been reported to transmit via maternal vertical transmission [32, 33]. This indicates that the negative effects on offspring born to mothers infected with influenza virus during pregnancy are mediated not by direct infection of placenta and fetus, but indirect causes such as dysregulated hormonal signaling, increased inflammation, or immune system activation against placental and/or fetal tissue.

Progesterone and PGF2 α regulate compartment-specific cytokine signaling during gestation in the absence of infection. Progesterone promotes endometrium and uterine changes to support embryo implantation and feto-placental development. Insufficient progesterone concentrations can

lead to preterm delivery and miscarriage in humans and rodents [34, 35]. To assess the effect of influenza virus infection on systemic progesterone levels and subsequently in pre-term labor, we first measured cytokine expression and progesterone levels in serum of uninfected pregnant and non-pregnant mice (Fig 3).

Serum progesterone was 7-fold higher ($p < 0.01$) in uninfected pregnant mice compared to non-pregnant controls as is expected during healthy gestation (Fig 3A). These levels inversely correlated with the levels of pro-inflammatory cytokines IL-1 β , IL-12p40 and GM-CSF showing a reduction of 41%, 50% and 63% respectively when compared to their levels in non-pregnant mice ($p = .01$) (Fig 3B, S1 Table). None of the Th2 (IL-3, IL-4, IL-5, IL-10, IL-13) or Th1 (IL-2, IL-12p70, IFN- γ) cytokines showed any differences between pregnant and non-pregnant mice (S1 Table).

To further establish the threshold of inflammation in the pregnant mouse model, we measured the levels of serum prostaglandin F2 α (PGF2 α) and prostaglandin E2 (PGE2) in uninfected pregnant mice and compared them to uninfected non-pregnant controls. PGE2 selectively suppresses effector functions of macrophages and neutrophils and the Th1, CTL and NK cell-mediated type-1 immunity, but promotes Th2, Th17, and T_{reg} responses [36]. In contrast to increased levels of progesterone during pregnancy, PGF2 α and PGE2 were reduced by 50% and 33% respectively in serum of pregnant mice compared to non-pregnant controls (Fig 3C, D). Thus, we established in our mouse model that pregnancy hormones or hormone-like mediators of homeostasis are subjected to systemic changes to prepare an immune environment trending toward anti-inflammatory responses.

Infected pregnant mice show lower levels of serum inflammatory markers than non-pregnant controls. Hormonal and cytokine responses were further confounded during pregnancy following influenza virus infection. Infection caused a 5-fold reduction of serum progesterone in pregnant mice 4 d.p.i. to levels similar to those seen in non-pregnant mice (Fig 3A). There was a significant inverse correlation between serum progesterone levels and lung viral load ($r^2=0.8$, $p=0.04$) (S1 Fig C). Similarly, serum PGF2 α levels were approximately 5 times lower than pre-infection in both pregnant and non-pregnant cohorts ($p=0.02$) (Fig 3C) whereas PGE2 did not show any significant differences (Fig 3D).

Infection in pregnancy elevated the serum inflammatory cytokines IL-1 β , IL-12p40, GM-CSF and eotaxin from 2 to 10 times whereas it significantly reduced RANTES (Fig 3E; S1 Table). When compared to infected non-pregnant controls, pregnant mice had less than half the number of upregulated inflammatory cytokines (IL-1 β , IL-6, IL-12p40, eotaxin, G-CSF, GM-CSF, MIP-1 α , TNF- α , RANTES,) (S1 Table). The majority of these cytokines had approximately 50% lower levels in pregnant mice (Fig 3F). Interestingly, IL-10 increased significantly only in infected pregnant mice ($p=0.02$) suggesting a robust regulatory response to infection (Fig 3E). Pro-inflammatory IL-17 which is detected mainly in serum and placenta [37] was elevated 2-fold during pregnancy (Fig 3B, F). Although IL-17 production was not affected by virus infection, its levels were significantly higher than those observed in infected non-pregnant animals (Fig 3F, S1 Table). These data show that pregnancy results in a unique signature of systemic antiviral cytokine expression. Progesterone and PGF2 α reduction led to an inflammatory response although its magnitude was lower than the response seen in the control group.

Pregnancy increases inflammation in the lungs following H1N1 influenza virus infection.

Progesterone increase in pregnancy results in relaxation of smooth muscles in the airways, dilating the bronchial tissue [38]. PGE2 and PGF2 α are key players in lung's physiological response to infection and airway reactivity [38]. PGE2 is a vasodilator that increases the permeability of the lung vasculature [39, 40] and works with PGF2 α , a bronchoconstrictive hormone to finely tune lung function [41]. Influenza virus infection damages lung epithelial cells, releasing free reactive oxygen species (ROS) that activate cyclooxygenase-2 (COX-2) via the arachidonic acid pathway and upregulate synthesis of PGE2 [42]. In order to assess the effect of these hormones on inflammatory responses in infected lungs of pregnant mice, we determined their levels along with a panel of 23 cytokines and chemokines in tissue lysates of pregnant and non-pregnant mice 4 d.p.i.

Pregnancy increased expression of lung progesterone 11.6-fold ($p < 0.001$) and PGF2 α 2.7-fold ($p = 0.03$) (Fig 4A, B), while no detectable changes were found in PGE2 levels between pregnant and non-pregnant mice (Fig 4C). Notably, in the absence of infection, pregnant uninfected mice overexpressed lung neutrophil-recruiting chemokines (KC, 1.37 times higher) and cytokines (IL-1 β , IL-6 and G-CSF; 1.64-, 7.6- and 3-times higher respectively) relative to non-pregnant controls (Fig 4D, S2 Table) [43]. These data suggest that these changes may prepare the lung environment during pregnancy to fight microbial insults, more so than during a non-pregnant state.

Infection reduced progesterone expression in the lungs of pregnant animals by 5-fold ($p < 0.0001$) when compared to non-pregnant mice that showed a 2-fold reduction ($p = 0.01$) (Fig 4A). Moreover we observed a strong correlation between lung progesterone with viral load ($r^2 = 0.79$, $p = 0 < 0.0001$) (S1 Fig D). Following the same trend, PGE2 levels were significantly

decreased ($p=0.008$) (Fig 4C). However, $\text{PGF2}\alpha$ lung expression was not altered after infection in either pregnant or non-pregnant mice (Fig 4B).

While influenza virus infection caused dramatic increases in expression of inflammatory cytokines and chemokines in lungs of both pregnant and non-pregnant mice (S2 Table) we detected a few differences between these groups. The levels of $\text{IL-1}\alpha$, $\text{IL-1}\beta$ and KC were 50%, 200% and 40% higher than those estimated in infected non-pregnant controls, while IL-6 levels were 50% lower in the pregnant group (Fig 4E, S2 Table). The results on $\text{IL-1}\alpha$ and IL-6 are in agreement with previous reports on the role of $\text{IL-1}\alpha$ as a negative regulator of IL-6 expression [44]. Influenza virus infection upregulated $\text{MIP-1}\alpha$ expression in both pregnant and non-pregnant cohorts reaching similar levels (S2 Table) whereas $\text{MIP-1}\beta$ expression was 40% lower in pregnant animals (Fig 4E, S2 Table). While both cytokines are involved in cellular recruitment and inflammation at the site of infection, they signal through different receptors. $\text{MIP-1}\alpha$ signals through CCR1, CCR4, and CCR5 and $\text{MIP-1}\beta$ signals directly through the CCR5 [45], suggesting that pregnancy may induce different pathways signaling in response to infection.

Our findings point to a model for the excessive morbidity seen in infected pregnant mice. Pregnancy induces a combination of physiological changes, including vasoconstriction in the lungs via $\text{PGF2}\alpha$, the negative impact of infection on progesterone and PGE2 expression, and robust inflammatory responses in the lungs. Decreased bronchodilation and intense neutrophil infiltration in the alveolar spaces leads to respiratory failure, which is evident also in lung histopathology (Fig 2A) [46-48].

Infection upregulates labor-inducing hormones and inflammatory cytokines in the placenta.

In addition to their effects on lung architecture and immune responses, progesterone, PGE2 and

PGF2 α were measured following infection of pregnant mice because of their respective roles in uterine contractility. Progesterone elevation in pregnancy supports fetal development by thickening the endometrium to allow for embryo implantation and suppressing inflammation in the uterus. PGE2 increases vasodilation, induces uterine contractions, and decreases T-cell proliferation and lymphocyte migration [49] while PGF2 α initiates vasoconstriction of uterine and endometrial blood vessels [50], resulting in induction of labor [6, 12, 13, 51-53]. At the same time, PGF2 α stimulates the production of pro-inflammatory cytokines and may enhance uterine production of leukotriene B4 (LTB4) that in turn activates various neutrophil functions [54]. We found that progesterone levels in the placentas of infected pregnant mice were decreased by 40% compared to uninfected pregnant mice ($p=.04$) (Fig 5A). In contrast, PGF2 α levels were almost 5-fold higher in the same group compared to uninfected controls ($p=.0002$) (Fig 5B). Placental lysates did not show a difference in PGE2 expression (Fig 5C) after infection.

Progesterone and PGF2 α expression were inversely correlated with viral load following infection although significant association between measured parameters was only observed in progesterone ($r^2=0.46$, $p=0.007$ and $r^2=0.44$, $p=0.22$ respectively) (S1 Fig B, E). The association of serum, lung or placental progesterone with viral load supports the notion that seasonal influenza virus infection during gestation disrupts the production of progesterone and provides evidence an explanation for early termination of pregnancy and spontaneous abortions.

Fold changes of cytokine expression in the placentas and fetuses of pregnant mice were also compared before and after infection. Eleven placental cytokines showed suppressed expression ranging from 29-72% after infection (S2 Fig, S3 Table). G-CSF and RANTES however were enhanced by 4.8- and 1.5-fold respectively. Similarly, fetuses showed a dramatic decrease in immune responses, although pre-infection cytokine and chemokine levels were very low compared

to the placental compartment. With the exception of IL-1 α , which was increased following infection, cytokine expression was decreased in the fetus post-infection by at least 60% (S2 Fig, S3 Table). This suppression indicates that the placenta and fetus are effectively shielded from the inflammatory cytokine signature of the mother's circulatory system and that the physiological changes induced by progesterone and prostaglandins are likely causes of poor fetal and offspring outcome.

Infection disrupts placental architecture via inflammation and protein degradation. Placenta is the sole source of nutrients and oxygen to the developing fetus. The placenta in both humans and rodents is derived from the maternal endometrial decidua and fetal trophoblasts [55]. The development of this critical organ is carefully negotiated through regulation by pregnancy hormones, initiated by prolactin and progesterone, and tightly regulated immune tolerance by uterine regulatory T cells [56]. Inflammation in the uterus and placenta due to infection or autoimmune responses has been linked to preeclampsia, endometriosis, and spontaneous abortion [57, 58] yet influenza virus has not been definitively shown to cross the maternal-fetal barrier in mice or humans. Viral infection in the placenta was examined and yet no viral RNA (M gene) was detected via qPCR (Fig 2C). Hence, the effect of influenza infection on placental function and health was examined via histology and molecular assays. Placentas from uninfected mothers at E16 (16 days of gestation) (Fig 6A: a, b, c, g) and mothers 4 d.p.i. (Fig 6A: d, e, f, h) were compared. Placentas from uninfected mothers maintained structural integrity between the maternal decidual layer, the fetal spongiotrophoblast layer, and the placental labyrinth (Fig 6A: a) while placentas from infected mothers (Fig 6A: d) showed increased regions of fetal endothelial cellular death (**stars**) with dark-blue nuclei suspended within the tissue, indicating that infection increases

cellular death within the placenta. Infection increased gaps within the spongiotrophoblast layer (\blacktriangle), a region through which maternal spiral arteries cross to deliver oxygen to fetal blood within the labyrinth (Fig 6A: b, e, f). Infection also increased the incidence of fibrinoid necrosis in-between the maternal decidual layer and the fetal spongiotrophoblast (\blacksquare) region. (Fig 6A: h) [59]. Histology slides were scored for the incidence of fetal endothelial cellular death (FED), degradation of the spongiotrophoblast layer, and fibrinoid necrosis (FN); infection increased the occurrence of these indicators of poor placental health (Fig 6B).

To determine underlying molecular causes of the placental spongiotrophoblast degradation, matrix metalloproteinase (MMP) expression was quantified via Western Blot in placental lysates from infected and uninfected pregnant mice at E16 (Fig 6C). MMPs are proteolytic enzymes, localized in the placenta, that remodel tissues throughout the body via endopeptidase activity towards extracellular membranes (ECM), breaking down tightly adherent cells within the tissue [60-62]. MMP-2 and MMP-9 are gelatinases that have been widely implicated in placental pathology and preterm labor, both in rodent models and in humans [57, 63-66]. MMP-9 can be induced by high levels of IL-1 β via the p38 MAPK signaling pathway [61, 67, 68], consistent with the increased levels of IL-1 β observed in placentas of infected mice (S3 Table). Infection increased placental expression of the pro-enzyme and activated enzyme form of MMP-2 and MMP-9 (Fig 6C), thus exposing both the placenta and the amniotic membranes surrounding the fetus and placenta to degradation.

Infection alters the expression of immune-responsive hormone regulators COX-2 and PIBF.

Sex hormone synthesis and feedback pathways are intrinsically linked with innate immune signaling pathways of TNF- α , IL-1 β , IL-4, IL-6, IL-10, IL-17, and IFN- γ [42, 69, 70]. Hence, we

quantified hormone regulators, progesterone-induced blocking factor (PIBF) and COX-2 in order to examine the interdependent relationships in endocrine and innate signaling in our pregnancy model. Successful outcome of gestation requires expression of PIBF, a progesterone-responsive immunomodulatory protein with multiple active isoforms: 90kD, 66kD, and 55kD [71, 72]. PIBF promotes Th2 cytokine production [73] and inhibition of natural killer (NK) cell activity [34, 51]. While this function is crucial to limiting cytolytic activity in the uterus and placenta reduction of NK activity in lungs leaves the pregnant mother vulnerable to infection. Expression of PIBF isoform 66kD in the placenta was nearly abrogated following infection while 90 kD and 55 kD isoforms were undetectable (Fig 7A and 7B). In non-infected non-pregnant and pregnant mouse lungs, these isoforms were differentially expressed. The isoforms 90 kD and 55 kD showed 3-fold and 9-fold higher expression respectively in pregnant mice as compared to non-pregnant controls. In contrast, the levels of 66 kD isoform were 2-fold lower when comparing the pregnant to the non-pregnant group. Following infection of pregnant mice, isoform 66 kD was reduced 3-fold and isoform 55 kD was increased 2-fold. In infected pregnant mice, all isoforms were uniformly suppressed by 2-fold (Fig 7C, 7D, 7E). The results of this study demonstrate that different isoforms are highly expressed in placenta and lungs of pregnant mice, that infection down-regulates all isoforms and that there is a differential expression of isoforms in lungs during pregnancy. Notably the regulation of isoform 55 kD in pregnant and non-pregnant population follows opposite trends, suggesting a role in immunomodulation of placental-fetal interface.

COX-2 is a key regulator in the arachidonic acid and prostaglandin synthesis pathway. Influenza virus infection induces COX-2 expression, thus increasing secretion of PGF2 α in bronchial epithelial cells [42]. Previous studies demonstrated that COX-2 deficiencies reduce the recruitment of macrophages and neutrophils to the site of influenza viral infection, and COX-2^{-/-}

mice infected with influenza virus had reduced lung viral clearance compared to wild-type infected mice [69] [74]. COX-2 placental expression was decreased upon infection (Fig 8A, 8B) which is consistent with lack of upregulation of PGE2 in the placenta following infection (Fig 5C). Thus, preterm birth in our model is correlated with the physiological changes mediated by the withdrawal of pregnancy-supportive progesterone, the increased expression of labor-inducing PGF2 α , and upregulation of structure-damaging degradative proteinases in the placenta rather than increased inflammation mediated by COX-2, PGE2, or cytokines.

Pregnancy elevated expression of active COX-2 45kD in the lungs (Fig 8C, 8E). Infection did not exert a significant effect on active 45 kD COX-2 expression in the lungs of non-pregnant mice but resulted in a 2-fold increase during pregnancy (Fig 8E). Enhanced COX-2 expression during pregnancy may explain increased expression of neutrophil-recruiting chemokines in the lungs (Fig 4E), providing a regulatory mechanism for the enhanced immunopathology seen following infection.

Discussion

Influenza viral infection disrupts the supportive molecular environment for fetal development and offspring health. The objective of this study was to investigate how seasonal H1N1 influenza virus infection affects the outcomes of pregnancy and how pregnancy alters the innate immune response during infection in a BALB/c mouse model. This study is unique in that it ties together hormonal changes induced by infection with cytokine dysregulation across three compartments; maternal, placental and fetal. We demonstrate that influenza virus infection alters key hormone levels required to maintain healthy pregnancy, and results in increased immunopathology thus compromising maternal and fetal health. Our study expands upon previously published work from Kim HM et al [27], Kim JC et al [75], Klein and Robinson [17, 19, 76, 77], and Moran et al [18, 78] by examining compartmental changes in hormone and cytokine expression following influenza virus infection. We linked seasonal influenza virus infection to clinical observations of adverse outcomes in pregnancy (preterm birth, SGA, stillbirth, increased maternal morbidity), enhanced lung and placental histopathology and reduced control of viral replication in lungs of infected pregnant mothers. We provide a model for how influenza virus infection, while contained in the lung, results in global dysregulation of the hormonal signaling required to sustain healthy gestation. In our study, the state of pregnancy dampens innate immune responses compared to non-pregnant controls by at least 50%; in some compartments, the maternal body maintains some form of systemic tolerance, while in the respiratory compartment, the lungs remain primed to fight invading pathogens.

Consistent with previous clinical reports and animal studies, we found that pregnancy increases the severity of seasonal influenza virus infection and thus impairs maternal and offspring health and recovery [25-27, 75, 79-81]. Pregnant mice exhibited increased viral replication in the

lungs by 8-fold compared to infected, non-pregnant controls, a trend that was also found in similar studies looking at pandemic H1N1 influenza virus in 2012 and influenza B virus in 2014 [27, 75]. We found a significant correlation between lung viral load and progesterone levels in lung, placenta and serum suggesting that seasonal influenza virus infection during gestation disrupts the production of progesterone leading to preterm labor, SGA and increased fetal mortality. We also observed a dramatic increase of placental PGF2 α after infection pointing to the role of this prostaglandin in the intense local inflammatory response. We also documented that the immune responses are compartment-specific in the mouse model, resulting in distinct signatures of inflammation within each compartment (Fig S2). Similar to findings by Kim et al with pandemic 2009 H1N1 influenza virus, we demonstrated that seasonal H1N1 influenza virus enhanced lung pathology in pregnant mice via an increase in IL-6, IL-1 α , and G-CSF expression and that infection reduced serum concentrations of progesterone during pregnancy [27]. The differences in systemic responses between pregnant and non-pregnant groups in our mouse model suggest that the unique endocrine environment supporting gestation compromises most of the innate immune responses to infection. These shifts in response to infection during pregnancy may have evolved to protect the fetus from activation of inappropriate activation of T cell responses, at the expense of increased inflammation in the lungs.

There are a few caveats to our pregnant mouse model of infection. Most obvious is that the average length of pregnancy in humans is 40 weeks while gestational length in mice is around 19-21 days depending on the mouse strain. However, both mice and humans possess a hemochorial placenta where the fetal chorion is in direct contact with maternal blood [82, 83]. Common transcription factors involving the expression of various placental genes have been identified in both human and mouse placenta [84]. Another caveat is the different mechanisms for maintaining

progesterone secretions during gestation in mice and humans. In mice, progesterone is produced by the placental corpus luteum, which is regulated by prolactin for the first half of pregnancy and then by trophoblastic giant cells for the remainder of gestation [84]. In humans, prolactin is not required for the maintenance of pregnancy and the corpus luteum depends on the human chorionic gonadotropin (hCG) produced by trophoblasts to stimulate progesterone. After 8 weeks of gestation, the progesterone produced by the placenta is sufficient to maintain pregnancy in humans [84]. These differences should be taken into account when interpreting the role of progesterone in pregnancy following influenza virus infection. Lastly, Periolo et al. studied nasopharyngeal swab samples obtained in the second and third trimester of 41 pregnant women with confirmed pandemic H1N1 influenza A virus infection [2]. The authors reported increased expression of inflammatory cytokines IL-8, IL-6, and TNF- α and significantly lower levels of TGF- β and IFN- β compared to the pregnant women who survived or non-pregnant controls, with particular emphasis in the role of IL-6 in severity of disease. We have not seen these differences in seasonal H1N1 influenza virus-infected pregnant mouse model, and to our knowledge, there have been no studies examining the extent of cytokine expression in response to seasonal influenza virus infection in human pregnant women.

Influenza virus infection in our mouse model interfered with progesterone-mediated anti-inflammatory effects during pregnancy. Elevated levels of progesterone in the lungs during pregnancy suppress the activation of COX-2 by blocking IL-1 β activation of NF- κ B thus creating an anti-inflammatory environment at the expense of a quick response to foreign antigen [85]. However, when slow immune response results in uncontrolled viral growth, NF- κ B initiates transcription of a host of immunomodulatory genes, including COX-2 [86]. It has been reported that influenza virus infection results in epithelial cell damage, which releases free oxygen radicals

and activates COX-2 [42]. In our pregnant model we demonstrate that influenza virus infection induced COX-2 activation and upregulation of PGF2 α in the lungs resulting in vasoconstriction and inflammation. These changes reduce the amount of oxygen available to the mother and developing fetus that may lead to respiratory distress, increased morbidity and retardation of fetal growth.

Previous studies have indicated that progesterone treatment at levels equivalent to hormonal birth control are sufficient to limit immunopathology of H1N1 influenza virus infection in non-pregnant mice [87, 88]. In our study, influenza A virus infection resulted in a decrease of progesterone expression in pregnant mice, and progesterone therapy may be a promising treatment to mitigate the effects of viral infection on lung pathology and to prevent PROM and early delivery of the fetus. COX-2 inhibitors have been proposed as antivirals for treating inflammation caused by influenza virus infection [89, 90]. This study demonstrates that pregnancy has a unique relationship with COX-2 upregulation in the lungs and that pregnant women may benefit from these molecular inhibitors following influenza virus infection.

Vertical transplacental transmission of influenza virus has been debated [29, 30, 91]. In our study, influenza virus was not detectable in the placenta and fetus. Instead, poor offspring health was likely due to imbalances in the maternal endocrine and immune physiology responsible for proper fetal development. Influenza virus infection resulted in a breakdown of the placental architecture, likely caused by inflammation, reduced progesterone expression and activation of structure-remodeling MMP-2 and MMP-9. Programmed cell death in amnion membranes is routine to normal parturition in rodents; membranes rupture in part due to tissue weakening rather than solely dependent on mechanical stress of labor [92]. Weakened strength of the amniotic membrane combined with reduced placental health creates an impetus for premature rupture of

membranes (PROM) and thus, preterm birth. Increases in the placental concentrations of vasoconstrictor $\text{PGF2}\alpha$ and immune cellular activators G-CSF and RANTES following infection create an environment where uterine contractility is triggered prematurely and immune cells can be activated against fetal cells at the maternal-fetal interface (Fig 5B, S2). While we have shown disruption of key hormonal regulators in the lungs following infection during pregnancy, COX-2 does not seem to be involved in the phenotype of pre-term labor following viral infection during pregnancy. COX-2 is directly correlated with PGE2 levels, which do not change in the placenta following influenza virus infection. Rather, major changes in progesterone and $\text{PGF2}\alpha$ production have been shown to induce pre-term labor, while synthesis of $\text{PGF2}\alpha$ does not depend on COX-2 cellular expression [74]. Compromise of placental structure and function may lead to reduced oxygen and nutritional supply and buildup of gas and waste in the fetus, resulting in retardation of fetal growth and neural development or stillbirth. Clinical studies indicate that maternal influenza A virus infection during pregnancy may predispose offspring to psychosis and schizophrenia due to fetal neurodevelopment being dysregulated by hypoxia and inflammation [93, 94]. In future studies, offspring of influenza virus-infected mothers will be followed to adulthood and examined for neurological disorders as well as variation in the timing of viral dose at early, mid, and late gestation.

These data support a model where influenza virus infection “breaks through” the balance of maternal systemic tolerance towards developing fetuses, enhancing pathogenesis in the lungs and triggering pre-term birth thus affecting the health of both mother and offspring. We hypothesize that fetal health is impaired by the spillover of inflammatory cytokines, whose expression is influenced by pregnancy hormones, and structural remodeling proteins intended to repair maternal airways have long ranging effects outside the compartments they were intended to work in, such

as the placenta. Previous studies have examined the effect of individual hormones on male and female innate immune responses to influenza virus infection. Klein et al have demonstrated that 17β -estradiol and progesterone treatments reduce influenza virus infection immunopathology, promoting expression of TGF β , IL-22, and IL-6 and suppressing inflammatory cytokine production [77, 87, 95]. We found that reduced expression of progesterone in the lungs and placenta might be a causative factor for fetal and maternal respiratory distress and early termination of pregnancy.

Infection in the maternal lungs resulted in the upregulation of cellular activation markers in the placenta and inflammatory signaling in the fetus, indicating that while *in utero* offspring are not in contact with influenza virus; they are nevertheless negatively impacted by maternal infection. Our findings also suggest a breach of feto-placental tolerance, which relies on suppression of uterine and placental immune cells to ensure an inflammation-free environment for the developing fetus.

This study further explains the interconnected nature of hormonal and cytokine signaling during pregnancy and the unique predicament of maternal tolerance during respiratory viral infection. Recent work has shown that immunosuppression in the lungs during pregnancy creates an ideal environment for adaptation of influenza viruses to more virulent strains [81]. Thus, understanding how pregnancy hormones modulate immune responses to influenza virus infection is not just necessary for developing clinical interventions for a high-risk population but also as part of a global strategy to reduce the incidence of highly pathogenic influenza viruses with pandemic potential. Pregnant women are a target population for improving vaccination efficacy in order to reduce their risk of pregnancy complications due to infection and to increase protective strength of passive immunity to their offspring [96, 97]. We demonstrate that increased progesterone

expression required to support pregnancy results in an immunosuppressive lung environment and that pregnancy increases susceptibility to prostaglandin-induced inflammation as a result of infection. These conclusions are important for understanding respiratory viral pathogenesis in a pregnant mother.

Materials and Methods

Cells and virus stocks. Madin-Darby canine kidney (MDCK) cells (ATCC CCL 34, American Type Culture Collection, Manassas, VA) were maintained in Dulbecco's Modified Eagle's Medium (DMEM) (Mediatech, Herndon, VA) containing 10% fetal bovine serum (Hyclone, Thermo Scientific, Rockford, IL). A/Brisbane/59/07 (H1N1) virus stock was propagated in MDCK cells. The hemagglutination (HA) activity was determined using turkey blood cells (LAMPIRE Biological Laboratories, Pipersville, PA) [98]. The mouse-adapted A/Brisbane/59/07 (H1N1) strain was obtained by serially passaging the virus in lungs of BALB/c mice. The LD₅₀ was determined by Reed-Munch formula [99] and the viral titers were determined by plaque assay [100]; 2xLD₅₀ mouse-adapted virus is approximately 155 plaque forming units (p.f.u) per infection.

Animals. 8-week-old female BALB/c mice (Harlan Laboratories, Dublin, VA) were bred and housed in a biosafety level 1 facility for breeding; infections were conducted in a biosafety level 2 at Emory University Whitehead animal facility. All animal studies were approved by the IACUC at Emory University.

Protocol for timed pregnancies. The mouse estrous cycle is divided into four stages: estrous, metestrous, diestrous, and proestrous. Each stage can be determined by visual examination of vaginal opening [101]. Tagged female mice were used for breeding. Cages were set up with three to four female mice in proestrous or estrus and one a male for 3 days [102]. Females were monitored for the presence of a copulation plug, indicative of mating and body weight changes were monitored daily. In uninfected BALB/c pregnant mice, gestation lasts approximately 21 days,

and pregnancy can be determined when mice gain 20% of their initial body weight. Pregnant mice were placed in separate cages, two females per cage, and the remaining mice were mated again.

Animal infection with seasonal influenza virus and sample collection. Pregnant females that had noticeable body weight increases (in the range of 20-25%) of their initial bodyweights between days 12-14 after mating were infected with 2xLD₅₀ mouse-adapted A/Brisbane/59/07 (dose calculated for non-pregnant, healthy 8-week-old female mice). Intranasal infections were performed under light isoflurane anesthetization, and euthanasia was performed via CO₂ asphyxiation. Severity of infection, completion of gestation, and health outcome of offspring (i.e. healthy, small for gestational age, or stillborn) were all closely monitored and compared to uninfected pregnant mice.

In another cohort of mice, sera, lungs, placenta, and fetuses were collected 4 d.p.i. in order to assess viral presence and extend of inflammation in various compartments, host innate immune responses, and hormone expression. Serum was stored at -20°C in the presence of Halt Protease Inhibitor (Thermo Fisher) until further use.

PCR. Lung and placental lysates were harvested from infected and uninfected pregnant mice and homogenized, filtered through 70µm filters and stored in 1x DMEM, 1x Halt Protease Inhibitor and/or RNase Later (Ambion). Viral RNA was isolated using a QIAamp Viral RNA Mini Kit (Qiagen) and probed for the presence of H1N1 HA and M genes via qPCR. Viral RNA was converted to cDNA iTaq Universal SYBR Green Supermix (Bio-Rad) and amplified using 3 nmol of commercially available or synthesized primers in a CFX96 Real-Time PCR Detection System (Bio-Rad). PCR mixtures were heated at 50°C for 10 minutes to convert RNA to cDNA, 95°C for

1 minute, and cycled 40x (95°C for 10 seconds, annealing temperatures were varied dependent on primer melting curve for 15 seconds, and 72°C for 30 seconds). A melting curve from 65°C to 95°C was performed to assess quality of primer binding. H1 HA was amplified using Influenza A Virus H1 Primers (BEI Resources, NR-12316, with an annealing temperature of 61°C. H1 M was amplified using synthesized primers (FLUAM-1F: AAGACCAATCCTGTCACCTCTGA; FLUAM-1R: CAAAGCGTCTACGCTGCAGTCC; Operon) with an annealing temperature of 61°C, and mouse GAPDH (realtimeprimers.com, VMPS-7317) with an annealing temperature of 50°C [103]. Analysis of threshold values and normalization to GAPDH were performed in CFX Manager Software (Bio-Rad). PCR products were electrophoresed on a 1% agarose/TAE gel and imaged using ethidium bromide.

Plaque Assays. Viral titers in the lung tissue samples were quantified via plaque assay in MDCK cells as described previously [104]. Viral titers were assessed per gram of tissue.

Determination of hormone levels. Progesterone, prostaglandin F₂ α (PGF₂ α) and prostaglandin E₂ (PGE₂) were quantified via ELISA kits from ALPCO (Salem, NH). Experimental values for lungs and placentas were normalized by the mass of the tissue and the volume in which samples were homogenized.

Cytokine Expression. For cytokine expression, a 23-plex Luminex assay from Bio-Rad (Hercules, CA) was used. Experimental values for lungs, placentas, and fetuses were normalized by volume and mass of the tissues. Fold changes were expressed relative to uninfected controls. A

heat map was constructed to visualize fold changes within the tissues in pregnant and non-pregnant mice.

MMP, COX-2, and PIBF quantification in tissue lysates. Molecular analysis of protein expression was performed on 5 mg of placental tissue lysate via Western blot. Purified anti-murine MMP-9 (BioLegend 819701, 1:500) and anti-murine MMP-2 (BioLegend 680002, 1:500) were used to detect degradative proteins and secondary antibodies (goat anti-mouse, 1:10,000). Rabbit anti-murine COX-2 (Abcam, ab52237) and rabbit anti-murine C13orf24 (PIBF) (Abcam, ab156267) were used to detect markers for oxidative and hormonal stress in the lungs and placenta, and goat anti-rabbit (1:10,000) antibodies were used as secondary antibodies. Rabbit anti-murine β -actin (1:2000) was used as a loading control with secondary antibodies (goat anti-rabbit, 1:10,000). Blots were developed with Super Signal Femto Maximum Sensitivity Substrate (Thermo Scientific 34096) and imaged using a Bio-Rad ChemiDoc Touch. Volume intensity of MMP-2 and MMP-9 was normalized to β -actin loading controls. A two-way ANOVA analyzing factors of protein maturation ($p < 0.0001$, ***) and infection ($P < 0.0296$, *) was performed in GraphPad Prism 5.

Histology. Placentas were isolated 4 d.p.i. (day 16 of gestation) and submerged in histology cassettes in 4% paraformaldehyde overnight at 4°C. Tissues were embedded in paraffin, sectioned in 4 μ m, and fixed to glass microscopy slides. Hematoxylin and eosin staining was performed by Yerkes National Primate Research Center Pathology Core, and slides were imaged on a Zeiss Akioskop with SpotFlex 15.2 camera with Spot Advanced 4.7 software. Pathology scores were determined by randomizing histology slides prior to imaging and blindly scoring the incidence of

exposed fetal endothelial nuclei (FEN), degradation in the spongiotrophoblast layer, and fibrinoid necrosis (FN).

Statistics. All statistical analysis used a student's t-test, linear regression, or one-way ANOVA using GraphPad Prism statistical software with a significance level (α) of 0.05.

Ethics statement. Emory University Division of Animal Resources veterinary staff ascertained welfare of animals in addition to research scientists, and DAR staff performed regular care and wellness assessments. Animal work was conducted according to Emory University Institutional Animal Care and Use Committee (IACUC) guidelines according to an approved protocol (DAR2002950-122617BN) in accordance with the United States federal Animal Welfare Act (PL 89-544) and subsequent amendments. Emory University is registered with the United States Department of Agriculture (57-R-003) and has filed an Assurance of Compliance statement with the Office of Laboratory Animal Welfare of the National Institutes of Health (D16-00113). Emory University has been fully and continuously accredited by AAALAC International since 1992 (Unit 000781). The Georgia Fee-Exempt Wild Animal Permit Customer Number for animals maintained by the Division of Animal Resources is 22257.

Accession Numbers. The sequence for each genomic segment of the mouse-adapted virus used in this study may be found at NCBI GenBank MG460793 (HA), MG460794 (M1), MG460795 (NA), MG460796 (NP), MG460797 (NS1), MG460798 (PA), MG460799 (PB1), MG460800 (PB2).

Acknowledgements

Special thanks to David Lee at the Immunological Core at the Yerkes National Primate Center for assistance in Luminex Assays, Ben Isett at the Emory Integrated Genomics Core and Gaurav Kumar at the Emory Integrated Computing Core for sequencing and analysis of mouse adapted viral genomes, Dahnide T. Williams for her lab managerial support, and Nadia Lelutiu for critical reading of this manuscript.

References

1. Omer SB, Bednarczyk R, Madhi SA, Klugman KP. Benefits to mother and child of influenza vaccination during pregnancy. *Hum Vaccin Immunother.* 2012;8(1):130-7. Epub 2012/01/19. doi: 10.4161/hv.8.1.18601. PubMed PMID: 22251998.
2. Periolo N, Avaro M, Czech A, Russo M, Benedetti E, Pontoriero A, et al. Pregnant women infected with pandemic influenza A(H1N1)pdm09 virus showed differential immune response correlated with disease severity. *J Clin Virol.* 2015;64:52-8. doi: 10.1016/j.jcv.2015.01.009. PubMed PMID: 25728079.
3. Cox S, Posner SF, McPheeters M, Jamieson DJ, Kourtis AP, Meikle S. Influenza and pregnant women: hospitalization burden, United States, 1998-2002. *J Womens Health (Larchmt).* 2006;15(8):891-3. doi: 10.1089/jwh.2006.15.891. PubMed PMID: 17087611.
4. Cox S, Posner SF, McPheeters M, Jamieson DJ, Kourtis AP, Meikle S. Hospitalizations with respiratory illness among pregnant women during influenza season. *Obstet Gynecol.* 2006;107(6):1315-22. doi: 10.1097/01.AOG.0000218702.92005.bb. PubMed PMID: 16738158.
5. Yudin MH. Risk management of seasonal influenza during pregnancy: current perspectives. *Int J Womens Health.* 2014;6:681-9. doi: 10.2147/IJWH.S47235. PubMed PMID: 25114593; PubMed Central PMCID: PMC4122531.
6. Rasmussen SA, Jamieson DJ, Uyeki TM. Effects of influenza on pregnant women and infants. *Am J Obstet Gynecol.* 2012;207(3 Suppl):S3-8. doi: 10.1016/j.ajog.2012.06.068. PubMed PMID: 22920056.

7. Raj RS, Bonney EA, Phillippe M. Influenza, immune system, and pregnancy. *Reprod Sci.* 2014;21(12):1434-51. doi: 10.1177/1933719114537720. PubMed PMID: 24899469; PubMed Central PMCID: PMC4231130.
8. Lai PL, Panatto D, Ansaldi F, Canepa P, Amicizia D, Patria AG, et al. Burden of the 1999-2008 seasonal influenza epidemics in Italy: comparison with the H1N1v (A/California/07/09) pandemic. *Human vaccines.* 2011;7 Suppl:217-25. PubMed PMID: 21922688.
9. CDC. Estimates of Deaths Associated with Seasonal Influenza --- United States, 1976--2007. Atlanta, GA: 2010.
10. Siston AM, Rasmussen SA, Honein MA, Fry AM, Seib K, Callaghan WM, et al. Pandemic 2009 influenza A(H1N1) virus illness among pregnant women in the United States. *JAMA : the journal of the American Medical Association.* 2010;303(15):1517-25. doi: 10.1001/jama.2010.479. PubMed PMID: 20407061.
11. Hartel C, Humberg A, Viemann D, Stein A, Orlikowsky T, Rupp J, et al. Preterm Birth during Influenza Season Is Associated with Adverse Outcome in Very Low Birth Weight Infants. *Front Pediatr.* 2016;4:130. doi: 10.3389/fped.2016.00130. PubMed PMID: 27965950; PubMed Central PMCID: PMC45129678.
12. Brown AS, Derkits EJ. Prenatal infection and schizophrenia: a review of epidemiologic and translational studies. *Am J Psychiatry.* 2010;167(3):261-80. doi: 10.1176/appi.ajp.2009.09030361. PubMed PMID: 20123911; PubMed Central PMCID: PMC3652286.

13. Solano ME, Jago C, Pincus MK, Arck PC. Highway to health; or How prenatal factors determine disease risks in the later life of the offspring. *J Reprod Immunol.* 2011;90(1):3-8. doi: 10.1016/j.jri.2011.01.023. PubMed PMID: 21641655.
14. Memoli MJ, Harvey H, Morens DM, Taubenberger JK. Influenza in pregnancy. *Influenza Other Respi Viruses.* 2012. Epub 2012/11/23. doi: 10.1111/irv.12055. PubMed PMID: 23170853.
15. Kay AW, Blish CA. Immunogenicity and Clinical Efficacy of Influenza Vaccination in Pregnancy. *Front Immunol.* 2015;6:289. doi: 10.3389/fimmu.2015.00289. PubMed PMID: 26089824; PubMed Central PMCID: PMC4455389.
16. Cunningham AF, Khan M, Ball J, Toellner KM, Serre K, Mohr E, et al. Responses to the soluble flagellar protein FliC are Th2, while those to FliC on Salmonella are Th1. *Eur J Immunol.* 2004;34(11):2986-95. Epub 2004/09/24. doi: 10.1002/eji.200425403. PubMed PMID: 15384042.
17. Klein SL, Hodgson A, Robinson DP. Mechanisms of sex disparities in influenza pathogenesis. *J Leukoc Biol.* 2012;92(1):67-73. doi: 10.1189/jlb.0811427. PubMed PMID: 22131346; PubMed Central PMCID: PMC4046247.
18. Pazos MA, Kraus TA, Munoz-Fontela C, Moran TM. Estrogen mediates innate and adaptive immune alterations to influenza infection in pregnant mice. *PLoS One.* 2012;7(7):e40502. doi: 10.1371/journal.pone.0040502. PubMed PMID: 22792357; PubMed Central PMCID: PMC3390370.
19. Robinson DP, Klein SL. Pregnancy and pregnancy-associated hormones alter immune responses and disease pathogenesis. *Horm Behav.* 2012;62(3):263-71. doi:

- 10.1016/j.yhbeh.2012.02.023. PubMed PMID: 22406114; PubMed Central PMCID: PMC3376705.
20. Kourtis AP, Read JS, Jamieson DJ. Pregnancy and infection. *N Engl J Med*. 2014;370(23):2211-8. doi: 10.1056/NEJMra1213566. PubMed PMID: 24897084; PubMed Central PMCID: PMC4459512.
 21. Takeda S, Hisano M, Komano J, Yamamoto H, Sago H, Yamaguchi K. Influenza vaccination during pregnancy and its usefulness to mothers and their young infants. *J Infect Chemother*. 2015;21(4):238-46. doi: 10.1016/j.jiac.2015.01.015. PubMed PMID: 25708925.
 22. Germain SJ, Sacks GP, Sooranna SR, Sargent IL, Redman CW. Systemic inflammatory priming in normal pregnancy and preeclampsia: the role of circulating syncytiotrophoblast microparticles. *Journal of immunology*. 2007;178(9):5949-56. PubMed PMID: 17442979.
 23. Kraus TA, Sperling RS, Engel SM, Lo Y, Kellerman L, Singh T, et al. Peripheral blood cytokine profiling during pregnancy and post-partum periods. *Am J Reprod Immunol*. 2010;64(6):411-26. doi: 10.1111/j.1600-0897.2010.00889.x. PubMed PMID: 20712812.
 24. PrabhuDas M, Bonney E, Caron K, Dey S, Erlebacher A, Fazleabas A, et al. Immune mechanisms at the maternal-fetal interface: perspectives and challenges. *Nature immunology*. 2015;16(4):328-34. doi: 10.1038/ni.3131. PubMed PMID: 25789673; PubMed Central PMCID: PMCPMC5070970.
 25. Chan KH, Zhang AJ, To KK, Chan CC, Poon VK, Guo K, et al. Wild type and mutant 2009 pandemic influenza A (H1N1) viruses cause more severe disease and higher mortality in pregnant BALB/c mice. *PLoS One*. 2010;5(10):e13757. doi:

- 10.1371/journal.pone.0013757. PubMed PMID: 21060798; PubMed Central PMCID: PMC2966430.
26. Marcelin G, Aldridge JR, Duan S, Ghoneim HE, Rehg J, Marjuki H, et al. Fatal outcome of pandemic H1N1 2009 influenza virus infection is associated with immunopathology and impaired lung repair, not enhanced viral burden, in pregnant mice. *J Virol*. 2011;85(21):11208-19. doi: 10.1128/JVI.00654-11. PubMed PMID: 21865394; PubMed Central PMCID: PMC3194964.
 27. Kim HM, Kang YM, Song BM, Kim HS, Seo SH. The 2009 pandemic H1N1 influenza virus is more pathogenic in pregnant mice than seasonal H1N1 influenza virus. *Viral Immunol*. 2012;25(5):402-10. doi: 10.1089/vim.2012.0007. PubMed PMID: 22985287.
 28. Martin A, Cox S, Jamieson DJ, Whiteman MK, Kulkarni A, Tepper NK. Respiratory illness hospitalizations among pregnant women during influenza season, 1998-2008. *Maternal and child health journal*. 2013;17(7):1325-31. doi: 10.1007/s10995-012-1135-3. PubMed PMID: 23001819.
 29. Kanmaz HG, Erdeve O, Oguz SS, Uras N, Celen S, Korukluoglu G, et al. Placental transmission of novel pandemic influenza A virus. *Fetal Pediatr Pathol*. 2011;30(5):280-5. doi: 10.3109/15513815.2011.572956. PubMed PMID: 21612336.
 30. Cetinkaya M, Ozkan H, Celebi S, Koksall N, Hacimustafaoglu M. Human 2009 influenza A (H1N1) virus infection in a premature infant born to an H1N1-infected mother: placental transmission? *Turk J Pediatr*. 2011;53(4):441-4. PubMed PMID: 21980848.
 31. Komine-Aizawa S, Suzuki A, Trinh QD, Izumi Y, Shibata T, Kuroda K, et al. H1N1/09 influenza A virus infection of immortalized first trimester human trophoblast cell lines.

- Am J Reprod Immunol. 2012;68(3):226-32. doi: 10.1111/j.1600-0897.2012.01172.x.
PubMed PMID: 22762384.
32. Gu J, Xie Z, Gao Z, Liu J, Korteweg C, Ye J, et al. H5N1 infection of the respiratory tract and beyond: a molecular pathology study. *Lancet*. 2007;370(9593):1137-45. doi: 10.1016/S0140-6736(07)61515-3. PubMed PMID: 17905166.
33. Nicholls JM, Bourne AJ, Chen H, Guan Y, Peiris JS. Sialic acid receptor detection in the human respiratory tract: evidence for widespread distribution of potential binding sites for human and avian influenza viruses. *Respir Res*. 2007;8:73. doi: 10.1186/1465-9921-8-73. PubMed PMID: 17961210; PubMed Central PMCID: PMCPMC2169242.
34. Arck P, Hansen PJ, Mulac Jericevic B, Piccinni MP, Szekeres-Bartho J. Progesterone during pregnancy: endocrine-immune cross talk in mammalian species and the role of stress. *Am J Reprod Immunol*. 2007;58(3):268-79. doi: 10.1111/j.1600-0897.2007.00512.x. PubMed PMID: 17681043.
35. Lissauer D, Eldershaw SA, Inman CF, Coomarasamy A, Moss PA, Kilby MD. Progesterone promotes maternal-fetal tolerance by reducing human maternal T-cell polyfunctionality and inducing a specific cytokine profile. *Eur J Immunol*. 2015;45(10):2858-72. doi: 10.1002/eji.201445404. PubMed PMID: 26249148.
36. Kalinski P. Regulation of immune responses by prostaglandin E2. *J Immunol*. 2012;188(1):21-8. doi: 10.4049/jimmunol.1101029. PubMed PMID: 22187483; PubMed Central PMCID: PMCPMC3249979.
37. Choi GB, Yim YS, Wong H, Kim S, Kim H, Kim SV, et al. The maternal interleukin-17a pathway in mice promotes autism-like phenotypes in offspring. *Science*.

- 2016;351(6276):933-9. doi: 10.1126/science.aad0314. PubMed PMID: 26822608; PubMed Central PMCID: PMC4782964.
38. LoMauro A, Aliverti A. Respiratory physiology of pregnancy: Physiology masterclass. *Breathe (Sheff)*. 2015;11(4):297-301. doi: 10.1183/20734735.008615. PubMed PMID: 27066123; PubMed Central PMCID: PMC4818213.
39. Serhan CN, Levy B. Success of prostaglandin E2 in structure-function is a challenge for structure-based therapeutics. *Proceedings of the National Academy of Sciences of the United States of America*. 2003;100(15):8609-11. doi: 10.1073/pnas.1733589100. PubMed PMID: 12861081; PubMed Central PMCID: PMC166355.
40. Cheng SE, Lee IT, Lin CC, Wu WL, Hsiao LD, Yang CM. ATP mediates NADPH oxidase/ROS generation and COX-2/PGE2 expression in A549 cells: role of P2 receptor-dependent STAT3 activation. *PloS one*. 2013;8(1):e54125. doi: 10.1371/journal.pone.0054125. PubMed PMID: 23326583; PubMed Central PMCID: PMC3543320.
41. Cuthbert MF. *Clinical Effects of the Prostaglandins on the Respiratory System*. F. Bertin BSaGPV, editor: Springer; 1977. 179-90 p.
42. Mizumura K, Hashimoto S, Maruoka S, Gon Y, Kitamura N, Matsumoto K, et al. Role of mitogen-activated protein kinases in influenza virus induction of prostaglandin E2 from arachidonic acid in bronchial epithelial cells. *Clin Exp Allergy*. 2003;33(9):1244-51. PubMed PMID: 12956746.
43. Soehnlein O, Weber C, Lindbom L. Neutrophil granule proteins tune monocytic cell function. *Trends Immunol*. 2009;30(11):538-46. doi: 10.1016/j.it.2009.06.006. PubMed PMID: 19699683.

44. Schmitz N, Kurrer M, Bachmann MF, Kopf M. Interleukin-1 is responsible for acute lung immunopathology but increases survival of respiratory influenza virus infection. *J Virol.* 2005;79(10):6441-8. doi: 10.1128/JVI.79.10.6441-6448.2005. PubMed PMID: 15858027; PubMed Central PMCID: PMCPMC1091664.
45. Menten P, Wuyts A, Van Damme J. Macrophage inflammatory protein-1. *Cytokine Growth Factor Rev.* 2002;13(6):455-81. PubMed PMID: 12401480.
46. Williams TJ, Peck MJ. Role of prostaglandin-mediated vasodilatation in inflammation. *Nature.* 1977;270(5637):530-2. PubMed PMID: 593374.
47. Raud J, Dahlen SE, Sydbom A, Lindbom L, Hedqvist P. Enhancement of acute allergic inflammation by indomethacin is reversed by prostaglandin E2: apparent correlation with in vivo modulation of mediator release. *Proceedings of the National Academy of Sciences of the United States of America.* 1988;85(7):2315-9. PubMed PMID: 2451246; PubMed Central PMCID: PMCPMC279982.
48. O'Byrne PM. *Asthma and COPD: Basic Mechanisms and Clinical Management.* Barnes PJ, Drazen, J.M., Rennard, S.I. and Thomson, N.C., editor. London, UK: Academic Press; 2002.
49. Kirkwood JM, Butterfield LH, Tarhini AA, Zarour H, Kalinski P, Ferrone S. Immunotherapy of cancer in 2012. *CA Cancer J Clin.* 2012;62(5):309-35. doi: 10.3322/caac.20132. PubMed PMID: 22576456; PubMed Central PMCID: PMC3445708.
50. Kota SK, Gayatri K, Jammula S, Kota SK, Krishna SV, Meher LK, et al. Endocrinology of parturition. *Indian J Endocrinol Metab.* 2013;17(1):50-9. doi: 10.4103/2230-8210.107841. PubMed PMID: 23776853; PubMed Central PMCID: PMCPMC3659907.

51. Szekeres-Bartho J, Polgar B. PIBF: the double edged sword. Pregnancy and tumor. *Am J Reprod Immunol.* 2010;64(2):77-86. doi: 10.1111/j.1600-0897.2010.00833.x. PubMed PMID: 20367622.
52. Arck PC, Hecher K. Fetomaternal immune cross-talk and its consequences for maternal and offspring's health. *Nat Med.* 2013;19(5):548-56. doi: 10.1038/nm.3160. PubMed PMID: 23652115.
53. Beatty PR, Puerta-Guardo H, Killingbeck SS, Glasner DR, Hopkins K, Harris E. Dengue virus NS1 triggers endothelial permeability and vascular leak that is prevented by NS1 vaccination. *Sci Transl Med.* 2015;7(304):304ra141. doi: 10.1126/scitranslmed.aaa3787. PubMed PMID: 26355030.
54. Montuschi P, Kharitonov SA, Ciabattini G, Barnes PJ. Exhaled leukotrienes and prostaglandins in COPD. *Thorax.* 2003;58(7):585-8. PubMed PMID: 12832671; PubMed Central PMCID: PMC1746732.
55. Rossant J, Cross JC. Placental development: lessons from mouse mutants. *Nat Rev Genet.* 2001;2(7):538-48. doi: 10.1038/35080570. PubMed PMID: 11433360.
56. John RM. Epigenetic regulation of placental endocrine lineages and complications of pregnancy. *Biochem Soc Trans.* 2013;41(3):701-9. doi: 10.1042/BST20130002. PubMed PMID: 23697929.
57. Lockwood CJ, Basar M, Kayisli UA, Guzeloglu-Kayisli O, Murk W, Wang J, et al. Interferon-gamma protects first-trimester decidual cells against aberrant matrix metalloproteinases 1, 3, and 9 expression in preeclampsia. *Am J Pathol.* 2014;184(9):2549-59. doi: 10.1016/j.ajpath.2014.05.025. PubMed PMID: 25065683; PubMed Central PMCID: PMC4188280.

58. Meijer WJ, Wensing AM, Bruinse HW, Nikkels PG. High rate of chronic villitis in placentas of pregnancies complicated by influenza A/H1N1 infection. *Infect Dis Obstet Gynecol.* 2014;2014:768380. doi: 10.1155/2014/768380. PubMed PMID: 24693211; PubMed Central PMCID: PMCPMC3947755.
59. Yamashita K, Yoshioka Y, Higashisaka K, Mimura K, Morishita Y, Nozaki M, et al. Silica and titanium dioxide nanoparticles cause pregnancy complications in mice. *Nat Nanotechnol.* 2011;6(5):321-8. doi: 10.1038/nnano.2011.41. PubMed PMID: 21460826.
60. Vincent ZL, Mitchell MD, Ponnampalam AP. Regulation of MT1-MMP/MMP-2/TIMP-2 axis in human placenta. *J Inflamm Res.* 2015;8:193-200. doi: 10.2147/JIR.S88039. PubMed PMID: 26491367; PubMed Central PMCID: PMCPMC4599070.
61. Mittal R, Patel AP, Debs LH, Nguyen D, Patel K, Grati M, et al. Intricate Functions of Matrix Metalloproteinases in Physiological and Pathological Conditions. *J Cell Physiol.* 2016;231(12):2599-621. doi: 10.1002/jcp.25430. PubMed PMID: 27187048.
62. Majali-Martinez A, Hiden U, Ghaffari-Tabrizi-Wizsy N, Lang U, Desoye G, Dieber-Rotheneder M. Placental membrane-type metalloproteinases (MT-MMPs): Key players in pregnancy. *Cell Adh Migr.* 2016;10(1-2):136-46. doi: 10.1080/19336918.2015.1110671. PubMed PMID: 26745344; PubMed Central PMCID: PMCPMC4853033.
63. Li W, Mata KM, Mazzuca MQ, Khalil RA. Altered matrix metalloproteinase-2 and -9 expression/activity links placental ischemia and anti-angiogenic sFlt-1 to uteroplacental and vascular remodeling and collagen deposition in hypertensive pregnancy. *Biochem Pharmacol.* 2014;89(3):370-85. doi: 10.1016/j.bcp.2014.03.017. PubMed PMID: 24704473; PubMed Central PMCID: PMCPMC4034157.

64. Zhu J, Zhong M, Pang Z, Yu Y. Dysregulated expression of matrix metalloproteinases and their inhibitors may participate in the pathogenesis of pre-eclampsia and fetal growth restriction. *Early Hum Dev.* 2014;90(10):657-64. doi: 10.1016/j.earlhumdev.2014.08.007. PubMed PMID: 25194834.
65. Flores-Pliego A, Espejel-Nunez A, Castillo-Castrejon M, Meraz-Cruz N, Beltran-Montoya J, Zaga-Clavellina V, et al. Matrix Metalloproteinase-3 (MMP-3) Is an Endogenous Activator of the MMP-9 Secreted by Placental Leukocytes: Implication in Human Labor. *PLoS One.* 2015;10(12):e0145366. doi: 10.1371/journal.pone.0145366. PubMed PMID: 26713439; PubMed Central PMCID: PMC4699849.
66. Tian FJ, Cheng YX, Li XC, Wang F, Qin CM, Ma XL, et al. The YY1/MMP2 axis promotes trophoblast invasion at the maternal-fetal interface. *J Pathol.* 2016;239(1):36-47. doi: 10.1002/path.4694. PubMed PMID: 27071480.
67. Mauris J, Woodward AM, Cao Z, Panjwani N, Argueso P. Molecular basis for MMP9 induction and disruption of epithelial cell-cell contacts by galectin-3. *J Cell Sci.* 2014;127(Pt 14):3141-8. doi: 10.1242/jcs.148510. PubMed PMID: 24829150; PubMed Central PMCID: PMC4095856.
68. Hong JM, Kwon OK, Shin IS, Song HH, Shin NR, Jeon CM, et al. Anti-inflammatory activities of *Physalis alkekengi* var. *franchetii* extract through the inhibition of MMP-9 and AP-1 activation. *Immunobiology.* 2015;220(1):1-9. doi: 10.1016/j.imbio.2014.10.004. PubMed PMID: 25454812.
69. Carey MA, Bradbury JA, Seubert JM, Langenbach R, Zeldin DC, Germolec DR. Contrasting effects of cyclooxygenase-1 (COX-1) and COX-2 deficiency on the host

- response to influenza A viral infection. *Journal of immunology*. 2005;175(10):6878-84.
PubMed PMID: 16272346.
70. Raghupathy R, Al-Mutawa E, Al-Azemi M, Makhseed M, Azizieh F, Szekeres-Bartho J. Progesterone-induced blocking factor (PIBF) modulates cytokine production by lymphocytes from women with recurrent miscarriage or preterm delivery. *Journal of reproductive immunology*. 2009;80(1-2):91-9. doi: 10.1016/j.jri.2009.01.004. PubMed PMID: 19371956.
71. Szekeres-Bartho J, Wegmann TG. A progesterone-dependent immunomodulatory protein alters the Th1/Th2 balance. *J Reprod Immunol*. 1996;31(1-2):81-95. Epub 1996/08/01. PubMed PMID: 8887124.
72. Faust Z, Laskarin G, Rukavina D, Szekeres-Bartho J. Progesterone-induced blocking factor inhibits degranulation of natural killer cells. *Am J Reprod Immunol*. 1999;42(2):71-5. PubMed PMID: 10476687.
73. Szekeres-Bartho J, Faust Z, Varga P, Szereday L, Kelemen K. The immunological pregnancy protective effect of progesterone is manifested via controlling cytokine production. *Am J Reprod Immunol*. 1996;35(4):348-51. Epub 1996/04/01. PubMed PMID: 8739452.
74. Charpigny G, Reinaud P, Creminon C, Tamby JP. Correlation of increased concentration of ovine endometrial cyclooxygenase 2 with the increase in PGE2 and PGD2 in the late luteal phase. *J Reprod Fertil*. 1999;117(2):315-24. PubMed PMID: 10690199.
75. Kim JC, Kim HM, Kang YM, Ku KB, Park EH, Yum J, et al. Severe pathogenesis of influenza B virus in pregnant mice. *Virology*. 2014;448:74-81. doi: 10.1016/j.virol.2013.10.001. PubMed PMID: 24314638.

76. Klein SL, Passaretti C, Anker M, Olukoya P, Pekosz A. The impact of sex, gender and pregnancy on 2009 H1N1 disease. *Biology of sex differences*. 2010;1(1):5. doi: 10.1186/2042-6410-1-5. PubMed PMID: 21208468; PubMed Central PMCID: PMC3010100.
77. Robinson DP, Lorenzo ME, Jian W, Klein SL. Elevated 17beta-estradiol protects females from influenza A virus pathogenesis by suppressing inflammatory responses. *PLoS Pathog*. 2011;7(7):e1002149. doi: 10.1371/journal.ppat.1002149. PubMed PMID: 21829352; PubMed Central PMCID: PMC3145801.
78. Pazos M, Sperling RS, Moran TM, Kraus TA. The influence of pregnancy on systemic immunity. *Immunol Res*. 2012;54(1-3):254-61. doi: 10.1007/s12026-012-8303-9. PubMed PMID: 22447351.
79. Jamieson DJ, Theiler RN, Rasmussen SA. Emerging infections and pregnancy. *Emerg Infect Dis*. 2006;12(11):1638-43. Epub 2007/02/08. doi: 10.3201/eid1211.060152. PubMed PMID: 17283611; PubMed Central PMCID: PMC3372330.
80. Chan JF, To KK, Tse H, Lau CC, Li IW, Hung IF, et al. The lower serum immunoglobulin G2 level in severe cases than in mild cases of pandemic H1N1 2009 influenza is associated with cytokine dysregulation. *Clin Vaccine Immunol*. 2011;18(2):305-10. doi: 10.1128/CVI.00363-10. PubMed PMID: 21123524; PubMed Central PMCID: PMC3067346.
81. Engels G, Hierweger AM, Hoffmann J, Thieme R, Thiele S, Bertram S, et al. Pregnancy-Related Immune Adaptation Promotes the Emergence of Highly Virulent H1N1 Influenza Virus Strains in Allogeneically Pregnant Mice. *Cell host & microbe*. 2017;21(3):321-33. doi: 10.1016/j.chom.2017.02.020. PubMed PMID: 28279344.

82. Schmidt A, Morales-Prieto DM, Pastuschek J, Frohlich K, Markert UR. Only humans have human placentas: molecular differences between mice and humans. *J Reprod Immunol.* 2015;108:65-71. doi: 10.1016/j.jri.2015.03.001. PubMed PMID: 25817465.
83. Krishnan L, Nguyen T, McComb S. From mice to women: the conundrum of immunity to infection during pregnancy. *Journal of reproductive immunology.* 2013;97(1):62-73. doi: 10.1016/j.jri.2012.10.015. PubMed PMID: 23432873; PubMed Central PMCID: PMC3748615.
84. Malassine A, Frenzo JL, Evain-Brion D. A comparison of placental development and endocrine functions between the human and mouse model. *Hum Reprod Update.* 2003;9(6):531-9. PubMed PMID: 14714590.
85. Lei K, Chen L, Georgiou EX, Sooranna SR, Khanjani S, Brosens JJ, et al. Progesterone acts via the nuclear glucocorticoid receptor to suppress IL-1beta-induced COX-2 expression in human term myometrial cells. *PloS one.* 2012;7(11):e50167. doi: 10.1371/journal.pone.0050167. PubMed PMID: 23209664; PubMed Central PMCID: PMC3509141.
86. Hardy DB, Janowski BA, Corey DR, Mendelson CR. Progesterone receptor plays a major antiinflammatory role in human myometrial cells by antagonism of nuclear factor-kappaB activation of cyclooxygenase 2 expression. *Mol Endocrinol.* 2006;20(11):2724-33. doi: 10.1210/me.2006-0112. PubMed PMID: 16772530.
87. Hall OJ, Limjunyawong N, Vermillion MS, Robinson DP, Wohlgenuth N, Pekosz A, et al. Progesterone-Based Therapy Protects Against Influenza by Promoting Lung Repair and Recovery in Females. *PLoS pathogens.* 2016;12(9):e1005840. doi:

- 10.1371/journal.ppat.1005840. PubMed PMID: 27631986; PubMed Central PMCID: PMC5025002.
88. Hall OJ, Nachbagauer R, Vermillion MS, Fink AL, Phuong V, Krammer F, et al. Progesterone-Based Contraceptives Reduce Adaptive Immune Responses and Protection against Sequential Influenza A Virus Infections. *J Virol*. 2017;91(8). doi: 10.1128/JVI.02160-16. PubMed PMID: 28179523; PubMed Central PMCID: PMC5375688.
89. Lee MY, Cheung CY, Peiris JS. Role of cyclooxygenase-2 in H5N1 viral pathogenesis and the potential use of its inhibitors. *Hong Kong Med J*. 2013;19 Suppl 4:29-35. PubMed PMID: 23775184.
90. Lee SM, Gai WW, Cheung TK, Peiris JS. Antiviral effect of a selective COX-2 inhibitor on H5N1 infection in vitro. *Antiviral Res*. 2011;91(3):330-4. doi: 10.1016/j.antiviral.2011.07.011. PubMed PMID: 21798291.
91. Xu L, Bao L, Deng W, Qin C. Highly pathogenic avian influenza H5N1 virus could partly be evacuated by pregnant BALB/c mouse during abortion or preterm delivery. *Virology journal*. 2011;8:342. doi: 10.1186/1743-422X-8-342. PubMed PMID: 21740553; PubMed Central PMCID: PMC3148567.
92. Lei H, Furth EE, Kalluri R, Chiou T, Tilly KI, Tilly JL, et al. A program of cell death and extracellular matrix degradation is activated in the amnion before the onset of labor. *J Clin Invest*. 1996;98(9):1971-8. doi: 10.1172/JCI119001. PubMed PMID: 8903315; PubMed Central PMCID: PMC507640.

93. Brown AS. Exposure to prenatal infection and risk of schizophrenia. *Front Psychiatry*. 2011;2:63. doi: 10.3389/fpsy.2011.00063. PubMed PMID: 22131978; PubMed Central PMCID: PMC3222883.
94. Khandaker GM, Zimbron J, Lewis G, Jones PB. Prenatal maternal infection, neurodevelopment and adult schizophrenia: a systematic review of population-based studies. *Psychol Med*. 2013;43(2):239-57. doi: 10.1017/S0033291712000736. PubMed PMID: 22717193; PubMed Central PMCID: PMC3479084.
95. Robinson DP, Hall OJ, Nilles TL, Bream JH, Klein SL. 17beta-estradiol protects females against influenza by recruiting neutrophils and increasing virus-specific CD8 T cell responses in the lungs. *J Virol*. 2014;88(9):4711-20. doi: 10.1128/JVI.02081-13. PubMed PMID: 24522912; PubMed Central PMCID: PMC3993800.
96. Baum U, Leino T, Gissler M, Kilpi T, Jokinen J. Perinatal survival and health after maternal influenza A(H1N1)pdm09 vaccination: A cohort study of pregnancies stratified by trimester of vaccination. *Vaccine*. 2015;33(38):4850-7. doi: 10.1016/j.vaccine.2015.07.061. PubMed PMID: 26238723.
97. Regan AK, de Klerk N, Moore HC, Omer SB, Shellam G, Effler PV. Effect of Maternal Influenza Vaccination on Hospitalization for Respiratory Infections in Newborns: A Retrospective Cohort Study. *The Pediatric infectious disease journal*. 2016;35(10):1097-103. doi: 10.1097/INF.0000000000001258. PubMed PMID: 27314823.
98. Souvannavong V, Brown S, Adam A. Muramyl dipeptide (MDP) synergizes with interleukin 2 and interleukin 4 to stimulate, respectively, the differentiation and proliferation of B cells. *Cell Immunol*. 1990;126(1):106-16. PubMed PMID: 2105848.

99. Muench LJRaH. A simple method of estimating fifty percent endpoints. . Journal of Hygiene 1938;29(493).
100. Sha Z, Compans RW. Induction of CD4(+) T-cell-independent immunoglobulin responses by inactivated influenza virus. J Virol. 2000;74(11):4999-5005. PubMed PMID: 10799573.
101. Byers SL, Wiles MV, Dunn SL, Taft RA. Mouse estrous cycle identification tool and images. PLoS One. 2012;7(4):e35538. doi: 10.1371/journal.pone.0035538. PubMed PMID: 22514749; PubMed Central PMCID: PMC3325956.
102. Esser ES, Romanyuk A, Vassilieva EV, Jacob J, Prausnitz MR, Compans RW, et al. Tetanus vaccination with a dissolving microneedle patch confers protective immune responses in pregnancy. J Control Release. 2016;236:47-56. doi: 10.1016/j.jconrel.2016.06.026. PubMed PMID: 27327766.
103. WHO. Immunization Surveillance assessment and monitoring. Geneva, Switzerland: 2009.
104. Skountzou I, Quan FS, Jacob J, Compans RW, Kang SM. Transcutaneous immunization with inactivated influenza virus induces protective immune responses. Vaccine. 2006;24(35-36):6110-9. doi: 10.1016/j.vaccine.2006.05.014. PubMed PMID: 16766095.

Figures

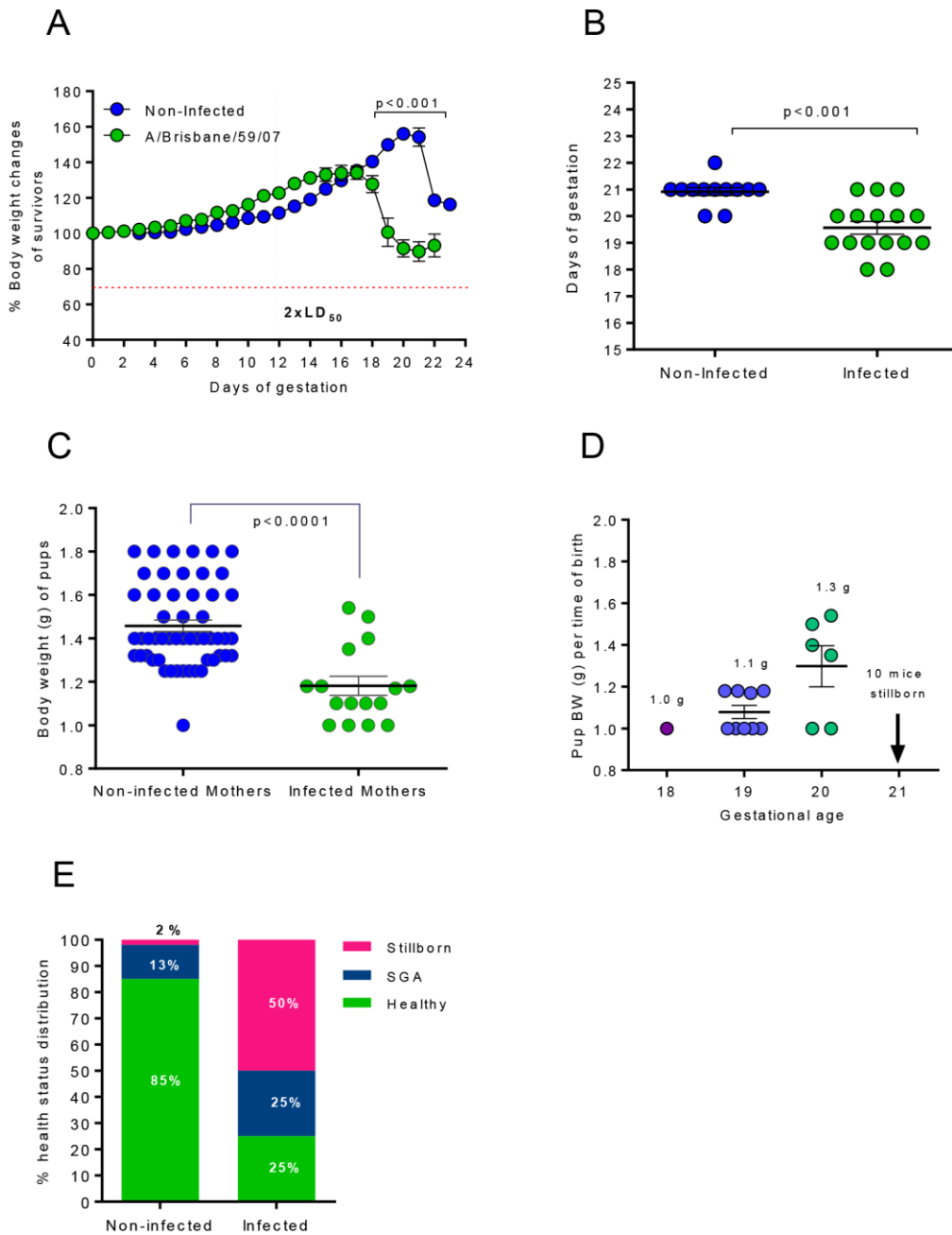


Fig 1. Influenza infection inhibits gestational development and offspring health. (A) Body weight (BW) fluctuations of pregnant BALB/c mice were tracked over the course of gestation. At day 12 of gestation (dashed vertical line) a cohort of pregnant mice (N=6) was infected with

2xLD₅₀ A/Brisbane/59/07. Weight changes were compared to uninfected pregnant controls (N=12). *P*-values were calculated by two-way ANOVA. Error bars represent Standard Error of Mean (SEM). (B) Mean gestational length for infected (N=13) and uninfected (N=9) groups was calculated based on the dates of successful copulation and parturition of offspring. *P*-value was calculated by Student's *t*-test. (C) The body weights (BW) of pups born to infected (N=16 to 6 mothers) and uninfected mothers (N=53 to 12 mothers) were recorded upon delivery. (D) The BW distribution of pups was categorized based on gestational age. Pups less than 1.25g were designated SGA. Pups greater than 1.25g were considered healthy. Average BW and SEM were plotted and *P*-value was calculated by Student's *t*-test for C and D. (E) Percent distribution of health status of pups born to uninfected and infected mothers.

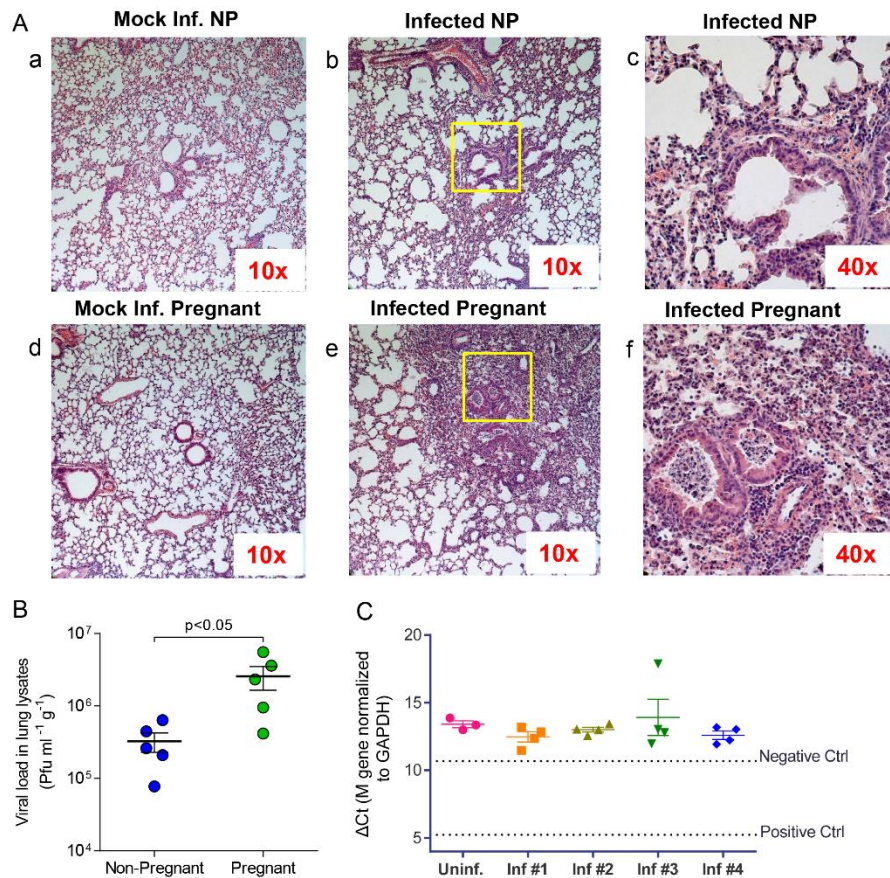


Fig 2. Pregnancy results in increased inflammation in the lungs and enhanced viral growth in lungs but not detected in placenta. A. Lungs from mock infected (a, d) and infected (b, c, e, f) pregnant and non-pregnant mice were stained with hematoxylin and eosin (H&E) 4 d.p.i. with mouse-adapted A/Brisbane/59/07 or mouse lung lysate at an equivalent dilution. (b, e) Lung sections at 10x magnification; (c, f) Inset boxes in (b, e) at 40x magnification represent lung structures. B. Viral load was quantified from lung lysates (N=5 per group) 4 d.p.i via plaque assay in MDCK-derived cell lines and normalized per gram of tissue weight. C. Viral RNA was isolated from placental lysates (N=4-5 per group) and probed for the presence of M gene RNA (A/Brisbane/59/07) via qPCR. Influenza-virus specific RNA was not detected below the negative

control threshold (RNA isolated from mock-infected BALB/c lungs) or positive control threshold (RNA isolated from infected BALB/c lungs). Inf.: Infected mice; NP: Non-pregnant mice.

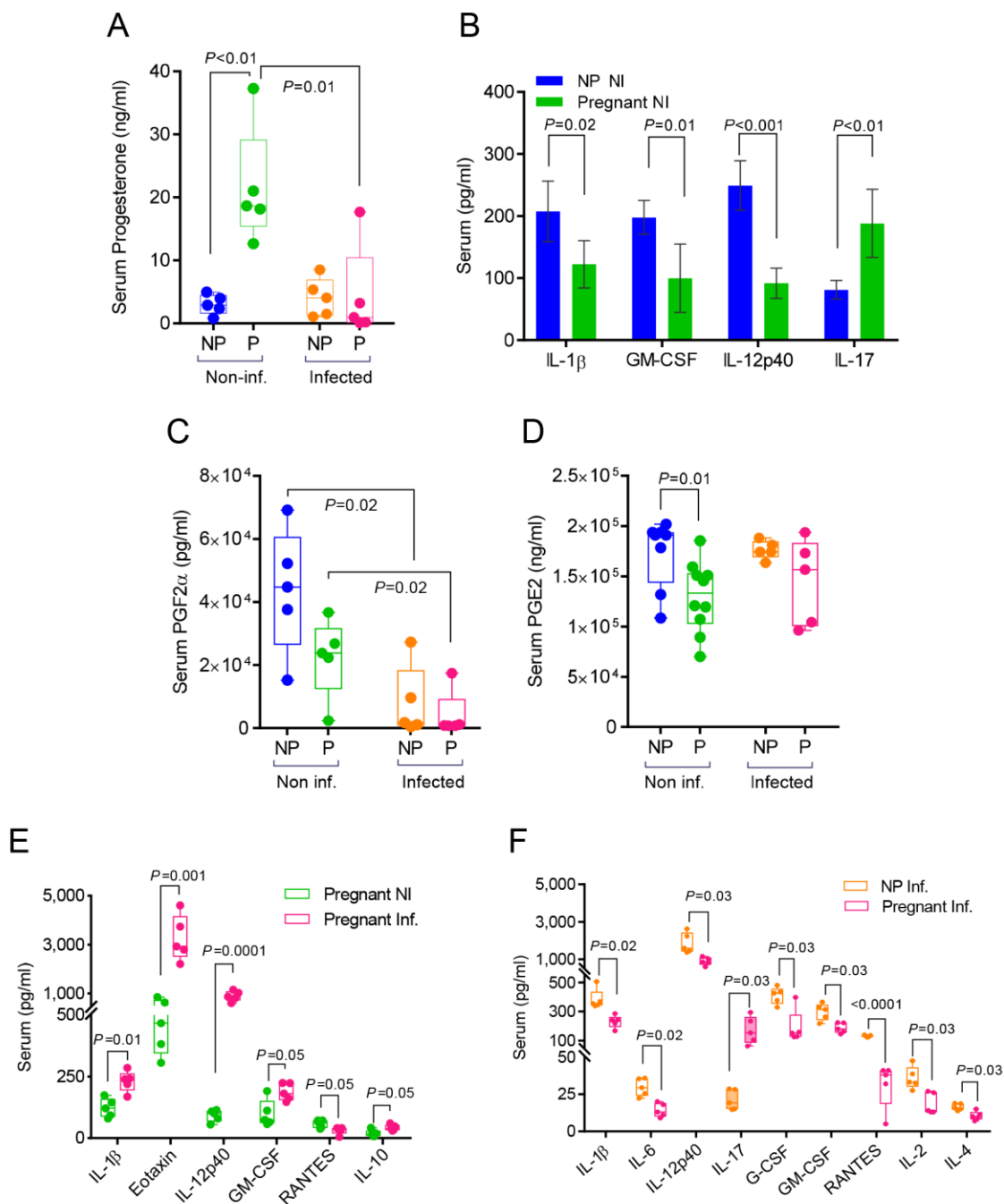


Fig 3. Viral infection disproportionately reduces cytokine and hormone expression in the sera and lungs during pregnancy. Hormone expression in sera was quantified via ELISA in uninfected and infected non-pregnant mice for A. progesterone; C. prostaglandin F2 α (PGF2 α); and D. prostaglandin E2 (PGE2). Cytokine and chemokine expression in sera was quantified via

Bio-Rad 23-plex assay in B. uninfected pregnant (E16) (N=5) and non-pregnant mice (N=5); E. uninfected and infected pregnant (E16; 4 d.p.i) (N=5 per group); and F. infected (4 d.p.i) non-pregnant and pregnant (E16) mice (N=5 per group). Student's t-test was performed between selected groups and significance noted above asterisk brackets. Inf.: infected; Uninf: uninfected; NP: non-pregnant; P: pregnant mice.

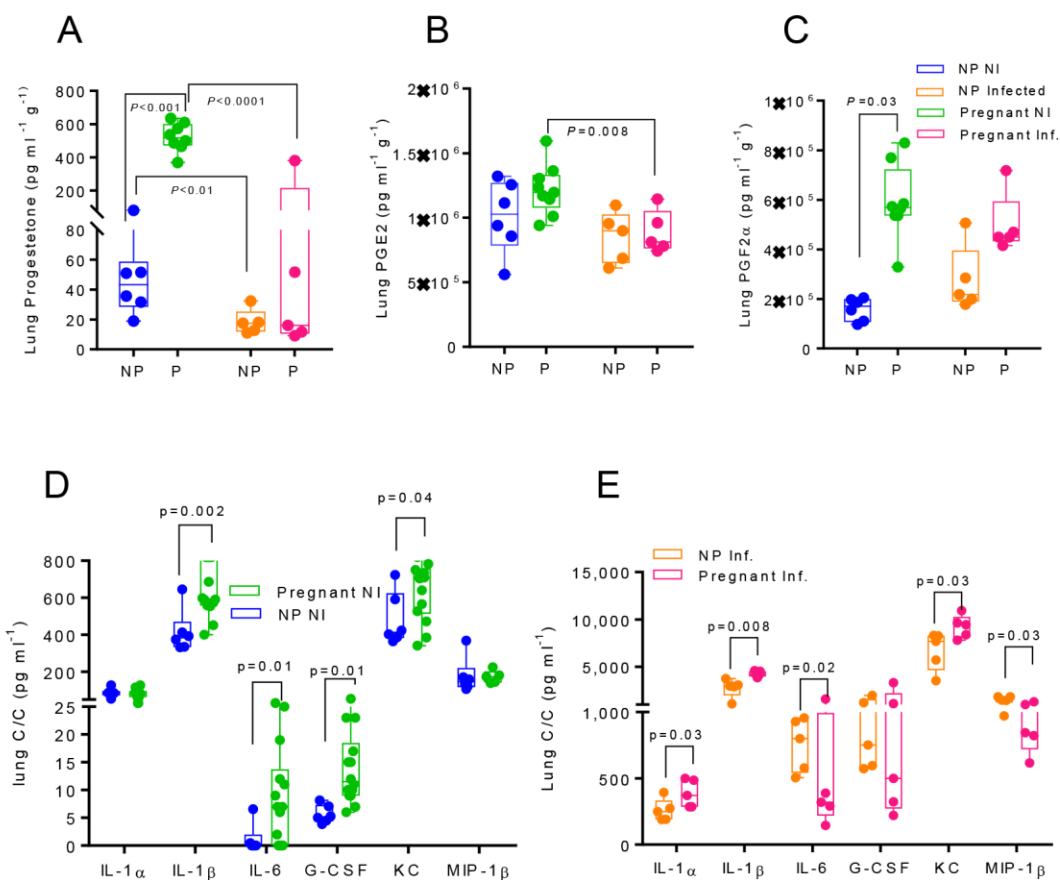


Fig 4. Pregnancy increases lung tissue expression of proinflammatory cytokines and chemokines while dampening the upregulation of progesterone and PGF2 α following infection. Hormone expression in lung lysates was quantified via ELISA in uninfected (N=6) and infected (N=5) non-pregnant and pregnant mice for A. progesterone; B. prostaglandin F2 α (PGF2 α); and C. prostaglandin E2 (PGE2). Cytokine and chemokine expression in sera was quantified in lung lysates of D. uninfected pregnant (E16) (N=8) and non-pregnant mice (N=6); E. infected pregnant (4 d.p.i., E16) (N=5) and non-pregnant mice (N=5). Student's t-test was performed between selected groups and significance noted above asterisk brackets. Abbreviations for groups are as described in Fig 3.

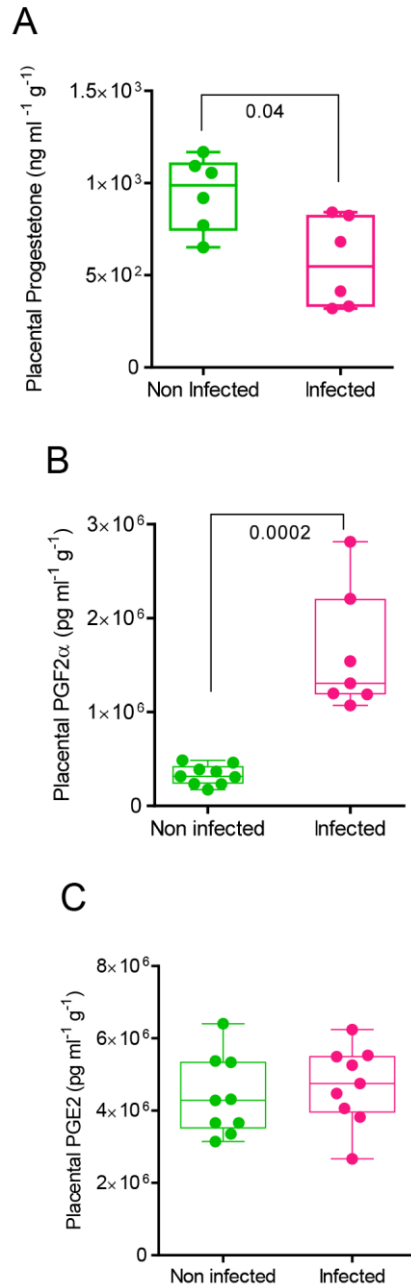


Fig 5. Infection increases placental expression of contraction-inducing PGF2 α and reduces pregnancy-supportive progesterone. Placental lysates were isolated from uninfected and infected pregnant mice (E16). Hormone expression was quantified via ELISA for A. progesterone (N=6 per group); B. prostaglandin F2 α (PGF2 α) (N=9, uninfected, N=7, infected) and C.

prostaglandin E2 (PGE2) (N=9 per group). Student's t-test was performed between selected groups and significance noted above asterisk brackets.

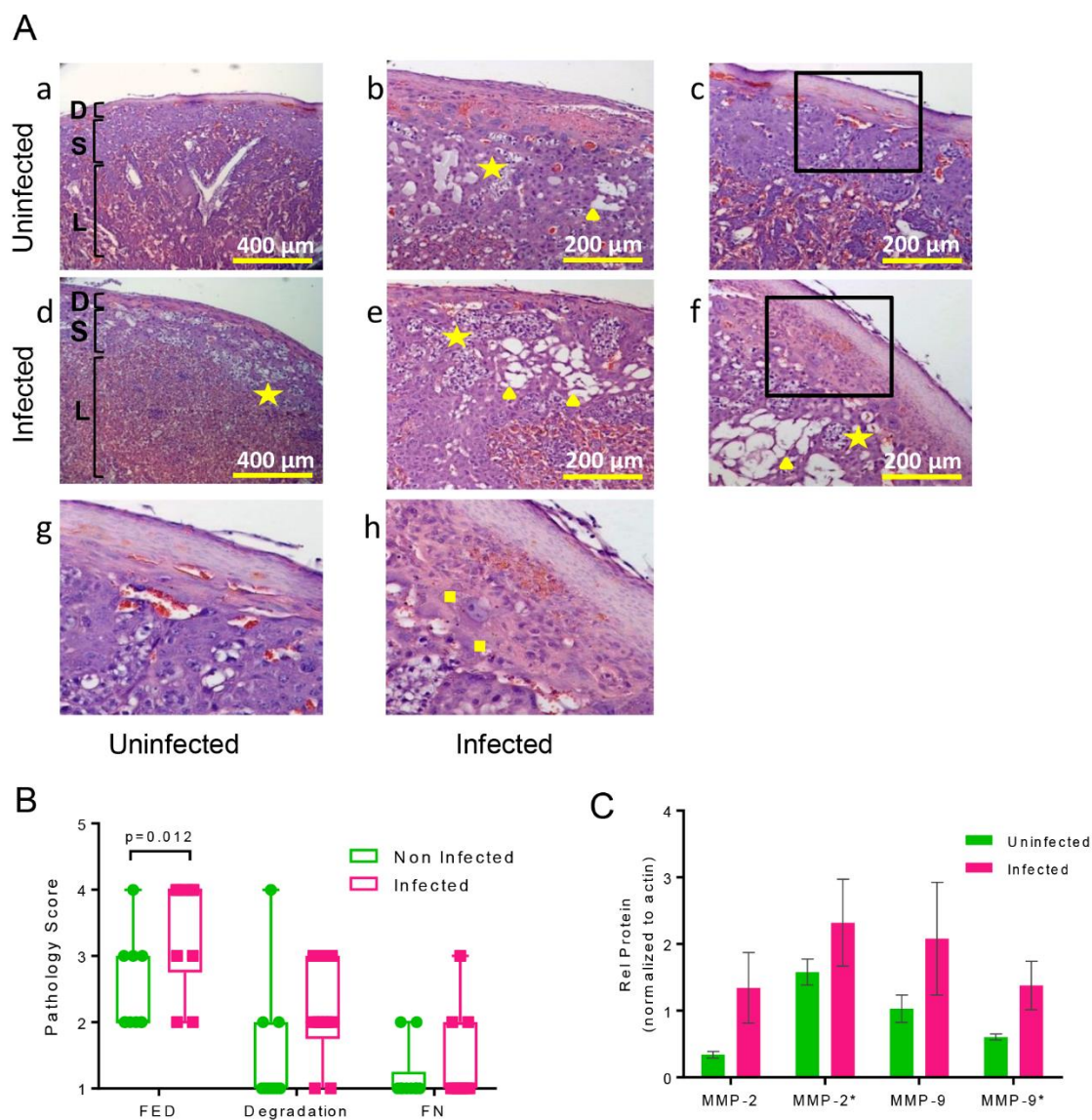


Fig 6. Infection damages placental architecture and increases activation of structural protein degrading matrix metalloproteinases (MMPs). A. Placentas from uninfected [a, b, c, g] (N=8) and infected [d, e, f, h] (N=8) pregnant mice (E16) were embedded in paraffin, sectioned in 4 μ M, H&E stained and imaged with a Zeiss brightfield microscope. Infection increases gaps within the spongiosotrophoblast layer (S) between the decidual layer (D) and the placental labyrinth (L) [a, d;

10x]. Gaps are marked by fetal endothelial nuclei suspended in tissue [stars] and empty space [triangles] distinct from maternal blood sinuses and fetal blood vessels [**d, 10x; b, e, f, 20x**]. Fibrinoid necrosis [squares] beneath the decidual layer was increased in placentae from infected mice [**h, inset of box in f**] compared to uninfected mice [**g, inset of box in c**]. B. Histology slides were randomized prior to imaging and scored blindly for the incidence of fetal endothelial death (FED; N=10, p=0.012), degradation of the spongiotrophoblast layer (Degradation; N=10, p>0.05), and fibrinoid necrosis (FN; N=10, p>0.05). C. Protein expression of matrix metalloproteinases (MMP-2, MMP-9; active forms denoted with *) in placentas in uninfected and infected mice at E16 quantified by Western blot. Two-way ANOVA: protein maturation, p=0.064, ns; infection, p=0.007, **.

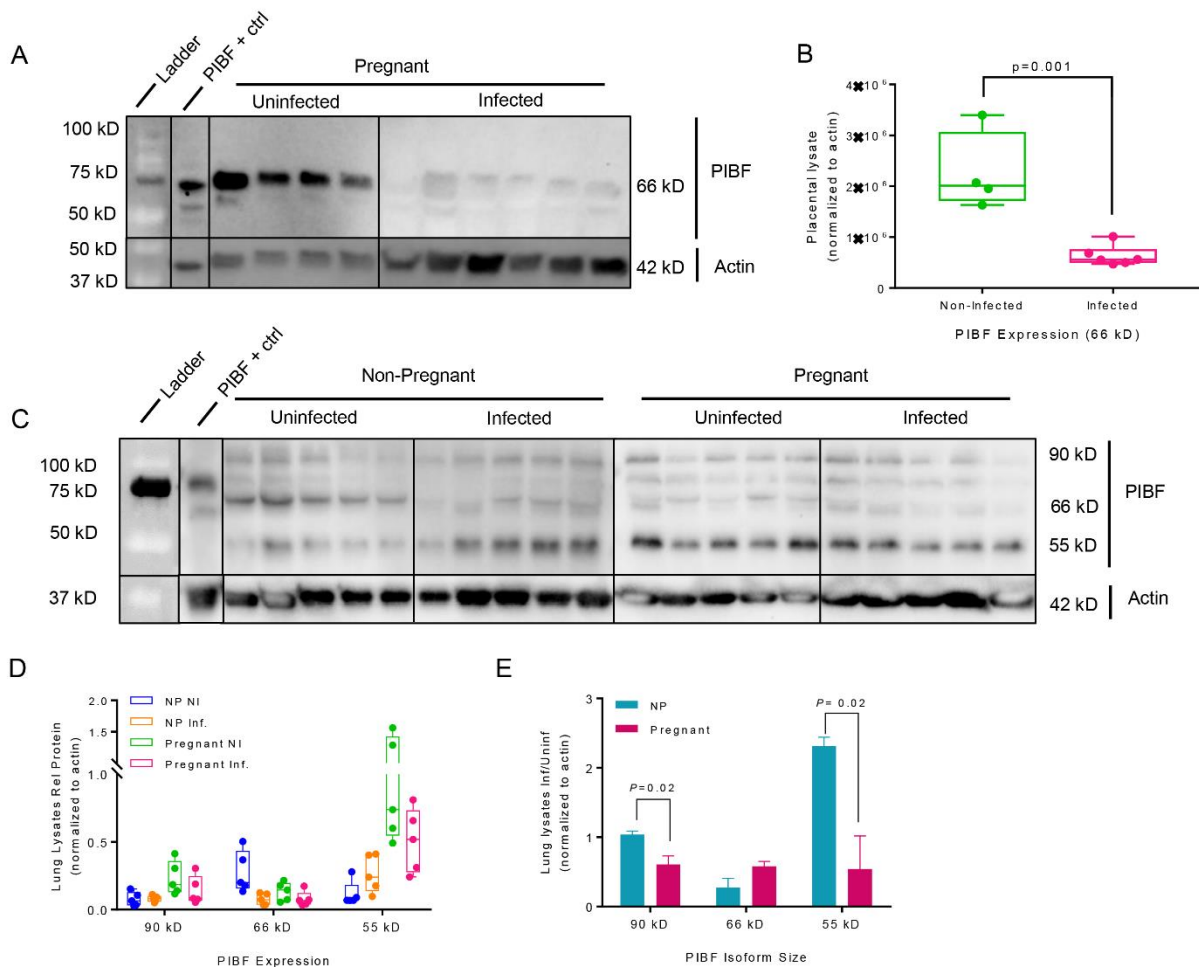


Fig 7. Infection changes pregnancy-supportive PIBF expression in the placenta and lungs.

PIBF isoforms (90 kD, 66 kD, 55 kD) were detected using Western blots of A. placental and C. lung lysates. Protein expression is represented as isoform density normalized to loading control anti-beta actin (42 kD) for each sample. The effect of infection was measured by dividing the average density of bands from tissues from infected mice by the uninfected controls for both pregnant and non-pregnant mice. (B) Relative protein normalized to actin for uninfected (N=4) and infected (N=6) placental lysates. (D) Relative protein normalized to actin for lung lysates (N=5 per group). (E) Ratio of infected vs uninfected lung lysates (normalized to actin). Uninf: uninfected; NP: Non-pregnant; Inf: Infected mice. P-values were determined by Student's t-test.

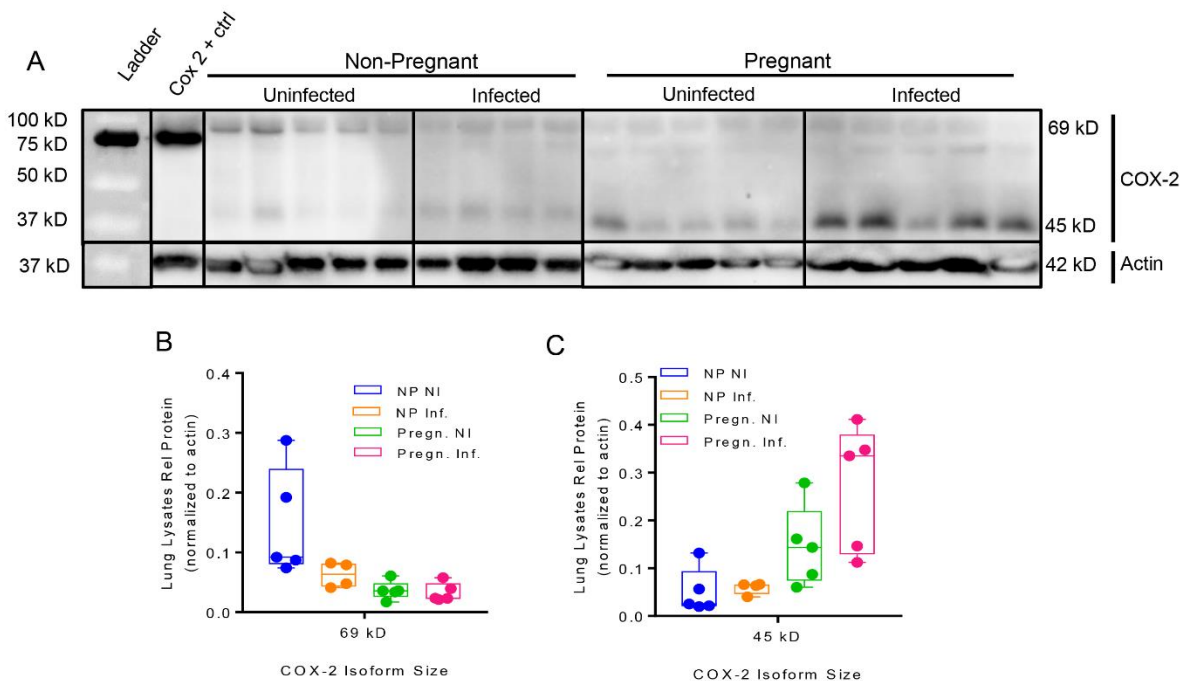
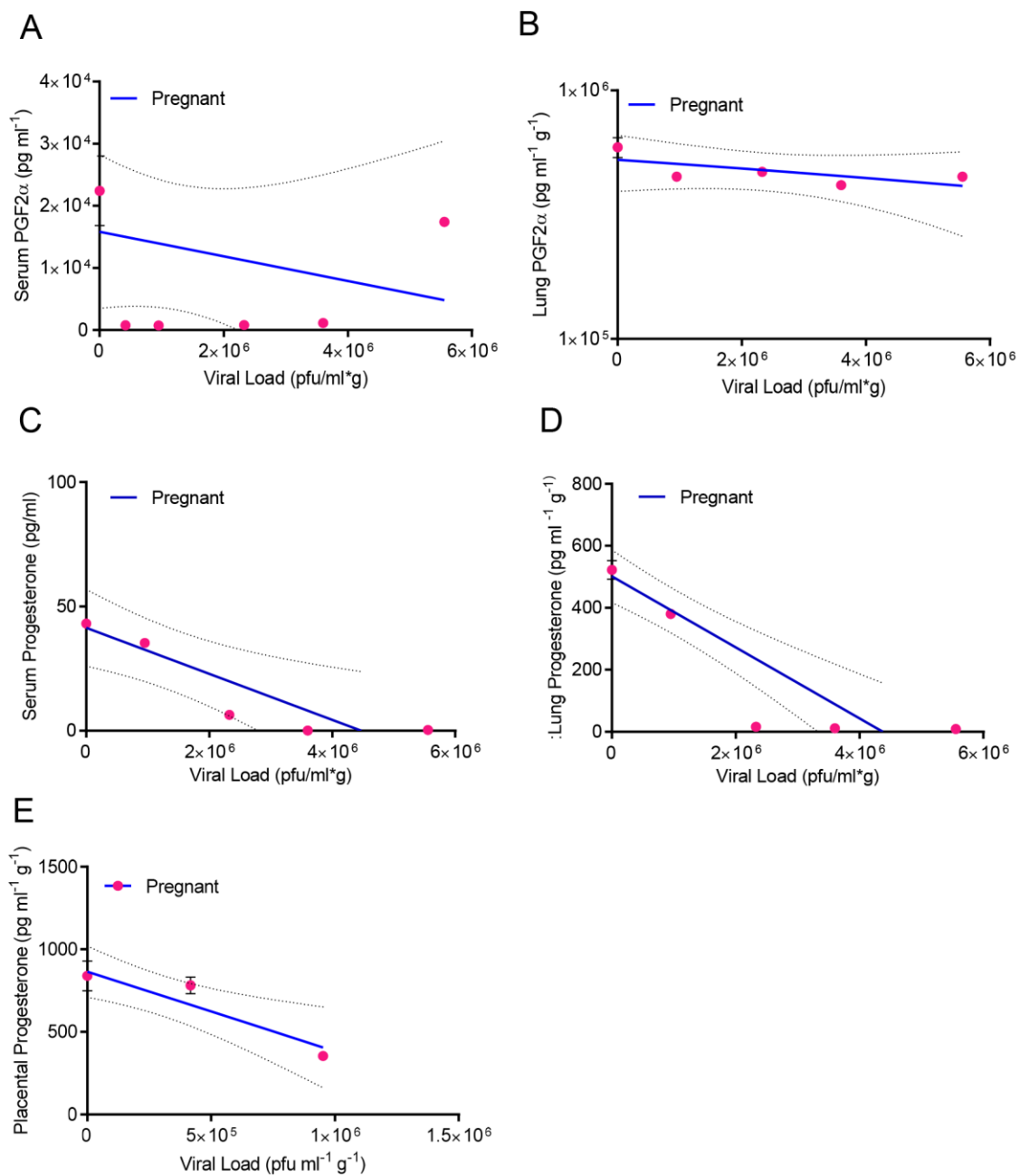


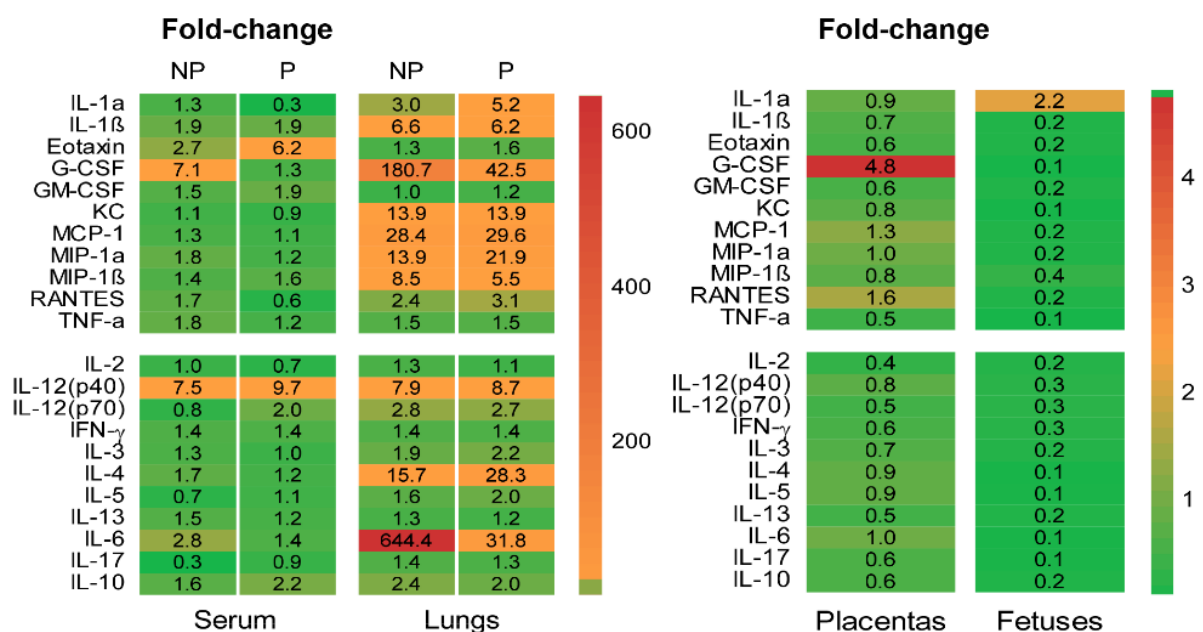
Fig 8. Infection and pregnancy increase COX-2 expression in the lungs. (A) Placental and (C) lung lysates collected 4 d.p.i were probed via Western blot for COX-2 expression. Protein expression is represented as isoform density normalized to loading control anti-beta actin (42 kD) for each sample. (B) COX-2 69 kD expression was the only detectable band in these placental lysates (Uninfected, N=4; Infected, N=6) and it was significantly lower in infected mice. COX-2 isoforms (D) 69 kD and (E) 45 kD were detected in lung lysates (N=5 per each group except NP Infected mice; N=4). Group annotations are as described in Fig 7. P-values were determined by Student's t-test.

Supporting Information



S1 Fig. Viral titer in the lungs affects expression of progesterone and PGF2 α in a compartment-specific manner. Hormone expression was quantified in sera, lung and placental lysates in pregnant infected mice with ELISA, and viral load was quantified with plaque assay in

MDCK-derived cells. Virus titer detected in the lungs was plotted against corresponding expression values; linear regression (blue line) was derived for each compartment and 95% confidence is represented by dashed lines. Serum PGF2 α was correlated with lung viral titer (A, $r^2 = 0.4$) and lungs (B, $r^2 = 0.6$) of pregnant mice, and progesterone was correlated with lung viral titer in serum (C, $r^2 = 0.8$), lung lysates (D, $r^2 = 0.7$), and placenta (E, $r^2 = 0.46$).



S2 Fig. Infection and pregnancy impact cytokine expression in a compartment-specific manner. Cytokine and chemokine expression in serum, lungs, placenta and fetuses was determined via Bio-Rad 23-plex Luminex Assay. The effect of infection on cytokine and chemokine expression is represented as fold-change of the average values of infected mice over average values of uninfected mice. Numerical values and fold changes are reported in Supplementary Tables S1-3.

S1 Table. Serum chemokine and cytokine levels 4 days post-infection.

Cytokine	Pregnant				Non-Pregnant			
	Non-Infected	Infected	Fold	<i>P</i>	Non-Infected	Infected	Fold	<i>P</i>
IL-1α	47.2 \pm 28.8	14.6 \pm 4.6	0.3	0.06	53.7 \pm 51.7	67.1 \pm 38.8	1.3	0.66
IL-1β	122.4 \pm 38.2	230.7 \pm 42.5	1.9	0.01	207.6 \pm 48.8	383 \pm 175.9	1.8	0.00
Eotaxin	528.0 \pm 219.0	3254.6 \pm 932.5	6.2	0.00	823.0 \pm 420.9	2245.7 \pm 952.2	2.7	0.01
G-CSF	150.8 \pm 92.7	192.6 \pm 115.7	1.3	0.55	57.9 \pm 53.1	409.7 \pm 194.7	7.1	0.00
GM-CSF	99.7 \pm 55.0	187 \pm 35.5	1.9	0.02	197.9 \pm 27.1	298.6 \pm 117.1	1.5	0.01
KC	23.9 \pm 5.1	20.3 \pm 7.0	0.9	0.39	36.3 \pm 18.2	39.6 \pm 22.4	1.1	0.81
MCP-1	216.2 \pm 41.2	238.3 \pm 68.1	1.1	0.55	225.7 \pm 71.3	288.6 \pm 105.8	1.3	0.27
MIP-1α	15.5 \pm 3.1	18.7 \pm 8.6	1.2	0.46	15.6 \pm 12.3	28.6 \pm 8.7	1.8	0.00
MIP-1β	41.4 \pm 7.3	66.9 \pm 23.5	1.6	0.07	39.9 \pm 16.0	53.8 \pm 18.1	1.3	0.26
RANTES	57.4 \pm 16.0	31.3 \pm 15.3	0.5*	0.03	78.6 \pm 18.5	131.4 \pm 38.0	1.7	0.00
TNF-α	456.8 \pm 122.5	565.7 \pm 188.4	1.2	0.32	385.4 \pm 111.8	702.6 \pm 198.9	1.8	0.00
IL-12p40	91.7 \pm 24.3	891.9 \pm 209.4	9.7	0.00	249.3 \pm 39.7	1856.7 \pm 945.5	7.4	0.00
IL-12p70	238.2 \pm 63.7	478.4 \pm 295.5	2.0	0.14	175.1 \pm 57.6	135.6 \pm 89.7	0.8	0.43
IL-6	10.4 \pm 4.8	14.3 \pm 4.6	1.4	0.23	10.5 \pm 3.1	29.7 \pm 8.9	2.8	0.00
IL-17	188.3 \pm 54.9	170.1 \pm 93.9	0.9	0.72	81.3 \pm 14.8	21.3 \pm 60.7	0.3	0.00
IL-2	27.6 \pm 5.5	18.7 \pm 7.3	0.7	0.06	36.9 \pm 17.1	35.9 \pm 8.9	1.0	0.91
IFN-γ	24.2 \pm 10.1	33.2 \pm 22.0	1.4	0.44	25.6 \pm 8.3	35.5 \pm 8.6	1.4	0.05
IL-3	11.2 \pm 5.4	11.2 \pm 3.7	1.0	0.99	9.4 \pm 3.4	12.5 \pm 5.7	1.3	0.32
IL-4	8.8 \pm 1.0	10.3 \pm 3.2	1.2	0.36	9.6 \pm 2.3	16.4 \pm 4.8	1.7	0.00
IL-5	10.6 \pm 2.8	11.5 \pm 3.1	1.1	0.64	22.2 \pm 11.9	14.8 \pm 6.2	0.7	0.26
IL-13	244.9 \pm 79.6	303.8 \pm 114.1	1.2	0.38	300.3 \pm 97.4	444.3 \pm 122.7	1.5	0.03
IL-10	18.9 \pm 13.7	42.3 \pm 12.2	2.2	0.02	28.5 \pm 19.7	45.6 \pm 48.5	1.6	0.48

The shaded fold-differences are significant ($p < 0.05$). * RANTES is the only chemokine that is significantly decreased after infection in serum of pregnant mice. *P* values were determined with t-test comparing infected and uninfected tissues ($n = 5-14$).

S1 Table. Serum chemokine and cytokine levels 4 days post-infection. Serum was collected

from pregnant and non-pregnant infected and non-infected mice 4 d.pi. (16 days post mating),

and cytokine and chemokine expression was quantified via Bio-Rad 23-plex Luminex Assay.

The shaded fold-differences are significant ($p < 0.05$). * RANTES is the only chemokine that is

significantly decreased after infection in serum of pregnant mice. *P* values were determined with

t-test comparing infected and uninfected tissues ($n =$

S2. Table. Lung chemokine and cytokine levels 4 days post-infection.

	Pregnant				Non-Pregnant			
	Non-Infected	Infected	Fold	<i>P</i>	Non-Infected	Infected	Fold	<i>P</i>
IL-1α	81 \pm 24.8	418.2 \pm 89.7	5.2	0.00	85 \pm 23.6	259.8 \pm 83.0	3.0	0.01
IL-1β	686 \pm 195.5	4238.9 \pm 303.5	6.2	0.00	416 \pm 116.8	2745.1 \pm 991.2	6.6	0.01
Eotaxin	6074 \pm 1861.1	9713.5 \pm 428.8	1.6	0.00	7492 \pm 2319.3	9414.2 \pm 2172.2	1.3	0.19
G-CSF	16 \pm 12.3	1095.8 \pm 1290.7	42.5	0.03	6 \pm 1.6	1020.1 \pm 587.6	180.7	0.02
GM-CSF	278 \pm 83.4	330.3 \pm 24.1	1.2	0.05	345 \pm 106.9	345.8 \pm 81.9	1.0	0.99
KC	665 \pm 194.6	9240.2 \pm 1210.3	13.9	0.00	483 \pm 143.3	6710.3 \pm 2062.1	13.9	0.00
MCP-1	915 \pm 339.6	27077.3 \pm 5265.3	29.6	0.00	745 \pm 296.5	21165.3 \pm 9307.2	28.4	0.01
MIP-1α	140 \pm 57.4	3062.7 \pm 572.2	21.9	0.00	233 \pm 168.7	3242.1 \pm 866.4	13.9	0.00
MIP-1β	166 \pm 46.6	920.2 \pm 257.0	5.5	0.00	177 \pm 96.8	1505 \pm 352.7	8.5	0.00
RANTES	3477 \pm 1936.2	10886.7 \pm 2398.6	3.1	0.00	5365 \pm 2721.6	12644.6 \pm 7420.3	2.4	0.39
TNF-α	1185 \pm 355.7	1764 \pm 478.0	1.5	0.05	1050 \pm 298.1	1593.12 \pm 381.0	1.5	0.03
IL-12p40	564 \pm 560.4	4879.9 \pm 2045.1	8.7	0.01	634 \pm 625.4	5021.8 \pm 2050.2	7.9	0.01
IL-12p70	201 \pm 53.5	534.5 \pm 46.1	2.7	0.00	208 \pm 77.7	578 \pm 145.3	2.8	0.00
IL-6	9 \pm 9.5	286.2 \pm 102.3	31.8	0.01	1.17 \pm 2.65	754.1 \pm 204.5	644.4	0.00
IL-17	38 \pm 6.0	50.8 \pm 7.8	1.3	0.02	35 \pm 7.4	49.9 \pm 9.2	1.4	0.02
IL-2	64 \pm 9.5	69.7 \pm 17.7	1.1	0.51	81 \pm 42.4	104.5 \pm 41.9	1.3	0.38
IFN-γ	47 \pm 9.3	65 \pm 12.1	1.4	0.03	54 \pm 18.9	77.9 \pm 9.4	1.4	0.03
IL-3	36 \pm 9.6	77.2 \pm 19.8	2.2	0.01	41 \pm 14.9	77.3 \pm 13.1	1.9	0.00
IL-4	2 \pm 5.2	68.6 \pm 20.1	28.3	0.00	5 \pm 11.3	72.3 \pm 22.9	15.7	0.00
IL-5	38 \pm 19.4	73.4 \pm 43.1	2.0	0.14	34 \pm 14.4	55.7 \pm 30.8	1.6	0.21
IL-13	796 \pm 286.1	920.5 \pm 72.9	1.2	0.15	715 \pm 152.4	895.3 \pm 205.4	1.3	0.15
IL-10	110 \pm 22.3	218.4 \pm 21.2	2.0	0.00	100 \pm 30.3	234.5 \pm 46.6	2.4	0.00

The shaded fold-differences are significant ($p \leq 0.05$). *P* values were determined with t-test comparing infected and uninfected tissues ($n=5-14$).

S2. Table. Lung chemokine and cytokine levels 4 days post-infection. Lungs were collected from pregnant and non-pregnant infected and non-infected mice 4 d.p.i. (E16 gestation), and cytokine and chemokine expression was quantified in homogenized lysates via Bio-Rad 23-plex Luminex Assay. The shaded fold-differences are significant ($p \leq 0.05$). *P* values were determined with t-test comparing infected and uninfected tissues ($n=5-14$).

S3 Table. Placental and fetal chemokine and cytokine levels 4 days post-infection

	Placentas				Fetuses			
	Non-Infected	Infected	Fold	<i>P</i>	Non-Infected	Infected	Fold	<i>P</i>
IL-1α	5299.6 \pm 3340.4	4710.7 \pm 1390.0	0.9	0.53	114.7 \pm 164.3	248.5 \pm 210.7	2.2*	0.05
IL-1β	10948.2 \pm 3540.3	7319.6 \pm 1032.6	0.7	0.00	477.8 \pm 371.8	95.5 \pm 46.3	0.2	0.00
Eotaxin	93402.3 \pm 29970.0	57049.4 \pm 14303.5	0.6	0.00	9701.6 \pm 8126.5	1561.9 \pm 527.6	0.2	0.00
G-CSF	7918.5 \pm 4603.7	38170.7 \pm 31120.6	4.8*	0.01	170.4 \pm 177.4	27.5 \pm 11.2	0.1	0.07
GM-CSF	4868.3 \pm 1507.5	2846.5 \pm 698.9	0.6	0.00	260.5 \pm 222.5	43.2 \pm 14.4	0.2	0.00
KC	12712.5 \pm 6675.8	10225.3 \pm 6773.7	0.8	0.33	331.7 \pm 538.8	41.8 \pm 16.2	0.1	0.04
MCP-1	15782.3 \pm 7165.0	21031.3 \pm 8454.5	1.3	0.09	761 \pm 754.0	141.4 \pm 45.4	0.2	0.01
MIP-1α	3229.6 \pm 2436.6	3311.3 \pm 1045.0	1.0	0.91	126.6 \pm 126.8	20 \pm 5.3	0.2	0.00
MIP-1β	1073.6 \pm 419.1	889.8 \pm 271.4	0.8	0.17	70.8 \pm 71.3	26.4 \pm 11.1	0.4	0.03
RANTES	871.7 \pm 347.8	1347.3 \pm 409.6	1.5*	0.00	63.7 \pm 92.7	10.4 \pm 3.7	0.2	0.04
TNF-α	14045.4 \pm 3807.7	6884.2 \pm 1370.9	0.5	0.00	859.7 \pm 597.5	113.9 \pm 54.2	0.1	0.00
IL-12p40	2486.6 \pm 823.7	2026.2 \pm 377.2	0.8	0.06	62.9 \pm 50.8	18.6 \pm 4.4	0.3	0.00
IL-12p70	4853.4 \pm 119.8	2620.9 \pm 603.7	0.5	0.00	252.2 \pm 221.5	73.7 \pm 15.3	0.3	0.01
IL-6	2105.2 \pm 987.4	2085.6 \pm 570.4	1.0	0.95	111 \pm 109.4	13.1 \pm 7.6	0.1	0.02
IL-17	462.7 \pm 88.0	297.8 \pm 82.6	0.6	0.00	37.6 \pm 29.1	4.9 \pm 2.4	0.1	0.00
IL-2	1868.9 \pm 472.1	701.4 \pm 175.1	0.4	0.00	106.1 \pm 71.8	25 \pm 12.5	0.2	0.00
IFN-γ	1327.7 \pm 378.1	795.3 \pm 211.2	0.6	0.00	140.3 \pm 132.7	38 \pm 13.2	0.3	0.01
IL-3	291.8 \pm 78.7	206.9 \pm 52.4	0.7	0.00	10.8 \pm 9.6	2.5 \pm 1.3	0.2	0.01
IL-4	434.1 \pm 111.7	373.3 \pm 117.5	0.9	0.17	90.6 \pm 16.4	9.8 \pm 4.5	0.1	0.09
IL-5	384.8 \pm 155	330.5 \pm 183.8	0.9	0.40	67.9 \pm 51.2	8.6 \pm 4.6	0.1	0.00
IL-13	24155.9 \pm 6693.4	12923.9 \pm 2948.0	0.5	0.00	917.6 \pm 768.7	177.7 \pm 50.7	0.2	0.00
IL-10	1402.6 \pm 418.5	894.7 \pm 212.9	0.6	0.00	53.3 \pm 47.4	10.2 \pm 3.5	0.2	0.00

The shaded fold-differences are significant ($p \leq 0.05$). *: depicts increases after infection. G-CSF and RANTES are increased in placenta and IL-1 α is increased in fetus after infection. *P* values were determined with t-test comparing infected and uninfected tissues (n=5-14).

S3 Table. Placental and fetal chemokine and cytokine levels 4 days post-infection. Placentae

and fetuses were collected from pregnant and non-pregnant infected and non-infected mice 4 d.p.i. (E16 gestation), and cytokine and chemokine expression was quantified in homogenized lysates via Bio-Rad 23-plex Luminex Assay. The shaded fold-differences are significant ($p \leq 0.05$). *: depicts increases after infection. G-CSF and RANTES are increased in placenta and IL-1 α is increased in fetus after infection. *P* values were determined with t-test comparing infected and uninfected tissues (n=5-14).

**Chapter III: Pregnancy dysregulates innate immune responses to 2009 H1N1
influenza viral infection and the efficacy of long term anti-influenza
antibodies**

Elizabeth Q. Littauer, Katherine M. Bricker, E. Stein Esser, Olivia Q. Antao, Dahnide T.
Williams, Lisa K. Mills, Jacob T. Beaver, Richard W. Compans, Ioanna Skountzou

*Manuscript in preparation for submission. April 2018.

Emory University School of Medicine
1518 Clifton Road, CNR 5050
Atlanta, GA 30322

*Corresponding author: iskount@emory.edu

Abstract

Successful pregnancy requires complex regulation of the maternal immune system in order to tolerate the developing fetus, limit inflammation, and protect mother and offspring from infections. The 2009 H1N1 influenza pandemic increased the incidence of hospitalizations of pregnant women due to acute respiratory distress syndrome (ARDS) and viral pneumonia and was implicated with increased risk for preterm birth and small-for-gestational age (SGA) infants. The pregnant mouse model will be used to recapitulate clinical phenotypes of preterm birth and low birth weight offspring and enhanced maternal morbidity and mortality. Here we characterize the role of pregnancy in modulating the cellular and humoral response to seasonal H1N1 infection. We report that pregnancy dysregulated chemoattractant cytokine signaling in the lungs, resulting in reduced recruitment of dendritic cells (DCs) and natural killer (NK) cells to the infected lungs. While B and T cell activation following infection was unaffected by pregnancy, virus-specific IgA-secreting cells and IFN- γ secreting cells were increased in the lungs of mice infected during pregnancy at 6 weeks post-infection. Pregnancy increased expression of serum anti-influenza IgG but these antibodies had reduced avidity and hemagglutination binding titers. Lastly, mice vaccinated mid-gestation generated antibodies at a similar titer to non-pregnant vaccinated mice but generated fewer virus-specific T cells in the spleen and lungs; however, boost vaccination was able to increase the number of virus-specific IFN- γ secreting T cells in the spleen and lungs relative to non-pregnant controls. These findings can inform improved treatment strategies of influenza-infected pregnant women and provide evidence supporting boost vaccination in strengthening the maternal immune responses post-partum.

Introduction

Influenza A virus (IAV) infection during pregnancy has been widely documented to cause significant risks to pregnant women and their offspring, not only during gestation but also in maternal immune responses and offspring development [1, 2]. During the 1918, 1957, 1968, and 2009 pandemics, incidence of maternal and fetal death in pregnant women was raised significantly relative to their non-pregnant peers, with an increased risk of acute respiratory distress syndrome (ARDS), viral pneumonia and secondary bacterial infection, pre-term birth, low birth weight, and congenital heart malformations [1, 3-5]. Admittance to an intensive care unit (ICU) or death following pandemic 2009 H1N1 IAV infection during pregnancy was linked to asthma, obesity, and pre-gestational and gestational diabetes; early antiviral treatment was associated with improved outcomes [6]. Overall, during the 2009 influenza pandemic, pregnant women comprised 5% of the deaths due to confirmed H1N1 influenza virus infection, although they represent just 1% of the United States population [4, 6].

The mechanisms by which IAV infection worsens pregnant women's outcomes are clearly related to hormone expression [1, 7]. Pregnancy is regulated by sex hormones, namely progesterone, estrogen, luteinizing hormone (LH) and follicular stimulating hormone (FSH) [8]. Sex hormones coordinate to reduce uterine and placental inflammatory cytokine expression and T cell activation during pregnancy that might cause fetal developmental damage, in part by upregulating regulatory T cell activity and downregulating natural killer (NK) cell activity in the uterus [9-11]. Pregnancy also poses increased respiratory burden on the mother's lungs, and increased progesterone concentrations have been linked to labored respiration in pregnant women; *in vitro* studies in primary lung epithelial culture showed that the addition of progesterone altered cilia function [12-15]. This increase in immunosuppression in the lung combined with respiratory

stress due to hormonal and physiological changes during pregnancy results in an inefficient immune response to influenza A virus infection.

Pregnant mice infected with seasonal or pandemic H1N1 IAV strains or influenza B virus exhibited increased lung pathology and expression of inflammatory cytokines KC (CXCL1), granulocyte-colony stimulating factor (G-CSF), RANTES, interleukin (IL)-1 α , and IL-6 compared to non-pregnant mice [16-18]. Infection reduced progesterone expression in uterine and tissue and the expression of estrogen in the lungs and sera [16]. Previous studies have shown low levels of 17- β estradiol and other estrogens to reduce viral pathology in female mice [19-21].

We have previously shown that seasonal H1N1 influenza infection during pregnancy results in dysregulated hormonal and cytokine expression, placental degradation through upregulation of prostaglandins and matrix metalloproteinases (MMPs), and increased inflammation and cyclooxygenase 2 (COX-2) expression in the lungs [22]. Withdrawal of progesterone, increased prostaglandin expression, and premature rupture of amniotic membranes (PROM) via placental degradation is linked to the early induction of labor and spontaneous abortion [23, 24]. Although preterm birth and poor offspring outcomes are well documented, transplacental transmission of IAV from mother to fetus is rarely observed [25, 26]. Rather, damage to the placenta is more likely the cause of low birth weight and fetal demise. Lastly, there is evidence that pregnancy-induced suppression of type I interferon (IFN) and CD8⁺ T cell migration in the lungs can foster the development of more virulent 2009 H1N1 IAV strains [27]. Thus, the prevention of influenza virus infection in pregnant women is particularly important in clinical treatment and in public health vaccination initiatives.

The dysregulation of innate immune cells and inflammatory cytokines may result in impaired activation of humoral immunity. It has been reported that progesterone negatively regulates pre-B

and pro-B cell lymphopoiesis, and progesterone administered to female mice at levels comparable to oral contraceptives reduced antibody responses and memory CD8⁺ T cell activity following primary H1N1 IAV infection [28-31]. Pregnant women infected with the 2009 H1N1 pandemic showed reduced IgG2 expression compared to non-pregnant infected women [32, 33]. The development of strong humoral immunity during pregnancy is of special importance in pregnant women because antibody transfer of IgG, primarily IgG1 subisotypes, through the placenta and IgA through the breastmilk is a significant source of passive immunity for the newborn [34, 35]. Clinical studies have demonstrated that maternal vaccination during pregnancy reduces neonatal hospitalization due to respiratory illness and is not associated with a significant risk of adverse effects for mother or child [36-38]. However, vaccination coverage was estimated at 50% of pregnant women in the 2011-2012 flu season in the United States [39]. Additionally, there is evidence that pregnancy reduces antibody binding responses to H1N1 A/California/07/2009 vaccine; other studies show an increase in plasmablast circulation following vaccination during pregnancy compared to vaccinated non-pregnant women but no increase in anti-influenza antibody titers [40, 41]. There is a need to better characterize how pregnancy affects the development of humoral immunity following mid-gestation infection and vaccination.

Here we examine the long range of effects of pregnancy on the development of cellular and humoral immunity induced by sublethal infection or vaccination of mice at mid-gestation with a 2009 H1N1 pandemic influenza strain which is of historical and clinical significance.

Materials and Methods

Animal infections and vaccination

Animal studies were conducted according to Emory University Institutional Animal Care and Use Committee (IACUC) guidelines outlined in an approved protocol (DAR2002950-122617BN) in compliance with the United States Federal Animal Welfare Act (PL 89–544) and subsequent amendments. Timed pregnancies were generated in eight- to twelve-week female BALB/c mice (Envigo, Huntingdon, United Kingdom) as described previously [22]. On day 12 of pregnancy (determined by 20% weight gain and/or presence of a copulation plug), pregnant mice and non-pregnant controls were lightly anesthetized with isoflurane and infected intranasally with 30 μ l 0.5xLD₅₀ of mouse adapted A/California/07/09, approximately 30 plaque forming units (p.f.u.). Non-infected mice were intranasally dosed with a dilution of BALB/c lung lysate in sterile PBS. For vaccination studies, 1 μ g recombinant H1N1 A/California/07/09 (BEI Resources, Manassas, VA) was administered intramuscularly (IM) in the right hind leg on day 12 of pregnancy. For short-term studies, mice were euthanized, and their organs were harvested at 2, 4, 7, 10, and 14 days post-infection. For long-term studies, mice were bled biweekly post-infection and euthanized at 6 and 12 weeks post-infection. Blood was collected submandibularly, and sera was isolated and stored in 1x Halt Protease Inhibitor (ThermoFisher, Waltham, Massachusetts) at -20°C. Lung and placental samples were weighed, homogenized into 1x DMEM (ThermoFisher)/1 x Halt Protease Inhibitor and stored at -80°C. Lymphocytes were isolated from lungs, spleen, mediastinal lymph nodes, and bone marrow, and ELISPOTs and FACS staining were performed immediately. Peripheral blood monocytes were isolated from whole blood with 4% sodium citrate as anti-coagulant through a HistoPaque density gradient centrifugation at 1500 g for 15 minutes. Remaining cells were suspended in 80% fetal bovine serum (Corning Cellgro, Tewksbury,

Massachusetts)/20% dimethyl sulfoxide (DMSO) (Sigma-Aldrich, St. Louis, Missouri) and stored at -80°C. Left lung lobes were homogenized in serum-free DMEM and stored in 1x Halt Protease Inhibitor (ThermoFisher) for viral titers. The titers were determined by plaque assay in MDCK cells (American Type Culture Collection, Manassas, Virginia) as described previously [42].

Cytokine and hormone quantification in the lungs, sera, and placenta

Cytokines were quantified in sera, lungs, and placentas at days 4 and 7 post-infection using a Bio-Rad 23-plex Mouse Group I Cytokine Assay Kit from Bio-Rad (Hercules, CA). Progesterone, prostaglandin F₂ α and E₂ (PGF₂ α and PGE₂), and estradiol 17- α were quantified with hormone ELISA kits from ALPCO (Salem, NH). Cytokine and hormone expression values were normalized by dilution and tissue lysate concentration. Fold changes are plotted in heat maps and raw values are reported in supplementary tables.

Antibody characterization and binding studies

Antibody titers were determined via ELISA with biotinylated anti-IgG, IgG1, IgG2a antibodies (Southern Biotech, Birmingham, AL) against recombinant HA A/California/07/2009 as described previously [43]. Hemagglutination inhibition (HAI) assays were performed with PBS washed turkey red blood cells in accordance with the WHO Laboratory Diagnostics Manual [44]. Antibody avidity was measured by ELISA in the presence of increasing concentrations (0 - 2.0 M) of the chaotropic agent guanidine thiocyanate (GTC) (Sigma Aldrich) following binding to recombinant HA A/California/07/2009 (BEI Resources) as previously described [43]. The avidity index was calculated in Prism 7.03 Software (GraphPad, La Jolla, CA) by determining the GTC molar concentration (IC₅₀) needed to reduce the initial optical density of bound IgG antibody by 50%.

Innate immune cell and germinal center activation.

Single cell suspensions were obtained from blood, spleen, liver, uterus, placenta, and lung-draining mediastinal lymph nodes (MLN). For innate immune cell analysis, cells were stained with anti-CD11c (N418), -CD11b (M1/70), -Ly6G (1A8), -F4/80 (BM8), -CD45 (30-F11), -IA/IE (M5/114.15.2), -CD64 (C54-5/7.1), and -CD24 (30-F1) (BioLegend, San Diego, California). For plasmablast and germinal center (GC+) cell analysis, cells were stained with anti-CD4 (GK1.5), -CD8a (53-6.7), -CD11b (M1/70), -CD19 (6D5), -B220 (RA3-6B2), -CD138 (281-2), and -GL7 (BioLegend). Dead cells were excluded by gating out cells positive for Live/Dead fixable dead stain (eBioscience). Following fixation in 2% paraformaldehyde, samples were acquired with an LSRII (BD Biosciences, San Jose, California) and analyzed using FlowJo v 9 (FlowJo LLC, BD, Franklin Lakes, NJ). Gating methodologies for innate immune cell and germinal center activated populations are depicted in Supplemental Figure 1.

Quantification of antibody and cytokine secreting cells from lymph nodes, spleens, and lungs

To quantify antibody-secreting cells (ASCs), poly-vinylidene fluoride ELISPOT plates (EMD Millipore, Burlington, MA) were coated with 200 ng/well recombinant H1 A/California/07/2009 HA protein (NR-13691) (BEI Resources). Splenocytes and lung lymphocytes (1×10^6 cells/well) were incubated at 37°C for 16 hours. Influenza-specific antibodies were detected using isotype-specific, biotinylated murine Ig antibodies (IgA, IgM, and IgG, Southern Biotech, Birmingham, AL). To detect cytokine secreting cells (CSC), 5×10^5 cells/well were overlaid in ELISPOT plates (EMD Millipore, Burlington, MA) coated with 100 ng/well of capture antibody (BD Biosciences, San Jose, CA). Cells were stimulated with 200 ng/well H1N1 A/Christchurch/16/2010 for 48 hours

at 37°C. CSC plates were washed and incubated with 100 ng/well biotinylated detection antibodies (IL-4 and IFN- γ , BD Biosciences) and developed with streptavidin-HRP and diaminobenzidine. Plates were analyzed via ImmunoSpot Reader 5.0 (Cellular Technology Limited, **Shaker Heights, OH**) and normalized to 1×10^6 cells/well.

Statistical Analysis

Student t-tests (unpaired, uncorrected, parametric), one-way ANOVAs and two-way ANOVAs were performed in GraphPad Prism 7. Data was graphed and annotated in Prism 7 also. Data available upon request.

Results

Infection reduces gestation length and increases offspring morbidity and placental degradation.

To establish a long-lived model of influenza infection and to more accurately simulate a low dose infection, cohorts of female 8-week-old pregnant and non-pregnant BALB/c mice were infected with 0.5xLD₅₀ mouse-adapted H1N1 A/California/07/2009 mid-gestation, on day 12 of pregnancy (E12) as determined by a 20% weight gain from initial body weight (Fig 1A). Non-pregnant mice sub-lethally infected lost up to 10% of their initial body weight at 7 d.p.i. and regained that weight at the end of the observational period (14 d.p.i.). Pregnant mice infected at E12 lost 10% more body weight than naïve pregnant controls following parturition (7 d.p.i., E19) and remained 16% lower than pregnant controls at 14 d.p.i. (Fig 1A). Viral growth was initially increased in the lungs of pregnant mice at 2 days post infection (d.p.i.) but otherwise, viral clearance was not affected by pregnancy status (Fig 1B). Delivery is evident when weight loss drops significantly in pregnant mice; infection reduced gestation length by 2 days (Fig 1C). Lung histology sections at 4 d.p.i. from mock-infected and virus-infected pregnant and non-pregnant mice showed that airway inflammation is elevated during pregnancy even prior to infection, and that infection increased cellular infiltration and airway inflammation in pregnant mice compared with non-pregnant mice (Fig 1E). Placental histology showed that infection increased the incidence of fetal endothelial death in the spongiotrophoblast layer, as have previously observed in studies of lethal seasonal H1N1 infection during pregnancy [22].

Pregnancy affects the expression of chemoattractant cytokines in the lungs following infection.

Lethal doses of H1N1 virus have been shown to interfere with hormonal expression during pregnancy [16]. Hormonal and cytokine expression was quantified in the lungs to determine how

pregnancy alters the innate immune response to virus infection at 4 d.p.i and at the height of immunopathology at 7 d.p.i. (Fig 2). Lung expression of estradiol was increased by influenza virus infection in both pregnant and non-pregnant mice, while lung expression of progesterone was decreased by 50% during pregnancy (Fig 2A, B). IL-6 upregulation was delayed in pregnancy at 4 d.p.i. compared to infected non-pregnant mice, with IL-6 expression abating in non-pregnant mice at 7 d.p.i. but increasing in pregnant mice (Fig 2C). Similarly, IL-12p40, KC, and MIP-1 α were reduced in pregnant lungs at 4 d.p.i. (Fig 2D, 2E, 2F); these cytokines are secreted by activated lung endothelium and recruit neutrophils to the site of infection [45-47]. MCP-1 expression was elevated at the same levels in pregnant and non-pregnant mice at 4 d.p.i but increased 4-fold while non-pregnant lung expression of MCP-1 remained nearly constant during the infection response period (Fig 2G). Notably, MIP-1 β expression was elevated equally in pregnant and non-pregnant mice following infection (Fig 2H), while RANTES expression was decreased at both 4 and 7 d.p.i (Fig 2I). Infection resulted in the upregulation of inflammatory and innate cell recruiting cytokines at days 4 and 7 post infection, and the subtleties by which pregnancy impacts their expression are summarized in a heat map (Fig 2J) and Suppl Table 1. These data illustrate the early suppression of inflammation in the lungs following infection during pregnancy and followed by late stage inflammation that correlates with immunopathology and the initiation of pre-term birth at 7 d.p.i. (Fig 1).

Effects of infection in the lungs spillover into serum expression in pregnant females. To measure the extent of systemic hormonal and cytokine signaling post infection, hormones and cytokines were quantified in the sera at 4 d.p.i and 7 d.p.i. (Fig 3). Similar to lung tissue response following infection, serum expression of estradiol was elevated during pregnancy post-infection; however,

unlike expression in the lungs, serum levels of estradiol in non-pregnant mice were unaffected by infection (Fig 3A). Progesterone expression was significantly elevated at 4 d.p.i (Fig 3B). These differences between pregnant and non-pregnant responses suggest that infection requires a broader hormonal coordination of cytokine expression during pregnancy than needed by non-pregnant females. Infection increased serum expression of IL-17 significantly during pregnancy (Fig 3C). Interleukin-17 is noted for its induction of Th17 cells; both are hallmarks of immunopathology during viral respiratory illness [48, 49]. IL-1 β and IL-12p40 expression was upregulated at approximately similar levels in pregnant and non-pregnant mice post-infection (Fig 3D, E), while pregnancy prolonged the expression of G-CSF at 7 d.p.i. (Fig 3F). While sublethal H1N1 virus infection in the lungs had limited impact on the number and variety of systemic inflammatory cytokine activation, infection activated a broader array of inflammatory cytokines in pregnant mice that take require longer time to resolve than in mice that are not pregnant (Fig 3G) (Suppl. Table 2).

Influenza viral infection in maternal lungs results in upregulation of placental inflammatory cytokines. Placental health and successful pregnancy is dependent on suppression of inflammatory cytokines and the continuous expression of progesterone. Viral RNA was not detected in the placenta via RT-PCR (data not shown), and low dose infection did not appear to disrupt abortifacient prostaglandin F2 α (PGF2 α), progesterone, and estradiol expression in placental tissue 7 d.p.i. (Fig 4A, B, C). Infection during pregnancy resulted in expression of IL-1 α (Fig 4D) and IL-9 (Fig 4E) which are associated with enhanced immunopathology following H1N1 influenza A viral infection [50, 51]. Infection increased the expression of G-CSF (Fig 4F), MIP-1 α (Fig 4G), RANTES (Fig 4H), and KC (Fig 4I), which are all involved in the recruitment of innate immune

and T cells following influenza A virus infection [52]. Infection slightly upregulated most cytokines at 7 d.p.i. in the placenta (Fig 4J); these values and fold changes are reported in Suppl. Table 3. These contrasting effects of activation highlight the tension between cellular activation and immunosuppression and describe the immune environment in which antiviral cellular activation occurs.

Pregnancy reduces innate immune cell populations activated by influenza viral infection.

Immunosuppression of uterine and placental natural killer (NK) cells via regulatory T cells (Tregs) is a commonly described tenet of reproductive immunology [1, 53]. In order to determine how pregnancy had affected innate immune cell activation in response to infection, lymphocytes from the uterus, placenta, lungs and peripheral blood mononuclear cells (PBMCs) were harvested at 2 d.p.i and stained for innate immune cell markers (Suppl. Figure 1A). Uterine monocyte numbers were elevated in naïve pregnant mice, and infection increased this population significantly (Fig 5A). While infection increased uterine dendritic cells (DCs) in non-pregnant mice, pregnancy downregulated the number of DCs in naïve and infected mice (Fig 5B). While uterine NK cells were low, lung NK cells were elevated in naïve pregnant mice; infection caused significant reduction of NK cells in both compartments (Fig 5C, D). Similarly, pregnancy reduced the lung DC response to infection compared with non-pregnant infected mice (Fig 5D) (Fig E). PBMCs were elevated marginally following infection during pregnancy relative to non-pregnant mice (Fig 5F). With the exception of monocytes in the lung and blood, infection at mid-gestation resulted in the reduction of innate immune cell populations, indicating a protective effect against inflammation in the uterus and placenta.

Pregnancy delays GC activation of B cells in the spleen following infection. Influenza virus-neutralizing antibodies are secreted by plasmablasts following antigen presentation from lung dendritic cells and macrophages; naïve B cells with BCRs specific for the virus are activated with co-stimulation from follicular T cells (TFHs) and mature in germinal centers (GCs) in the mediastinal lymph nodes (MLNs) located adjacent to the lungs and in the spleen [54]. Lymphocytes from MLNs, spleens, and lungs were isolated and stained for B cell markers to determine how the pregnancy-altered innate immune environment affected the GC-activation of B cells and their development into plasmablasts in the spleen and lungs (Suppl. Fig 1B). The rate of activation of GC⁺ (CD19⁺GL7⁺) B cells in the MLNs was similar between pregnant and non-pregnant mice (Fig 6A). However, as these cells were trafficked to the spleen to undergo secondary maturation, the numbers of GC⁺ cells in pregnant mice were decreased compared to non-pregnant mice (Fig 6B). This indicates that pregnancy may reduce the cellular trafficking of activated B cells to secondary lymphoid tissue to avoid the development of anti-fetal antibodies.

Pregnancy results increased IgA-secreting cells in the lungs 6 weeks post infection. Influenza virus-specific B cells in the spleen and lungs were measured in order to quantify how delayed trafficking of plasmablasts in the spleen affected the longevity of virus-specific antibody secreting cells (ASCs) in these compartments. Importantly, mice infected during pregnancy have given birth at 7 d.p.i.; offspring that survived were weaned at 21 days of age (28 d.p.i.). Surprisingly, anti-H1N1 A/California/07/2009 IgA⁻, IgM⁻, and IgG-secreting cells in the spleen were not significantly different between mice infected during pregnancy and non-pregnant infected mice (Fig 7A, B, C). At 42 d.p.i., memory B cell populations were equivalent between pregnant and non-pregnant mice in the spleen and in the lungs (Fig 7D). However, virus-specific IgA-secreting

cells were increased in the lungs at 42 d.p.i. (Figure 7E). Pregnancy has been shown to increase the homing of IgA⁺ B cells to mammary ducts which affords offspring improved immunity through breastmilk [35]. Enhanced IgA-secreting cells in mucosal tissues may be one advantage pregnancy confers to mothers infected by influenza virus mid-gestation.

Pregnancy reduced influenza-specific class-switched antibody expression, binding avidity to H1 recombinant protein, and HAI titers. Circulating antibody expression is important for preventing future viral infection. We found that serum levels of IgG, IgG1, and IgG2a against recombinant H1 A/California/07/2009 were the same between mice infected during pregnancy and non-pregnant infected mice. Interestingly, the former group had significantly greater virus-specific IgG antibody expression with equivalent or reduced class-switched IgG1 and IgG2a sub-isotypes compared to the latter (Figure 8A, B, C). Mice infected during pregnancy generated antibodies with reduced antibody avidity and virus hemagglutinin inhibition (HAI) titers, indicating that despite equivalent activation of IgG-secreting cells in the spleen, influenza virus infection during pregnancy reduces the maternal immune system's ability to generate highly specific, virus-binding antibodies (Fig 8D, E; Fig 7C).

Pregnancy enhances long lived virus-specific inflammatory T cell responses in the lungs. In order to determine how pregnancy impacted the development of cellular memory responses following influenza virus infection, lymphocytes were isolated from the spleen and lungs and stimulated with recombinant H1 A/California/07/2009 protein. Similarly to ASCs, pregnancy did not alter the activation of splenic populations of H1-specific IL-4⁻, IFN- γ ⁻, and IL-10-secreting cells up to 42 d.p.i. (Fig 9A, B, C). Pregnancy did not affect the number of CD4⁺ or CD8⁺ cells

in spleen or lungs 42 d.p.i. (Figure 9D). However, pregnancy increased the number of IFN- γ -secreting cells in the lungs substantially, which may be a result of the increased inflammatory cytokine signaling at later time points during infection (Figure 9E, Figure 2). It is also possible that a difference in viral load (Fig 1C) induced the increase of IgA-secreting cells (Fig 7E) and INF- γ -secreting cells (Fig 9E) in mice infected during pregnancy. Henceforth the variation in vaccination and infection responses during pregnancy on cellular and humoral immunity was examined as well.

Boost vaccination during pregnancy improves IgG2a expression and enhances vaccine-specific IFN- γ secreting cells in the spleen. Influenza vaccination primes the immune system to respond quickly and efficiently to influenza virus with neutralizing antibodies and virus-specific T cell help. Mice were vaccinated with 1 μ g H1 of A/California/07/2009 recombinant protein at E12 and boosted with the same dose 42 days later (d.p.p.) to study antibody expression and class switching during and post pregnancy. Serum levels of IgM, IgG, and IgG1 were equivalent between vaccinated groups after prime immunization (Fig 10A, B, C). Interestingly, pregnancy amplified the IgG2a response to boost vaccination (Fig 10D).

Antibody- and cytokine-secreting cells were measured at early time points in cellular maturation and pre- and post-boost. Vaccine-specific ASCs were generated at similar levels in pregnant and non-pregnant mice at 7 d.p.p., while at 14 d.p.p., mice vaccinated during pregnancy showed elevated IgA-secreting cell numbers in the spleen and the lungs (Fig 11A). By day 42 ASC populations in the lungs and spleen were equivalent between mice that were pregnant or non-pregnant during vaccination (Fig 11B). Upon boost vaccination, mice from the pregnant cohort expressed reduced IgA secreting cells in the spleen and increased IgG cells compared to the non-

pregnant cohort (Fig 11C). Mice vaccinated during pregnancy generated increased numbers of IL-4-secreting cells at 7 d.p.p. but no significant difference was observed in activation of CSCs between vaccinated groups by 14 d.p.p. (Fig 11D). Pregnancy reduced the numbers of splenic IL-4- and IFN- γ -secreting cells at 42 d.p.p. (Fig 11E); however, boost vaccination resulted in a 10-fold increase in vaccine-specific IFN- γ -secreting cells (Fig 11F). This improvement in systemic cellular immune responses may warrant further examination as an opportunity for improving maternal vaccination.

Discussion

The 2009 H1N1 influenza virus pandemic caused a surge of research into the mechanisms leading to enhanced pathogenesis. Clinical research highlighted the intensity of the lung pathology and increased maternal and fetal demise in infected pregnant human population that was further observed in murine models [1, 5-7]. However, in the years since the pandemic, the H1N1 A/California/07/2009 strain became a circulating seasonal strain and was incorporated into the subunit vaccine[55]. In this work, we revisited how a swine origin reassortant influenza virus caused severe illness in an immunologically naïve pregnant population and their offspring and how pregnancy hormones and dysregulated cytokine expression affected the development of cellular and humoral immunity. This work is significant in that novel avian species may unpredictably cause a human pandemic; avian H5N1 and H7N9 viruses have been shown to cause excessive mortality in pregnant women in the few instances of human infection [56, 57].

Immediately following the 2009 H1N1 influenza virus pandemic, several groups examined how the pandemic virus strain caused increased mortality in pregnant mice and their offspring, enhanced lung immunopathology and dysregulated progesterone and estrogen expression [16, 17, 58]. Here, we demonstrated that even low doses of H1N1 A/California/07/2009 (30 p.f.u.) could recapitulate the preterm labor, low birth-weight and lung immunopathology typical of severe but non-fatal 2009 H1N1 pandemic cases in pregnant women [58-60]. Similar to the Marcelin et al report immunopathology was not dependent on increased viremia, but rather on inflammatory cytokines and CD8⁺ T cell infiltration [61]. We demonstrate that H1N1 A/California/07/2009 dysregulated serum and lung estrogen and progesterone expression and increased lung expression of IL-6, MCP-1, MIP-1 α , MIP-1 β , and RANTES in infected pregnant mice within 7 d.p.i. In clinical reports from the 2009 pandemic, increased expression of these cytokines was associated

with fatal influenza viral disease [51, 62, 63]. Elevated serum IL-17 and G-CSF expression was associated with fatal outcome in humans during the 2009 pandemic, and IL-17 and activated Th17 cells are linked to acute lung injury in 2009 H1N1 viral infection in mice [48, 49]. In our pregnant murine model, we found increased serum expression of IL-17 following H1N1 influenza A viral infection, and serum and placental G-CSF expression. Pregnant mice activated fewer NK cells and DCs in the lungs following infection than non-pregnant infected mice. Thus, pregnancy increases maternal vulnerability to sublethal viral infection through ineffective cytokine expression and innate cellular recruitment to the site of infection, which may result in enhanced stress on the maternal endocrine system and placental health.

Here we demonstrate the long-term implications of pregnancy on anti-H1N1 immune responses and describe improved mucosal immunity via increased numbers of IgA- secreting cells and virus-specific IFN- γ secreting T cells in the lungs. However, pregnancy decreased antibody specificity and virus-binding in the sera, indicating there may be some benefit to modifying immune products that might activate inflammation in the placenta. GC activation of B cells appeared to be delayed in the spleens of mice infected during pregnancy, but activation levels in the pregnant cohort following delivery caught up with non-pregnant infected mice. This indicates that pregnancy hormones may play some role in reducing systemic immune responses that may be circulated to the fetus until after gestation. Flow cytometry analysis of trafficking markers expressed on lymphocytes from the MLNs, spleen, and lungs following infection during pregnancy or following exposure to progesterone and estrogen may further elucidate how hormones may coordinate this phenotype. Sequencing analysis of immunoglobulin genes in activated plasmablasts and memory B cells following influenza A virus infection during pregnancy are

needed to determine how progesterone expression may be influencing somatic hypermutation and the generation of high affinity antibodies against influenza antigens.

We also studied the effect of pregnancy on cellular and humoral responses to H1N1 A/California/07/2009 in part because replicating virus in the lungs during infection may increase the antigen load, and thus, the variability in our results and because pregnant women are recommended to get the quadrivalent vaccination which until recently included subunit H1N1 A/California/07/2009 [64-66]. Vaccination generated similar serum levels of antibody expression between mice vaccinated during pregnancy and vaccinated non-pregnant controls; however, surprisingly, upon boost vaccination pregnancy increased the IgG2a recall response typically induced by Th1 cytokine expression [9, 67]. Unlike infection-induced ASCs in pregnant mice, prime-boost vaccination during pregnancy did not confer superior IgA⁺ ASCs in the lungs but did increase the splenic population of vaccine specific IFN- γ -secreting cells.

Correlating these results to clinical results is challenging, in part because there are few studies comparing vaccination of healthy pregnant women with healthy non-pregnant women and also because clinical studies tend to report few correlates of immunity beyond HAI titer and IgG titer. Plasmablast induction by vaccination has been shown to be unaffected by pregnancy in women, but whether pregnancy affects seroconversion (based on a 4-fold change in HAI titers following vaccination) is disputed [40, 41, 68, 69]. Sperling et al. reported that the rate of seroconversion in cohorts of women vaccinated during pregnancy is dependent on the trimester in which vaccination occurred, with the highest rates of conversion occurring in women vaccinated in late third trimester or post-partum [70]. They also determined that higher baseline antibody levels and previous vaccination history reduced pregnant women's antibody responses to annual vaccination. Analysis of serum antibody titers in pregnant vaccinated women and in the cord blood of their neonates

showed that 25 μg of subunit H1 A/California/07/09 was sufficient to generate HAI titers $\geq 1:40$ [71]. We present a study in which influenza virus infection and vaccination during pregnancy conferred improved mucosal immunity compared with non-pregnant mice; however, class-switched, high affinity anti-H1N1 antibodies were reduced in maternal sera. Further studies are needed to elucidate the mechanisms by which pregnancy causes these phenotypes and whether these are specific to influenza vaccination or apply more broadly to immunization during pregnancy.

Acknowledgements

We thank Ali Ellebedy (Washington University in St. Louis) for technical training and Nadia Lelutiu for critical reading of this manuscript. We would also like to thank Kiran Gill and Barbara Cervalho in the Flow Cytometry Core and David Lee in the Immunology Core for facility and technical support at the Emory Vaccine Center/Yerkes National Primate Research Center and the staff in the Division of Animal Resources in Whitehead Biomedical Research Building at Emory University.

Funding Sources

Funding for this research was provided through Centers of Excellence for Influenza Research and Surveillance (HHSN272201400004C; Walt Orenstein, MD/DSc, Center PI).

References

1. Raj RS, Bonney EA, Phillippe M. Influenza, immune system, and pregnancy. *Reprod Sci.* 2014;21(12):1434-51. doi: 10.1177/1933719114537720. PubMed PMID: 24899469; PubMed Central PMCID: PMC4231130.
2. Louie JK, Salibay CJ, Kang M, Glenn-Finer RE, Murray EL, Jamieson DJ. Pregnancy and severe influenza infection in the 2013-2014 influenza season. *Obstet Gynecol.* 2015;125(1):184-92. Epub 2015/01/07. doi: 10.1097/AOG.0000000000000593. PubMed PMID: 25560123.
3. Mosby LG, Rasmussen SA, Jamieson DJ. 2009 pandemic influenza A (H1N1) in pregnancy: a systematic review of the literature. *Am J Obstet Gynecol.* 2011;205(1):10-8. Epub 2011/02/25. doi: 10.1016/j.ajog.2010.12.033. PubMed PMID: 21345415.
4. Callaghan WM, Creanga AA, Jamieson DJ. Pregnancy-Related Mortality Resulting From Influenza in the United States During the 2009-2010 Pandemic. *Obstet Gynecol.* 2015;126(3):486-90. Epub 2015/08/06. doi: 10.1097/AOG.0000000000000996. PubMed PMID: 26244541; PubMed Central PMCID: PMC4557717.
5. Jamieson DJ, Honein MA, Rasmussen SA, Williams JL, Swerdlow DL, Biggerstaff MS, et al. H1N1 2009 influenza virus infection during pregnancy in the USA. *Lancet.* 2009;374(9688):451-8. Epub 2009/08/01. doi: 10.1016/S0140-6736(09)61304-0. PubMed PMID: 19643469.
6. Siston AM, Rasmussen SA, Honein MA, Fry AM, Seib K, Callaghan WM, et al. Pandemic 2009 influenza A(H1N1) virus illness among pregnant women in the United States. *JAMA : the journal of the American Medical Association.* 2010;303(15):1517-25. doi: 10.1001/jama.2010.479. PubMed PMID: 20407061.

7. Robinson DP, Klein SL. Pregnancy and pregnancy-associated hormones alter immune responses and disease pathogenesis. *Hormones and behavior*. 2012;62(3):263-71. doi: 10.1016/j.yhbeh.2012.02.023. PubMed PMID: 22406114; PubMed Central PMCID: PMC3376705.
8. Wira CR, Rodriguez-Garcia M, Patel MV. The role of sex hormones in immune protection of the female reproductive tract. *Nat Rev Immunol*. 2015;15(4):217-30. Epub 2015/03/07. doi: 10.1038/nri3819. PubMed PMID: 25743222; PubMed Central PMCID: PMC4716657.
9. Druckmann R, Druckmann MA. Progesterone and the immunology of pregnancy. *The Journal of steroid biochemistry and molecular biology*. 2005;97(5):389-96. doi: 10.1016/j.jsbmb.2005.08.010. PubMed PMID: 16198558.
10. Engler JB, Kursawe N, Solano ME, Patas K, Wehrmann S, Heckmann N, et al. Glucocorticoid receptor in T cells mediates protection from autoimmunity in pregnancy. *Proc Natl Acad Sci U S A*. 2017;114(2):E181-E90. Epub 2017/01/05. doi: 10.1073/pnas.1617115114. PubMed PMID: 28049829; PubMed Central PMCID: PMC5240705.
11. Hughes GC, Clark EA, Wong AH. The intracellular progesterone receptor regulates CD4+ T cells and T cell-dependent antibody responses. *J Leukoc Biol*. 2013;93(3):369-75. Epub 2013/01/12. doi: 10.1189/jlb.1012491. PubMed PMID: 23307939; PubMed Central PMCID: PMC3579022.
12. Garcia-Rio F, Pino JM, Gomez L, Alvarez-Sala R, Villasante C, Villamor J. Regulation of breathing and perception of dyspnea in healthy pregnant women. *Chest*. 1996;110(2):446-53. Epub 1996/08/01. PubMed PMID: 8697850.

13. Milne JA. The respiratory response to pregnancy. *Postgrad Med J.* 1979;55(643):318-24. Epub 1979/05/01. PubMed PMID: 382162; PubMed Central PMCID: PMC2425453.
14. Jain R, Ray JM, Pan JH, Brody SL. Sex hormone-dependent regulation of cilia beat frequency in airway epithelium. *Am J Respir Cell Mol Biol.* 2012;46(4):446-53. Epub 2011/10/29. doi: 10.1165/rcmb.2011-0107OC. PubMed PMID: 22033264; PubMed Central PMCID: PMC3359952.
15. Sathish V, Martin YN, Prakash YS. Sex steroid signaling: implications for lung diseases. *Pharmacol Ther.* 2015;150:94-108. Epub 2015/01/18. doi: 10.1016/j.pharmthera.2015.01.007. PubMed PMID: 25595323; PubMed Central PMCID: PMC4523383.
16. Kim HM, Kang YM, Song BM, Kim HS, Seo SH. The 2009 pandemic H1N1 influenza virus is more pathogenic in pregnant mice than seasonal H1N1 influenza virus. *Viral immunology.* 2012;25(5):402-10. doi: 10.1089/vim.2012.0007. PubMed PMID: 22985287.
17. Chan KH, Zhang AJ, To KK, Chan CC, Poon VK, Guo K, et al. Wild type and mutant 2009 pandemic influenza A (H1N1) viruses cause more severe disease and higher mortality in pregnant BALB/c mice. *PloS one.* 2010;5(10):e13757. doi: 10.1371/journal.pone.0013757. PubMed PMID: 21060798; PubMed Central PMCID: PMC2966430.
18. Kim JC, Kim HM, Kang YM, Ku KB, Park EH, Yum J, et al. Severe pathogenesis of influenza B virus in pregnant mice. *Virology.* 2014;448:74-81. doi: 10.1016/j.virol.2013.10.001. PubMed PMID: 24314638.

19. Pazos MA, Kraus TA, Munoz-Fontela C, Moran TM. Estrogen mediates innate and adaptive immune alterations to influenza infection in pregnant mice. *PloS one*. 2012;7(7):e40502. doi: 10.1371/journal.pone.0040502. PubMed PMID: 22792357; PubMed Central PMCID: PMC3390370.
20. Robinson DP, Hall OJ, Nilles TL, Bream JH, Klein SL. 17beta-estradiol protects females against influenza by recruiting neutrophils and increasing virus-specific CD8 T cell responses in the lungs. *J Virol*. 2014;88(9):4711-20. doi: 10.1128/JVI.02081-13. PubMed PMID: 24522912; PubMed Central PMCID: PMC3993800.
21. Robinson DP, Lorenzo ME, Jian W, Klein SL. Elevated 17beta-estradiol protects females from influenza A virus pathogenesis by suppressing inflammatory responses. *PLoS pathogens*. 2011;7(7):e1002149. doi: 10.1371/journal.ppat.1002149. PubMed PMID: 21829352; PubMed Central PMCID: PMC3145801.
22. Littauer EQ, Esser ES, Antao OQ, Vassilieva EV, Compans RW, Skountzou I. H1N1 influenza virus infection results in adverse pregnancy outcomes by disrupting tissue-specific hormonal regulation. *PLoS pathogens*. 2017;13(11):e1006757. doi: 10.1371/journal.ppat.1006757. PubMed PMID: 29176767; PubMed Central PMCID: PMC5720832.
23. Wetendorf M, DeMayo FJ. Progesterone receptor signaling in the initiation of pregnancy and preservation of a healthy uterus. *Int J Dev Biol*. 2014;58(2-4):95-106. Epub 2014/07/16. doi: 10.1387/ijdb.140069mw. PubMed PMID: 25023675; PubMed Central PMCID: PMC4413906.
24. Phillips RJ, Fortier MA, Lopez Bernal A. Prostaglandin pathway gene expression in human placenta, amnion and chorion is differentially affected by preterm and term

- labour and by uterine inflammation. *BMC Pregnancy Childbirth*. 2014;14:241. Epub 2014/07/23. doi: 10.1186/1471-2393-14-241. PubMed PMID: 25048443; PubMed Central PMCID: PMC4223419.
25. Mackenzie JS, Williams K, Papadimitriou J. Influenza A virus and its influence on the outcome of pregnancy in the mouse. *Developments in biological standardization*. 1977;39:489-96. PubMed PMID: 604135.
26. Meijer WJ, Wensing AM, Bruinse HW, Nikkels PG. High rate of chronic villitis in placentas of pregnancies complicated by influenza A/H1N1 infection. *Infect Dis Obstet Gynecol*. 2014;2014:768380. doi: 10.1155/2014/768380. PubMed PMID: 24693211; PubMed Central PMCID: PMC4223419.
27. Engels G, Hierweger AM, Hoffmann J, Thieme R, Thiele S, Bertram S, et al. Pregnancy-Related Immune Adaptation Promotes the Emergence of Highly Virulent H1N1 Influenza Virus Strains in Allogeneically Pregnant Mice. *Cell host & microbe*. 2017;21(3):321-33. doi: 10.1016/j.chom.2017.02.020. PubMed PMID: 28279344.
28. Hall OJ, Nachbagauer R, Vermillion MS, Fink AL, Phuong V, Krammer F, et al. Progesterone-Based Contraceptives Reduce Adaptive Immune Responses and Protection against Sequential Influenza A Virus Infections. *J Virol*. 2017;91(8). doi: 10.1128/JVI.02160-16. PubMed PMID: 28179523; PubMed Central PMCID: PMC5375688.
29. Zhang L CK, Li MQ, Li DJ, Yao XY. Mouse endometrial stromal cells and progesterone inhibit the activation and regulate the differentiation and antibody secretion of mouse B cells. *Int J Clin Exp Pathol* 2014;7(1):123-33. PubMed Central PMCID: PMC4223419.

30. Pazos M, Sperling RS, Moran TM, Kraus TA. The influence of pregnancy on systemic immunity. *Immunologic research*. 2012;54(1-3):254-61. doi: 10.1007/s12026-012-8303-9. PubMed PMID: 22447351.
31. Kay L, Medina GS, and Paul W. Kincade. Suppression of B Lymphopoiesis during Nomial Pregnancy. *The Journal of experimental medicine*. 1993;93(11):1507-15.
32. Zheng R, Qin X, Li Y, Yu X, Wang J, Tan M, et al. Imbalanced anti-H1N1 immunoglobulin subclasses and dysregulated cytokines in hospitalized pregnant women with 2009 H1N1 influenza and pneumonia in Shenyang, China. *Human immunology*. 2012;73(9):906-11. doi: 10.1016/j.humimm.2012.06.005. PubMed PMID: 22750537; PubMed Central PMCID: PMC2750537.
33. Gordon CL, Johnson PD, Permezel M, Holmes NE, Gutteridge G, McDonald CF, et al. Association between severe pandemic 2009 influenza A (H1N1) virus infection and immunoglobulin G(2) subclass deficiency. *Clinical infectious diseases : an official publication of the Infectious Diseases Society of America*. 2010;50(5):672-8. doi: 10.1086/650462. PubMed PMID: 20121412; PubMed Central PMCID: PMC20121412.
34. Takeda S, Hisano M, Komano J, Yamamoto H, Sago H, Yamaguchi K. Influenza vaccination during pregnancy and its usefulness to mothers and their young infants. *J Infect Chemother*. 2015;21(4):238-46. doi: 10.1016/j.jiac.2015.01.015. PubMed PMID: 25708925.
35. Mbawuike IN, Six HR, Cate TR, Couch RB. Vaccination with inactivated influenza A virus during pregnancy protects neonatal mice against lethal challenge by influenza A viruses representing three subtypes. *J Virol*. 1990;64(3):1370-4. PubMed PMID: 2304146; PubMed Central PMCID: PMC249259.

36. Jamieson DJ, Kissin DM, Bridges CB, Rasmussen SA. Benefits of influenza vaccination during pregnancy for pregnant women. *Am J Obstet Gynecol.* 2012;207(3 Suppl):S17-20. Epub 2012/09/07. doi: 10.1016/j.ajog.2012.06.070. PubMed PMID: 22920053; PubMed Central PMCID: PMC4552345.
37. Omer SB, Bednarczyk R, Madhi SA, Klugman KP. Benefits to mother and child of influenza vaccination during pregnancy. *Human vaccines & immunotherapeutics.* 2012;8(1):130-7. Epub 2012/01/19. doi: 10.4161/hv.8.1.18601. PubMed PMID: 22251998.
38. Ludvigsson JF, Zugna D, Cnattingius S, Richiardi L, Ekblom A, Ortqvist A, et al. Influenza H1N1 vaccination and adverse pregnancy outcome. *Eur J Epidemiol.* 2013;28(7):579-88. Epub 2013/05/30. doi: 10.1007/s10654-013-9813-z. PubMed PMID: 23715672.
39. Groom HC, Henninger ML, Smith N, Koppolu P, Cheetham TC, Glanz JM, et al. Influenza Vaccination During Pregnancy: Influenza Seasons 2002-2012, Vaccine Safety Datalink. *Am J Prev Med.* 2016;50(4):480-8. Epub 2015/11/04. doi: 10.1016/j.amepre.2015.08.017. PubMed PMID: 26526159.
40. Schlaudecker EP, McNeal MM, Dodd CN, Ranz JB, Steinhoff MC. Pregnancy modifies the antibody response to trivalent influenza immunization. *The Journal of infectious diseases.* 2012;206(11):1670-3. doi: 10.1093/infdis/jis592. PubMed PMID: 22984116.
41. Kay AW, Bayless NL, Fukuyama J, Aziz N, Dekker CL, Mackey S, et al. Pregnancy Does Not Attenuate the Antibody or Plasmablast Response to Inactivated Influenza Vaccine. *J Infect Dis.* 2015;212(6):861-70. Epub 2015/03/06. doi: 10.1093/infdis/jiv138. PubMed PMID: 25740957; PubMed Central PMCID: PMC4548461.

42. Skountzou I, Quan FS, Jacob J, Compans RW, Kang SM. Transcutaneous immunization with inactivated influenza virus induces protective immune responses. *Vaccine*. 2006;24(35-36):6110-9. doi: 10.1016/j.vaccine.2006.05.014. PubMed PMID: 16766095.
43. Esser ES, Romanyuk A, Vassilieva EV, Jacob J, Prausnitz MR, Compans RW, et al. Tetanus vaccination with a dissolving microneedle patch confers protective immune responses in pregnancy. *Journal of controlled release : official journal of the Controlled Release Society*. 2016;236:47-56. doi: 10.1016/j.jconrel.2016.06.026. PubMed PMID: 27327766.
44. WHO/CDS/CSR/NCS. WHO Manual of Animal Influenza Diagnosis and Surveillance. : Department of Communicable Disease Surveillance and Response; 2002.
45. Wareing MD, Lyon A, Inglis C, Giannoni F, Charo I, Sarawar SR. Chemokine regulation of the inflammatory response to a low-dose influenza infection in CCR2^{-/-} mice. *J Leukoc Biol*. 2007;81(3):793-801. Epub 2006/12/21. doi: 10.1189/jlb.0506299. PubMed PMID: 17179466.
46. Driscoll KE. Macrophage inflammatory proteins: biology and role in pulmonary inflammation. *Exp Lung Res*. 1994;20(6):473-90. Epub 1994/11/01. doi: 10.3109/01902149409031733. PubMed PMID: 7882902.
47. Sugamata R, Dobashi H, Nagao T, Yamamoto K, Nakajima N, Sato Y, et al. Contribution of neutrophil-derived myeloperoxidase in the early phase of fulminant acute respiratory distress syndrome induced by influenza virus infection. *Microbiol Immunol*. 2012;56(3):171-82. Epub 2012/01/04. doi: 10.1111/j.1348-0421.2011.00424.x. PubMed PMID: 22211924.

48. Almansa R, Socias L, Ramirez P, Martin-Loeches I, Valles J, Loza A, et al. Imbalanced pro- and anti-Th17 responses (IL-17/granulocyte colony-stimulating factor) predict fatal outcome in 2009 pandemic influenza. *Crit Care*. 2011;15(5):448. Epub 2011/11/02. doi: 10.1186/cc10426. PubMed PMID: 22040730; PubMed Central PMCID: PMC3334743.
49. Li C, Yang P, Sun Y, Li T, Wang C, Wang Z, et al. IL-17 response mediates acute lung injury induced by the 2009 pandemic influenza A (H1N1) virus. *Cell Res*. 2012;22(3):528-38. Epub 2011/10/26. doi: 10.1038/cr.2011.165. PubMed PMID: 22025253; PubMed Central PMCID: PMC3292301.
50. Schmitz N, Kurrer M, Bachmann MF, Kopf M. Interleukin-1 is responsible for acute lung immunopathology but increases survival of respiratory influenza virus infection. *J Virol*. 2005;79(10):6441-8. doi: 10.1128/JVI.79.10.6441-6448.2005. PubMed PMID: 15858027; PubMed Central PMCID: PMC1091664.
51. Hagau N, Slavcovici A, Gongnanau DN, Oltean S, Dirzu DS, Brezoszki ES, et al. Clinical aspects and cytokine response in severe H1N1 influenza A virus infection. *Crit Care*. 2010;14(6):R203. Epub 2010/11/11. doi: 10.1186/cc9324. PubMed PMID: 21062445; PubMed Central PMCID: PMC3220006.
52. Matsukura S, Kokubu F, Kubo H, Tomita T, Tokunaga H, Kadokura M, et al. Expression of RANTES by normal airway epithelial cells after influenza virus A infection. *Am J Respir Cell Mol Biol*. 1998;18(2):255-64. Epub 1998/02/26. doi: 10.1165/ajrcmb.18.2.2822. PubMed PMID: 9476913.

53. Alijotas-Reig J, Llorba E, Gris JM. Potentiating maternal immune tolerance in pregnancy: a new challenging role for regulatory T cells. *Placenta*. 2014;35(4):241-8. Epub 2014/03/04. doi: 10.1016/j.placenta.2014.02.004. PubMed PMID: 24581729.
54. Chiu C, Ellebedy AH, Wrammert J, Ahmed R. B cell responses to influenza infection and vaccination. *Current topics in microbiology and immunology*. 2015;386:381-98. doi: 10.1007/82_2014_425. PubMed PMID: 25193634.
55. Beigi RH. Emerging Infectious Diseases in Pregnancy. *Obstet Gynecol*. 2017;129(5):896-906. Epub 2017/04/07. doi: 10.1097/AOG.0000000000001978. PubMed PMID: 28383378.
56. Liu S, Sha J, Yu Z, Hu Y, Chan TC, Wang X, et al. Avian influenza virus in pregnancy. *Rev Med Virol*. 2016;26(4):268-84. Epub 2016/05/18. doi: 10.1002/rmv.1884. PubMed PMID: 27187752.
57. Beigi RH. Pandemic influenza and pregnancy: a call for preparedness planning. *Obstet Gynecol*. 2007;109(5):1193-6. Epub 2007/05/02. doi: 10.1097/01.AOG.0000262051.71925.ac. PubMed PMID: 17470605.
58. van Riel D, Mittrucker HW, Engels G, Klingel K, Markert UR, Gabriel G. Influenza pathogenicity during pregnancy in women and animal models. *Semin Immunopathol*. 2016;38(6):719-26. Epub 2016/07/09. doi: 10.1007/s00281-016-0580-2. PubMed PMID: 27387428.
59. Bowkalow S, Brauer M, Gross W, Schleussner E. Severe H1N1-infection during pregnancy. *Arch Gynecol Obstet*. 2011;284(5):1133-5. Epub 2011/07/13. doi: 10.1007/s00404-011-1967-x. PubMed PMID: 21748316.

60. Marchiori R, Brecht CS, Campos MM, Negretti F, Duarte PA. Pandemic influenza A/H1N1: comparative analysis of microscopic lung histopathological findings. *Einstein (Sao Paulo)*. 2012;10(3):306-11. Epub 2013/02/07. PubMed PMID: 23386009.
61. Brown CM, Mulcahey TA, Filipek NC, Wise PM. Production of proinflammatory cytokines and chemokines during neuroinflammation: novel roles for estrogen receptors alpha and beta. *Endocrinology*. 2010;151(10):4916-25. Epub 2010/08/06. doi: 10.1210/en.2010-0371. PubMed PMID: 20685874; PubMed Central PMCID: PMC2946152.
62. Gao R, Bhatnagar J, Blau DM, Greer P, Rollin DC, Denison AM, et al. Cytokine and chemokine profiles in lung tissues from fatal cases of 2009 pandemic influenza A (H1N1): role of the host immune response in pathogenesis. *Am J Pathol*. 2013;183(4):1258-68. Epub 2013/08/14. doi: 10.1016/j.ajpath.2013.06.023. PubMed PMID: 23938324.
63. Betakova T, Kostrabova A, Lachova V, Turianova L. Cytokines Induced During Influenza Virus Infection. *Curr Pharm Des*. 2017;23(18):2616-22. Epub 2017/03/18. doi: 10.2174/1381612823666170316123736. PubMed PMID: 28302021.
64. Litchfield SM. Summary recommendations by the Advisory Committee on Immunization Practices (ACIP) for the use of H1N1 influenza vaccine for the 2009-2010 vaccination season. *AAOHN J*. 2009;57(9):354. Epub 2009/10/22. doi: 10.3928/08910162-20090826-02. PubMed PMID: 19842610.
65. Centers for Disease C, Prevention. Prevention and control of seasonal influenza with vaccines. Recommendations of the Advisory Committee on Immunization Practices-- United States, 2013-2014. *MMWR Recommendations and reports : Morbidity and*

- mortality weekly report Recommendations and reports / Centers for Disease Control. 2013;62(RR-07):1-43. PubMed PMID: 24048214.
66. Nicoll A. A new decade, a new seasonal influenza: the Council of the European Union Recommendation on seasonal influenza vaccination. *Euro Surveill.* 2010;15(1). Epub 2010/01/14. PubMed PMID: 20067749.
67. Proietti E, Bracci L, Puzelli S, Di Pucchio T, Sestili P, De Vincenzi E, et al. Type I IFN as a natural adjuvant for a protective immune response: lessons from the influenza vaccine model. *J Immunol.* 2002;169(1):375-83. Epub 2002/06/22. PubMed PMID: 12077267.
68. Bischoff AL, Folsgaard NV, Carson CG, Stokholm J, Pedersen L, Holmberg M, et al. Altered Response to A(H1N1)pnd09 Vaccination in Pregnant Women: A Single Blinded Randomized Controlled Trial. *PloS one.* 2013;8(4):e56700. Epub 2013/05/03. doi: 10.1371/journal.pone.0056700. PubMed PMID: 23637733; PubMed Central PMCID: PMC3630160.
69. Tsatsaris V, Capitant C, Schmitz T, Chazallon C, Bulifon S, Riethmuller D, et al. Maternal immune response and neonatal seroprotection from a single dose of a monovalent nonadjuvanted 2009 influenza A(H1N1) vaccine: a single-group trial. *Ann Intern Med.* 2011;155(11):733-41. Epub 2011/12/08. doi: 10.7326/0003-4819-155-11-201112060-00005. PubMed PMID: 22147712.
70. Sperling RS, Engel SM, Wallenstein S, Kraus TA, Garrido J, Singh T, et al. Immunogenicity of trivalent inactivated influenza vaccination received during pregnancy or postpartum. *Obstet Gynecol.* 2012;119(3):631-9. Epub 2012/02/23. doi:

10.1097/AOG.0b013e318244ed20. PubMed PMID: 22353963; PubMed Central PMCID: PMC3327739.

71. Jackson LA, Patel SM, Swamy GK, Frey SE, Creech CB, Munoz FM, et al. Immunogenicity of an inactivated monovalent 2009 H1N1 influenza vaccine in pregnant women. *J Infect Dis.* 2011;204(6):854-63. Epub 2011/08/19. doi: 10.1093/infdis/jir440. PubMed PMID: 21849282; PubMed Central PMCID: PMC3156926.

Figures

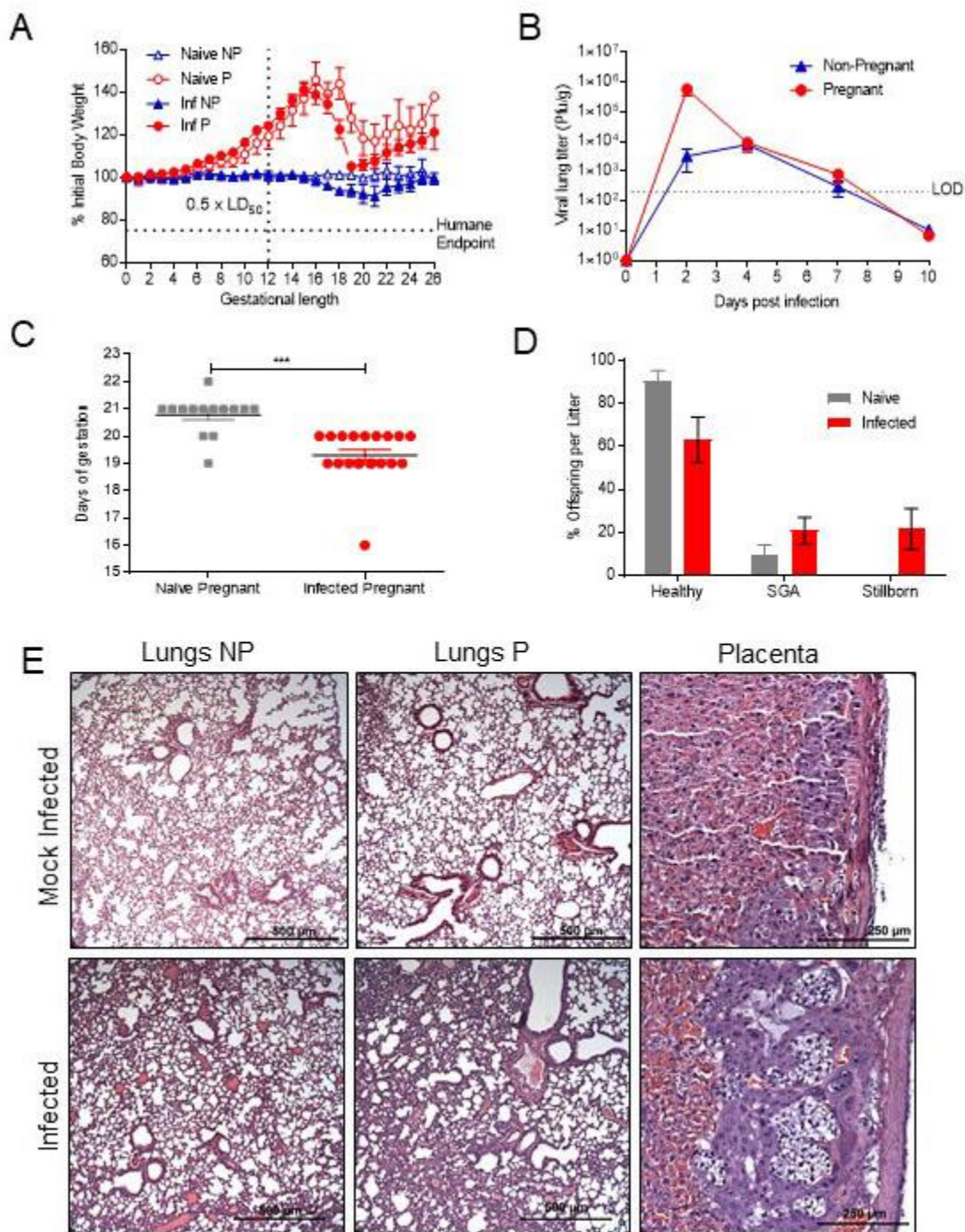


Fig 1. H1N1 influenza virus infection results in increased pathogenicity during pregnancy.

(A) Body weights of pregnant and non-pregnant mice infected either with 0.5xLD₅₀ mouse-adapted H1N1 A/California/07/2009 virus or mock-infected with PBS and lung tissue lysate. (B)

Viral titers in pregnant and non-pregnant mice until viral clearance at 10 days post-infection (d.p.i.). (C) Days of gestation in uninfected and infected pregnant mice. (D) Offspring outcomes calculated by % of pups/litter healthy, small-for-gestational age (SGA) defined as <1.2 g, and stillborn. € Hematoxylin and eosin (H&E) staining of lungs infected with virus or tissue lysate and PBS and placenta from infected and uninfected pregnant mice.

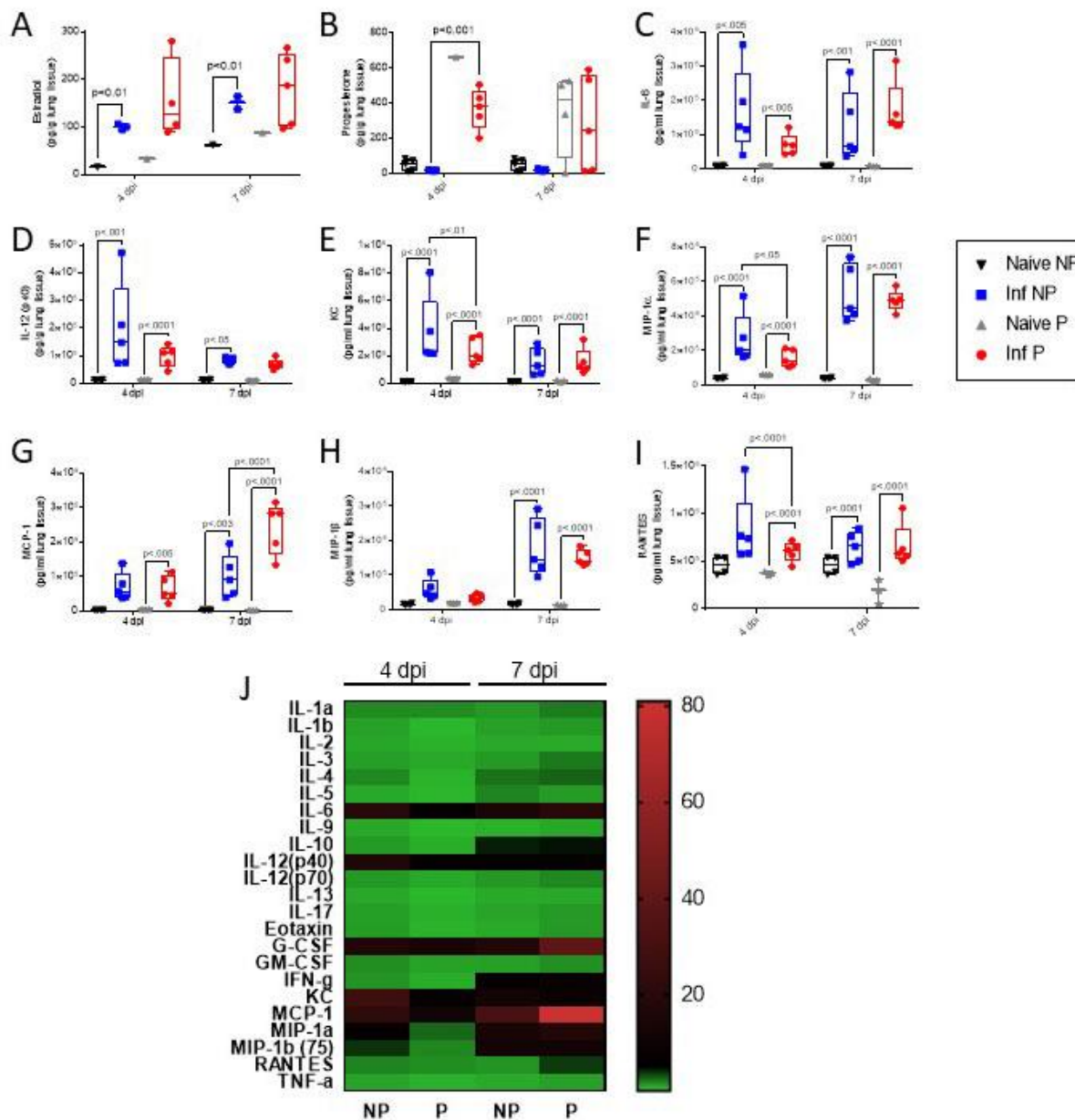


Fig 2. Hormone and cytokine expression in lung tissue 4 d.p.i. and 7 d.p.i. Lung expression of (A) estradiol and (B) progesterone was determined by ELISA and calculated per gram of tissue. Cytokine expression was determined by a 23-plex Luminex assay and cytokines of interest are depicted: (C) IL-6, (D) IL-12(p40), (E) KC, (F) MIP-1 α , (G) MCP-1, (H) MIP-1 β , and (I) RANTES. (J) Heat map indicating fold-changes following infection (infected/uninfected samples per group) at 4 and 7 d.p.i. in non-pregnant and pregnant mice. Significance was determined by

Student's t-test; all cytokine values, fold-changes, and p-values are reported in Supplemental Table

1.

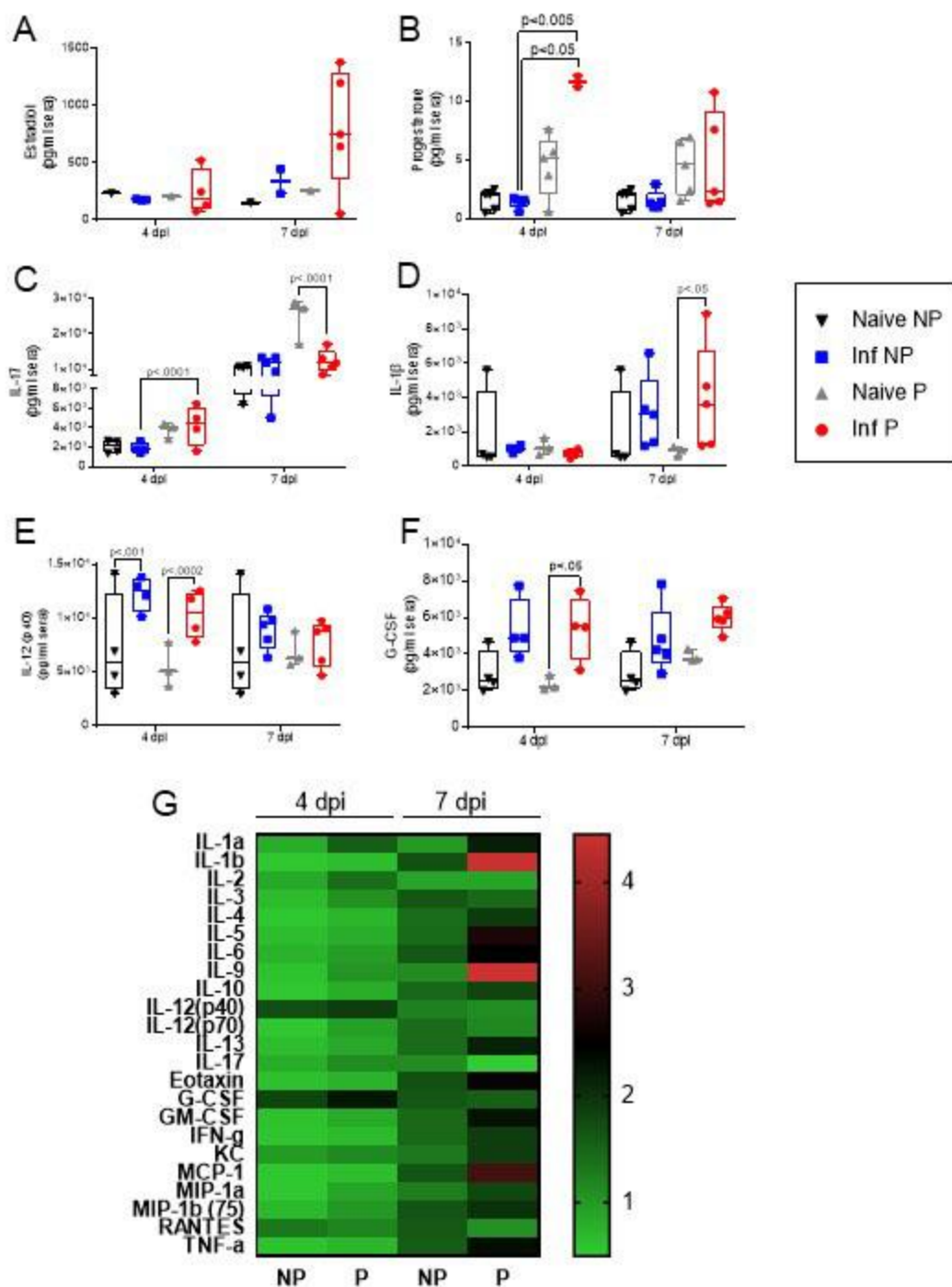


Fig 3. Hormone and cytokine expression in serum samples 4 d.p.i. and 7 d.p.i. Hormone expression of (A) estradiol and (B) progesterone was determined per ml of serum with ELISA. Cytokine expression was determined in a 23-plex Luminex assay; cytokines of interest are

depicted: (C) IL-17, (D) IL-1 β , (E) IL-12(p40), and (F) G-CSF. (G) Heat map indicating fold-changes following infection (infected/uninfected samples per group) at 4 and 7 d.p.i. in non-pregnant and pregnant mice. Significance was determined by Student's t-test; all cytokine values, fold-changes, and p-values are reported in Supplemental Table 2.

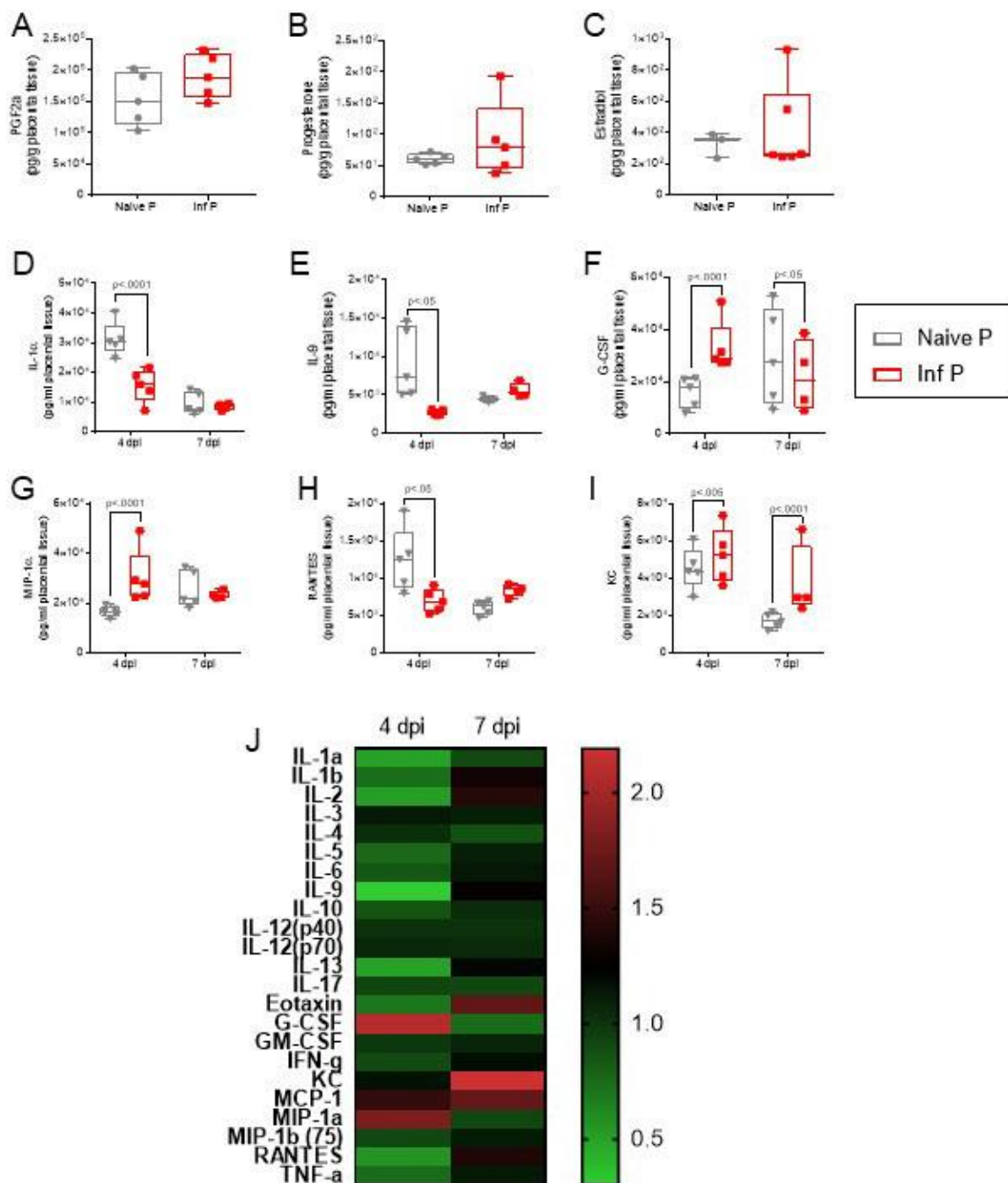


Fig 4. Hormone and cytokine expression in placental tissue 4 d.p.i. and 7 d.p.i. Hormone expression of (A) prostaglandin F2 α (PGF2 α), (B) progesterone and (C) estradiol was determined per gram of placental tissue with ELISA. Cytokine expression was determined in a 23-plex Luminex assay and cytokines of interest are plotted here: (D) IL-1 α , (E) IL-9, (F) G-CSF, (G)

MIP-1 α , (H) RANTES, and (I) KC. (J) Heat map indicating fold-changes following infection (infected/uninfected samples per group) at 4 and 7 d.p.i. in pregnant mice. Significance was determined by a student's t-test; all cytokine values, fold-changes, and p-values are reported in Supplemental Table 3.

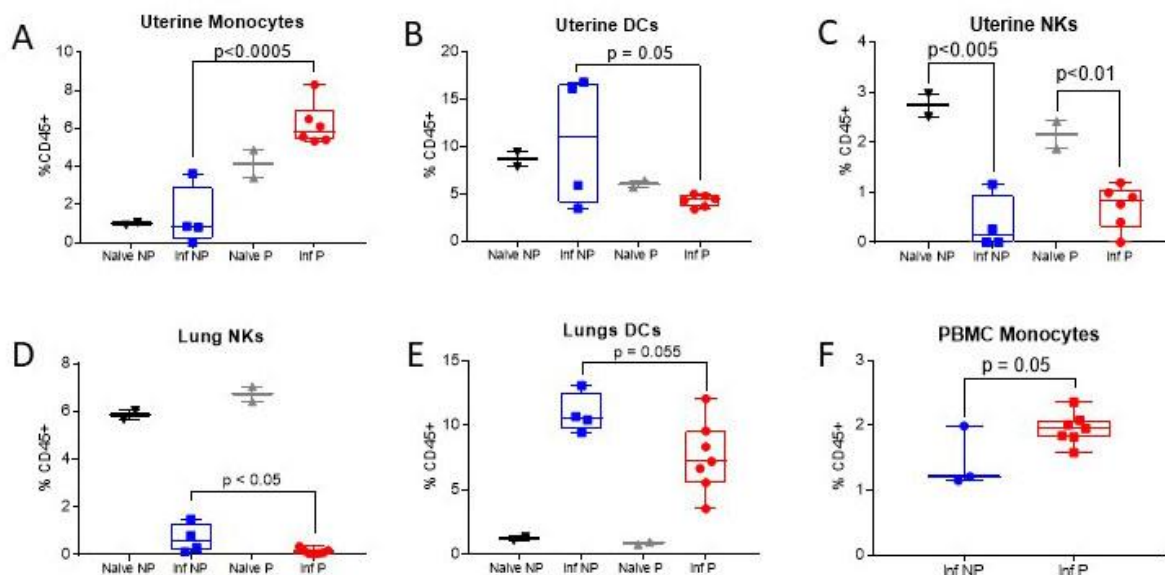


Fig 5. Innate immune activation following H1N1 influenza virus infection. Lymphocytes were isolated from pregnant and non-pregnant mice and uninfected controls at 2 d.p.i. in the uterus (A-C), lungs (D-F), and from peripheral blood mononuclear cells (PBMCs) (F). Monocytes, DCs, NK cells and neutrophils were determined in each tissue type as a percentage of CD45+ cells; significant findings are presented here. Gating strategy for innate immune cells is described in Suppl Figure 1A.

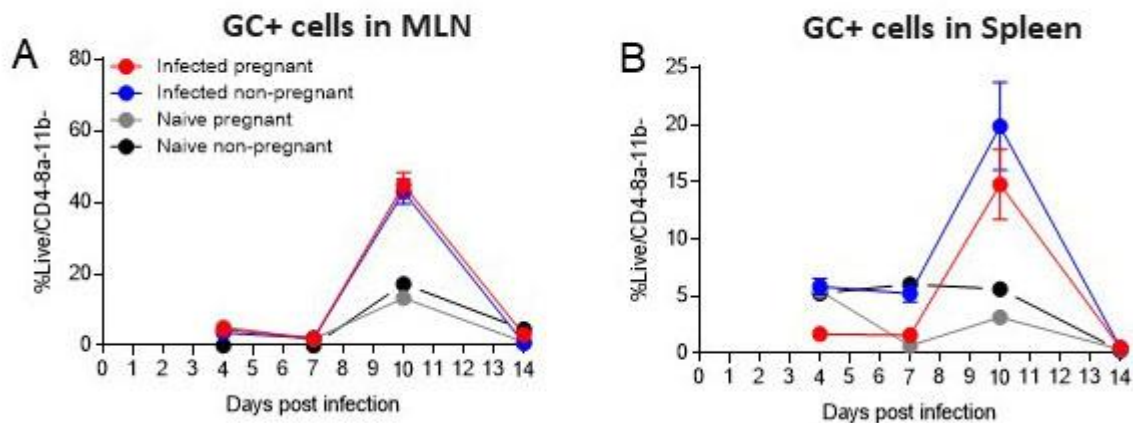


Fig 6. Germinal center reactions and plasmablast activation. Lymphocytes from the mediastinal lymph nodes (MLN), spleens, and lungs were isolated at 4, 7, 10, and 14 d.p.i. Germinal center + (GC+) cells (CD19+ GL7+) were determined in the (A) MLN and (B) spleens. Gating strategy for GC+ B cells and plasmablasts is described in Suppl Figure 1B.

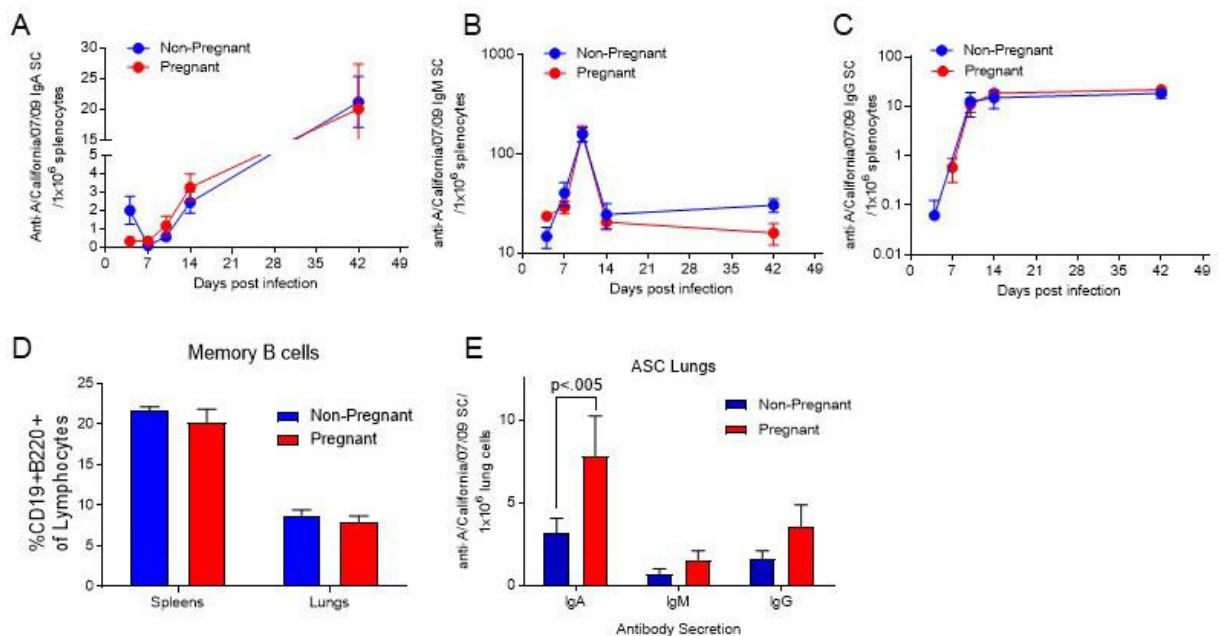


Fig 7. Pregnancy increases virus-specific IgA-secreting cells in the lungs 6 weeks post infection. Lung and spleen lymphocytes were isolated from pregnant and non-pregnant mice following 0.5xLD₅₀ H1N1 A/California/07/2009 infection. Virus-specific (A) IgA, (B) IgM and (C) IgG-secreting cells in the spleen were stimulated with recombinant H1 A/California/07/2009 bound to ELISPOT plates. (D) Memory B cells in spleen and lung lymphocyte populations from pregnant and non-pregnant mice post-infection were quantified via flow cytometry as a % frequency of CD19+ B220+ cells in the total lymphocyte population. (E) Antibody secreting cells specific for recombinant H1 A/California/07/09 were determined in the lungs at 42 d.p.i.

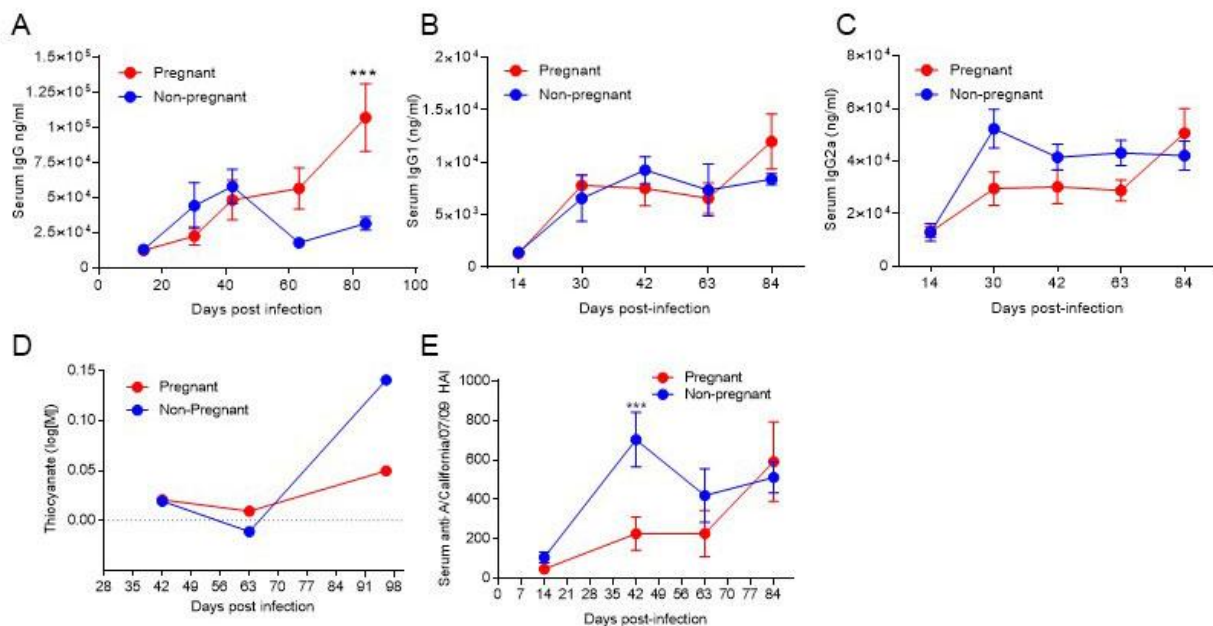


Fig 8. Pregnancy induces increased IgG expression with reduced avidity and HAI titers.

Serum antibody concentration of anti-A/California/07/2009-specific (A) IgG, (B) IgG1, and (C) IgG2a was determined with ELISA. (D) Antibody avidity was determined by measuring the IC50 of antibody binding to A/California/07/2009 following exposure to increasing concentrations of a chaotropic agent. (E) anti-A/California/07/2009 hemagglutinin inhibition titers (HAI) from sera of infected pregnant and non-pregnant mice.

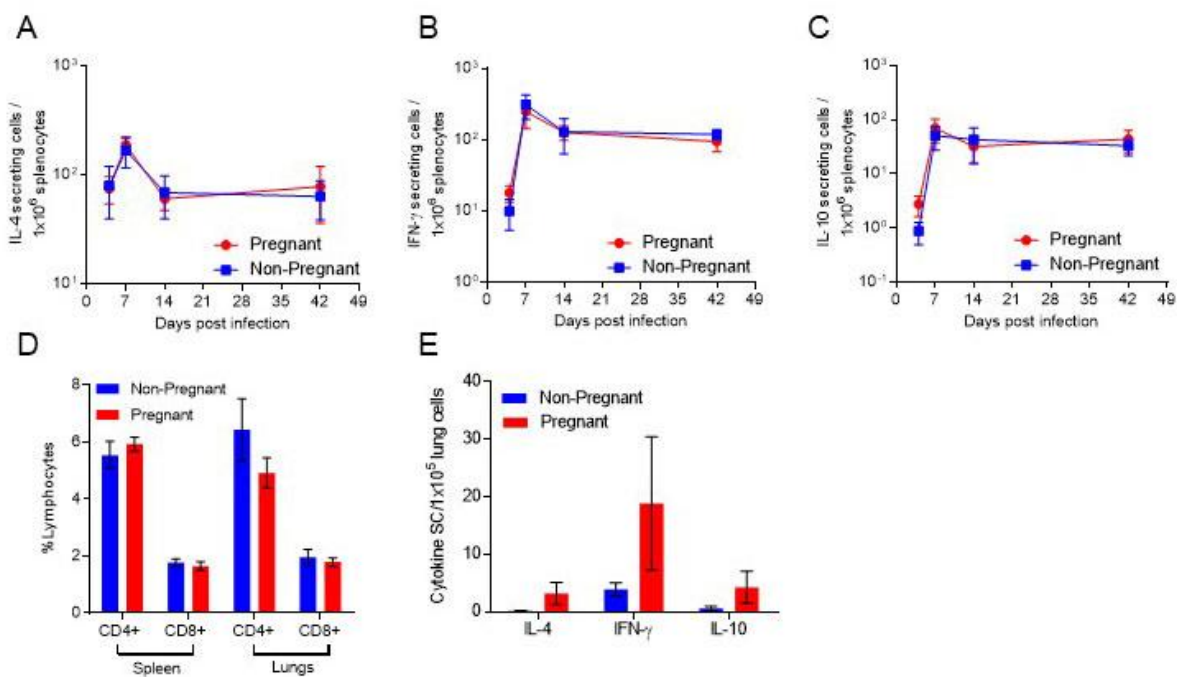


Fig 9. Pregnancy increases virus-specific IFN- γ secreting cells in the lungs 6 weeks post infection. Lung and spleen lymphocytes were isolated from pregnant and non-pregnant mice following 0.5xLD₅₀ H1N1 A/California/07/09 infection. A/California/07/2009-specific (A) IL-4, (B) IFN- γ and (C) IL-10-secreting cells in the spleen. (D) Spleen and lung CD4+ and CD8+ lymphocyte populations from pregnant and non-pregnant mice were quantified via flow cytometry as % CD4+ or CD8+ cells in the total lymphocyte population at 42 d.p.i. (E) A/California/07/09-specific cytokine secreting cells specific were determined in the lungs at 42 d.p.i.

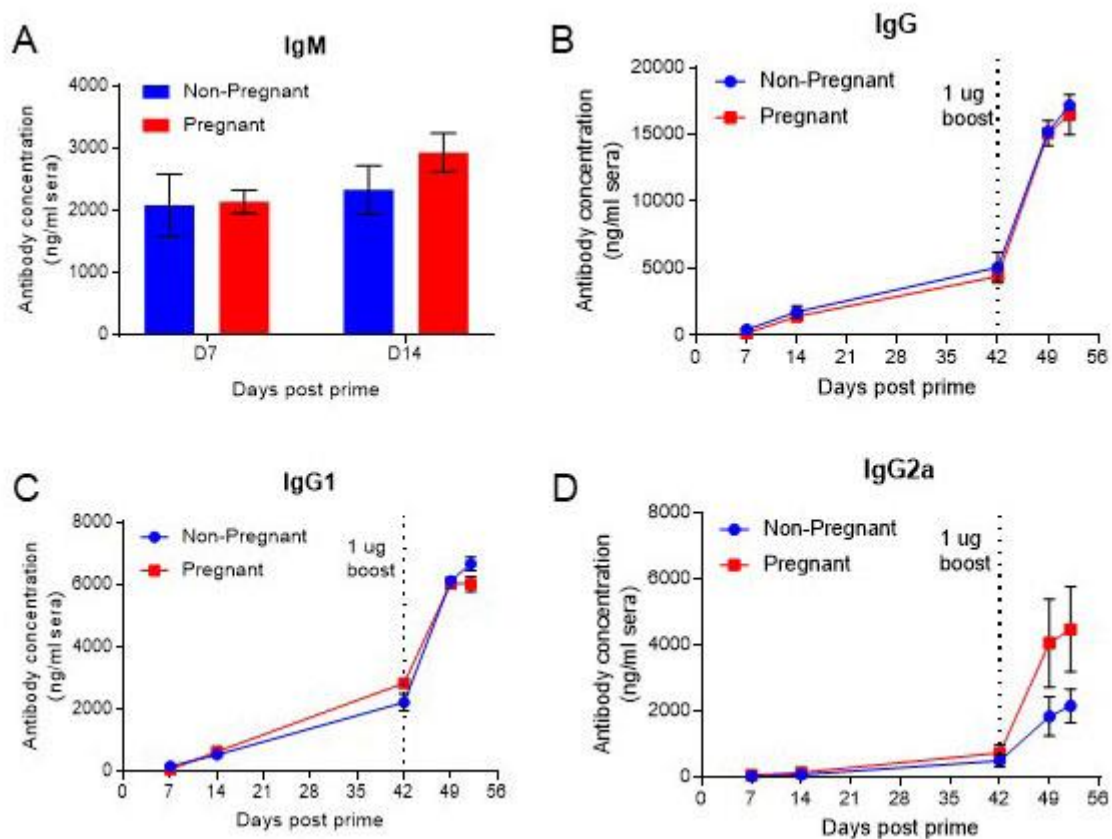


Fig 10. Pregnancy induces an IgG2a-specific response to boost vaccination 42 d.p.p. Pregnant mice (E12) and non-pregnant mice were primed and boosted 42 days apart with 1 μ g A/California/07/2009 recombinant protein. (A) Serum IgM expression was measured 7 and 14 days post-prime. Serum expression of vaccine-specific (B) IgG, (C) IgG1, and (D) IgG2a was measured up to 8 weeks following prime and boost vaccination.

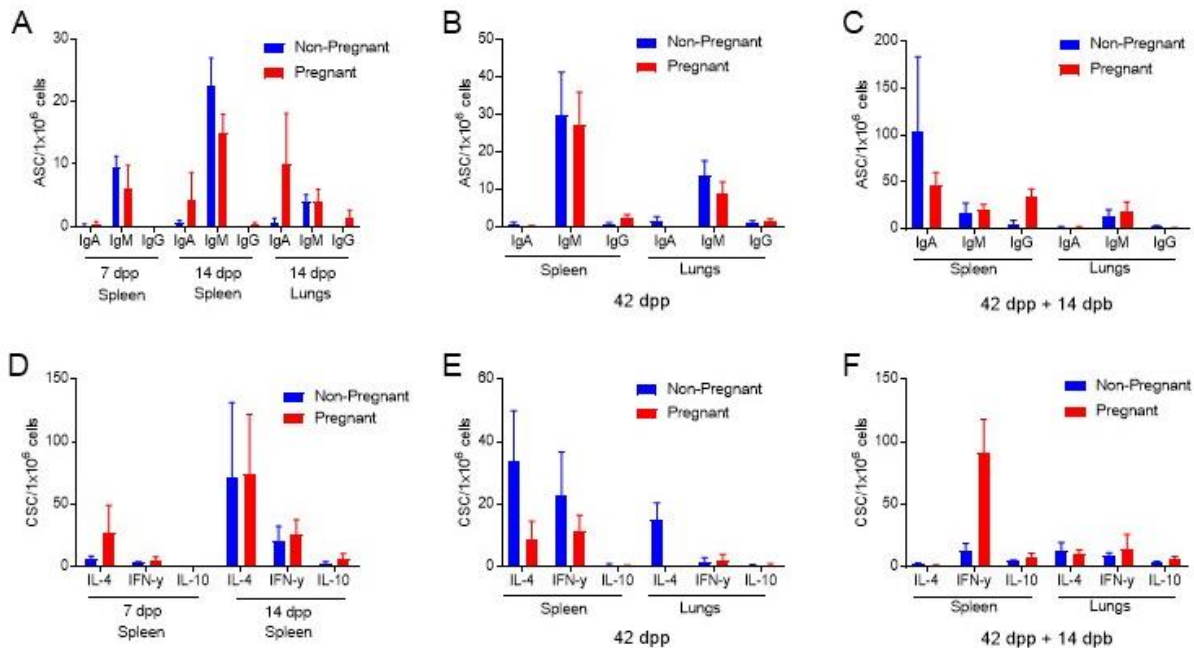
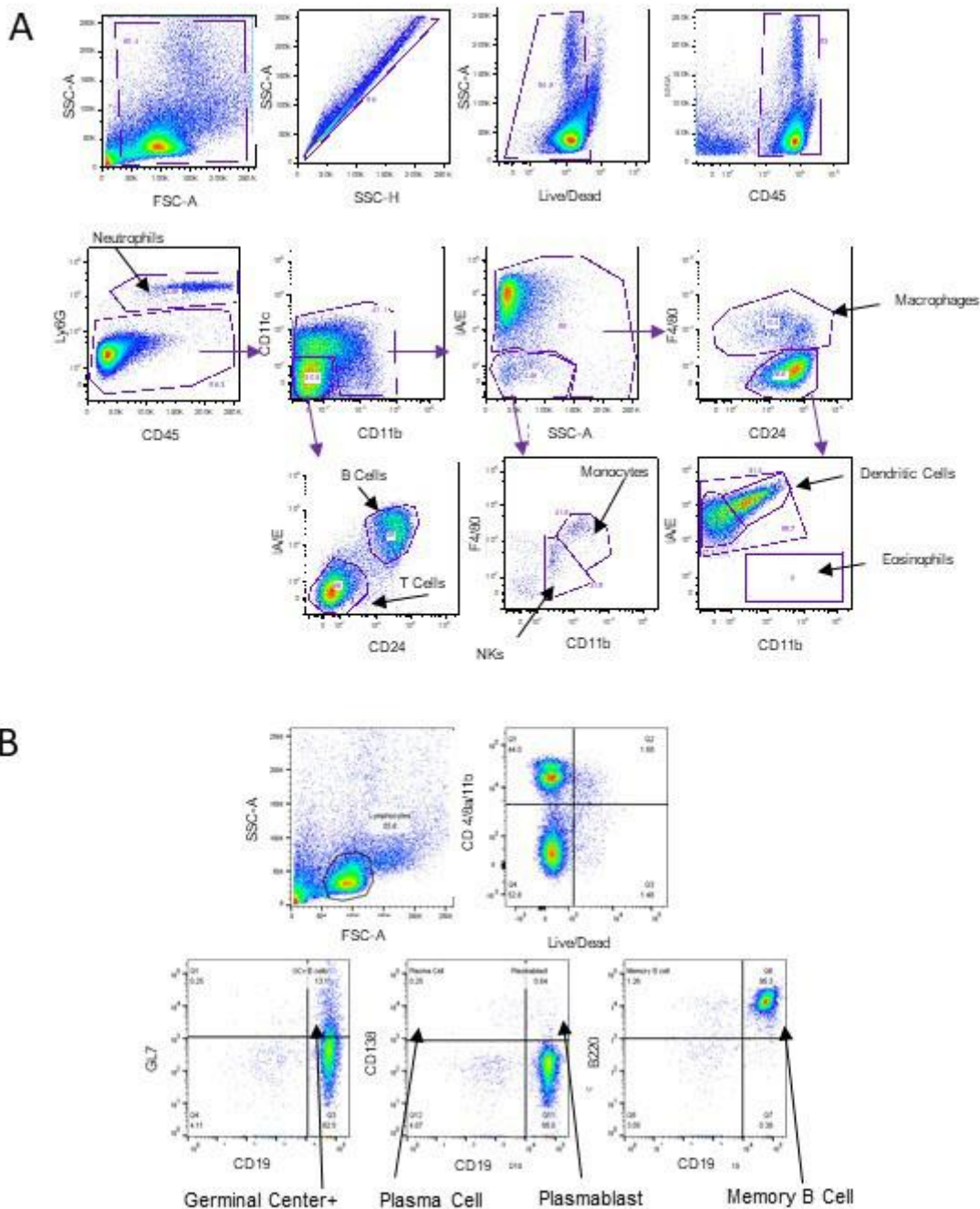


Fig 11. Activation of vaccine-specific B and T cells following vaccination during pregnancy and boost post-weaning. Pregnant mice (E12) and no-pregnant mice were primed and boosted with 1 μ g A/California/07/2009 recombinant protein 42 days apart. Vaccine-specific antibody-secreting cells (ASCs) in the spleen were determined at (A) 7 days post prime (d.p.p.) and in the spleen and lungs at 14 d.p.p., (B) 42 d.p.p and (C) 14 days post boost (d.p.b.). Vaccine-specific CSCs were determined in the spleen and lungs (E) 42 d.p.p and (F) 14 d.p.b.

Supplemental Figures and Tables



Suppl Fig 1. Gating settings for flow cytometry. (A) Innate immune cell populations were gated by gating out debris and non-singlet populations and selecting for CD45+ cells.

Neutrophils were gated as CD45+Ly6G positive, while double negative populations were further

gated CD11b/CD11c. Double negative populations were gated as B cells (CD24⁺ MHC II⁺) or T cells (CD24⁻ MHC II⁻). Non-negative CD11b/CD11c populations were gated for low SSC density as monocytes (CD11b⁺ F4/80) or NK cells (CD11b^{int} F4/80^{int}); MHC II⁺ cells were gated for macrophages (CD24^{int} F4/80⁺). CD24⁺F4/80⁻ cells were gated as dendritic cells (CD11b⁻ MHC II⁺). Eosinophils were gated as CD11b⁺ MHC II⁺. (B) Lymphocytes and populations negative for CD4, CD8a, CD11b, and Live/Dead stain were selected. CD19⁺ GL7⁺ cells were gated as germinal center + B cells. CD19⁺ CD138⁺ cells were determined to be plasmablasts; CD19⁻ CD138⁺ cells were determined to be plasma cells. Memory B cells were gated as CD19⁺ B220⁺.

Suppl Table 1. Lung cytokine expression.

LUNGS	Day 4										
	Sample	Naïve NP	Inf NP	Fold change	p-value	Naïve P	Inf P	Fold change	p-value	Fold change	p-value
	IL-1 α	14673.4 \pm 1123.7	24672.4 \pm 5028.9	1.68	0.994	1652.4 \pm 554.6	27231.6 \pm 3963.9	1.65	0.606	1.104	0.960
	IL-1 β	9604.6 \pm 771.5	11071.3 \pm 2111.9	1.15	0.987	11676.2 \pm 208.9	6981.7 \pm 728.1	0.60	0.821	0.631	0.936
	IL-2	12470.4 \pm 683.6	12897.2 \pm 1951.2	1.03	0.977	14009.5 \pm 247.5	10182.4 \pm 667.7	0.73	0.853	0.790	0.957
	IL-3	5238.4 \pm 370.2	6176.6 \pm 1146.1	1.18	0.996	5281.0 \pm 157.9	5201.0 \pm 384.0	0.98	0.997	0.842	0.985
	IL-4	2244.6 \pm 135.5	3838.6 \pm 842.6	1.71	0.005	4795.2 \pm 12.6	3303.4 \pm 379.2	0.69	0.943	0.861	0.992
	IL-5	7461.0 \pm 526.0	7176.6 \pm 1182.7	0.96	0.994	7004.8 \pm 169.1	4457.9 \pm 800.8	0.64	0.902	0.621	0.957
	IL-6	8677.5 \pm 517.4	167683.6 \pm 54854.9	19.32	0.976	9957.1 \pm 250.8	70530.2 \pm 14025.4	7.08	0.004	0.421	0.057
	IL-9	18751.9 \pm 2519.9	18343.7 \pm 2454.8	0.98	0.001	22381.0 \pm 1281.3	13913.2 \pm 1744.9	0.62	0.683	0.758	0.930
	IL-10	5844.9 \pm 504.9	7533.3 \pm 1739.9	1.29	0.957	6219.0 \pm 295.6	5234.6 \pm 411.9	0.84	0.962	0.695	0.964
	IL-12(p40)	11810.7 \pm 935.6	195755.4 \pm 73700.2	16.57	0.996	13804.8 \pm 189.9	97014.3 \pm 17100.4	7.03	0.000	0.496	0.053
	IL-12(p70)	8686.3 \pm 645.3	11663.9 \pm 2622.7	1.34	0.971	9061.9 \pm 261.9	8629.9 \pm 730.1	0.95	0.983	0.740	0.952
	IL-13	8947.9 \pm 744.6	8677.6 \pm 1471.1	0.97	0.969	9642.9 \pm 678.6	5823.1 \pm 720.0	0.60	0.854	0.671	0.955
	IL-17	10786.1 \pm 860.0	12793.8 \pm 2417.5	1.19	0.332	14047.6 \pm 272.2	11036.3 \pm 732.0	0.79	0.884	0.863	0.972
	Eotaxin	10940.3 \pm 1513.5	13113.3 \pm 2379.8	1.20	0.928	12771.4 \pm 882.6	8877.8 \pm 1386.6	0.70	0.851	0.677	0.934
	G-CSF	3373.6 \pm 232.9	57383.0 \pm 15342.8	17.01	0.943	4376.2 \pm 85.8	60293.1 \pm 9442.9	13.78	0.008	1.051	0.954
	GM-CSF	8382.4 \pm 426.8	13414.0 \pm 2680.1	1.60	0.000	8981.0 \pm 339.0	10052.9 \pm 1120.8	1.12	0.959	0.749	0.947
	IFN- γ	9236.7 \pm 667.0	13222.3 \pm 2419.6	1.43	0.227	9461.9 \pm 246.9	7926.5 \pm 418.1	0.84	0.941	0.599	0.917
	KC	13457.6 \pm 947.0	369929.8 \pm 113209.6	27.49	0.000	35014.3 \pm 1347.1	238626.2 \pm 43202.2	6.82	0.000	0.645	0.010
	MCP-1	3237.0 \pm 163.8	70509.4 \pm 18578.8	21.78	0.437	5695.2 \pm 66.7	64325.7 \pm 16607.1	11.29	0.005	0.912	0.903
	MIP-1 α	39455.8 \pm 1582.9	265706.7 \pm 65716.7	6.73	0.000	61414.3 \pm 611.3	155627.9 \pm 22905.2	2.53	0.000	0.586	0.031
	MIP-1 β	15531.3 \pm 1201.3	58773.7 \pm 13522.9	3.78	0.997	18961.9 \pm 361.9	33651.1 \pm 5236.6	1.77	0.478	0.573	0.621
	RANTES	454098.9 \pm 47642.7	826791.8 \pm 165093.4	1.82	0.994	373609.5 \pm 11592.5	599480.8 \pm 46690.2	1.60	0.000	0.725	0.000
	TNF- α	5048.0 \pm 539.0	5287 \pm 885	1.05	0.987	5490.5 \pm 217.8	4060.2 \pm 424.2	0.74	0.945	0.768	0.981

Supplemental Table 1. Lung cytokine expression.

Suppl Table 1. Lung cytokine expression.

Day 7											
LUNGS	Sample	Naïve NP	Inf NP	Fold change	p-value	Naïve P	Inf P	Fold change	p-value	Fold change	p-value
	IL-1α	14673.4 \pm 1123.7	19802.1 \pm 2402.8	1.35	0.876	13537.5 \pm 1251.7	26893.4 \pm 1476.2	1.99	0.722	1.558	0.855
	IL-1β	9604.6 \pm 771.5	10842.2 \pm 1641.8	1.13	0.970	8408.3 \pm 74.1	10792.8 \pm 1464.0	1.28	0.949	0.995	0.999
	IL-2	12470.4 \pm 683.6	12142.1 \pm 1996.5	0.97	0.992	12966.7 \pm 1482.6	11972.6 \pm 1860.5	0.92	0.979	0.986	0.997
	IL-3	5238.4 \pm 370.2	6707.8 \pm 948.3	1.28	0.964	4012.5 \pm 481.4	8370.0 \pm 814.1	2.09	0.908	1.248	0.966
	IL-4	2244.6 \pm 135.5	5083.0 \pm 881.9	2.26	0.931	2416.7 \pm 171.7	6323.3 \pm 761.9	2.62	0.917	1.244	0.974
	IL-5	7461.0 \pm 526.0	13449.6 \pm 7067.6	1.80	0.855	7369.4 \pm 1461.5	9221.1 \pm 1087.8	1.25	0.961	0.686	0.913
	IL-6	8677.5 \pm 517.4	121962.4 \pm 46179.4	14.06	0.001	8636.1 \pm 1084.2	173568.2 \pm 36277.8	20.10	0.000	1.423	0.184
	IL-9	18751.9 \pm 2519.9	13815.9 \pm 2410.6	0.74	0.881	17411.1 \pm 1719.5	16798.0 \pm 4262.2	0.96	0.987	1.216	0.939
	IL-10	5844.9 \pm 504.9	25115.5 \pm 6470.9	4.30	0.558	5366.7 \pm 263.6	24592.7 \pm 2935.5	4.58	0.609	0.979	0.989
	IL-12(p40)	11810.7 \pm 935.6	81709.0 \pm 4829.0	6.92	0.035	10050.0 \pm 1576.1	69853.4 \pm 8383.4	6.95	0.113	0.855	0.759
	IL-12(p70)	8686.3 \pm 645.3	11781.4 \pm 1325.5	1.36	0.925	7830.6 \pm 382.6	13372.8 \pm 1657.4	1.71	0.883	1.135	0.967
	IL-13	8947.9 \pm 744.6	8172.7 \pm 1074.0	0.91	0.981	7905.6 \pm 357.1	7631.1 \pm 1268.7	0.97	0.994	0.934	0.989
	IL-17	10786.1 \pm 860.0	11439.6 \pm 1359.3	1.06	0.984	10373.6 \pm 1032.6	13413.9 \pm 2299.0	1.29	0.935	1.173	0.959
	Eotaxin	10940.3 \pm 1513.5	9777.0 \pm 1147.3	0.89	0.972	8969.4 \pm 810.2	12243.0 \pm 2171.8	1.36	0.931	1.252	0.949
	G-CSF	3373.6 \pm 232.9	57396.2 \pm 7111.8	17.01	0.102	3043.1 \pm 320.7	120913.2 \pm 23664.4	39.73	0.002	2.107	0.102
	GM-CSF	8382.4 \pm 426.8	9707.6 \pm 1216.3	1.16	0.968	7348.6 \pm 942.1	11316.2 \pm 1634.3	1.54	0.916	1.166	0.967
	IFN-γ	9236.7 \pm 667.0	68553.7 \pm 25105.6	7.42	0.072	8883.3 \pm 635.1	75673.9 \pm 23469.7	8.52	0.077	1.104	0.854
	KC	13457.6 \pm 947.0	154905.8 \pm 43806.5	11.51	0.000	17412.5 \pm 3202.1	156443.1 \pm 42441.9	8.98	0.000	1.010	0.968
	MCP-1	3237.0 \pm 163.8	101245.8 \pm 28329.5	31.28	0.003	3004.2 \pm 223.2	243195.6 \pm 33617.4	80.95	0.000	2.402	0.000
	MIP-1α	39455.8 \pm 1582.9	529329.5 \pm 74771.4	13.42	0.000	28183.3 \pm 4811.0	491407.8 \pm 27024.1	17.44	0.000	0.928	0.328
	MIP-1β	15531.3 \pm 1201.3	180193.3 \pm 37619.4	11.60	0.000	13259.7 \pm 1010.2	150194.7 \pm 10524.7	11.33	0.000	0.834	0.439
	RANTES	454098.9 \pm 47642.7	645769.2 \pm 72087.6	1.42	0.000	186470.8 \pm 74356.4	665643.1 \pm 100838.3	3.57	0.000	1.031	0.608
	TNF-α	5048.1 \pm 539.2	4625.8 \pm 551.8	0.92	0.990	4750.0 \pm 573.5	5421.3 \pm 715.8	1.14	0.986	1.172	0.984

Suppl Table 2. Sera cytokine expression.

Supplemental Table 2. Sera cytokine expression.

SERA	Day 4									
	Naïve NP	Inf NP	Fold change	p-value	Naïve P	Inf P	Fold change	p-value	Fold Change	p-value
IL-1α	1637.5 \pm 138.9	1309.0 \pm 127.8	0.80	0.832	830.7 \pm 101.9	1296.0 \pm 84.9	1.56	0.708	0.990	0.990
IL-1β	1842.0 \pm 1254.6	1018.5 \pm 100.2	0.55	0.594	1120.7 \pm 283.9	731.5 \pm 118.4	0.65	0.754	0.718	0.784
IL-2	1123.0 \pm 128.7	945.0 \pm 131.1	0.84	0.908	806.0 \pm 41.1	1127.5 \pm 278.8	1.40	0.796	1.193	0.862
IL-3	1634.5 \pm 686.0	1075.0 \pm 26.4	0.66	0.717	1172.0 \pm 135.2	1248.0 \pm 224.7	1.06	0.951	1.161	0.869
IL-4	1451.5 \pm 771.6	786.5 \pm 49.7	0.54	0.667	1045.3 \pm 225.9	751.5 \pm 150.4	0.72	0.813	0.955	0.973
IL-5	1839.0 \pm 976.3	1197.5 \pm 138.3	0.65	0.678	1393.3 \pm 271.1	1113.5 \pm 166.6	0.80	0.822	0.930	0.936
IL-6	2820.0 \pm 1553.5	2124.5 \pm 104.9	0.75	0.652	2100.0 \pm 498.0	2024.5 \pm 373.8	0.96	0.952	0.953	0.924
IL-9	2728.5 \pm 1180.3	1647.0 \pm 263.2	0.60	0.484	997.3 \pm 88.7	1037.0 \pm 231.9	1.04	0.975	0.630	0.560
IL-10	2289.0 \pm 1432.8	1250.5 \pm 110.8	0.55	0.501	1744.0 \pm 278.5	1378.5 \pm 345.5	0.79	0.769	1.102	0.903
IL-12(p40)	7169.0 \pm 2465.5	12235.5 \pm 789.4	1.71	0.001	5478.7 \pm 1195.4	10289.5 \pm 1119.3	1.88	0.000	0.841	0.065
IL-12(p70)	4344.0 \pm 1603.5	2380.0 \pm 297.5	0.55	0.205	3650.0 \pm 67.3	3408.0 \pm 629.9	0.93	0.846	1.432	0.327
IL-13	1549.5 \pm 878.4	1003.5 \pm 32.6	0.65	0.724	1143.3 \pm 206.5	966.5 \pm 150.8	0.85	0.887	0.963	0.972
IL-17	9618.0 \pm 1077.8	7653.0 \pm 1028.5	0.80	0.204	15038.7 \pm 1848.2	16946.5 \pm 4084.0	1.13	0.127	2.214	0.000
Eotaxin	2438.0 \pm 1240.9	1515.0 \pm 152.2	0.62	0.550	1726.7 \pm 359.4	1297.5 \pm 191.3	0.75	0.730	0.856	0.835
G-CSF	2943.0 \pm 587.5	5336.0 \pm 841.1	1.81	0.123	2393.3 \pm 237.1	5404.5 \pm 884.8	2.26	0.017	1.013	0.948
GM-CSF	3165.0 \pm 1577.0	1899.5 \pm 150.4	0.60	0.413	2026.0 \pm 217.9	1667.5 \pm 201.2	0.82	0.773	0.878	0.825
IFN-γ	5319.5 \pm 2685.5	3042.0 \pm 308.8	0.57	0.142	4363.3 \pm 616.7	2961.5 \pm 581.5	0.68	0.261	0.974	0.939
KC	2772.0 \pm 1391.6	2750.5 \pm 270.9	0.99	0.989	2604.7 \pm 579.7	3002.5 \pm 202.6	1.15	0.749	1.092	0.810
MCP-1	2295.0 \pm 1475.1	1244.5 \pm 128.5	0.54	0.497	1530.0 \pm 354.2	983.0 \pm 177.4	0.64	0.660	0.790	0.803
MIP-1α	6383.5 \pm 2128.9	3495.0 \pm 184.5	0.55	0.063	4549.3 \pm 386.3	4044.5 \pm 299.7	0.89	0.685	1.157	0.600
MIP-1β	2580.5 \pm 1487.3	1773.5 \pm 148.7	0.69	0.601	1812.0 \pm 391.7	1830.5 \pm 394.2	1.01	0.988	1.032	0.957
RANTES	5180.0 \pm 1778.4	6816.5 \pm 649.0	1.32	0.290	4004.0 \pm 332.8	4795.0 \pm 1002.2	1.20	0.525	0.703	0.055
TNF-α	4193.0 \pm 2346.4	2439.0 \pm 305.1	0.58	0.257	3373.3 \pm 527.8	2380.0 \pm 547.7	0.71	0.425	0.976	0.955

Suppl Table 2. Sera cytokine expression.

SERA	Day 7									
	Native NP	Inf NP	Fold change	p-value	Native P	Inf P	Fold change	p-value	Fold Change	p-value
Sample										
IL-1α	1637.5 \pm 138.9	1624.8 \pm 205.0	0.99	0.857	1720.0 \pm 479.3	3732.0 \pm 1824.3	2.17	0.191	2.297	0.154
IL-1β	1842.0 \pm 1254.6	3108.8 \pm 971.5	1.69	0.979	890.0 \pm 152.4	3934.4 \pm 1409.0	4.42	0.049	1.266	0.576
IL-2	1123.0 \pm 128.7	994.4 \pm 117.8	0.89	0.994	1384.7 \pm 126.8	1239.2 \pm 137.2	0.89	0.925	1.246	0.868
IL-3	1634.5 \pm 686.0	2673.6 \pm 647.7	1.64	0.987	1780.0 \pm 261.6	2590.0 \pm 509.3	1.46	0.598	0.969	0.955
IL-4	1451.5 \pm 771.6	2064.8 \pm 466.5	1.42	0.977	1145.3 \pm 45.4	2170.8 \pm 518.6	1.90	0.504	1.051	0.943
IL-5	1839.0 \pm 976.3	2663.2 \pm 720.1	1.45	0.996	1082.7 \pm 188.1	2943.2 \pm 544.9	2.72	0.227	1.105	0.849
IL-6	2820.0 \pm 1553.5	4610.4 \pm 1160.1	1.63	0.005	2084.0 \pm 221.6	5176.0 \pm 973.9	2.48	0.046	1.123	0.701
IL-9	2728.5 \pm 1180.3	3057.2 \pm 329.8	1.12	0.994	1086.7 \pm 1.3	4835.6 \pm 1016.7	4.45	0.016	1.582	0.229
IL-10	2289.0 \pm 1432.8	3395.2 \pm 916.6	1.48	0.976	1793.3 \pm 240.8	3239.6 \pm 621.0	1.81	0.347	0.954	0.916
IL-12(p40)	7169.0 \pm 2465.5	8864.8 \pm 778.6	1.24	0.001	6916.7 \pm 964.1	7646.4 \pm 969.9	1.11	0.635	0.863	0.409
IL-12(p70)	4344.0 \pm 1603.5	6193.6 \pm 1386.1	1.43	0.957	5216.0 \pm 679.3	6090.4 \pm 997.6	1.17	0.569	0.983	0.944
IL-13	1549.5 \pm 878.4	2236.4 \pm 518.8	1.44	0.996	1144.0 \pm 89.0	2446.8 \pm 466.4	2.14	0.397	1.094	0.886
IL-17	9618.0 \pm 1077.8	10565.6 \pm 1567.1	1.10	0.971	24370.7 \pm 3709.8	12228.0 \pm 1423.5	0.50	0.000	1.157	0.260
Eotaxin	2438.0 \pm 1240.9	4129.6 \pm 1037.7	1.69	0.969	1550.0 \pm 168.7	3969.2 \pm 828.3	2.56	0.117	0.961	0.913
G-CSF	2943.0 \pm 587.5	4764.8 \pm 829.3	1.62	0.332	3893.3 \pm 189.6	6003.6 \pm 342.1	1.54	0.171	1.260	0.401
GM-CSF	3165.0 \pm 1577.0	4628.0 \pm 1050.9	1.46	0.928	2048.0 \pm 238.1	4684.0 \pm 1103.7	2.29	0.088	1.012	0.970
IFN-γ	5319.5 \pm 2685.5	7782.4 \pm 1669.2	1.46	0.943	4052.0 \pm 557.8	7626.4 \pm 1453.5	1.88	0.021	0.980	0.916
KC	2772.0 \pm 1391.6	3602.0 \pm 541.9	1.30	0.000	1918.7 \pm 140.2	3607.2 \pm 448.4	1.88	0.272	1.001	0.997
MCP-1	2295.0 \pm 1475.1	3805.6 \pm 1080.9	1.66	0.227	1276.7 \pm 147.4	3998.4 \pm 982.4	3.13	0.078	1.051	0.896
MIP-1α	6383.5 \pm 2128.9	8038.8 \pm 1481.6	1.26	0.000	4685.3 \pm 313.0	8392.8 \pm 1396.0	1.79	0.017	1.044	0.810
MIP-1β	2580.5 \pm 1487.3	4271.6 \pm 1183.5	1.66	0.437	2286.0 \pm 237.8	4546.0 \pm 822.2	1.99	0.142	1.064	0.852
RANTES	5180.0 \pm 1778.4	8347.6 \pm 1286.7	1.61	0.000	6256.7 \pm 1068.9	6719.2 \pm 1230.8	1.07	0.763	0.805	0.270
TNF-α	4193.0 \pm 2346.4	6638.8 \pm 1638.6	1.58	0.997	3192.7 \pm 473.1	7473.6 \pm 1713.5	2.34	0.006	1.126	0.571

Suppl Table 3. Placental cytokine expression.

Supplemental Table 3. Placental Cytokine Expression.

PLACENTA	Day 4					Day 7				
	Naïve P	Inf P	Fold change	p-value		Naïve P	Inf P	Fold change	p-value	
IL-1α	31260.0 \pm 2555.3	15576.0 \pm 2479.8	0.50	0.000		9589.2 \pm 1630.8	8586.1 \pm 564.6	0.90	0.748	
IL-1β	2462.4 \pm 124.1	1789.0 \pm 151.0	0.73	0.787		1882.8 \pm 51.8	2493.2 \pm 337.5	1.32	0.845	
IL-2	7674.0 \pm 575.2	3904.4 \pm 296.2	0.51	0.132		3088.8 \pm 101.8	4388.6 \pm 364.2	1.42	0.677	
IL-3	2252.4 \pm 37.3	2526.4 \pm 194.8	1.12	0.913		2270.4 \pm 77.2	2488.1 \pm 162.5	1.10	0.944	
IL-4	979.2 \pm 29.8	1003.8 \pm 90.0	1.03	0.992		1062.0 \pm 66.4	927.1 \pm 44.9	0.87	0.965	
IL-5	1550.4 \pm 53.6	1184.1 \pm 68.5	0.76	0.883		1098.0 \pm 22.6	1212.0 \pm 52.6	1.10	0.971	
IL-6	3144.0 \pm 80.7	2640.1 \pm 117.1	0.84	0.840		2834.4 \pm 116.1	3212.7 \pm 175.5	1.13	0.903	
IL-9	9118.8 \pm 2022.4	2693.3 \pm 165.8	0.30	0.011		4411.2 \pm 144.2	5599.5 \pm 466.8	1.27	0.703	
IL-10	1893.6 \pm 57.9	1609.3 \pm 94.3	0.85	0.909		1674.0 \pm 31.7	1743.3 \pm 54.7	1.04	0.982	
IL-12(p40)	7386.0 \pm 211.5	7448.9 \pm 220.0	1.01	0.980		5636.4 \pm 509.7	5673.7 \pm 641.2	1.01	0.990	
IL-12(p70)	3660.0 \pm 66.6	3872.8 \pm 352.5	1.06	0.932		3391.2 \pm 138.4	3563.0 \pm 159.9	1.05	0.956	
IL-13	3189.6 \pm 137.7	1572.3 \pm 67.0	0.49	0.517		1658.4 \pm 66.3	2001.1 \pm 122.4	1.21	0.912	
IL-17	4314.0 \pm 185.8	3962.6 \pm 421.8	0.92	0.888		3910.8 \pm 191.6	3555.1 \pm 187.3	0.91	0.909	
Eotaxin	3897.6 \pm 269.7	2737.4 \pm 158.3	0.70	0.642		3117.6 \pm 214.9	5225.1 \pm 547.0	1.68	0.499	
G-CSF	15913.2 \pm 2669.0	33178.7 \pm 4464.2	2.08	0.000		29504.4 \pm 8299.3	22117.2 \pm 6815.4	0.75	0.019	
GM-CSF	4114.8 \pm 57.1	4086.4 \pm 180.9	0.99	0.991		4088.4 \pm 126.9	4377.8 \pm 180.9	1.07	0.926	
IFN-γ	3895.2 \pm 127.9	3499.0 \pm 285.1	0.90	0.874		3471.6 \pm 122.2	4103.2 \pm 265.6	1.18	0.839	
KC	45151.2 \pm 4996.2	52324.6 \pm 6605.8	1.16	0.004		17089.2 \pm 1814.5	37420.3 \pm 9681.0	2.19	0.000	
MCP-1	2234.4 \pm 268.0	3315.2 \pm 295.4	1.48	0.665		2481.6 \pm 364.6	4222.2 \pm 850.4	1.70	0.577	
MIP-1α	16624.8 \pm 956.0	30334.9 \pm 4884.6	1.82	0.000		25503.6 \pm 3339.1	23203.0 \pm 826.3	0.91	0.461	
MIP-1β	4576.8 \pm 329.5	4181.7 \pm 328.5	0.91	0.874		4530.0 \pm 548.5	5089.2 \pm 580.4	1.12	0.858	
RANTES	12465.6 \pm 1901.7	6981.1 \pm 688.8	0.56	0.029		6019.2 \pm 418.8	8367.8 \pm 423.0	1.39	0.452	
TNF-α	1808.4 \pm 97.6	1362.6 \pm 68.8	0.75	0.858		1294.8 \pm 54.8	1455.6 \pm 60.1	1.12	0.959	

Chapter IV: Conclusions

Influenza viral illness causes significant socioeconomic and clinical burden each year [88]. The interlinked immunology of viral pathogenesis and reproductive endocrinology makes the field of infectious disease in pregnant women complicated, exciting, and clinically significant. Investigations into the immunological components of infertility, recurrent miscarriage, and preeclampsia have yielded a wealth of information regarding the requirements of immune tolerance and rejection, and this information can provide a platform for understanding healthy pregnancy and how inflammation and hormonal dysregulation will impact maternal health and fetal development.

This dissertation focused on the effect of H1N1 influenza A virus infection during pregnancy due to the wide availability of clinical data on how H1N1 pandemics have affected pregnant populations. However, there is need for evaluating how other influenza groups and subtypes affect women. In this research, I found that seasonal H1N1 A/Brisbane/59/2007 (Chapter 2) induced increased inflammation in the lungs and sera following mid-gestation infection while pandemic H1N1 A/California/07/2009 (Chapter 3) induced a wider variety of chemokines in the lungs, sera, and placenta. While these experiments cannot be directly compared due to the differences in dose, it is interesting that a lower dose of H1N1 A/California/07/2009 was able to produce the same phenotype of pre-term birth and placental degradation; still, lethal infection of mothers with H1N1 A/Brisbane/59/2007 unsurprisingly increased the incidence of stillborn mice and prostaglandins in the placenta. While most research into influenza A viral infection during pregnancy has focused on H1N1 subtypes, there is evidence that influenza B virus can also cause significant maternal and fetal complications following mid-gestation infection [89, 90]. It remains unclear if seasonal H3N2 infection, excluding neurotropic WSN strains, contributes to the poor clinical outcomes of

influenza virus-infected pregnant women infected in a similar manner to H1N1 and B virus strains [89, 91-93]. Lastly, emerging pandemic avian H7N9 and H5N1 influenza strains have been shown to cause enhanced disease during pregnancy, and the knowledge gained through research of the pandemic H1N1 swine-derived influenza virus may provide the clinical and research community with early resources for a novel pandemic virus entering a naïve pregnant population [94-97]. These studies demonstrate the vulnerability of pregnant women to infectious disease, and the fact that neonate health is directly dependent on maternal health, doubles the significance of research that results in improved therapies and treatment strategies.

Respiratory infection during pregnancy is of broad interest. While influenza A virus has generated some of the highest morbidity rates following maternal infection, coronavirus outbreaks have also been associated with similar outcomes in mothers and neonates following mid-gestation infection. Infection with severe acute respiratory syndrome (SARS) virus and Middle Eastern respiratory syndrome (MERS) virus have been associated with spontaneous abortion, fetal growth retardation, and maternal and neonate mortality [98-100]. Mid-gestation infection with respiratory syncytial virus (RSV) has been described in rare severe adult cases and has also been associated with pre-term birth and low birth weight in a cohort in Nepal [101, 102]. High rates of mortality among infants and toddlers infected with RSV highlights the need for improved understanding of maternal immunity to RSV infection and vaccination during pregnancy, and there is hope that vaccination of mothers during pregnancy can provide transplacental immunity that will protect the fetus for months after birth [103]. None of these viruses were transmitted transplacentally to fetuses, and yet respiratory infection during pregnancy still induced significant maternal illness, pre-term labor, low birth weight, or spontaneous abortion. The pork industry also provides an interesting connection to pregnant immunology and fetal susceptibility to respiratory viruses

during pregnancy. Pregnancy increases the mortality of pregnant sows infected with porcine reproductive and respiratory syndrome (PRRSV) virus, and gilts born to sows infected with PRRSV during pregnancy had increased mortality associated with fetal exposure to type I inflammatory cytokines and activation of CD8⁺ T cells at the maternal fetal interface [104-107]. These clinical and veterinary data both demonstrate the broad effects of pregnancy on the immune response to respiratory illness and that these effects may not be limited to humans.

Animal models are necessary to conduct experiments on viral pathogenesis mid-gestation because obtaining placental samples can only occur with the termination of pregnancy. Guinea pigs and ferrets are widely accepted as the best models for the study of influenza virus transmission studies, while mice are more frequently used for the study of cellular activation and immune response due to their similarity to humans in cytokine signaling in the lung and B and T cells responses [108-113]. The addition of pregnancy to research studies of influenza virus pathogenesis and immune responses required an additional layer of homology with human physiology: similarity between uterine and placental cytokine and hormonal expression and cellular composition. While non-human primates are the closest to humans in placentation and hormone expression, they are expensive and require intensive care regimens; guinea pigs are alternative model but have fewer reagents available [114, 115]. Therefore, this research utilized timed pregnancies in mice, who have haemochorial placenta similar to humans [116]. While the diffusion properties of amino acids, nutrient macromolecules, and cytokines across the maternal-fetal interface are similar between mice and humans, mice have are haemotrichorial, meaning they have three layers of spongiotrophoblasts in comparison with the single syncytiotrophoblast layer found in human placenta [116]. Previously, common models examining the interplay of hormonal regulation and immune responses to viral infection employed hormone-secreting intradermal

implants or injections into often ovariectomized mice [117, 118]. These models have shown how progesterone and estrogen can protect female mice from influenza virus immunopathology via the down-regulation of inflammatory cytokines IL-1 α , IFN- γ , and IFN- β [57, 118, 119]. However, these studies do not fully recapitulate the maternal-fetal environment, with systemic changes that include not just progesterone and estrogen increases, but also the complexities of placental signaling and fetal development. The use of a pregnant animal model allows for the examination of the effect of placental hormonal secretion and fetal antigen stimulation of the immune system and is thus more physiologically similar, although much more complicated, than single hormone implant or dosing. This dissertation utilized a BALB/c murine model due to the combined immunological and placental shared physiology with pregnant women and for the ease of use, facility concerns, reagent availability, and cost-efficiency across multiple timepoints; a more detailed comparison is available in Chapter 2 [115, 116, 120]. This work is the first to provide a mechanism for placental degradation as a result of H1N1 influenza virus infection in maternal lungs and the first to provide a description of how pregnancy-induced cytokine and hormonal dysregulation impacts the long-term development of systemic and mucosal immunity.

Early antiviral therapy following H1N1 influenza A virus infection during pregnancy has been shown to significantly reduce preterm birth, hospitalization in intensive care units (ICUs), and maternal death [9, 121]. In Chapter 2, I showed how seasonal H1N1 influenza A virus induced increased levels of cyclooxygenase-2 (COX-2) and prostaglandin-F 2α in the lungs and placenta, which provides a mechanism for lung immunopathology and preterm labor in pregnant mice. The anti-inflammatory potential of COX-2 inhibitor therapy has already been proposed for high-pathogenesis avian influenza strains H5N1 and H7N9 and attenuates lung expression of G-CSF and KC, cytokines I found to be elevated in pregnant mice infected by H1N1 A/Brisbane/59/2007

and H1N1 A/California/07/2009 (Chapter 3) [122-125]. However, while non-steroidal anti-inflammatory drugs (NSAIDs) have been shown to be safe during pregnancy, COX-2 specific inhibitors may induce pre-term labor and musculoskeletal defects [126-128]. I also identified that viral load was negatively associated with progesterone and that reduced progesterone expression was correlated with preterm labor in influenza virus-infected pregnant mothers. Administration of progesterone to female mice following H1N1 influenza virus infection has already been identified to reduce immunopathology and improved lung epithelial cell regeneration, although it had no effect on reducing viral load [119, 129]. Hence, limiting viral replication should be one of many aims for anti-influenza therapy during pregnancy, including the limiting of immunopathology caused by cytokine dysregulation and promoting the healing of damaged airway epithelium following viral clearance.

Pregnancy hormones may coordinate the down-regulation of class-switching or post-translational modifications (i.e. glycosylation, fucosylation, sialylation, etc) of the antigen-binding (Fab) or receptor binding (Fc) regions of antibodies in order to attenuate potentially inflammatory or anti-fetal immune responses. As described in Chapter 3, H1N1 influenza A virus infection caused an increase in virus-specific IgG antibodies but a reduction in virus-specific IgG1, IgG2a, and hemagglutinin inhibition (HAI) titers and IgG avidity. There have also been reports that pregnant women infected with H1N1 pandemic virus in Shenyang, China in 2009 produced an imbalanced proportion of anti-H1N1 IgG1, IgG2, IgG3, and IgG4 antibody subtypes compared with infected non-pregnant women in the same hospital [130]. Interestingly, IgG1 is preferentially transported from maternal circulation across the placenta compared to other IgG classes, especially IgG2, although this phenomenon has not been directly linked to influenza infection and vaccination previously [131-133]. While preferential transport is linked to affinity with the

neonatal FcRn receptors on placental syncytiotrophoblasts into the fetal blood stream, how pregnancy shifts expression from virus-specific IgG2 to IgG1 requires further investigation [133].

Antibody isotype classes and generation of specificity are governed by the class-switching of Ig genes and somatic hypermutation of their variable chain-encoding regions [69, 134]. Variability is induced primarily by activation-induced cytidine deaminase (AID) and uracil-DNA glycosylase (UNG) that selectively damage DNA and repair it randomly [69, 134, 135]. B cells that have complementarity-determining regions (CDRs) that bind best to antigen are selected for by T follicular helper cells (TFHs) and clonally amplified to flood the circulatory system with virus neutralizing antibodies [136, 137]. Estrogen and progesterone seem to work in opposition to each other on the regulation of AID: estrogen receptors bind the HoxC4 promoter to induce AID activation, while progesterone receptors can bind directly to the AID promoter to inhibit activation [138-140]. Glucocorticoids have also been described as negative regulators of AID activation [141]. These phenomena are typically described in the context of autoimmune disease regulation and have not been described in the multi-hormonal environment of pregnancy.

Asymmetric glycosylation, or the single glycosylation of one side rather than both sides of the Fab or Fc antibody chains, can result in finely tuned interactions with antigen and Fc receptors, and these binding affinities are important for antibody-dependent cellular cytotoxicity (ADCC) [142, 143]. Pregnancy has been shown to increase the serum and placental concentrations of asymmetrically glycosylated IgG and may provide an explanation for the reduced avidity and virus-binding capability demonstrated in Chapter 3 following viral infection during pregnancy [144, 145]. Human and murine placental expression of IL-6 has been shown to induce asymmetrical glycosylation of IgG from hybridomas [146, 147]. Trophoblast-produced asymmetric antibodies have been documented throughout the placenta [144, 148]. However,

whether these signaling effects can extend outside the uterus has yet to be determined and would be a major finding in maternal immunity. By reducing binding specificity for antibody effector cells via asymmetric glycosylation, the maternal immune system may be able to mitigate the negative effects of any anti-fetal antibodies that may have developed while still maintaining a population of semi-functional or selectively-functional antibodies that can neutralize pathogens and non-self-entities [145].

In summary, this dissertation bridges research disciplines in reproductive immunology and viral pathogenesis to describe how the maternal immune system is initially disadvantaged by increased immunopathology but is not dampened by reduced activation of virus-specific B and T cells. I demonstrate that boost vaccination following an initial vaccination during pregnancy results in improved immune responses over non-pregnant mice with the same vaccination strategy. Further research is needed to describe how progesterone specifically alters B cell expression and function in our model despite similar activation levels. The balance of immune tolerance of the fetus and immune rejection, clearance, and memory of pathogens complicates our current understanding of influenza viral pathogenesis and likely requires specialized antiviral therapies and vaccination strategies to prevent maternal and fetal health complications.

References

1. Webster RG, Bean WJ, Gorman OT, Chambers TM, Kawaoka Y. Evolution and ecology of influenza A viruses. *Microbiol Rev.* 1992;56(1):152-79. Epub 1992/03/01. PubMed PMID: 1579108; PubMed Central PMCID: PMCPMC372859.
2. Kidd M. Influenza viruses: update on epidemiology, clinical features, treatment and vaccination. *Curr Opin Pulm Med.* 2014;20(3):242-6. Epub 2014/03/19. doi: 10.1097/MCP.0000000000000049. PubMed PMID: 24637227.
3. Taubenberger JK, Kash JC. Influenza virus evolution, host adaptation, and pandemic formation. *Cell Host Microbe.* 2010;7(6):440-51. Epub 2010/06/15. doi: 10.1016/j.chom.2010.05.009. PubMed PMID: 20542248; PubMed Central PMCID: PMCPMC2892379.
4. Tao H, Steel J, Lowen AC. Intrahost dynamics of influenza virus reassortment. *J Virol.* 2014;88(13):7485-92. Epub 2014/04/18. doi: 10.1128/JVI.00715-14. PubMed PMID: 24741099; PubMed Central PMCID: PMCPMC4054463.
5. Hannoun C. The evolving history of influenza viruses and influenza vaccines. *Expert Rev Vaccines.* 2013;12(9):1085-94. Epub 2013/09/13. doi: 10.1586/14760584.2013.824709. PubMed PMID: 24024871.
6. Jamieson DJ, Honein MA, Rasmussen SA, Williams JL, Swerdlow DL, Biggerstaff MS, et al. H1N1 2009 influenza virus infection during pregnancy in the USA. *Lancet.* 2009;374(9688):451-8. Epub 2009/08/01. doi: 10.1016/S0140-6736(09)61304-0. PubMed PMID: 19643469.

7. Longman RE, Johnson TR. Viral respiratory disease in pregnancy. *Curr Opin Obstet Gynecol.* 2007;19(2):120-5. Epub 2007/03/14. doi: 10.1097/GCO.0b013e328028fdc7. PubMed PMID: 17353679.
8. Creanga AA, Johnson TF, Graitcer SB, Hartman LK, Al-Samarrai T, Schwarz AG, et al. Severity of 2009 pandemic influenza A (H1N1) virus infection in pregnant women. *Obstet Gynecol.* 2010;115(4):717-26. Epub 2010/03/24. doi: 10.1097/AOG.0b013e3181d57947. PubMed PMID: 20308830.
9. Siston AM, Rasmussen SA, Honein MA, Fry AM, Seib K, Callaghan WM, et al. Pandemic 2009 influenza A(H1N1) virus illness among pregnant women in the United States. *JAMA.* 2010;303(15):1517-25. Epub 2010/04/22. doi: 10.1001/jama.2010.479. PubMed PMID: 20407061.
10. Rasmussen SA, Jamieson DJ, Uyeki TM. Effects of influenza on pregnant women and infants. *Am J Obstet Gynecol.* 2012;207(3 Suppl):S3-8. Epub 2012/09/07. doi: 10.1016/j.ajog.2012.06.068. PubMed PMID: 22920056.
11. Pierce M, Kurinczuk JJ, Spark P, Brocklehurst P, Knight M, Ukoss. Perinatal outcomes after maternal 2009/H1N1 infection: national cohort study. *BMJ.* 2011;342:d3214. Epub 2011/06/16. doi: 10.1136/bmj.d3214. PubMed PMID: 21672992; PubMed Central PMCID: PMC3114455.
12. Mendez-Figueroa H, Raker C, Anderson BL. Neonatal characteristics and outcomes of pregnancies complicated by influenza infection during the 2009 pandemic. *Am J Obstet Gynecol.* 2011;204(6 Suppl 1):S58-63. Epub 2011/04/05. doi: 10.1016/j.ajog.2011.02.058. PubMed PMID: 21457913; PubMed Central PMCID: PMC3111839.

13. Kay AW, Blish CA. Immunogenicity and Clinical Efficacy of Influenza Vaccination in Pregnancy. *Front Immunol.* 2015;6:289. Epub 2015/06/20. doi: 10.3389/fimmu.2015.00289. PubMed PMID: 26089824; PubMed Central PMCID: PMC4455389.
14. Schlaudecker EP, McNeal MM, Dodd CN, Ranz JB, Steinhoff MC. Pregnancy modifies the antibody response to trivalent influenza immunization. *J Infect Dis.* 2012;206(11):1670-3. Epub 2012/09/18. doi: 10.1093/infdis/jis592. PubMed PMID: 22984116.
15. Adegbola R, Nesin M, Wairagkar N. Immunogenicity and efficacy of influenza immunization during pregnancy: recent and ongoing studies. *Am J Obstet Gynecol.* 2012;207(3 Suppl):S28-32. Epub 2012/09/07. doi: 10.1016/j.ajog.2012.07.001. PubMed PMID: 22920055.
16. Salomon R, Webster RG. The influenza virus enigma. *Cell.* 2009;136(3):402-10. Epub 2009/02/11. doi: 10.1016/j.cell.2009.01.029. PubMed PMID: 19203576; PubMed Central PMCID: PMC2971533.
17. van Riel D, den Bakker MA, Leijten LM, Chutinimitkul S, Munster VJ, de Wit E, et al. Seasonal and pandemic human influenza viruses attach better to human upper respiratory tract epithelium than avian influenza viruses. *Am J Pathol.* 2010;176(4):1614-8. Epub 2010/02/20. doi: 10.2353/ajpath.2010.090949. PubMed PMID: 20167867; PubMed Central PMCID: PMC2843453.
18. Lakadamyali M, Rust MJ, Zhuang X. Endocytosis of influenza viruses. *Microbes Infect.* 2004;6(10):929-36. Epub 2004/08/18. doi: 10.1016/j.micinf.2004.05.002. PubMed PMID: 15310470; PubMed Central PMCID: PMC2715838.

19. Luo M. Influenza virus entry. *Adv Exp Med Biol.* 2012;726:201-21. Epub 2012/02/03. doi: 10.1007/978-1-4614-0980-9_9. PubMed PMID: 22297515.
20. Leung HS, Li OT, Chan RW, Chan MC, Nicholls JM, Poon LL. Entry of influenza A Virus with a alpha2,6-linked sialic acid binding preference requires host fibronectin. *J Virol.* 2012;86(19):10704-13. Epub 2012/07/28. doi: 10.1128/JVI.01166-12. PubMed PMID: 22837202; PubMed Central PMCID: PMC3457276.
21. Watanabe T, Watanabe S, Kawaoka Y. Cellular networks involved in the influenza virus life cycle. *Cell Host Microbe.* 2010;7(6):427-39. Epub 2010/06/15. doi: 10.1016/j.chom.2010.05.008. PubMed PMID: 20542247; PubMed Central PMCID: PMC3167038.
22. Canini L, Carrat F. Population modeling of influenza A/H1N1 virus kinetics and symptom dynamics. *J Virol.* 2011;85(6):2764-70. Epub 2010/12/31. doi: 10.1128/JVI.01318-10. PubMed PMID: 21191031; PubMed Central PMCID: PMC3067928.
23. Kuiken T, Riteau B, Fouchier RA, Rimmelzwaan GF. Pathogenesis of influenza virus infections: the good, the bad and the ugly. *Curr Opin Virol.* 2012;2(3):276-86. Epub 2012/06/20. doi: 10.1016/j.coviro.2012.02.013. PubMed PMID: 22709515.
24. Hsu AC, Parsons K, Barr I, Lowther S, Middleton D, Hansbro PM, et al. Critical role of constitutive type I interferon response in bronchial epithelial cell to influenza infection. *PLoS One.* 2012;7(3):e32947. Epub 2012/03/08. doi: 10.1371/journal.pone.0032947. PubMed PMID: 22396801; PubMed Central PMCID: PMC3292582.
25. Yamaya M, Nadine LK, Ota C, Kubo H, Makiguchi T, Nagatomi R, et al. Magnitude of influenza virus replication and cell damage is associated with interleukin-6 production in

- primary cultures of human tracheal epithelium. *Respir Physiol Neurobiol.* 2014;202:16-23. Epub 2014/07/30. doi: 10.1016/j.resp.2014.07.010. PubMed PMID: 25064661.
26. Fukuyama S, Kawaoka Y. The pathogenesis of influenza virus infections: the contributions of virus and host factors. *Curr Opin Immunol.* 2011;23(4):481-6. Epub 2011/08/16. doi: 10.1016/j.coi.2011.07.016. PubMed PMID: 21840185; PubMed Central PMCID: PMC3163725.
27. Schultz-Cherry S. Role of NK cells in influenza infection. *Curr Top Microbiol Immunol.* 2015;386:109-20. Epub 2014/07/06. doi: 10.1007/82_2014_403. PubMed PMID: 24992894.
28. McCullers JA. The co-pathogenesis of influenza viruses with bacteria in the lung. *Nat Rev Microbiol.* 2014;12(4):252-62. Epub 2014/03/05. doi: 10.1038/nrmicro3231. PubMed PMID: 24590244.
29. Liderot K, Ahl M, Ozenci V. Secondary bacterial infections in patients with seasonal influenza A and pandemic H1N1. *Biomed Res Int.* 2013;2013:376219. Epub 2013/07/19. doi: 10.1155/2013/376219. PubMed PMID: 23865050; PubMed Central PMCID: PMC3705841.
30. Taubenberger JK, Morens DM. The pathology of influenza virus infections. *Annu Rev Pathol.* 2008;3:499-522. Epub 2007/11/28. doi: 10.1146/annurev.pathmechdis.3.121806.154316. PubMed PMID: 18039138; PubMed Central PMCID: PMC3163725.
31. De Serres G, Rouleau I, Hamelin ME, Quach C, Skowronski D, Flamand L, et al. Contagious period for pandemic (H1N1) 2009. *Emerg Infect Dis.* 2010;16(5):783-8.

- Epub 2010/04/23. doi: 10.3201/eid1605.091894. PubMed PMID: 20409367; PubMed Central PMCID: PMCPMC2954014.
32. Bot A, Reichlin A, Isobe H, Bot S, Schulman J, Yokoyama WM, et al. Cellular mechanisms involved in protection and recovery from influenza virus infection in immunodeficient mice. *J Virol.* 1996;70(8):5668-72. Epub 1996/08/01. PubMed PMID: 8764086; PubMed Central PMCID: PMCPMC190532.
 33. Chiu C, Ellebedy AH, Wrammert J, Ahmed R. B cell responses to influenza infection and vaccination. *Curr Top Microbiol Immunol.* 2015;386:381-98. Epub 2014/09/07. doi: 10.1007/82_2014_425. PubMed PMID: 25193634.
 34. Hogan BL, Barkauskas CE, Chapman HA, Epstein JA, Jain R, Hsia CC, et al. Repair and regeneration of the respiratory system: complexity, plasticity, and mechanisms of lung stem cell function. *Cell Stem Cell.* 2014;15(2):123-38. Epub 2014/08/12. doi: 10.1016/j.stem.2014.07.012. PubMed PMID: 25105578; PubMed Central PMCID: PMCPMC4212493.
 35. Grabiec AM, Hussell T. The role of airway macrophages in apoptotic cell clearance following acute and chronic lung inflammation. *Semin Immunopathol.* 2016;38(4):409-23. Epub 2016/03/10. doi: 10.1007/s00281-016-0555-3. PubMed PMID: 26957481; PubMed Central PMCID: PMCPMC4896990.
 36. Pichyangkul S, Yongvanitchit K, Limsalakpetch A, Kum-Arb U, Im-Erbsin R, Boonnak K, et al. Tissue Distribution of Memory T and B Cells in Rhesus Monkeys following Influenza A Infection. *J Immunol.* 2015;195(9):4378-86. Epub 2015/09/27. doi: 10.4049/jimmunol.1501702. PubMed PMID: 26408671; PubMed Central PMCID: PMCPMC4642841.

37. Boyden AW, Frickman AM, Legge KL, Waldschmidt TJ. Primary and long-term B-cell responses in the upper airway and lung after influenza A virus infection. *Immunol Res.* 2014;59(1-3):73-80. Epub 2014/05/20. doi: 10.1007/s12026-014-8541-0. PubMed PMID: 24838149.
38. Laidlaw BJ, Zhang N, Marshall HD, Staron MM, Guan T, Hu Y, et al. CD4+ T cell help guides formation of CD103+ lung-resident memory CD8+ T cells during influenza viral infection. *Immunity.* 2014;41(4):633-45. Epub 2014/10/14. doi: 10.1016/j.immuni.2014.09.007. PubMed PMID: 25308332; PubMed Central PMCID: PMC4324721.
39. Wetendorf M, DeMayo FJ. Progesterone receptor signaling in the initiation of pregnancy and preservation of a healthy uterus. *Int J Dev Biol.* 2014;58(2-4):95-106. Epub 2014/07/16. doi: 10.1387/ijdb.140069mw. PubMed PMID: 25023675; PubMed Central PMCID: PMC4413906.
40. Mulac-Jericevic B, Conneely OM. Reproductive tissue selective actions of progesterone receptors. *Reproduction.* 2004;128(2):139-46. Epub 2004/07/29. doi: 10.1530/rep.1.00189. PubMed PMID: 15280552.
41. Sathish V, Martin YN, Prakash YS. Sex steroid signaling: implications for lung diseases. *Pharmacol Ther.* 2015;150:94-108. Epub 2015/01/18. doi: 10.1016/j.pharmthera.2015.01.007. PubMed PMID: 25595323; PubMed Central PMCID: PMC4523383.
42. Wira CR, Rodriguez-Garcia M, Patel MV. The role of sex hormones in immune protection of the female reproductive tract. *Nat Rev Immunol.* 2015;15(4):217-30. Epub

- 2015/03/07. doi: 10.1038/nri3819. PubMed PMID: 25743222; PubMed Central PMCID: PMC4716657.
43. James JL, Carter AM, Chamley LW. Human placentation from nidation to 5 weeks of gestation. Part I: What do we know about formative placental development following implantation? *Placenta*. 2012;33(5):327-34. Epub 2012/03/01. doi: 10.1016/j.placenta.2012.01.020. PubMed PMID: 22374510.
44. Saito S. Cytokine network at the feto-maternal interface. *J Reprod Immunol*. 2000;47(2):87-103. Epub 2000/08/05. PubMed PMID: 10924744.
45. Robinson DP, Klein SL. Pregnancy and pregnancy-associated hormones alter immune responses and disease pathogenesis. *Horm Behav*. 2012;62(3):263-71. Epub 2012/03/13. doi: 10.1016/j.yhbeh.2012.02.023. PubMed PMID: 22406114; PubMed Central PMCID: PMC3376705.
46. Druckmann R, Druckmann MA. Progesterone and the immunology of pregnancy. *The Journal of steroid biochemistry and molecular biology*. 2005;97(5):389-96. doi: 10.1016/j.jsbmb.2005.08.010. PubMed PMID: 16198558; PubMed Central PMCID: PMC16198558.
47. Tan IJ, Peeva E, Zandman-Goddard G. Hormonal modulation of the immune system - A spotlight on the role of progestogens. *Autoimmun Rev*. 2015;14(6):536-42. Epub 2015/02/24. doi: 10.1016/j.autrev.2015.02.004. PubMed PMID: 25697984.
48. Szekeres-Bartho J, Polgar B. PIBF: the double edged sword. *Pregnancy and tumor*. *Am J Reprod Immunol*. 2010;64(2):77-86. Epub 2010/04/07. doi: 10.1111/j.1600-0897.2010.00833.x. PubMed PMID: 20367622.

49. Tai P, Wang J, Jin H, Song X, Yan J, Kang Y, et al. Induction of regulatory T cells by physiological level estrogen. *J Cell Physiol*. 2008;214(2):456-64. Epub 2007/07/27. doi: 10.1002/jcp.21221. PubMed PMID: 17654501.
50. Coyne CB, Lazear HM. Zika virus - reigniting the TORCH. *Nat Rev Microbiol*. 2016;14(11):707-15. Epub 2016/08/31. doi: 10.1038/nrmicro.2016.125. PubMed PMID: 27573577.
51. Adams Waldorf KM, McAdams RM. Influence of infection during pregnancy on fetal development. *Reproduction*. 2013;146(5):R151-62. Epub 2013/07/26. doi: 10.1530/REP-13-0232. PubMed PMID: 23884862; PubMed Central PMCID: PMC4060827.
52. Meijer WJ, Wensing AM, Bruinse HW, Nikkels PG. High rate of chronic villitis in placentas of pregnancies complicated by influenza A/H1N1 infection. *Infect Dis Obstet Gynecol*. 2014;2014:768380. Epub 2014/04/03. doi: 10.1155/2014/768380. PubMed PMID: 24693211; PubMed Central PMCID: PMC3947755.
53. Komine-Aizawa S, Suzaki A, Trinh QD, Izumi Y, Shibata T, Kuroda K, et al. H1N1/09 influenza A virus infection of immortalized first trimester human trophoblast cell lines. *Am J Reprod Immunol*. 2012;68(3):226-32. Epub 2012/07/06. doi: 10.1111/j.1600-0897.2012.01172.x. PubMed PMID: 22762384.
54. Parboosing R, Bao Y, Shen L, Schaefer CA, Brown AS. Gestational influenza and bipolar disorder in adult offspring. *JAMA Psychiatry*. 2013;70(7):677-85. Epub 2013/05/24. doi: 10.1001/jamapsychiatry.2013.896. PubMed PMID: 23699867.
55. Brown AS, Derkits EJ. Prenatal infection and schizophrenia: a review of epidemiologic and translational studies. *Am J Psychiatry*. 2010;167(3):261-80. Epub 2010/02/04. doi:

- 10.1176/appi.ajp.2009.09030361. PubMed PMID: 20123911; PubMed Central PMCID: PMC3652286.
56. Zerbo O, Qian Y, Yoshida C, Fireman BH, Klein NP, Croen LA. Association Between Influenza Infection and Vaccination During Pregnancy and Risk of Autism Spectrum Disorder. *JAMA Pediatr.* 2017;171(1):e163609. Epub 2016/11/29. doi: 10.1001/jamapediatrics.2016.3609. PubMed PMID: 27893896.
57. Pazos MA, Kraus TA, Munoz-Fontela C, Moran TM. Estrogen mediates innate and adaptive immune alterations to influenza infection in pregnant mice. *PLoS One.* 2012;7(7):e40502. doi: 10.1371/journal.pone.0040502. PubMed PMID: 22792357; PubMed Central PMCID: PMC3390370.
58. Robinson DP, Hall OJ, Nilles TL, Bream JH, Klein SL. 17beta-estradiol protects females against influenza by recruiting neutrophils and increasing virus-specific CD8 T cell responses in the lungs. *J Virol.* 2014;88(9):4711-20. Epub 2014/02/14. doi: 10.1128/JVI.02081-13. PubMed PMID: 24522912; PubMed Central PMCID: PMC3993800.
59. Forbes RL, Wark PA, Murphy VE, Gibson PG. Pregnant women have attenuated innate interferon responses to 2009 pandemic influenza A virus subtype H1N1. *J Infect Dis.* 2012;206(5):646-53. Epub 2012/06/14. doi: 10.1093/infdis/jis377. PubMed PMID: 22693225.
60. Forbes RL, Gibson PG, Murphy VE, Wark PA. Impaired type I and III interferon response to rhinovirus infection during pregnancy and asthma. *Thorax.* 2012;67(3):209-14. Epub 2011/09/16. doi: 10.1136/thoraxjnl-2011-200708. PubMed PMID: 21917654.

61. Kim HM, Kang YM, Song BM, Kim HS, Seo SH. The 2009 pandemic H1N1 influenza virus is more pathogenic in pregnant mice than seasonal H1N1 influenza virus. *Viral immunology*. 2012;25(5):402-10. Epub 2012/09/19. doi: 10.1089/vim.2012.0007. PubMed PMID: 22985287; PubMed Central PMCID: PMC22985287.
62. Gao R, Bhatnagar J, Blau DM, Greer P, Rollin DC, Denison AM, et al. Cytokine and chemokine profiles in lung tissues from fatal cases of 2009 pandemic influenza A (H1N1): role of the host immune response in pathogenesis. *Am J Pathol*. 2013;183(4):1258-68. Epub 2013/08/14. doi: 10.1016/j.ajpath.2013.06.023. PubMed PMID: 23938324.
63. Meijer WJ, van Noortwijk AG, Bruinse HW, Wensing AM. Influenza virus infection in pregnancy: a review. *Acta Obstet Gynecol Scand*. 2015;94(8):797-819. Epub 2015/05/28. doi: 10.1111/aogs.12680. PubMed PMID: 26012384.
64. Raj RS, Bonney EA, Phillippe M. Influenza, immune system, and pregnancy. *Reprod Sci*. 2014;21(12):1434-51. Epub 2014/06/06. doi: 10.1177/1933719114537720. PubMed PMID: 24899469; PubMed Central PMCID: PMC4231130.
65. Harwood NE, Batista FD. Early events in B cell activation. *Annu Rev Immunol*. 2010;28:185-210. Epub 2010/03/03. doi: 10.1146/annurev-immunol-030409-101216. PubMed PMID: 20192804.
66. Niiro H, Clark EA. Regulation of B-cell fate by antigen-receptor signals. *Nat Rev Immunol*. 2002;2(12):945-56. Epub 2002/12/04. doi: 10.1038/nri955. PubMed PMID: 12461567.

67. Batista FD, Harwood NE. The who, how and where of antigen presentation to B cells. *Nat Rev Immunol*. 2009;9(1):15-27. Epub 2008/12/17. doi: 10.1038/nri2454. PubMed PMID: 19079135.
68. Shulman Z, Gitlin AD, Targ S, Jankovic M, Pasqual G, Nussenzweig MC, et al. T follicular helper cell dynamics in germinal centers. *Science*. 2013;341(6146):673-7. Epub 2013/07/28. doi: 10.1126/science.1241680. PubMed PMID: 23887872; PubMed Central PMCID: PMC3941467.
69. Matthews AJ, Zheng S, DiMenna LJ, Chaudhuri J. Regulation of immunoglobulin class-switch recombination: choreography of noncoding transcription, targeted DNA deamination, and long-range DNA repair. *Adv Immunol*. 2014;122:1-57. Epub 2014/02/11. doi: 10.1016/B978-0-12-800267-4.00001-8. PubMed PMID: 24507154; PubMed Central PMCID: PMC4150736.
70. Chu VT, Berek C. The establishment of the plasma cell survival niche in the bone marrow. *Immunol Rev*. 2013;251(1):177-88. Epub 2013/01/03. doi: 10.1111/imr.12011. PubMed PMID: 23278749.
71. Assad S, Khan HH, Ghazanfar H, Khan ZH, Mansoor S, Rahman MA, et al. Role of Sex Hormone Levels and Psychological Stress in the Pathogenesis of Autoimmune Diseases. *Cureus*. 2017;9(6):e1315. Epub 2017/07/12. doi: 10.7759/cureus.1315. PubMed PMID: 28690949; PubMed Central PMCID: PMC5498122.
72. Grimaldi CM, Cleary J, Dagtas AS, Moussai D, Diamond B. Estrogen alters thresholds for B cell apoptosis and activation. *J Clin Invest*. 2002;109(12):1625-33. Epub 2002/06/19. doi: 10.1172/JCI14873. PubMed PMID: 12070310; PubMed Central PMCID: PMC151010.

73. Bynoe MS, Grimaldi CM, Diamond B. Estrogen up-regulates Bcl-2 and blocks tolerance induction of naive B cells. *Proc Natl Acad Sci U S A*. 2000;97(6):2703-8. Epub 2000/03/01. doi: 10.1073/pnas.040577497. PubMed PMID: 10694576; PubMed Central PMCID: PMCPMC15993.
74. Zhang L CK, Li MQ, Li DJ, Yao XY. Mouse endometrial stromal cells and progesterone inhibit the activation and regulate the differentiation and antibody secretion of mouse B cells. *Int J Clin Exp Pathol* 2014;7(1):123-33. PubMed Central PMCID: PMCPMC3885466
75. Pazos M, Sperling RS, Moran TM, Kraus TA. The influence of pregnancy on systemic immunity. *Immunol Res*. 2012;54(1-3):254-61. doi: 10.1007/s12026-012-8303-9. PubMed PMID: 22447351.
76. Kay L. Medina GS, and Paul W. Kincade. Suppression of B Lymphopoiesis during Nomial Pregnancy. *The Journal of experimental medicine*. 1993;93(11):1507-15.
77. Medina KL SG, Kincade PW. Suppression of B Lymphopoiesis during Normal Pregnancy. *The Journal of experimental medicine*. 1993;93(11):1507-15. PubMed Central PMCID: PMC8228804.
78. Clark MR, Mandal M, Ochiai K, Singh H. Orchestrating B cell lymphopoiesis through interplay of IL-7 receptor and pre-B cell receptor signalling. *Nat Rev Immunol*. 2014;14(2):69-80. doi: 10.1038/nri3570. PubMed PMID: 24378843; PubMed Central PMCID: PMC4276135.
79. Bosco N, Ceredig R, Rolink A. Transient decrease in interleukin-7 availability arrests B lymphopoiesis during pregnancy. *Eur J Immunol*. 2008;38(2):381-90. Epub 2008/01/19. doi: 10.1002/eji.200737665. PubMed PMID: 18203141.

80. Tanneau GM H-SOL, Chevaleyre CC, Salmon HP. Differential Recruitment of T- and IgA B-lymphocytes in the Developing Mammary Gland in Relation to Homing Receptors and Vascular Addressins. *The journal of histochemistry and cytochemistry : official journal of the Histochemistry Society*. 1999;47(12):1581-92. PubMed Central PMCID: PMC10567442.
81. Kruse A MM, Hallmann R, Butcher EC. Evidence of specialized leukocyte-vascular homing interactions at the maternal/fetal interface. *Eur J Immunol*. 1999;29(4):1116-26. PubMed Central PMCID: PMC 10229078.
82. Ludvigsson JF, Zugna D, Cnattingius S, Richiardi L, Ekblom A, Ortqvist A, et al. Influenza H1N1 vaccination and adverse pregnancy outcome. *Eur J Epidemiol*. 2013;28(7):579-88. Epub 2013/05/30. doi: 10.1007/s10654-013-9813-z. PubMed PMID: 23715672.
83. Omer SB, Goodman D, Steinhoff MC, Rochat R, Klugman KP, Stoll BJ, et al. Maternal influenza immunization and reduced likelihood of prematurity and small for gestational age births: a retrospective cohort study. *PLoS Med*. 2011;8(5):e1000441. Epub 2011/06/10. doi: 10.1371/journal.pmed.1000441. PubMed PMID: 21655318; PubMed Central PMCID: PMC3104979.
84. Ahrens KA, Louik C, Kerr S, Mitchell AA, Werler MM. Seasonal influenza vaccination during pregnancy and the risks of preterm delivery and small for gestational age birth. *Paediatr Perinat Epidemiol*. 2014;28(6):498-509. Epub 2014/10/22. doi: 10.1111/ppe.12152. PubMed PMID: 25331380; PubMed Central PMCID: PMC4813306.

85. Takeda S, Hisano M, Komano J, Yamamoto H, Sago H, Yamaguchi K. Influenza vaccination during pregnancy and its usefulness to mothers and their young infants. *J Infect Chemother.* 2015;21(4):238-46. Epub 2015/02/25. doi: 10.1016/j.jiac.2015.01.015. PubMed PMID: 25708925.
86. Steinhoff MC, Omer SB, Roy E, Arifeen SE, Raqib R, Altaye M, et al. Influenza immunization in pregnancy--antibody responses in mothers and infants. *N Engl J Med.* 2010;362(17):1644-6. Epub 2010/04/30. doi: 10.1056/NEJMc0912599. PubMed PMID: 20427817.
87. Kay AW, Bayless NL, Fukuyama J, Aziz N, Dekker CL, Mackey S, et al. Pregnancy Does Not Attenuate the Antibody or Plasmablast Response to Inactivated Influenza Vaccine. *J Infect Dis.* 2015;212(6):861-70. Epub 2015/03/06. doi: 10.1093/infdis/jiv138. PubMed PMID: 25740957; PubMed Central PMCID: PMC4548461.
88. Gasparini R, Amicizia D, Lai PL, Panatto D. Clinical and socioeconomic impact of seasonal and pandemic influenza in adults and the elderly. *Hum Vaccin Immunother.* 2012;8(1):21-8. Epub 2012/01/19. doi: 10.4161/hv.8.1.17622. PubMed PMID: 22252007.
89. Regan AK, Moore HC, Sullivan SG, N DEK, Effler PV. Epidemiology of seasonal influenza infection in pregnant women and its impact on birth outcomes. *Epidemiol Infect.* 2017;145(14):2930-9. Epub 2017/09/12. doi: 10.1017/S0950268817001972. PubMed PMID: 28891463.
90. Kim JC, Kim HM, Kang YM, Ku KB, Park EH, Yum J, et al. Severe pathogenesis of influenza B virus in pregnant mice. *Virology.* 2014;448:74-81. Epub 2013/12/10. doi: 10.1016/j.virol.2013.10.001. PubMed PMID: 24314638.

91. Mackenzie JS, Williams K, Papadimitriou J. Influenza A virus and its influence on the outcome of pregnancy in the mouse. *Dev Biol Stand.* 1977;39:489-96. Epub 1977/06/01. PubMed PMID: 604135.
92. Puig-Barbera J, Natividad-Sancho A, Trushakova S, Sominina A, Pisareva M, Ciblak MA, et al. Epidemiology of Hospital Admissions with Influenza during the 2013/2014 Northern Hemisphere Influenza Season: Results from the Global Influenza Hospital Surveillance Network. *PLoS One.* 2016;11(5):e0154970. Epub 2016/05/20. doi: 10.1371/journal.pone.0154970. PubMed PMID: 27196667; PubMed Central PMCID: PMC4873033.
93. Stanwell-Smith R, Parker AM, Chakraverty P, Soltanpoor N, Simpson CN. Possible association of influenza A with fetal loss: investigation of a cluster of spontaneous abortions and stillbirths. *Commun Dis Rep CDR Rev.* 1994;4(3):R28-32. Epub 1994/03/04. PubMed PMID: 7513232.
94. Liu S, Sha J, Yu Z, Hu Y, Chan TC, Wang X, et al. Avian influenza virus in pregnancy. *Rev Med Virol.* 2016;26(4):268-84. Epub 2016/05/18. doi: 10.1002/rmv.1884. PubMed PMID: 27187752.
95. Xu L, Bao L, Deng W, Qin C. Highly pathogenic avian influenza H5N1 virus could partly be evacuated by pregnant BALB/c mouse during abortion or preterm delivery. *Virol J.* 2011;8:342. Epub 2011/07/12. doi: 10.1186/1743-422X-8-342. PubMed PMID: 21740553; PubMed Central PMCID: PMC3148567.
96. Guo Q, Zhao D, Dong F, Liu S, Chen Y, Jin J, et al. Delivery of fetus death with misoprostol in a pregnant woman with H7N9 avian influenza A virus pneumonia and

- ARDS. Crit Care. 2014;18(5):589. Epub 2015/02/13. doi: 10.1186/s13054-014-0589-7. PubMed PMID: 25672440; PubMed Central PMCID: PMC4210470.
97. Qi X, Cui L, Xu K, Wu B, Tang F, Bao C, et al. Avian influenza A(H7N9) virus infection in pregnant woman, China, 2013. Emerg Infect Dis. 2014;20(2):333-4. Epub 2014/01/25. doi: 10.3201/eid2002.131109. PubMed PMID: 24457138; PubMed Central PMCID: PMC43901503.
98. Alserehi H, Wali G, Alshukairi A, Alraddadi B. Impact of Middle East Respiratory Syndrome coronavirus (MERS-CoV) on pregnancy and perinatal outcome. BMC Infect Dis. 2016;16:105. Epub 2016/03/05. doi: 10.1186/s12879-016-1437-y. PubMed PMID: 26936356; PubMed Central PMCID: PMC4776369.
99. Malik A, El Masry KM, Ravi M, Sayed F. Middle East Respiratory Syndrome Coronavirus during Pregnancy, Abu Dhabi, United Arab Emirates, 2013. Emerg Infect Dis. 2016;22(3):515-7. Epub 2016/02/20. doi: 10.3201/eid2203.151049. PubMed PMID: 26890613; PubMed Central PMCID: PMC4766880.
100. Wong SF, Chow KM, Leung TN, Ng WF, Ng TK, Shek CC, et al. Pregnancy and perinatal outcomes of women with severe acute respiratory syndrome. Am J Obstet Gynecol. 2004;191(1):292-7. Epub 2004/08/06. doi: 10.1016/j.ajog.2003.11.019. PubMed PMID: 15295381.
101. Wheeler SM, Dotters-Katz S, Heine RP, Grotegut CA, Swamy GK. Maternal Effects of Respiratory Syncytial Virus Infection during Pregnancy. Emerg Infect Dis. 2015;21(11):1951-5. Epub 2015/10/21. doi: 10.3201/eid2111.150497. PubMed PMID: 26485575; PubMed Central PMCID: PMC4622246.

102. Chu HY, Katz J, Tielsch J, Khatry SK, Shrestha L, LeClerq SC, et al. Clinical Presentation and Birth Outcomes Associated with Respiratory Syncytial Virus Infection in Pregnancy. *PLoS One*. 2016;11(3):e0152015. Epub 2016/04/01. doi: 10.1371/journal.pone.0152015. PubMed PMID: 27031702; PubMed Central PMCID: PMC4816499.
103. Munoz FM. Respiratory syncytial virus in infants: is maternal vaccination a realistic strategy? *Curr Opin Infect Dis*. 2015;28(3):221-4. Epub 2015/04/29. doi: 10.1097/QCO.0000000000000161. PubMed PMID: 25918956.
104. Karniychuk UU, De Spiegelaere W, Nauwynck HJ. Porcine reproductive and respiratory syndrome virus infection is associated with an increased number of Sn-positive and CD8-positive cells in the maternal-fetal interface. *Virus Res*. 2013;176(1-2):285-91. Epub 2013/05/28. doi: 10.1016/j.virusres.2013.05.005. PubMed PMID: 23707347.
105. Karniychuk UU, Nauwynck HJ. Pathogenesis and prevention of placental and transplacental porcine reproductive and respiratory syndrome virus infection. *Vet Res*. 2013;44:95. Epub 2013/10/09. doi: 10.1186/1297-9716-44-95. PubMed PMID: 24099529; PubMed Central PMCID: PMC4021427.
106. Ladinig A, Lunney JK, Souza CJ, Ashley C, Plastow G, Harding JC. Cytokine profiles in pregnant gilts experimentally infected with porcine reproductive and respiratory syndrome virus and relationships with viral load and fetal outcome. *Vet Res*. 2014;45:113. Epub 2014/12/07. doi: 10.1186/s13567-014-0113-8. PubMed PMID: 25479904; PubMed Central PMCID: PMC4333882.
107. Ladinig A, Foxcroft G, Ashley C, Lunney JK, Plastow G, Harding JC. Birth weight, intrauterine growth retardation and fetal susceptibility to porcine reproductive and

- respiratory syndrome virus. PLoS One. 2014;9(10):e109541. Epub 2014/10/03. doi: 10.1371/journal.pone.0109541. PubMed PMID: 25275491; PubMed Central PMCID: PMC4183575.
108. Thangavel RR, Bouvier NM. Animal models for influenza virus pathogenesis, transmission, and immunology. *J Immunol Methods*. 2014;410:60-79. Epub 2014/04/09. doi: 10.1016/j.jim.2014.03.023. PubMed PMID: 24709389; PubMed Central PMCID: PMC4163064.
109. Carolan LA, Rockman S, Borg K, Guarnaccia T, Reading P, Mosse J, et al. Characterization of the Localized Immune Response in the Respiratory Tract of Ferrets following Infection with Influenza A and B Viruses. *J Virol*. 2015;90(6):2838-48. Epub 2016/01/01. doi: 10.1128/JVI.02797-15. PubMed PMID: 26719259; PubMed Central PMCID: PMC4810641.
110. Kash JC, Basler CF, Garcia-Sastre A, Carter V, Billharz R, Swayne DE, et al. Global host immune response: pathogenesis and transcriptional profiling of type A influenza viruses expressing the hemagglutinin and neuraminidase genes from the 1918 pandemic virus. *J Virol*. 2004;78(17):9499-511. Epub 2004/08/17. doi: 10.1128/JVI.78.17.9499-9511.2004. PubMed PMID: 15308742; PubMed Central PMCID: PMC506954.
111. Kang YM, Song BM, Lee JS, Kim HS, Seo SH. Pandemic H1N1 influenza virus causes a stronger inflammatory response than seasonal H1N1 influenza virus in ferrets. *Arch Virol*. 2011;156(5):759-67. Epub 2011/01/15. doi: 10.1007/s00705-010-0914-7. PubMed PMID: 21234768.
112. Maines TR, Belser JA, Gustin KM, van Hoeven N, Zeng H, Svittek N, et al. Local innate immune responses and influenza virus transmission and virulence in ferrets. *J Infect Dis*.

- 2012;205(3):474-85. Epub 2011/12/14. doi: 10.1093/infdis/jir768. PubMed PMID: 22158704.
113. Lowen AC, Bouvier NM, Steel J. Transmission in the guinea pig model. *Curr Top Microbiol Immunol.* 2014;385:157-83. Epub 2014/07/09. doi: 10.1007/82_2014_390. PubMed PMID: 25001209.
114. Grigsby PL. Animal Models to Study Placental Development and Function throughout Normal and Dysfunctional Human Pregnancy. *Semin Reprod Med.* 2016;34(1):11-6. Epub 2016/01/12. doi: 10.1055/s-0035-1570031. PubMed PMID: 26752715; PubMed Central PMCID: PMC4799492.
115. Clark DA. The use and misuse of animal analog models of human pregnancy disorders. *J Reprod Immunol.* 2014;103:1-8. Epub 2014/04/15. doi: 10.1016/j.jri.2014.02.006. PubMed PMID: 24725995.
116. Dilworth MR, Sibley CP. Review: Transport across the placenta of mice and women. *Placenta.* 2013;34 Suppl:S34-9. Epub 2012/11/17. doi: 10.1016/j.placenta.2012.10.011. PubMed PMID: 23153501.
117. Davis SM, Sweet LM, Oppenheimer KH, Suratt BT, Phillippe M. Estradiol and progesterone influence on influenza infection and immune response in a mouse model. *Am J Reprod Immunol.* 2017;78(4). Epub 2017/05/31. doi: 10.1111/aji.12695. PubMed PMID: 28557314; PubMed Central PMCID: PMC5623159.
118. Robinson DP, Lorenzo ME, Jian W, Klein SL. Elevated 17beta-estradiol protects females from influenza A virus pathogenesis by suppressing inflammatory responses. *PLoS Pathog.* 2011;7(7):e1002149. Epub 2011/08/11. doi: 10.1371/journal.ppat.1002149. PubMed PMID: 21829352; PubMed Central PMCID: PMC3145801.

119. Hall OJ, Limjunyawong N, Vermillion MS, Robinson DP, Wohlgemuth N, Pekosz A, et al. Progesterone-Based Therapy Protects Against Influenza by Promoting Lung Repair and Recovery in Females. *PLoS Pathog.* 2016;12(9):e1005840. Epub 2016/09/16. doi: 10.1371/journal.ppat.1005840. PubMed PMID: 27631986; PubMed Central PMCID: PMC5025002.
120. Avni R, Neeman M, Garbow JR. Functional MRI of the placenta--From rodents to humans. *Placenta.* 2015;36(6):615-22. Epub 2015/04/29. doi: 10.1016/j.placenta.2015.04.003. PubMed PMID: 25916594; PubMed Central PMCID: PMC4452090.
121. Yates L, Pierce M, Stephens S, Mill AC, Spark P, Kurinczuk JJ, et al. Influenza A/H1N1v in pregnancy: an investigation of the characteristics and management of affected women and the relationship to pregnancy outcomes for mother and infant. *Health Technol Assess.* 2010;14(34):109-82. Epub 2010/07/16. doi: 10.3310/hta14340-02. PubMed PMID: 20630123.
122. Carey MA, Bradbury JA, Reboloso YD, Graves JP, Zeldin DC, Germolec DR. Pharmacologic inhibition of COX-1 and COX-2 in influenza A viral infection in mice. *PLoS One.* 2010;5(7):e11610. Epub 2010/07/27. doi: 10.1371/journal.pone.0011610. PubMed PMID: 20657653; PubMed Central PMCID: PMC2904706.
123. Lee SM, Gai WW, Cheung TK, Peiris JS. Antiviral effect of a selective COX-2 inhibitor on H5N1 infection in vitro. *Antiviral Res.* 2011;91(3):330-4. Epub 2011/07/30. doi: 10.1016/j.antiviral.2011.07.011. PubMed PMID: 21798291.
124. Li C, Li C, Zhang AJ, To KK, Lee AC, Zhu H, et al. Avian influenza A H7N9 virus induces severe pneumonia in mice without prior adaptation and responds to a

- combination of zanamivir and COX-2 inhibitor. *PLoS One*. 2014;9(9):e107966. Epub 2014/09/19. doi: 10.1371/journal.pone.0107966. PubMed PMID: 25232731; PubMed Central PMCID: PMC4169509.
125. Carey MA, Bradbury JA, Seubert JM, Langenbach R, Zeldin DC, Germolec DR. Contrasting effects of cyclooxygenase-1 (COX-1) and COX-2 deficiency on the host response to influenza A viral infection. *J Immunol*. 2005;175(10):6878-84. Epub 2005/11/08. PubMed PMID: 16272346.
126. Berard A, Sheehy O, Girard S, Zhao JP, Bernatsky S. Risk of preterm birth following late pregnancy exposure to NSAIDs or COX-2 inhibitors. *Pain*. 2018. Epub 2018/01/20. doi: 10.1097/j.pain.0000000000001163. PubMed PMID: 29351170.
127. Chan VS. A mechanistic perspective on the specificity and extent of COX-2 inhibition in pregnancy. *Drug Saf*. 2004;27(7):421-6. Epub 2004/05/15. PubMed PMID: 15141994.
128. Daniel S, Matok I, Gorodischer R, Koren G, Uziel E, Wiznitzer A, et al. Major malformations following exposure to nonsteroidal antiinflammatory drugs during the first trimester of pregnancy. *J Rheumatol*. 2012;39(11):2163-9. Epub 2012/09/18. doi: 10.3899/jrheum.120453. PubMed PMID: 22984274.
129. Hall OJ, Nachbagauer R, Vermillion MS, Fink AL, Phuong V, Krammer F, et al. Progesterone-Based Contraceptives Reduce Adaptive Immune Responses and Protection against Sequential Influenza A Virus Infections. *J Virol*. 2017;91(8). Epub 2017/02/10. doi: 10.1128/JVI.02160-16. PubMed PMID: 28179523; PubMed Central PMCID: PMC5375688.
130. Zheng R, Qin X, Li Y, Yu X, Wang J, Tan M, et al. Imbalanced anti-H1N1 immunoglobulin subclasses and dysregulated cytokines in hospitalized pregnant women

- with 2009 H1N1 influenza and pneumonia in Shenyang, China. *Hum Immunol.* 2012;73(9):906-11. Epub 2012/07/04. doi: 10.1016/j.humimm.2012.06.005. PubMed PMID: 22750537.
131. Malek A. Ex vivo human placenta models: transport of immunoglobulin G and its subclasses. *Vaccine.* 2003;21(24):3362-4. Epub 2003/07/10. PubMed PMID: 12850340.
132. Malek A, Sager R, Zakher A, Schneider H. Transport of immunoglobulin G and its subclasses across the in vitro-perfused human placenta. *Am J Obstet Gynecol.* 1995;173(3 Pt 1):760-7. Epub 1995/09/01. PubMed PMID: 7573239.
133. Malek A. Role of IgG antibodies in association with placental function and immunologic diseases in human pregnancy. *Expert Rev Clin Immunol.* 2013;9(3):235-49. Epub 2013/03/01. doi: 10.1586/eci.12.99. PubMed PMID: 23445198.
134. Hwang JK, Alt FW, Yeap LS. Related Mechanisms of Antibody Somatic Hypermutation and Class Switch Recombination. *Microbiol Spectr.* 2015;3(1):MDNA3-0037-2014. Epub 2015/06/25. doi: 10.1128/microbiolspec.MDNA3-0037-2014. PubMed PMID: 26104555; PubMed Central PMCID: PMC4481323.
135. Muramatsu M, Kinoshita K, Fagarasan S, Yamada S, Shinkai Y, Honjo T. Class switch recombination and hypermutation require activation-induced cytidine deaminase (AID), a potential RNA editing enzyme. *Cell.* 2000;102(5):553-63. Epub 2000/09/28. PubMed PMID: 11007474.
136. Shulman Z, Gitlin AD, Weinstein JS, Lainez B, Esplugues E, Flavell RA, et al. Dynamic signaling by T follicular helper cells during germinal center B cell selection. *Science.* 2014;345(6200):1058-62. Epub 2014/08/30. doi: 10.1126/science.1257861. PubMed PMID: 25170154; PubMed Central PMCID: PMC4519234.

137. Gitlin AD, Shulman Z, Nussenzweig MC. Clonal selection in the germinal centre by regulated proliferation and hypermutation. *Nature*. 2014;509(7502):637-40. Epub 2014/05/09. doi: 10.1038/nature13300. PubMed PMID: 24805232; PubMed Central PMCID: PMC4271732.
138. Mai T, Zan H, Zhang J, Hawkins JS, Xu Z, Casali P. Estrogen receptors bind to and activate the HOXC4/HoxC4 promoter to potentiate HoxC4-mediated activation-induced cytosine deaminase induction, immunoglobulin class switch DNA recombination, and somatic hypermutation. *J Biol Chem*. 2010;285(48):37797-810. Epub 2010/09/22. doi: 10.1074/jbc.M110.169086. PubMed PMID: 20855884; PubMed Central PMCID: PMC2988384.
139. Pauklin S, Sernandez IV, Bachmann G, Ramiro AR, Petersen-Mahrt SK. Estrogen directly activates AID transcription and function. *J Exp Med*. 2009;206(1):99-111. Epub 2009/01/14. doi: 10.1084/jem.20080521. PubMed PMID: 19139166; PubMed Central PMCID: PMC2626679.
140. Pauklin S, Petersen-Mahrt SK. Progesterone inhibits activation-induced deaminase by binding to the promoter. *J Immunol*. 2009;183(2):1238-44. Epub 2009/06/26. doi: 10.4049/jimmunol.0803915. PubMed PMID: 19553525.
141. Benko AL, Olsen NJ, Kovacs WJ. Glucocorticoid inhibition of activation-induced cytidine deaminase expression in human B lymphocytes. *Mol Cell Endocrinol*. 2014;382(2):881-7. Epub 2013/11/19. doi: 10.1016/j.mce.2013.11.001. PubMed PMID: 24239615.
142. Shatz W, Chung S, Li B, Marshall B, Tejada M, Phung W, et al. Knobs-into-holes antibody production in mammalian cell lines reveals that asymmetric afucosylation is

- sufficient for full antibody-dependent cellular cytotoxicity. *MAbs*. 2013;5(6):872-81. Epub 2013/09/03. doi: 10.4161/mabs.26307. PubMed PMID: 23995614; PubMed Central PMCID: PMC3896601.
143. Caaveiro JM, Kiyoshi M, Tsumoto K. Structural analysis of Fc/FcγR complexes: a blueprint for antibody design. *Immunol Rev*. 2015;268(1):201-21. Epub 2015/10/27. doi: 10.1111/imr.12365. PubMed PMID: 26497522.
144. Gu J, Lei Y, Huang Y, Zhao Y, Li J, Huang T, et al. Fab fragment glycosylated IgG may play a central role in placental immune evasion. *Hum Reprod*. 2015;30(2):380-91. Epub 2014/12/17. doi: 10.1093/humrep/deu323. PubMed PMID: 25505012; PubMed Central PMCID: PMC4303772.
145. Gutierrez G, Gentile T, Miranda S, Margni RA. Asymmetric antibodies: a protective arm in pregnancy. *Chem Immunol Allergy*. 2005;89:158-68. Epub 2005/09/01. doi: 10.1159/000087964. PubMed PMID: 16129962.
146. Gutierrez G, Malan Borel I, Margni RA. The placental regulatory factor involved in the asymmetric IgG antibody synthesis responds to IL-6 features. *J Reprod Immunol*. 2001;49(1):21-32. Epub 2001/01/04. PubMed PMID: 11137110.
147. Miranda S, Gentile T, Margni R. Enhancement of in vitro hsp72 expression by placental IL-6. *Am J Reprod Immunol*. 2001;46(5):358-65. Epub 2001/11/20. PubMed PMID: 11712765.
148. Li J, Korteweg C, Qiu Y, Luo J, Chen Z, Huang G, et al. Two ultrastructural distribution patterns of immunoglobulin G in human placenta and functional implications. *Biol Reprod*. 2014;91(5):128. Epub 2014/10/03. doi: 10.1095/biolreprod.114.122614. PubMed PMID: 25273527.

Appendix I: Stable incorporation of GM-CSF into dissolvable microneedle patch improves skin vaccination against influenza

Elizabeth Q. Littauer^{a,1}, Lisa K. Mills^{a,1}, Nicole Brock^a, E. Stein Esser^a, Andrey Romanyuk^b,
Joanna A. Pulit-Penalosa^a, Elena V. Vassilieva^a, Jacob T. Beaver^a, Florian Krammer^c,
Richard W. Compans^a, Mark R. Prausnitz^b and Ioanna Skountzou^{*, a}

^a Department of Microbiology & Immunology and Emory Vaccine Center,

Emory University School of Medicine, 1518 Clifton Road, Atlanta, GA 30322

^b School of Chemical and Biomolecular Engineering, Georgia Institute of Technology,

311 Ferst Drive, Atlanta, GA 30332-0100

^c Department of Microbiology, Icahn School of Medicine at Mount Sinai,

1 Gustave L. Levy Place, New York, New York 10029, USA

¹: Joint first authors

*: Corresponding author (email address: iskount@emory.edu)

Accepted. February 19, 2018. *Journal of Controlled Release*.

ABSTRACT

The widely used influenza subunit vaccine would benefit from increased protection rates in vulnerable populations. Skin immunization by microneedle (MN) patch can increase vaccine immunogenicity, as well as increase vaccination coverage due to simplified administration. To further increase immunogenicity, we used granulocyte-macrophage colony stimulating factor (GM-CSF), an immunomodulatory cytokine already approved for skin cancer therapy and cancer support treatment. GM-CSF has been shown to be upregulated in skin following MN insertion. The GM-CSF-adjuvanted vaccine induced robust and long-lived antibody responses cross-reactive to homosubtypic and heterosubtypic influenza viruses. Addition of GM-CSF resulted in increased memory B cell persistence relative to groups given influenza vaccine alone and led to rapid lung viral clearance following lethal infection with homologous virus in the mouse model. Here we demonstrate that successful incorporation of the thermolabile cytokine GM-CSF into MN resulted in improved vaccine-induced protective immunity holding promise as a novel approach to improved influenza vaccination. To our knowledge, this is the first successful incorporation of a cytokine adjuvant into dissolvable MNs, thus advancing and diversifying the rapidly developing field of MN vaccination technology.

Keywords: GM-CSF, Microneedle , Influenza , Adjuvant, Skin, Co-delivery

INTRODUCTION

Influenza A virus is a common respiratory pathogen that causes seasonal outbreaks, epidemics and occasional pandemics. Although influenza illness mostly presents with benign symptoms in healthy populations and resolves within 7-10 days, it can become life-threatening in elderly adults, pregnant women, infants and people with chronic conditions¹⁻³. Annual infection rates for seasonal influenza are 5-10% for adults and 20-30% for children⁴. Of the many influenza subtypes, H1N1 has the highest prevalence in laboratory-confirmed influenza-like illness (ILI), while H3N2 disproportionately affects individuals ≥ 65 -years of age causing higher morbidity and mortality rates⁵.

Influenza vaccination is the most effective public health strategy for reducing influenza mortality rate and economic burden of treatment and hospitalization costs and lost productivity and wages^{6,7}. However, during the 2015–2016 flu season influenza vaccination demonstrated modest protection against ILI, with an overall effectiveness of 47%⁸. In addition to the need for increased immunogenicity, current influenza vaccination approaches face obstacles such as limited duration of immunity and lack of protection in high risk groups, such as young children and the elderly, as well as low coverage and participation in vaccination⁹⁻¹¹.

Skin vaccination by microneedle (MN) patch has the potential to overcome the aforementioned hurdles observed in vaccination strategies by generating superior immune responses to vaccine antigen and increasing access to vaccination through improved vaccination logistics and greater patient acceptance¹²⁻¹⁵. MN vaccine patches have specifically been shown to enhance influenza vaccination, including increased immunogenicity^{12,13,16}, improved acceptability^{17,18} and long-lasting stability outside the cold-chain¹⁹. Additionally, a recent phase I clinical trial showed that influenza vaccination by MN patch administered by study personnel or self-administered by

study participants was well tolerated, strongly immunogenic and overwhelmingly preferred compared to intramuscular (IM) vaccination²⁰.

We previously demonstrated that influenza vaccination by MN patch leads to accelerated viral clearance and increased recall immune responses when compared to IM vaccination^{21,22}. Antigen delivery with this novel platform targets the skin-resident antigen-presenting cells (APCs) and drives robust activation and mobilization of innate and adaptive immune cells²³. Cytokines shape the immune response by modulating the function of cellular targets, making them potential adjuvants for vaccines. Thus, inclusion of cytokines within vaccine-containing MNs could further boost vaccine effectiveness.

Granulocyte-macrophage colony stimulating factor (GM-CSF) is a monomeric 24 kDa cytokine that promotes the maturation of granulocytes and macrophages from bone marrow progenitor cells²⁴ and is secreted by a wide array of immune cells, keratinocytes, eosinophils, neutrophils, and endothelial cells²⁵. GM-CSF is particularly active in the skin, recruiting epidermal dendritic cells (DC) such as Langerhans cells into draining lymph nodes and enhancing activation and antigen presentation^{26,27}. These properties have made GM-CSF an effective therapy to treat neutropenia in cancer and AIDS patients for the past 20 years^{28,29} and a molecule of interest for adjuvant purposes in therapeutic vaccinations against skin cancers and autoimmune skin disorders^{30,31}. However, despite the potential for successful use as an adjuvant and demonstrated safety in cancer clinical trials³²⁻³⁴, development of GM-CSF as an adjuvant in vaccines against infectious microorganisms has been limited by variability in effectiveness³⁵.

Due to the immunomodulatory effects and activation of skin immune cells by GM-CSF, we hypothesized that incorporation of this cytokine in MN patches containing influenza subunit vaccine will increase immunogenicity compared to vaccine alone. This is further motivated by

prior findings that GM-CSF was identified as a potential adjuvant from a panel of cytokines and chemokines that were upregulated in the skin following insertion of influenza vaccine-coated MN arrays³⁶. We tested our hypothesis in the BALB/c mouse model using both intradermal (ID) injection and MN patch delivery. We elaborate on previous work showing the efficacy of MN patches as an improved vaccination technology and develop a pipeline for testing novel adjuvants to enhance the potency of this emerging technology.

MATERIALS AND METHODS

Cells and virus stocks. Madin-Darby canine kidney (MDCK) cells (ATCC, Manassas, VA) were maintained in Dulbecco's Modified Eagle's Medium (DMEM) (Mediatech, Herndon, VA) containing 10% fetal bovine serum (Thermo, Rockford, IL). Influenza virus stocks A/Brisbane/59/2007 (H1N1), A/California/07/2009 (H1N1), and A/Udorn/307/1972 (H3N2) were propagated in MDCK cells. Egg-grown subunit monovalent influenza vaccines, A/Brisbane/59/2007, A/California/07/2009, A/Christchurch/16/2010 and A/Victoria/210/2009 (A/Perth/16/2009-like) were generously provided by Seqirus (Maidenhead, UK). Vaccine processing for MN patch fabrication (reconstitution of lyophilized preparation and concentration), determination of protein concentration and assay of hemagglutinin (HA) content were carried out as previously described¹³. The following in-house MDCK-grown viruses were used for our studies: H1N1 A/California/07/2009, A/California/10/1978, A/FM/1/1947; and H3N2 A/Texas/50/2012, A/Victoria/210/2009, and A/Aichi/2/1968. Mouse adapted A/California/07/2009 and A/Udorn/307/1972 (H3N2) viruses were serially passaged in lungs of BALB/c mice. The LD₅₀ was determined using the Reed-Muench formula³⁷ and the viral titers were determined by plaque assay³⁸. Viruses were sequenced at Operon-MWG (Huntsville, AL) and Macrogen (Seoul, South Korea) and assembled via ClustalW alignment algorithms in MegAlign (DNASTAR Lasergene v7.0, Madison, WI) and BioEdit (Ibis Biosciences, Carlsbad, CA) software.

Animals. Eight-week-old female BALB/c mice (Charles River Laboratories, Wilmington, MA) were bred and housed in a biosafety level 1 facility at Emory University's Division of Animal Resources and viral infection experiments were performed on animals housed in a biosafety level 2 facility at Emory University's Division of Animal Resources. All experiments were conducted in accordance with protocols approved by Emory University's Institutional Animal Care and Use

Committee (IACUC) in accordance with guidelines with the United States Federal Animal Welfare Act (PL 89-544) and subsequent amendments.

Immunizations and Infections. Vaccines and adjuvant were prepared in sterile Ca^{2+} and Mg^{2+} deficient phosphate-buffered saline (PBS). Mice were intradermally (ID) vaccinated with a tuberculin syringe on the caudal site of dorsum with 1 or 3 μg HA H1N1 A/California/07/2009 subunit vaccine alone or 1 μg HA mixed with 100 ng recombinant murine GM-CSF (PeproTech, Rocky Hill, NJ). Mice were infected intranasally (IN) under isoflurane anesthesia with 25xLD₅₀ (1,500 p.f.u.) mouse-adapted A/California/07/2009 virus 2 months post vaccination.

The optimal GM-CSF concentration for microneedle (MN) vaccination was determined by an initial screen of GM-CSF doses (5, 20, 100 ng) administered ID with 1 μg HA of H3N2 (A/Victoria/210/2009 (A/Perth/16/2009-like)) subunit vaccine and was compared to 1 μg HA or 5 μg of the same vaccine without adjuvant. Sera was collected 90 days post vaccination (d.p.v.), and mice were infected IN with mouse adapted A/Udorn/307/1972 (H3N2) at a dose of 4xLD₅₀ (35 plaque forming units (p.f.u.)) 4 months post vaccination.

The best route of adjuvanted vaccine delivery was selected by comparing magnitude and breadth of immune responses induced by MN, ID or IM immunization of mice with A/California/07/2009 subunit vaccine. Skin surfaces for MN patch vaccination were prepared as previously described³⁹. Mice were anesthetized using xylazine/ketamine cocktail and MN patches were applied with direct pressure for 1 minute and left in place for 20 minutes. Unused and used patches were analyzed by ELISA for vaccine and adjuvant content to determine delivery efficiency. Sera was collected 28, 90, and 120 d.p.v. Mice were infected with 25xLD₅₀ (1,500 p.f.u.) mouse-adapted A/California/07/2009 virus 4 months post vaccination.

Cellular immune responses in MN vaccinated cohorts of mice with blank patches or patches containing monovalent subunit vaccine (A/Christchurch/16/2010, a A/California/07/2009-like strain), at 1 μ g HA, 3 μ g HA, or 1 μ g HA mixed with 100 ng recombinant murine GM-CSF. Mice were challenged with 10xLD₅₀ (600 p.f.u.) homologous mouse-adapted A/California/07/2009 virus one-month post vaccination. In survival studies, animals were monitored daily for morbidity (body weight loss, hunched posture, ruffled hair and decreased mobility) and mortality for 2 weeks. Mice that lost 25% of their weight were euthanized according to IACUC guidelines. An independent cohort of mice from each group was euthanized at 4 days post-infection to harvest lungs, spleens and lymph nodes.

Microneedle patch fabrication. MN patches were fabricated in a two-step process with polydimethylsiloxane (PDMS) molds as previously described¹³. To measure stability of GM-CSF in the presence of excipients a first-cast solution was prepared containing recombinant GM-CSF (PeproTech, Rocky Hill, NJ) in 3% w/v poly-vinyl alcohol (PVA, Millipore, Bellerica, MA) in combination with one or more of the following: 0.1% w/v bovine serum albumin (BSA, Sigma), 10% w/v trehalose (Sigma), 1% w/v carboxymethyl cellulose (CMC, Spectrum, New Brunswick, NJ). A second-cast solution was prepared containing 18% w/v PVA and 18% w/v sucrose (Sigma). MN patches were prepared by sequentially casting the first-cast solution to fill the mold cavities and the second-cast solution to cover the mold surface (corresponding to the MN patch backing). The MN patches were removed from the molds and attached to adhesive paper discs. Patches were inspected via light microscopy for integrity and uniformity. Blank placebo patches were made identically, except no antigen was in the first-cast solution. Influenza HA concentration was measured by a modified SRID assay^{13,40}.

To measure stability of GM-CSF in the presence of influenza vaccine, the first-cast solution was prepared containing A/Brisbane/59/07 and murine recombinant GM-CSF in 3% w/v polyvinyl alcohol (PVA; Sigma-Aldrich St Louis, MO) or in combination with 10% w/v trehalose (Sigma) and 3% PVA. Based on pilot delivery efficiency data after microneedle insertion¹³, we encapsulated 20 ng GM-CSF per patch for a final working dose of 10 ng and 7 µg HA for a working concentration of 5 µg.

Bioactivity assays for GM-CSF. Bioactivity of GM-CSF was tested with proliferation assays using 2 cell types: murine bone marrow cells harvested from naïve female mice and TF-1 human erythroleukemia cell line (ATCC® CRL-2003, Manassas, VA). TF-1 cell growth and survival is dependent on GM-CSF or IL-3⁴¹. Cells were treated with either solubilized or dried and reconstituted microneedle coating solutions mixed with GM-CSF. Bone marrow was collected from the femurs of two naïve mice, centrifuged at 1,000 RPM for 7 minutes, and incubated in RBC Lysing Buffer Hybri-Max (Sigma-Aldrich, St. Louis, MO) for 10 minutes. Cells were washed and resuspended in RPMI with 10% FCS and 1% Penicillin-Streptomycin RPMI (Corning Cellgro, Thermo Fisher Scientific, Waltham, MA). Bioactivity was tested in bone marrow cells using: (i) first-cast solution (with 10% trehalose) without GM-CSF, (ii) GM-CSF suspended in RPMI-10 (200 µl of 200 ng/µl) (iii) first-cast solution mixed with 1:1 with GM-CSF (to reach a final concentration of 100 µg), with GM-CSF and (iv) first-cast solution with GM-CSF dried in microcentrifuge tubes and resuspended in 200 µl RPMI-10. After 2 days, cells were imaged via Axio Scope software (Carl Zeiss Microscopy, LLC, Thornwood, NY). Cell activation and proliferation was visualized with light microscopy throughout the incubation period. Every 2 days the cells were supplemented with RPMI-10. Following a 4-day incubation, we determined viable cells in proliferation with the colorimetric Promega Cell Titer 96® AQueous One Solution Cell

Proliferation Assay (Promega, Madison, WI). An additional liquid vaccine formulation control was included to ensure that the fabrication process did not cause a loss in activity.

Bioactivity of GM-CSF (10 ng delivery concentration) encapsulated in MN patches was tested in TF-1 cells with formulations used in the mold: 1) 0.1% w/v albumin 2) 0.1% albumin and 10% w/v trehalose 3) 1% CMC w/v and 10% trehalose or 4) 1% w/v gelatin for 4 days. Three patches from each group were resuspended in 200 μ l of RPMI-10 to overlay the cells. An additional liquid formulation control for each group was included to ensure that the fabrication process did not cause a loss in activity. As a second liquid control, we air-dried the same formulations in microtubes and reconstituted them in RPMI-10. At the end of 3-day incubation period cell proliferation was tested with Promega cell proliferation assay.

Subsequently bioactivity of GM-CSF with vaccine and MN excipients was measured in TF-1 cells by resuspending MN fabricated with GM-CSF (10 ng delivery concentration) and subunit influenza vaccine (A/Brisbane/59/2007) (5 μ g HA delivery concentration) in RPMI-10. The following controls were used in TF-1 cell proliferation: 1) GM-CSF dissolved in 200 PBS μ l 2) GM-CSF with 0.1% BSA in RPMI-10 3) GM-CSF with 10% trehalose in RPMI-10 4) GM-CSF with vaccine and 10% trehalose in RPMI-10. At the end of 3-day incubation period cell proliferation was tested with Promega cell proliferation assay.

Characterization and quantitation of humoral immune responses. Serum samples were collected at 14, 28, 56 or 60, 90 and 120 (d.p.v.). Antibody titers were quantified with ELISA as described previously with biotinylated anti-IgG, IgG1, IgG2 antibodies (Southern Biotech, Birmingham, AL) against 100 ng/well monovalent H1N1 A/California/07/2009 subunit vaccine, A/Christchurch/16/2010 subunit vaccine, or recombinant HA A/California/07/2009 from BEI Resources (Manassas, VA)⁴². Hemagglutination inhibition (HAI) assays were performed

according to the WHO laboratory diagnostics manual using washed turkey red blood cells⁴³. Virus-neutralizing (VN) antibody titers were determined by microneutralization assay for A/Perth/16/2009 and A/California/07/2009, as described previously²². IgG titers against chimeric HA proteins containing exotic HA head subtypes and commonly found seasonal HA stalks were measured to determine the antibody targets from H1N1 vaccinated mice; these chimeric proteins (cH6/1 and cH14/3) were created in a baculovirus system as described previously⁴⁴. Influenza-specific antibody avidity was measured by ELISA in the presence of increasing concentrations (0 - 2.0 M) of the chaotropic agent guanidine thiocyanate (GTC) (Sigma), as previously described⁴². The avidity index was determined using Prism 7.03 Software (GraphPad, La Jolla, CA) by calculating the molar concentration of the chaotropic agent required to reduce the initial optical density by 50%.

Antigen-specific cellular activity in spleen, lungs, and bone marrow. Lymphocytes were isolated from spleen and lung tissue 7 and 14 d.p.v. and 4 days post infection (d.p.i.). Bone marrow was isolated from mice 60 days d.p.v. Antibody secreting cells (ASCs) were quantified by overlaying 1×10^6 cells/well in ELISPOT plates coated with 200 ng/well H1N1 A/Christchurch/16/2010. ASCs were incubated at 37°C for 16 hours, washed, and then influenza-specific antibodies were detected using isotype-specific, biotinylated murine Ig antibodies. Cytokine secreting cells (CSC) were quantified by overlaying 5×10^5 cells/well in ELISPOT plates (EMD Millipore, Burlington, MA) coated with 100 ng/well of capture antibody (BD Biosciences, San Jose, CA). Cells were incubated with 200 ng/well H1N1 A/Christchurch/16/2010 for 48 hours at 37°C. ASC and CSC plates were washed and incubated with 100 ng/well biotinylated detection antibodies (IL-4 and IFN- γ , BD Biosciences; IgA, IgM, and IgG, Southern Biotech, Birmingham, AL) and developed with streptavidin-HRP and diaminobenzidine. Spots were counted via

ImmunoSpot Reader 5.0 (Cellular Technology Limited, Shaker Heights, OH), normalized to 1×10^6 cells/well and plotted with GraphPad Prism software.

Flow cytometry identification of activated cellular subsets. Skin draining (inguinal) lymph nodes were collected at 7 d.p.v. to evaluate the presence of activated T follicular helper cells (Tfh) and germinal center (GC) B cells by flow cytometry. Single-cell suspensions were incubated with anti-mouse CD16/32 antibody for 10 minutes on ice. Cells were then incubated with CD3 ϵ (145-2C11), CD4 (GK1.5), PD-1 (29F.1A12), CXCR5 (L138D7), CD19 (6D5), Fas (Jo2) and GL7 (GL7) on ice for 30 minutes. Antibodies were purchased from BioLegend (San Diego, CA) and BD Biosciences (San Jose, CA). Cells were washed and fixed in 2% paraformaldehyde. Samples were acquired on a LSR II flow cytometer (BD Biosciences) and data were analyzed with FlowJo (FlowJo LLC, BD, Franklin Lakes, NJ) (Suppl Figure 1).

Quantification of cytokines following infection. Lungs were weighed and homogenized in 0.5 mL DMEM and 1x Halt Protease Inhibitor. Lysates were diluted in 1x PBS and cytokines (GM-CSF, IFN- γ , IL-1 β , IL-2, IL-4, IL-5, IL-10, TNF- α) were quantified via a BioPlex Pro Mouse Cytokine 8-plex Assay (Bio-Rad, Hercules, California) at the Emory Vaccine Center Virology Core and normalized for dilution factor and original tissue concentration.

Measurement of lung viral titers. Viral titers in lung homogenates were quantified via plaque assay in MDCK cells³⁹. Viral titers were assessed per gram of tissue.

Statistics. For ELISA, ELISPOT and cell-based assays, the statistical significance of differences between two groups was calculated by two-tailed unpaired Student's *t*-test. Log₂ converted HAI and VN titers were analyzed with one or two-way ANOVA with Bonferroni post-hoc test. Unless otherwise stated, antibody assays were performed in duplicate. For survival curves, statistics were

calculated using a Log-rank (Mantel-Cox) test. Non-linear regression analyses were performed to determine the IC₅₀ (95% confidence interval). A p-value less than 0.05 was considered significant.

RESULTS

Intradermal vaccination screen identified GM-CSF as a promising adjuvant in microneedle influenza immunization. The efficacy of GM-CSF as vaccine adjuvant for skin immunization was initially carried out with ID injection studies. The dose of 100 ng for GM-CSF was based on published literature⁴⁵. The immune responses elicited to unadjuvanted A/California/07/2009 subunit vaccine at low or high dose (1 µg HA and 3 µg HA respectively) were compared to those induced by adjuvanted low dose vaccine (Figure 1). Mice that received the adjuvanted vaccine demonstrated 4-fold higher anti-A/California/07/2009 HAI titers ($p=0.07$) when compared to mice vaccinated with low dose unadjuvanted vaccine and similar HAI titers compared to the high-dose vaccinated group ($p=0.025$) at 8 weeks post-vaccination (Figure 1A).

Infection of all vaccinated groups, 2 months post-vaccination with 25xLD₅₀ homologous virus, conferred complete protection of the GM-CSF/1 µg HA and the unadjuvanted 3 µg HA vaccine groups ($p=0.04$ when comparing survival rates to unadjuvanted 1 µg vaccine group) (Figure 1B) and minimal morbidity with 5% body weight loss by day 6 (Figure 1C). In contrast, the group immunized with low-dose unadjuvanted vaccine showed 80% mortality and 20% body weight loss by the survivors. We observed that addition of GM-CSF as an adjuvant can boost protective immune responses comparable to a three-fold higher vaccine dose, thereby conserving the amount of vaccine required for protection.

H3N2 influenza A viruses are known to cause significant disease burden worldwide and the H3N2 strains in inactivated trivalent influenza vaccine have lower efficacy than the H1N1 strains. Hence, we assessed GM-CSF's ability to boost immune responses to a monovalent H3N2 subunit vaccine using a series of GM-CSF concentrations to optimize the adjuvant dose-response curve. Mice were ID vaccinated with 1 µg HA or 5 µg HA H3N2 A/Victoria/210/2009 (A/Perth/16/2009-

like) and a range of GM-CSF concentrations (5, 20, 100 ng) (Figure 2). Administration of 100 ng GM-CSF with 1 µg HA vaccine doubled the VN titers when compared to unadjuvanted low-dose vaccine at 90 d.p.v. (Figure 2A). Following infection with 4xLD₅₀ of A/Udorn/307/1972 4 months post-vaccination, the co-delivery of 100 ng GM-CSF increased survival rates (Figure 2B) and prevented significant body weight loss of infected survivors (Figure 2C) relative to mice that received a low-dose vaccine alone. Thus, we demonstrated that the adjuvanted formulation can improve protective immunity in a second clinically significant influenza subtype.

Effect of MN patch formulation on GM-CSF's ability to induce proliferation of bone marrow cells. The proliferative capacity of recombinant murine GM-CSF was initially tested in bone marrow cells (Figure 3A). Cells were stimulated with increasing concentrations of GM-CSF (0.6-400 ng per well) and supernatants were collected at 60 and 120 minutes of incubation to test for proliferation. We observed a time-dependent and dose-dependent response that was more significant above concentrations of 25 ng of GM-CSF/well. The maximum bone marrow proliferation occurred after 120 minutes of cellular exposure at 200 ng GM-CSF.

Since MN patch fabrication may affect the bioactivity of GM-CSF, we measured the ability of GM-CSF to induce activation and proliferation of bone marrow cells before and after incorporation and drying in casting solutions used to fabricate MN patches (Figure 3B). Bone marrow cells in culture were overlaid with casting solution alone (Figure 3Ba), murine recombinant GM-CSF dissolved in PBS (Figure 3Bb), GM-CSF dissolved in first-casting solution (Figure 3Bc) and GM-CSF in first-casting solution, air dried and resuspended in culture medium (Figure 3Bd). Visualization of cells with light microscopy showed that inclusion of GM-CSF in the first-casting solution in either liquid or dried formulation caused distinct morphological changes in bone marrow cultures similarly to GM-CSF dissolved in PBS, suggesting that the

cytokine retained its biological activity. We also found that the same formulations induced bone marrow cell proliferation and increased the overall cell numbers 4-fold compared to the control (Figure 3C). Thus, GM-CSF remained stable upon casting processes fundamental to MN production and retained the capacity to proliferate bone marrow cells following reconstitution.

Stability and bioactivity of GM-CSF following MN patch fabrication with excipients. We next analyzed whether GM-CSF (10 ng delivery concentration) would retain bioactivity following incorporation in MN patches using different formulations. The formulations included trehalose CMC, or gelatin, which have previously been used as structural and stabilizing excipients in MN patch fabrications^{13,46} and BSA alone or mixed with trehalose. Bioactivity of reconstituted patches was compared to lyophilized GM-CSF dissolved in PBS and from reconstituted dried solution. Bioactivity was determined by overlaying solutions on TF-1 cells and measuring proliferative capacity (Figure 4A). Among the formulations studied, MN patches containing 10 ng GM-CSF and fabricated using casting solutions comprised of 0.1% albumin and 10% trehalose generated the highest cellular proliferation within the standard curve (0.31-20 ng/ml). Formulations that induced the highest cellular proliferation in Figure 4A were reformulated with vaccine, excipients, and GM-CSF in order to validate bioactivity following co-incorporation of vaccine and adjuvant (Figure 4B).

Next, we tested the bioactivity of 10 ng GM-CSF mixed with subunit influenza vaccine (A/Brisbane/59/2007) (5 μ g delivery concentration) and encapsulated in MN patches to enhance TF-1 cell proliferation. These patches were dissolved in RPMI-10 and overlaid on TF-1 cells for 3 days. Bioactivity was compared to patches containing GM-CSF alone, GM-CSF formulated with BSA or trehalose and GM-CSF mixed with vaccine and trehalose (Figure 4B). Cells cultured in the presence of RPMI-alone were the negative control group. Each group of reconstituted patches

was compared to the same formulation in solution. Since reconstituted patches induced cell proliferation at similar levels, we concluded that the formulation that stabilized the adjuvants was also suitable for influenza vaccine.

Mechanical stability of MN patches formulated for GM-CSF delivery was also studied. MN patches containing a red dye were fabricated using a casting solution comprising 0.1% albumin and 10% trehalose and applied to skin. Before application, the red dye was localized mostly in the MNs and not in the patch backing (Figure 4Ca). After application to the skin, the MNs (and red dye) dissolved in the skin (Figure 4Cb). Altogether, these results demonstrate that MN patches were fabricated with GM-CSF that retained bioactivity and could be used to puncture and dissolve in skin.

Humoral and protective immune responses following delivery of recombinant murine GM-CSF-adjuvanted H1N1 vaccine. We previously demonstrated that MN patch delivery of antigen in skin can augment immune responses to influenza vaccination. The goal of this study was to determine if incorporation of GM-CSF into MN patches could induce superior and dose-sparing immune responses compared to conventional vaccination (IM or ID) without adjuvant. Mice were vaccinated either cutaneously (MN patches or ID injection) or systemically (IM injection) with the same vaccine (H1N1 A/California/07/2009) whereas the GM-CSF dose was 100 ng per patch and 200 ng for the IM and ID routes as determined in the *in vitro* bioactivity studies (Figure 3).

While MN patch vaccination generated superior vaccine-specific IgG responses when compared to IM and ID routes at 28, 90 and 120 d.p.v., we observed no differences in IgG titers among low- or high-dose unadjuvanted vaccine or in the presence of GM-CSF (Figure 5A). In contrast, the immunopotentiating effects of GM-CSF were demonstrated in antibody cross-reactivity of MN patch vaccinated mice against a heterologous (homosubtypic) seasonal influenza

strain H1N1 A/New Caledonia/20/1999 (Figure 5B) and the heterosubtypic H3N2 A/Brisbane/10/2007 strain (Figure 5C). The adjuvanted vaccine induced equivalent antigen-specific IgG serum titers to high vaccine doses at 120 d.p.v. Notably, vaccination in the presence of 2-fold higher dose GM-CSF generated comparable responses across ID and IM groups at 75% lower titers than those achieved with MN patch vaccination.

These data indicate that MN patch vaccination induced robust long-lived antibody responses, and that co-administration with GM-CSF further potentiated heterologous immune responses after MN patch vaccination, but not after ID or IM vaccination. Thus, the combination of MN patch vaccination and GM-CSF adjuvantation may play an important role on increasing breadth of immunity.

While all vaccinated groups showed protection (higher than 80%) (Figure 6A, 6C, 6E) following infection with homologous virus 4 months post-vaccination, only the MN group demonstrated least body weight losses (Figure 6B) compared to the ID group (Figure 6D) or IM group (Figure 6F). Contrary to the initial ID vaccination data (Figure 1) where administration of GM-CSF with low dose of vaccine improved protection compared to vaccine alone, in this experiment all vaccinated groups irrespectively of route of administration survived lethal infection. These findings are likely due to antibody maturation, considering that the infection study in this experiment took place 4 months post vaccination compared to 2 months in the initial ID vaccination study.

Longevity of antibody responses to MN vaccination with subunit influenza vaccine and GM-CSF. To assess the potential of GM-CSF to enhance long-term humoral and cellular immune memory, we fabricated MN patches containing low dose, high dose or low dose H1N1 vaccine (A/Christchurch/16/2010, A/California/07/2009-like) with GM-CSF in an experimental design

similar to the initial screening experiments in which we demonstrated superior immune responses after MN patch vaccination compared to the needle and syringe approach (Figure 7A).

We found that GM-CSF-adjuvanted patches increased by 2-fold A/California/07/2009-specific HAI titers up to 12 weeks post-vaccination (Figure 7B) and enhanced IgG binding avidity to subunit vaccine (Figure 7C), showing improved antibody specificity for the influenza antigen compared to non-adjuvanted patch vaccination. Addition of GM-CSF to the low-dose vaccine formulation augmented more than two-fold the levels of anti-A/Christchurch/16/2010 IgG antibodies when compared to the same dose of vaccine alone ($p=0.004$ at 10 weeks and $p=0.001$ for 12 weeks post-vaccination) (Figure 7D). When comparing the IgG1 titers between the same groups, we found a 2-fold difference by week 10 post-vaccination ($p=0.05$), which was further increased by week 12 ($p=0.003$). Notably, the adjuvanted formulation also induced 4-fold higher IgG1 responses than the unadjuvanted high-dose vaccine by week 12 ($p=0.003$) (Figure 7E). Although we did not see similar statistically significant differences in IgG2a titers among vaccinated groups due to a higher spread of responses, the antibody levels followed the same trend as in IgG1 subclass (Figure 7F). Thus, the inclusion of GM-CSF in MN patches increased the production, specificity and duration of antibodies in response to influenza vaccination.

Given the increase in long-term antibody expression for GM-CSF-adjuvanted MN patches, we also investigated whether mice vaccinated against influenza virus with GM-CSF had increased systemic B cell activation and memory responses. Indeed, co-administration of vaccine with GM-CSF doubled the number of influenza-specific IgM-secreting cells (Figure 8A) and tripled the number of influenza-specific IgG-secreting cells (Figure 8B) relative to non-adjuvanted low dose vaccine at 14 d.p.v. Most importantly, GM-CSF increased the number of vaccine-specific IgG-secreting cells in the bone marrow 60 d.p.v by 50% compared to all non-adjuvanted groups (Figure

8C-D). These results, combined with serological analysis, demonstrate that GM-CSF improved the development of humoral immunity through increased antibody avidity and IgG subtype expression, systemic IgM and IgG cell activation, and maintenance of vaccine-specific IgG-secreting cells in the bone marrow.

T cell activation in the inguinal lymph nodes (ILN) and spleen. Protective immune responses to influenza virus infection require both antibody responses to neutralize free virus and facilitate its opsonization and virus-specific cellular responses to kill infected cells and coordinate immune responses⁴⁷. Healthy adults expressing higher numbers of vaccine-specific CD8+ IFN- γ -secreting cells were less likely to have enhanced viral pathogenesis during the 2009 H1N1 pandemic⁴⁸. Thus, we investigated whether GM-CSF-adjuvanted vaccination could boost the number of activated T cells in draining inguinal lymph nodes (ILN) and the numbers of systemic vaccine-specific cytokine secreting cells. GM-CSF adjuvant-containing patches tripled the frequency of activated follicular CD8+ T cells (CD8+CXCR5+PD-1+) as early as day 7 (Figure 9A-E). In contrast, GM-CSF did not increase the frequency of CD4+ T follicular helper cells (CD4+, CXCR5+, PD-1+) (Suppl. Figure 2A). These findings suggest that GM-CSF adjuvant improves protective immunity following vaccination by enhancing activation of virus-specific CD8+ cytotoxic lymphocytes (CTLs).

To determine whether inclusion of GM-CSF in MN patches leads to the increased generation of vaccine-specific T cells, we enumerated vaccine-specific IFN- γ and IL-4 producing lymphocytes in ILN at 7 and 14 d.p.v. By day 14, the GM-CSF/ low-dose vaccine group induced a 3-fold increase in the number of IFN- γ secreting lymphocytes when compared to placebo ($p=0.02$), low dose ($p>0.05$) and high dose vaccine groups ($p=0.03$) (Figure 9F). Mice receiving

adjuvanted vaccine showed a 50% enhancement in the number of IL-4 secreting lymphocytes (Suppl. Figure 2B). Thus, in addition to previous results demonstrating the increase of vaccine-specific antibodies, the use of GM-CSF as an adjuvant in MN patches also exerted a positive effect on CTL activation and vaccine-specific IFN- γ and IL-4 secreting cell numbers, providing a range of cellular and humoral immune responses for an effective response to influenza viral infection.

Antibody response to H1N1 and H3N2 viruses. Effective influenza vaccination must demonstrate long-lasting and broadly neutralizing immune responses against commonly circulating influenza virus strains in order to reduce disease burden⁴⁹. Breadth of immunity adds value to current seasonal influenza vaccines and it is the goal of successful universal vaccine candidates⁵⁰. In order to measure the range of influenza-specific antibody responses elicited in animals that received the vaccine alone or in combination with GM-CSF, serum collected 3 months post-vaccination was tested for binding to various HAs within the same subtype (H1N1, group 1) or different subtype (H3N2, group 2).

With the exception of significantly higher antibody IgG titers to a homologous-like virus (anti-A/California/07/09) (Figure 10A), the GM-CSF adjuvanted vaccine generated comparable IgG titers to unadjuvanted vaccine against homosubtypic strains (Suppl. Fig. 3A, B). Interestingly, the adjuvanted vaccine induced 3-fold increase of IgG antibodies against 3 circulating H3N2 strains; A/Texas/50/2012 (Figure 10B), A/Victoria/210/2009 (Suppl. Fig.3C), A/Aichi/2/1969 (Suppl. Fig. 3D) relative to non-adjuvanted vaccine. Using recombinant baculovirus proteins containing rare HA heads (H6 and H14) and common seasonal stalks (H1 and H3), it was possible to determine whether the inclusion of GM-CSF as an adjuvant increased the number of antibodies able to bind to H1 and H3 stalks. While the combination of GM-CSF with low vaccine dose did not increase the antibody response to H1 stalks compared to vaccine alone (Figure 10C), it significantly

increased the titer of antibodies binding to H3 stalks (Figure 10D). These data suggest that the mechanism by which GM-CSF adjuvants increase antibody binding to H3N2 viruses is likely related to enhanced reactivity with H3 stalk rather than the H3 head or receptor binding domain. Thus, co-administration of GM-CSF with a licensed influenza vaccine encapsulated in MN patches generated antibodies with significant cross-reactivity, demonstrating the potential of this adjuvant to expand immune protection across various influenza subtypes.

Viral growth and immune responses to lethal challenge following MN patch vaccination with GM-CSF adjuvant. To determine the effect of skin vaccination with GM-CSF on protective immunity and identify the implicated mechanisms, mice were infected 30 days post-vaccination with 10xLD₅₀ A/California/07/2009. Survival and weights changes were monitored for 14 days post-infection. A second infected cohort of mice was sacrificed at 4 days post-infection to determine viral titers and cytokine profiles in the lungs and assess vaccine effectiveness in accelerating viral clearance and reducing virus-induced inflammation. Although all vaccinated groups maintained their weight and survived lethal infection (data not shown), immunization with adjuvanted vaccine induced a 2.7-log reduction in viral titers when compared to mice vaccinated with placebo MN patches (p=0.02), whereas immunization with high-dose vaccine was 42% less effective (2.5-log reduction in viral titers) (p=0.02). Mice vaccinated with low-dose vaccine in the absence of GM-CSF had one-log decrease in titers compared to placebo infected mice (p=0.03) (Figure 11A).

Lung lysates taken from vaccinated mice 4 days after lethal infection and tested for eight major Th1, Th2 and inflammatory cytokines showed significant expression of IL-4, IL-2 and GM-CSF. These cytokines were significantly elevated following lethal infection of mice that received adjuvanted vaccine when compared to the other vaccinated groups (Figure 11B, C, D). Early

expression of GM-CSF in the lungs has been shown to promote alveolar macrophage activation and recruitment in order to reduce viral replication^{51,52}. These findings may explain efficient viral clearance seen shortly after infection (Figure 11A). In contrast, IL-2 and IL-4 play important roles in reducing CTL-mediated immunopathogenesis⁵³ and promoting tissue repair through activation of innate lymphoid cells, respectively⁵⁴. These studies point to a potential role of GM-CSF in influenza vaccination by MN patch to elicit a unique signature of cytokines that promote elimination of virus from the respiratory compartment while reducing byproduct inflammation and tissue damage due to an overactive immune system.

DISCUSSION

Skin immunization is an innovative route of vaccination which takes advantage of a potent network of antigen-presenting cells (APCs) and other innate immune cells in skin that can interact with naive T and B cells proximal to the site of vaccination in draining lymph nodes⁵⁵⁻⁵⁸. We have previously reported the importance of langerin+ dendritic cells (DCs) in modulating adaptive immune responses following cutaneous MN vaccination⁵⁹. GM-CSF can recruit and activate APCs⁶⁰ and is a potent inducer of NF- κ B expression and nitric acid synthase in epithelial DCs⁶¹. CD103+ langerin+ DCs have shown GM-CSF dependent activation of follicular CD4+ T helper cells that subsequently led to the expression of IFN- γ and IL-17⁶². Thus, the presence of GM-CSF as an adjuvant is critical for enhancing the potency of vaccines with limited immunogenicity, such as the licensed subunit influenza vaccine, by promoting antigen capture and DC and T cell activation and regulation^{63,64}.

In this study, we investigated the role of GM-CSF to increase the efficiency of skin dendritic cells APCs and the recruitment and priming of antibody-secreting B cells and CD8+ follicular T cells in primary and secondary lymphoid tissues. Here we demonstrate stable co-incorporation of GM-CSF with influenza vaccine in MN patches that can be used to enhance the vaccine-specific humoral and cellular immune responses. We identified that ID administration of GM-CSF with H1N1 or H3N2 vaccines, improved antibody responses and protection against viral challenge^{65,66}. We then identified the formulations for efficient vaccine and adjuvant co-encapsulation within MN patches and delivery in the skin. We also identified adjuvant concentrations required for cellular activation, cytokine stabilization and bioreactivity.

Importantly, we demonstrated the superiority of MN patch vaccination over ID and IM vaccination in enhancement of vaccine-specific antibody responses. Mice cutaneously immunized

with H1N1 influenza vaccine and GM-CSF as adjuvant via ID and MN routes showed increased protection with lower morbidity and mortality rates following lethal infection, a phenomenon not seen in IM vaccination. These findings suggest that GM-CSF has unique properties as an adjuvant within the skin that can be exploited when developing MN patch delivery technologies.

Examination of the immune response to GM-CSF as an adjuvant showed increased activation of antigen-specific IFN- γ secreting cells following vaccination, which may explain the persistence of IgG2a antibodies 4 months post-vaccination⁶⁷. Following lethal infection, mice vaccinated against H1N1 virus in the presence of GM-CSF effectively controlled viral growth. Importantly, GM-CSF-adjuvanted H1N1 vaccination improved serum cross-reactivity with a homosubtypic (H1N1) and heterosubtypic (H3N2) viral strains. The broadly cross-reactive antibodies elicited in the presence of adjuvants were directed against the hemagglutinin stalk region. Ultimately, influenza immunization with a trivalent or quadrivalent vaccine co-encapsulated with appropriate adjuvants such as GM-CSF in a MN patch could significantly reduce disease burden due to strain mismatch or drift within an influenza season.

The role of GM-CSF in driving more potent humoral or cellular immune responses has been debated. Previous DNA vaccination studies in rhesus macaques showed that influenza HA responses were improved by the inclusion of recombinant rhGM-CSF⁶⁸. Intramuscular vaccination with GM-CSF encoded in a viral vector increased the frequency of APCs but decreased the antigen-specific CD8+ T cell responses in the draining lymph node⁶⁹. In our studies, MN patch vaccination with GM-CSF increased the number of CD8+ follicular T cells in ILN, highlighting the usefulness of administering this cytokine as an adjuvant during vaccination. Our findings are in alignment with data reported by Chou et al. on co-delivery of GM-CSF with hepatitis B subunit vaccine to skin in a biodegradable hydrogel⁷⁰. The authors demonstrated that presence of GM-CSF

increased antibody response to the vaccine and vaccine-specific T cell proliferation in addition to improved activation of APCs in the draining lymph node.

GIFT fusokines, engineered to have peptides from multiple cytokines, have been generated to combine the APC stimulation capabilities of GM-CSF with T cell differentiation signalers IL-4⁷¹. These fusokines have shown promise in prophylactic HIV vaccination studies in guinea pigs when anchored via glycolipids to virus-like particles (VLPs)⁷². These reports and our present findings suggest that the potency of GM-CSF as an adjuvant is dependent on administration route and formulation. To our knowledge, this is the first example of the use of MN patches to deliver a bioreactive cytokine as an adjuvant that can augment effective systemic and mucosal immune responses elicited to influenza vaccine.

CONCLUSIONS

In this study, we repurposed a cytokine already approved for clinical use for stimulating immune cell repopulation following chemotherapy for use as an adjuvant for skin immunization^{73,74}. Our preclinical studies in mice showed enhanced immunogenicity of influenza vaccine with recombinant murine GM-CSF administered with a MN patch, proposing a novel use for this cytokine as an active molecular adjuvant. Additionally, our process provides a pipeline to examine other active recombinant molecules as adjuvants and to optimize combined adjuvant doses for maximized vaccine efficacy and mucosal immunity. Lastly, these data demonstrate the usefulness of GM-CSF as an adjuvant in a single context; however, an effective adjuvant strategy may likely employ a combination of cytokines, TLR ligands or STING agonists^{75,76}.

ACKNOWLEDGEMENTS

We thank Nadia Lelutiu for her scientific feedback and editing of this manuscript, Dahnide Taylor-Williams for technical support, and Kiran Gill and David Lee for Emory Vaccine Center core facility expertise with flow cytometry and Luminex assays, respectively.

RESEARCH FUNDING

This work was supported by NIH grant 5R01AI111557.

COMPETING FINANCIAL INTERESTS

M.R.P. is an inventor of patents licensed to companies developing microneedle-based products, is a paid advisor to companies developing microneedle-based products and is a founder/shareholder of companies developing microneedle-based products (e.g., Micron Biomedical). This potential conflict of interest has been disclosed and is managed by Georgia Tech and Emory University.

E.Q.L, L.K.M., E.S.E., E.V.V, J.T.B., S.W., J.P.P., N.B., F.K. R.W.C, I.S. declare that they have no conflicts of interest.

REFERENCES

1. Taubenberger JK, Morens DM. The pathology of influenza virus infections. *Annu Rev Pathol.* 2008;3:499-522.
2. Kuiken T, Taubenberger JK. Pathology of human influenza revisited. *Vaccine.* Sep 12 2008;26 Suppl 4:D59-66.
3. CDC. Seasonal Influenza Vaccine Effectiveness, 2005-2015. In: CDC, ed. <http://www.cdc.gov/flu/professionals/vaccination/effectiveness-studies.htm>. Atlanta, GA: CDC; 2015.
4. WHO. Influenza (Seasonal). 2011; <http://www.who.int/mediacentre/factsheets/fs211/en/>.
5. Gilca R, Skowronski DM, Douville-Fradet M, et al. Mid-Season Estimates of Influenza Vaccine Effectiveness against Influenza A(H3N2) Hospitalization in the Elderly in Quebec, Canada, January 2015. *PloS one.* 2015;10(7):e0132195.
6. Clements KM, Meier G, McGarry LJ, Pruttivarasin N, Misurski DA. Cost-effectiveness analysis of universal influenza vaccination with quadrivalent inactivated vaccine in the United States. *Human vaccines & immunotherapeutics.* 2014;10(5):1171-1180.
7. Molinari NA, Ortega-Sanchez IR, Messonnier ML, et al. The annual impact of seasonal influenza in the US: measuring disease burden and costs. *Vaccine.* Jun 28 2007;25(27):5086-5096.
8. Flannery B, Chung J. Influenza Vaccine Effectiveness, Including LAIV vs IIV in Children and Adolescents, US Flu VE Network, 2015-16: Centers for Disease Control and Presentation 2016.

9. Kim YC, Jarrahan C, Zehrung D, Mitragotri S, Prausnitz MR. Delivery systems for intradermal vaccination. *Current topics in microbiology and immunology*. 2012;351:77-112.
10. Osterholm MT, Kelley NS, Sommer A, Belongia EA. Efficacy and effectiveness of influenza vaccines: a systematic review and meta-analysis. *The Lancet infectious diseases*. Jan 2012;12(1):36-44.
11. Ciancio BC, Rezza G. Costs and benefits of influenza vaccination: more evidence, same challenges. *BMC Public Health*. Aug 08 2014;14:818.
12. Chen X, Fernando GJ, Crichton ML, et al. Improving the reach of vaccines to low-resource regions, with a needle-free vaccine delivery device and long-term thermostabilization. *Journal of controlled release : official journal of the Controlled Release Society*. Jun 30 2011;152(3):349-355.
13. Vassilieva EV, Kalluri H, McAllister D, et al. Improved immunogenicity of individual influenza vaccine components delivered with a novel dissolving microneedle patch stable at room temperature. *Drug delivery and translational research*. Apr 17 2015.
14. Caffarel-Salvador E, Donnelly RF. Transdermal Drug Delivery Mediated by Microneedle Arrays: Innovations and Barriers to Success. *Curr Pharm Des*. 2016;22(9):1105-1117.
15. Prausnitz MR. Engineering Microneedle Patches for Vaccination and Drug Delivery to Skin. *Annu Rev Chem Biomol Eng*. Jun 07 2017;8:177-200.
16. Koutsonanos DG, Compans RW, Skountzou I. Targeting the skin for microneedle delivery of influenza vaccine. *Advances in experimental medicine and biology*. 2013;785:121-132.

17. Norman JJ, Arya JM, McClain MA, Frew PM, Meltzer MI, Prausnitz MR. Microneedle patches: Usability and acceptability for self-vaccination against influenza. *Vaccine*. Feb 11 2014.
18. Marshall S, Sahm LJ, Moore AC. Microneedle technology for immunisation: Perception, acceptability and suitability for paediatric use. *Vaccine*. Feb 03 2016;34(6):723-734.
19. Mistilis MJ, Joyce JC, Esser ES, et al. Long-term stability of influenza vaccine in a dissolving microneedle patch. *Drug delivery and translational research*. Feb 29 2016.
20. Roupheal NG. The safety, immunogenicity, and acceptability of inactivated influenza vaccine delivered by microneedle patch (TIV-MNP 2015): a randomised, partly blinded, placebo-controlled, phase 1 trial. Aug 12 2017;390(10095):649-658.
21. Hensley LE, Mulangu S, Asiedu C, et al. Demonstration of cross-protective vaccine immunity against an emerging pathogenic Ebolavirus Species. *PLoS pathogens*. May 2010;6(5):e1000904.
22. Koutsonanos DG, Vassilieva EV, Stavropoulou A, et al. Delivery of subunit influenza vaccine to skin with microneedles improves immunogenicity and long-lived protection. *Scientific reports*. 2012;2:357.
23. Skountzou I. Skin immunization with influenza vaccines. *Scientific reports*. 2015;386:343-369.
24. Na YR, Jung D, Gu GJ, Seok SH. GM-CSF Grown Bone Marrow Derived Cells Are Composed of Phenotypically Different Dendritic Cells and Macrophages. *Mol Cells*. Oct 2016;39(10):734-741.
25. Conti L, Gessani S. GM-CSF in the generation of dendritic cells from human blood monocyte precursors: recent advances. *Immunobiology*. 2008;213(9-10):859-870.

26. Bowne WB, Wolchok JD, Hawkins WG, et al. Injection of DNA encoding granulocyte-macrophage colony-stimulating factor recruits dendritic cells for immune adjuvant effects. *Cytokines Cell Mol Ther.* Dec 1999;5(4):217-225.
27. Yu T-WW, Chueh H-YY, Tsai C-CC, Lin C-TT, Qiu JT. Novel GM-CSF-based vaccines: One small step in GM-CSF gene optimization, one giant leap for human vaccines. *Human vaccines & immunotherapeutics.* 2016:1-9.
28. Manfredi R, Mastroianni A, Coronado O, Chiodo F. Recombinant human granulocyte-macrophage colony-stimulating factor (rHuGM-CSF) in leukopenic patients with advanced HIV disease. *J Chemother.* Jun 1996;8(3):214-220.
29. Burdach SE, Muschenich M, Josephs W, et al. Granulocyte-macrophage-colony stimulating factor for prevention of neutropenia and infections in children and adolescents with solid tumors. Results of a prospective randomized study. *Cancer.* Aug 01 1995;76(3):510-516.
30. Tarhini AA, Leng S, Moschos SJ, et al. Safety and immunogenicity of vaccination with MART-1 (26-35, 27L), gp100 (209-217, 210M), and tyrosinase (368-376, 370D) in adjuvant with PF-3512676 and GM-CSF in metastatic melanoma. *Journal of immunotherapy.* May 2012;35(4):359-366.
31. Tamura S, Kurata T. Defense mechanisms against influenza virus infection in the respiratory tract mucosa. *Japanese journal of infectious diseases.* Dec 2004;57(6):236-247.
32. Simmons SJ, Tjoa BA, Rogers M, et al. GM-CSF as a systemic adjuvant in a phase II prostate cancer vaccine trial. *Prostate.* Jun 01 1999;39(4):291-297.

33. Mittendorf EA, Clifton GT, Holmes JP, et al. Final report of the phase I/II clinical trial of the E75 (nelipepimut-S) vaccine with booster inoculations to prevent disease recurrence in high-risk breast cancer patients. *Ann Oncol*. Sep 2014;25(9):1735-1742.
34. Hoeller C, Michielin O, Ascierto PA, Szabo Z, Blank CU. Systematic review of the use of granulocyte-macrophage colony-stimulating factor in patients with advanced melanoma. *Cancer Immunol Immunother*. Sep 2016;65(9):1015-1034.
35. Chen H, Gao N, Wu J, et al. Variable effects of the co-administration of a GM-CSF-expressing plasmid on the immune response to flavivirus DNA vaccines in mice. *Immunology letters*. Nov 2014;162(1 Pt A):140-148.
36. del Pilar Martin M, Weldon WC, Zarnitsyn VG, et al. Local response to microneedle-based influenza immunization in the skin. *mBio*. 2012;3(2):e00012-00012.
37. Muench LJRaH. A simple method of estimating fifty percent endpoints. . *Journal of Hygiene* 1938;29(493).
38. Sha Z, Compans RW. Induction of CD4(+) T-cell-independent immunoglobulin responses by inactivated influenza virus. *J Virol*. 2000;74(11):4999-5005.
39. Skountzou I, Quan FS, Jacob J, Compans RW, Kang SM. Transcutaneous immunization with inactivated influenza virus induces protective immune responses. *Vaccine*. Aug 28 2006;24(35-36):6110-6119.
40. Williams MS. Single-radial-immunodiffusion as an in vitro potency assay for human inactivated viral vaccines. *Veterinary microbiology*. Nov 1993;37(3-4):253-262.
41. Klampfer L, Zhang J, Nimer SD. GM-CSF rescues TF-1 cells from growth factor withdrawal-induced, but not differentiation-induced apoptosis: the role of BCL-2 and MCL-1. *Cytokine*. Nov 1999;11(11):849-855.

42. Esser ES, Romanyuk A, Vassilieva EV, et al. Tetanus vaccination with a dissolving microneedle patch confers protective immune responses in pregnancy. *Journal of controlled release : official journal of the Controlled Release Society*. Aug 28 2016;236:47-56.
43. WHO/CDS/CSR/NCS. *WHO Manual of Animal Influenza Diagnosis and Surveillance*. : Department of Communicable Disease Surveillance and Response; 2002.
44. Krammer F, Pica N, Hai R, Margine I, Palese P. Chimeric hemagglutinin influenza virus vaccine constructs elicit broadly protective stalk-specific antibodies. *J Virol*. Jun 2013;87(12):6542-6550.
45. Eric M. Bonnem IAC, Elliot Stupak, Inventor; Schering Corporation, assignee. Use of gm-csf as a vaccine adjuvant US patent US5679356 A1997.
46. Sullivan SP, Koutsonanos DG, Del Pilar Martin M, et al. Dissolving polymer microneedle patches for influenza vaccination. *Nature medicine*. Aug 2010;16(8):915-920.
47. Kreijtz JH, Fouchier RA, Rimmelzwaan GF. Immune responses to influenza virus infection. *Virus Res*. Dec 2011;162(1-2):19-30.
48. Sridhar S, Begom S, Bermingham A, et al. Cellular immune correlates of protection against symptomatic pandemic influenza. *Nature medicine*. Oct 2013;19(10):1305-1312.
49. Jang YH, Seong BL. Options and obstacles for designing a universal influenza vaccine. *Viruses*. Aug 18 2014;6(8):3159-3180.
50. Krammer F, Palese P, Steel J. Advances in universal influenza virus vaccine design and antibody mediated therapies based on conserved regions of the hemagglutinin. *Current topics in microbiology and immunology*. 2015;386:301-321.

51. Huang FF, Barnes PF, Feng Y, et al. GM-CSF in the lung protects against lethal influenza infection. *American journal of respiratory and critical care medicine*. Jul 15 2011;184(2):259-268.
52. Sever-Chroneos Z, Murthy A, Davis J, et al. GM-CSF modulates pulmonary resistance to influenza A infection. *Antiviral Res*. Nov 2011;92(2):319-328.
53. Bot A, Holz A, Christen U, et al. Local IL-4 expression in the lung reduces pulmonary influenza-virus-specific secondary cytotoxic T cell responses. *Virology*. Mar 30 2000;269(1):66-77.
54. Monticelli LA, Sonnenberg GF, Abt MC, et al. Innate lymphoid cells promote lung-tissue homeostasis after infection with influenza virus. *Nature immunology*. Nov 2011;12(11):1045-1054.
55. Kawai K, Shimura H, Minagawa M, Ito A, Tomiyama K, Ito M. Expression of functional Toll-like receptor 2 on human epidermal keratinocytes. *J Dermatol Sci*. Dec 2002;30(3):185-194.
56. Matsushima H, Yamada N, Matsue H, Shimada S. TLR3-, TLR7-, and TLR9-mediated production of proinflammatory cytokines and chemokines from murine connective tissue type skin-derived mast cells but not from bone marrow-derived mast cells. *Journal of immunology*. Jul 1 2004;173(1):531-541.
57. Mitsui H, Inozume T, Kitamura R, Shibagaki N, Shimada S. Polyarginine-mediated protein delivery to dendritic cells presents antigen more efficiently onto MHC class I and class II and elicits superior antitumor immunity. *The Journal of investigative dermatology*. Aug 2006;126(8):1804-1812.
58. Miller LS. Toll-like receptors in skin. *Adv Dermatol*. 2008;24:71-87.

59. Pulit-Penalzoza JA, Esser ES, Vassilieva EV, et al. A protective role of murine langerin(+) cells in immune responses to cutaneous vaccination with microneedle patches. *Scientific reports*. 2014;4:6094.
60. Krakowski M, Abdelmalik R, Mocnik L, Krahl T, Sarvetnick N. Granulocyte macrophage-colony stimulating factor (GM-CSF) recruits immune cells to the pancreas and delays STZ-induced diabetes. *The Journal of pathology*. Jan 2002;196(1):103-112.
61. Cruz MT, Duarte CB, Goncalo M, Figueiredo A, Carvalho AP, Lopes MC. Granulocyte-macrophage colony-stimulating factor activates the transcription of nuclear factor kappa B and induces the expression of nitric oxide synthase in a skin dendritic cell line. *Immunology and cell biology*. Dec 2001;79(6):590-596.
62. Brown AS, Derkits EJ. Prenatal infection and schizophrenia: a review of epidemiologic and translational studies. *The American journal of psychiatry*. Mar 2010;167(3):261-280.
63. Pashine A, Valiante NM, Ulmer JB. Targeting the innate immune response with improved vaccine adjuvants. *Nature medicine*. Apr 2005;11(4 Suppl):S63-68.
64. Pulendran B. Division of labor and cooperation between dendritic cells. *Nature immunology*. Jul 2006;7(7):699-700.
65. Blanton L, Alabi N, Mustaquim D, et al. Update: Influenza Activity in the United States During the 2016-17 Season and Composition of the 2017-18 Influenza Vaccine. *MMWR. Morbidity and mortality weekly report*. Jun 30 2017;66(25):668-676.
66. Chen D, Endres RL, Erickson CA, et al. Epidermal immunization by a needle-free powder delivery technology: immunogenicity of influenza vaccine and protection in mice. *Nature medicine*. Oct 2000;6(10):1187-1190.

67. Kawano Y, Noma T, Yata J. Regulation of human IgG subclass production by cytokines. IFN-gamma and IL-6 act antagonistically in the induction of human IgG1 but additively in the induction of IgG2. *Journal of immunology*. Dec 01 1994;153(11):4948-4958.
68. Loudon PT, Yager EJ, Lynch DT, et al. GM-CSF increases mucosal and systemic immunogenicity of an H1N1 influenza DNA vaccine administered into the epidermis of non-human primates. *PloS one*. 2010;5(6):e11021.
69. Wanjalla CN, Goldstein EF, Wirblich C, Schnell MJ. A role for granulocyte-macrophage colony-stimulating factor in the regulation of CD8(+) T cell responses to rabies virus. *Virology*. May 10 2012;426(2):120-133.
70. Chou HY, Lin XZ, Pan WY, et al. Hydrogel-delivered GM-CSF overcomes nonresponsiveness to hepatitis B vaccine through the recruitment and activation of dendritic cells. *Journal of immunology*. Nov 01 2010;185(9):5468-5475.
71. Deng J, Pennati A, Cohen JB, et al. GIFT4 fusokine converts leukemic B cells into immune helper cells. *J Transl Med*. Apr 27 2016;14(1):106.
72. Feng H, Zhang H, Deng J, et al. Incorporation of a GPI-anchored engineered cytokine as a molecular adjuvant enhances the immunogenicity of HIV VLPs. *Scientific reports*. Jul 07 2015;5:11856.
73. Wood LC, Jackson SM, Elias PM, Grunfeld C, Feingold KR. Cutaneous barrier perturbation stimulates cytokine production in the epidermis of mice. *The Journal of clinical investigation*. Aug 1992;90(2):482-487.
74. Williams IR, Ort RJ, Daley D, et al. Constitutive expression of B7-1 (CD80) on mouse keratinocytes does not prevent development of chemically induced skin papillomas and carcinomas. *Journal of immunology*. May 1 1996;156(9):3382-3388.

75. Williams P, Galipeau J. GM-CSF-based fusion cytokines as ligands for immune modulation. *Journal of immunology*. May 15 2011;186(10):5527-5532.
76. Zhang C, Wang B, Wang M. GM-CSF and IL-2 as adjuvant enhance the immune effect of protein vaccine against foot-and-mouth disease. *Virology journal*. Jan 09 2011;8:7.

FIGURES

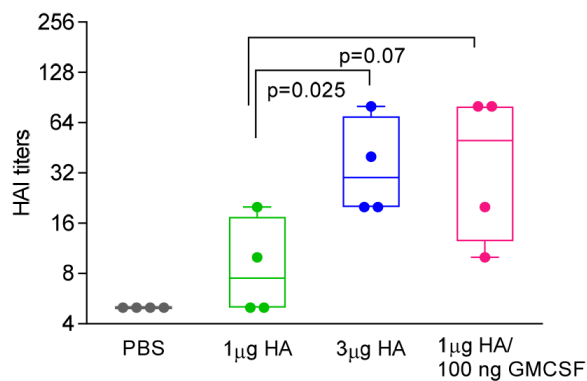
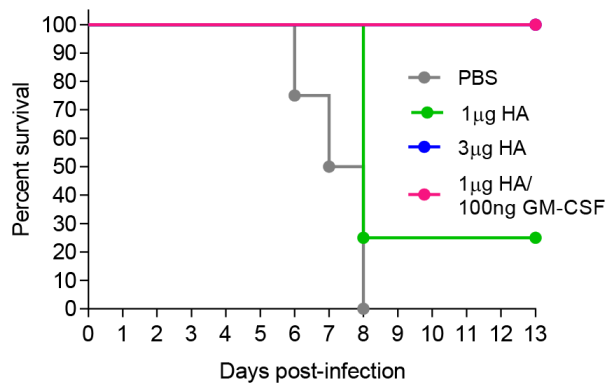
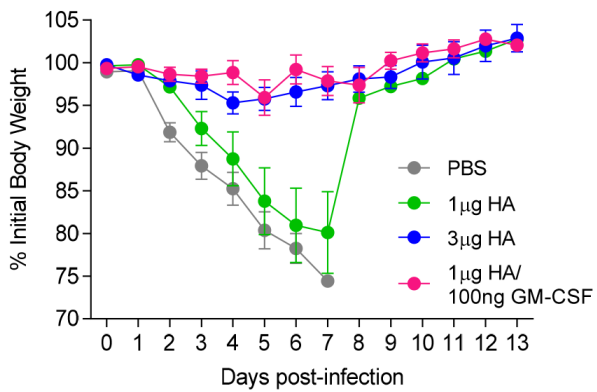
A**B****C**

Fig. 1. Adjuvantation with 100 ng GM-CSF in intradermal H1N1 A/California/07/09 subunit vaccination improves antibody responses and enhances protection to lethal virus challenge.

BALB/c mice (n=4) were vaccinated ID with PBS, 1 μ g HA, 3 μ g HA, or 1 μ g HA/100 ng GM-CSF. (A) Serum influenza-specific HAI titers are plotted at 8 weeks post-vaccination. Statistics for panel (A) were performed with Mann-Whitney test. Mice were challenged with 25xLD₅₀ homologous virus 3 months post-vaccination and (B) survival and (C) body weight changes were recorded for 13 days. Percent body weight values are expressed as mean \pm SEM. Statistics for panel (B) were performed with Mantel-Cox test.

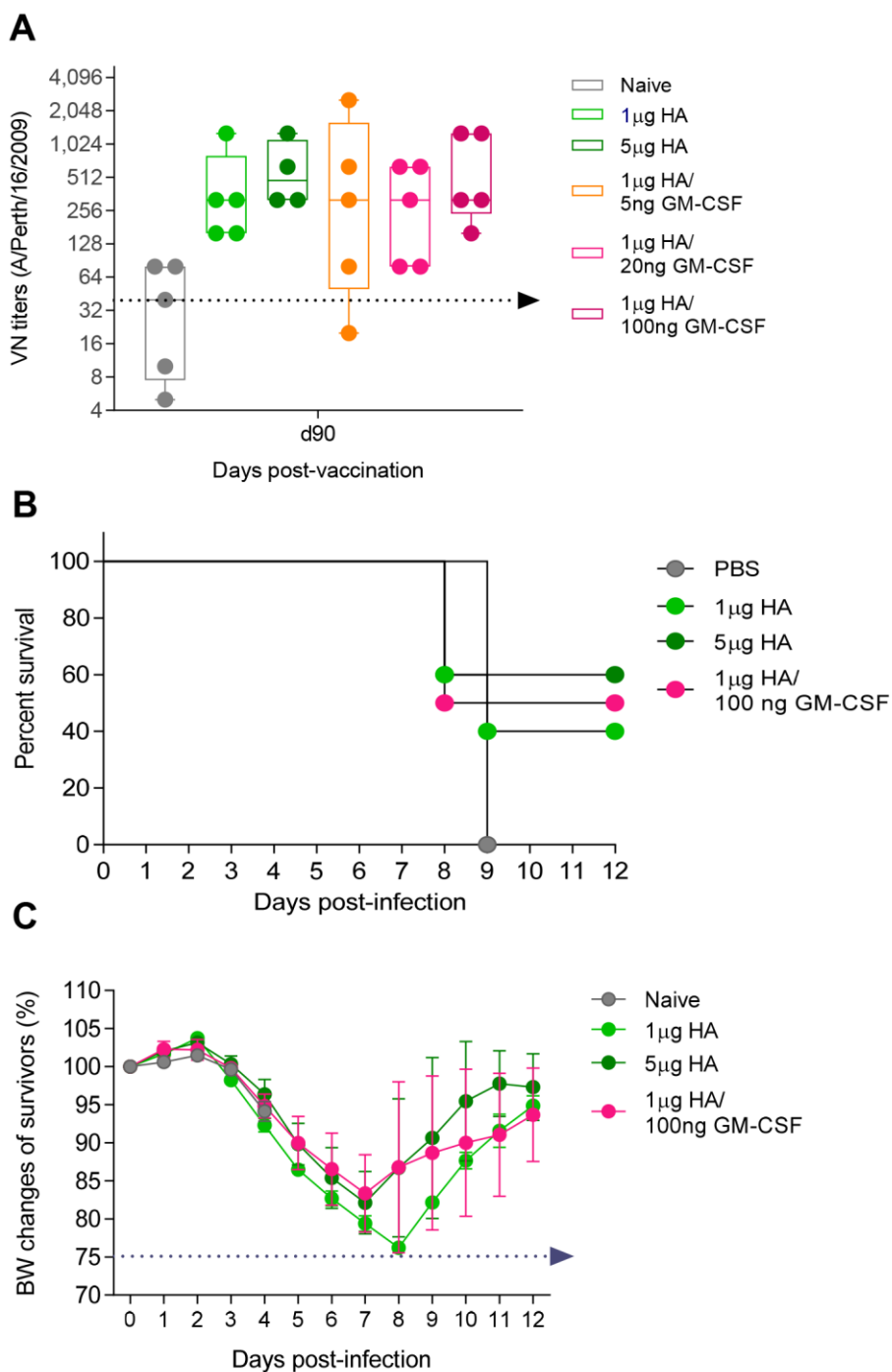


Fig. 2. GM-CSF is an effective adjuvant at low doses in H3N2 vaccinations. Mice were vaccinated ID with 1 μ g HA H3N2 A/Victoria/210/2009 with a range of GM-CSF concentrations: 5 ng, 20 ng, and 100 ng. A high vaccine dose (5 μ g) was used as a control for superlative immune

responses. Serum virus-neutralizing (VN) titers were assessed at 90 d.p.v. Vaccinated mice were challenged with 4xLD₅₀ mouse-adapted H3N2 A/Udorn/307/1972 for (C) survival and (D) body weight changes. VN titers were expressed as GMean \pm 95% CI. Percent body weight values are expressed as mean \pm SEM. Statistics for survival were performed with Mantel-Cox test.

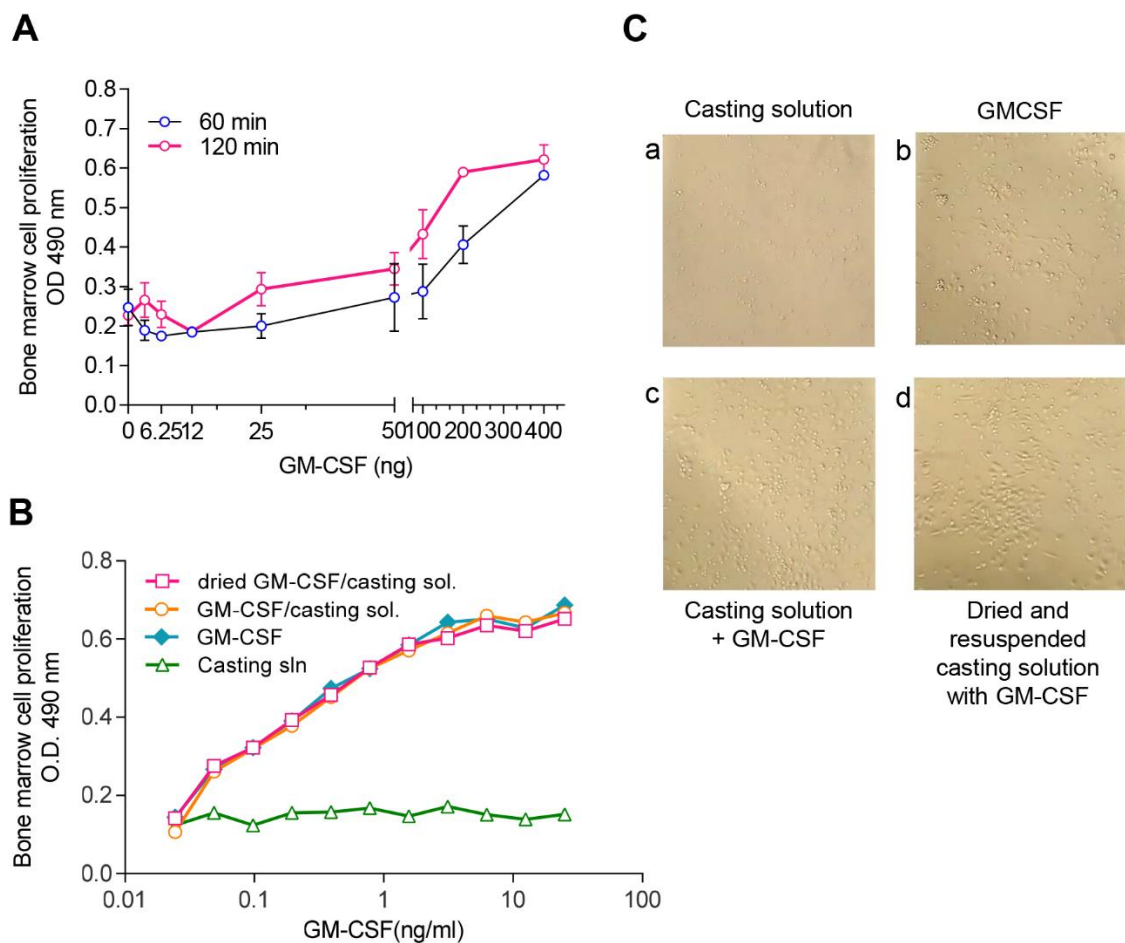


Fig. 3. GM-CSF retains proliferative capacity in bone marrow cells following MN patch fabrication and dissolution. (A) Dose-responsive cellular activation of bone marrow cells by murine GM-CSF in PBS at 60 and 120 minutes. (B) Bone marrow cells (5×10^5 cells/well) from naïve mice were incubated for 48 hours with (a) “first-cast” casting solution, (b) GM-CSF dissolved in PBS, (c) GM-CSF mixed 1:1 with casting solution, or (d) GM-CSF in casting solution air-dried in microcentrifuge tubes and reconstituted in PBS. Bioactivity was measured by determining cell proliferation at 48 hours post-exposure. (C) Bone marrow cells grown in tissue culture were imaged at 48 hours post-exposure to GM-CSF in formulations described in (B).

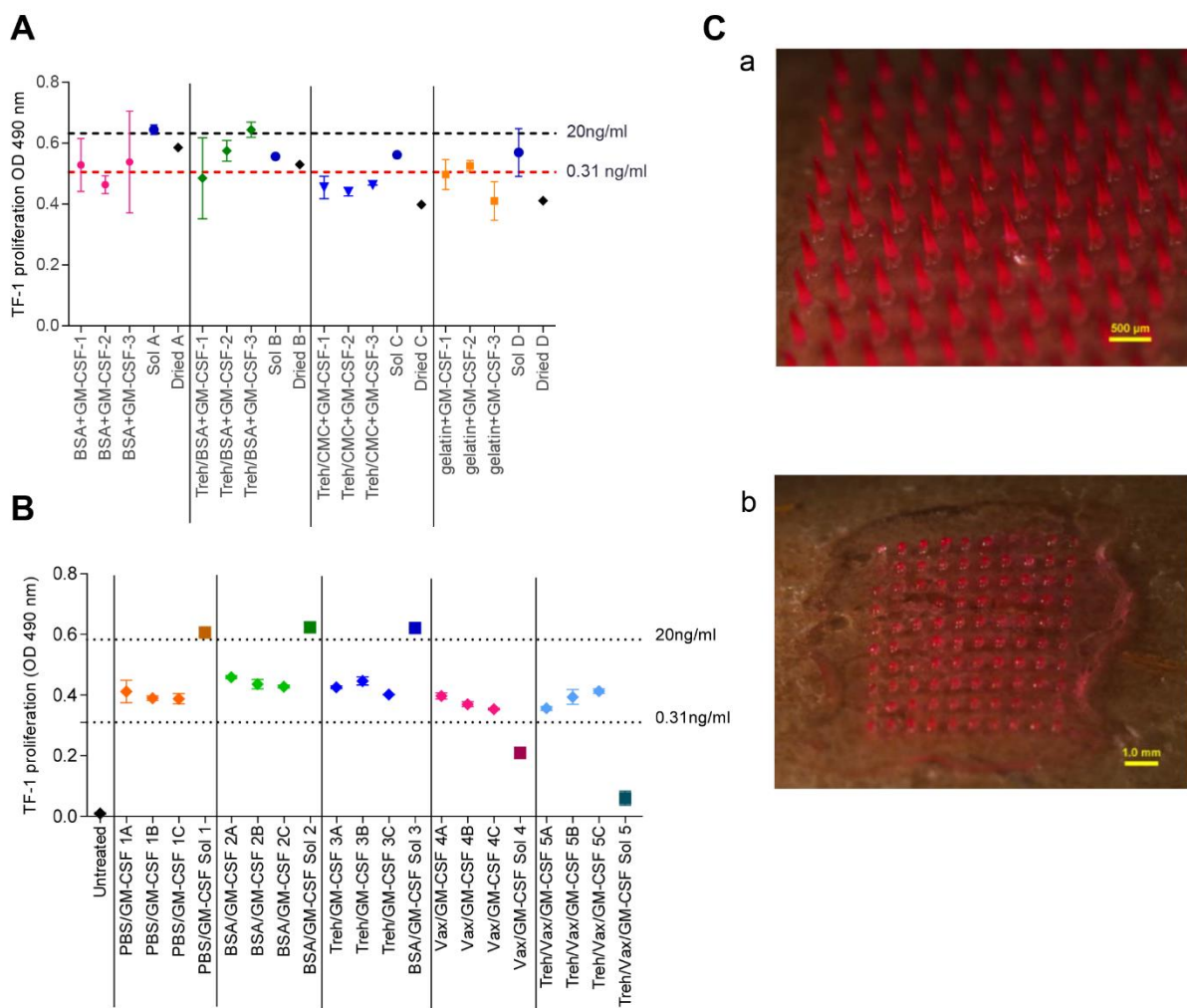


Fig. 4. GM-CSF retains bioactivity following fabrication with a range of MN excipients. (A)

The effect of first-cast solution excipients on GM-CSF stability and bioactivity was assessed by the proliferative capacity of GM-CSF using TF-1 cells. Triplicate MN patches containing 10 ng GM-CSF fabricated using various excipients in the first-cast solution were dissolved in culture medium and overlaid on TF-1 cells. They were compared to GM-CSF in fresh solution (Sol A-D) or air-dried and reconstituted in RPMI formulations (Dried A-D). (B) The effect of influenza vaccine (5 μ g HA delivery dose) on GM-CSF bioactivity when co-formulated in MN patches was assessed by TF-1 cell proliferation and compared to patches with GM-CSF alone. OD values for

panels (A) and (B) are expressed as mean \pm SEM. Dotted lines indicate upper and lower detection limits of the assay as determined by a standard curve, and “sol” and “dried” indicate casting solutions that were directly applied to TF-1 cells or dried and reconstituted before application. Each sample was run in duplicates in TF-1 cells. Images of MN patches containing sulforhodamine red dye were taken (Ca) before and (Cb) after application to skin in mice.

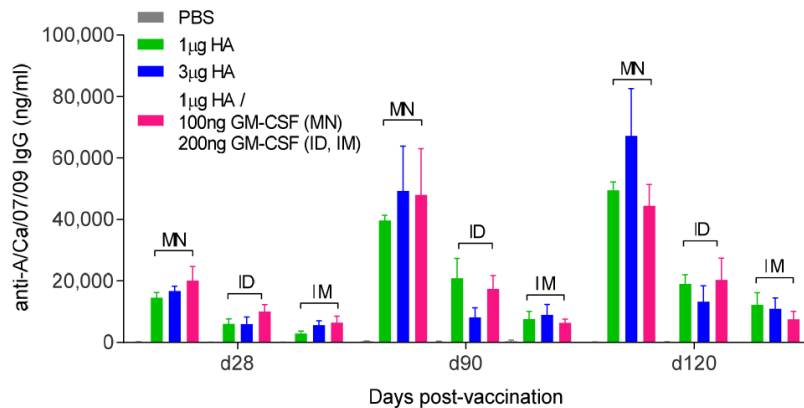
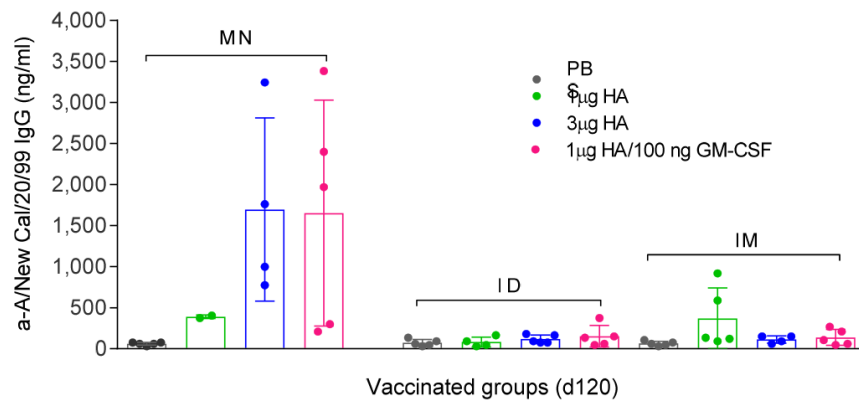
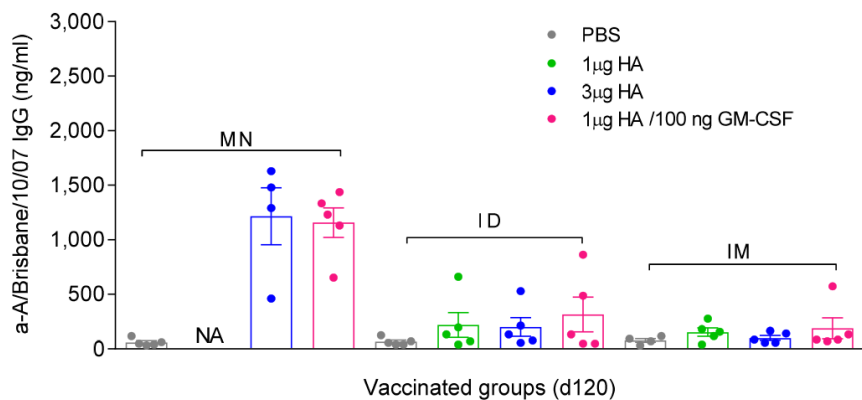
A**B****C**

Fig. 5. The inclusion of GM-CSF in MN patches in H1N1 influenza vaccination is dose-sparing and generates superior IgG expression against homologous and heterologous HAs compared to ID and IM vaccination. BALB/c mice were vaccinated with PBS, 1 μ g HA, 3 μ g HA A/California/07/2009 subunit vaccine or 1 μ g HA mixed with 100 ng murine GM-CSF in MN patch and 200 ng in solution for IM and ID injection. Serum IgG titers against (A) H1N1 A/California/07/2009 are plotted for days 28, 90, and 120 d.p.v. (B) H1N1 A/New Caledonia/20/1999-specific and (C) H3N2 A/Brisbane/10/2007-specific IgG titers were determined at 120 days post-vaccination. Values are expressed as mean \pm SEM.

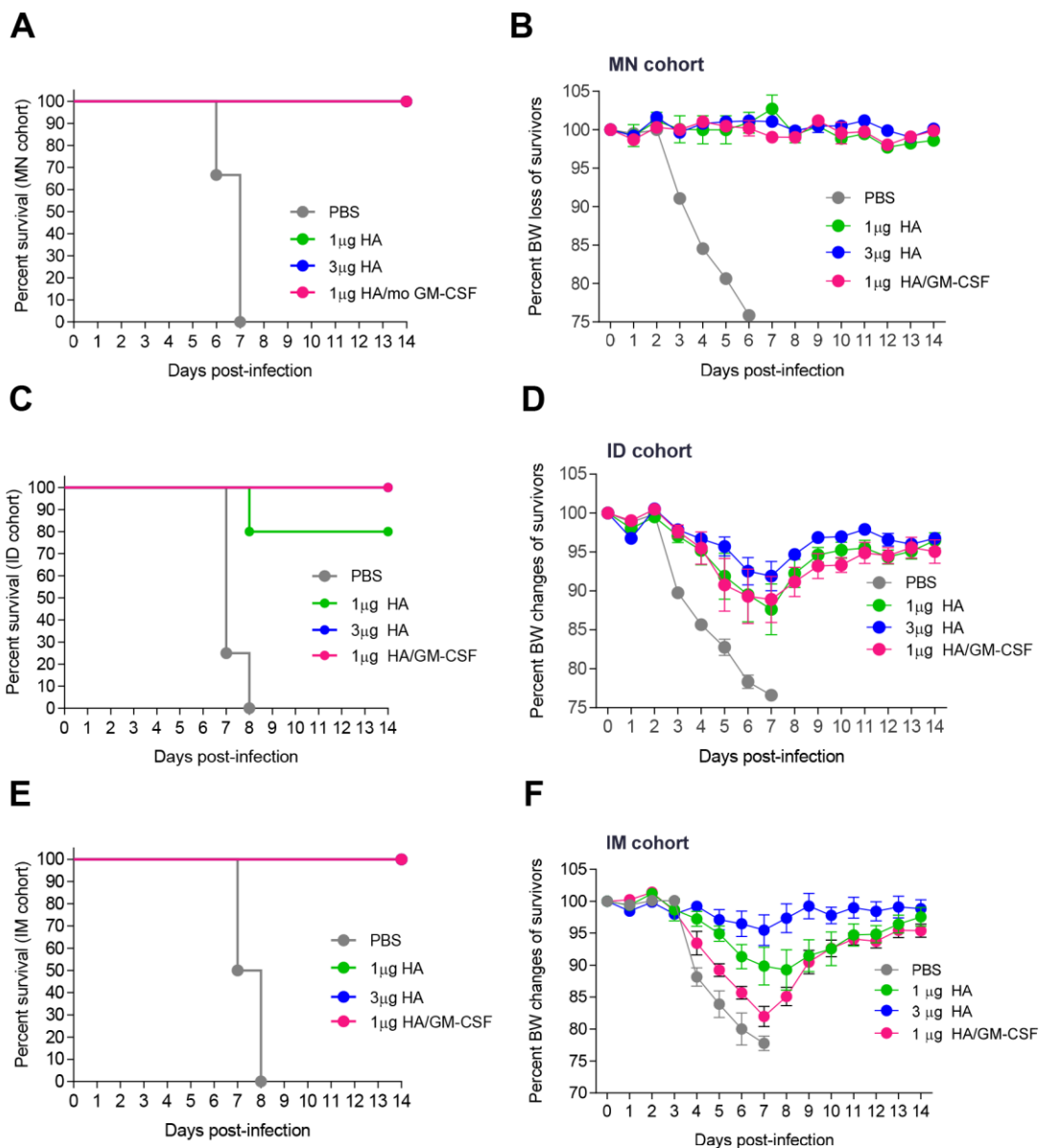


Fig. 6. H1N1 subunit vaccination with GM-CSF improved protection of mice from lethal H1N1 influenza challenge. Mice vaccinated with a single dose of A/California/07/2009 subunit vaccine via MN (A, B), ID (C, D), or IM (E, F) routes were challenged 17 weeks post-vaccination with 25xLD₅₀ homologous H1N1 A/California/07/2009 virus. Survival rates (A, C, E) and body weight changes (B, D, F) were recorded for 14 days post-challenge. Percent body weight values are expressed as mean \pm SEM.

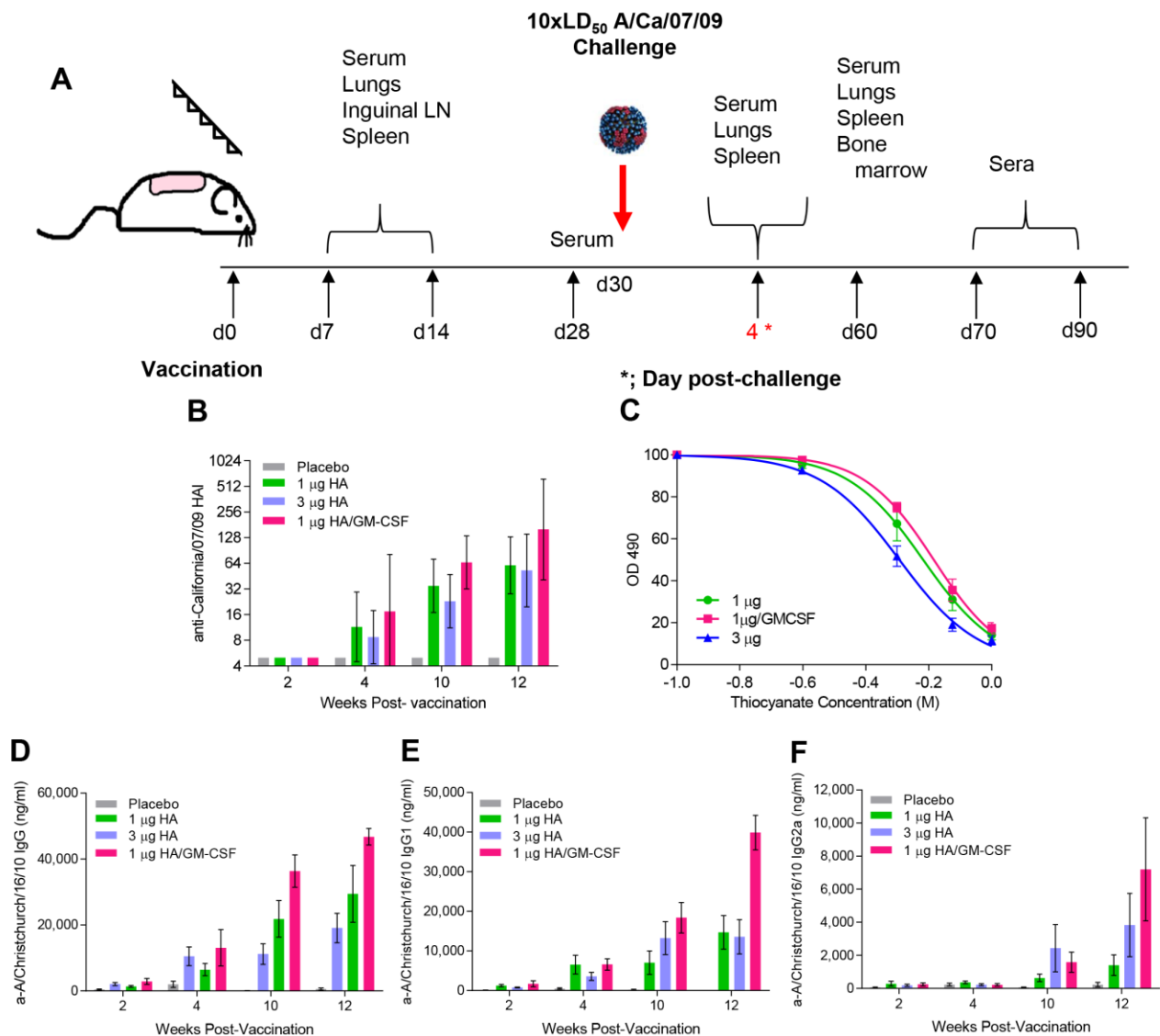


Fig. 7. GM-CSF improved antibody responses and avidity when included in MN patch vaccination. (A) Cohorts of BALB/c mice were vaccinated with MN patches containing vaccine formulation solution (placebo), 1 µg HA, 3 µg HA, or 1 µg HA of A/Christchurch/16/2010 mixed with recombinant murine GM-CSF. A total of 100 mice (n=25 per group) were used for this study. Serum samples were collected and analyzed at the time points depicted. (B) HAI titers against A/California/07/2009 virus (GMean ± 95% CI), and (C) antibody avidity against A/Christchurch/16/2010 subunit vaccine (n=5). Serum binding A/Christchurch/16/2010-specific

antibody titers were assessed with ELISA; (D) IgG, (E) IgG1, and (F) IgG2a (n=5). Statistics were performed with Mann-Whitney test. Antibody values are expressed as mean \pm SEM.

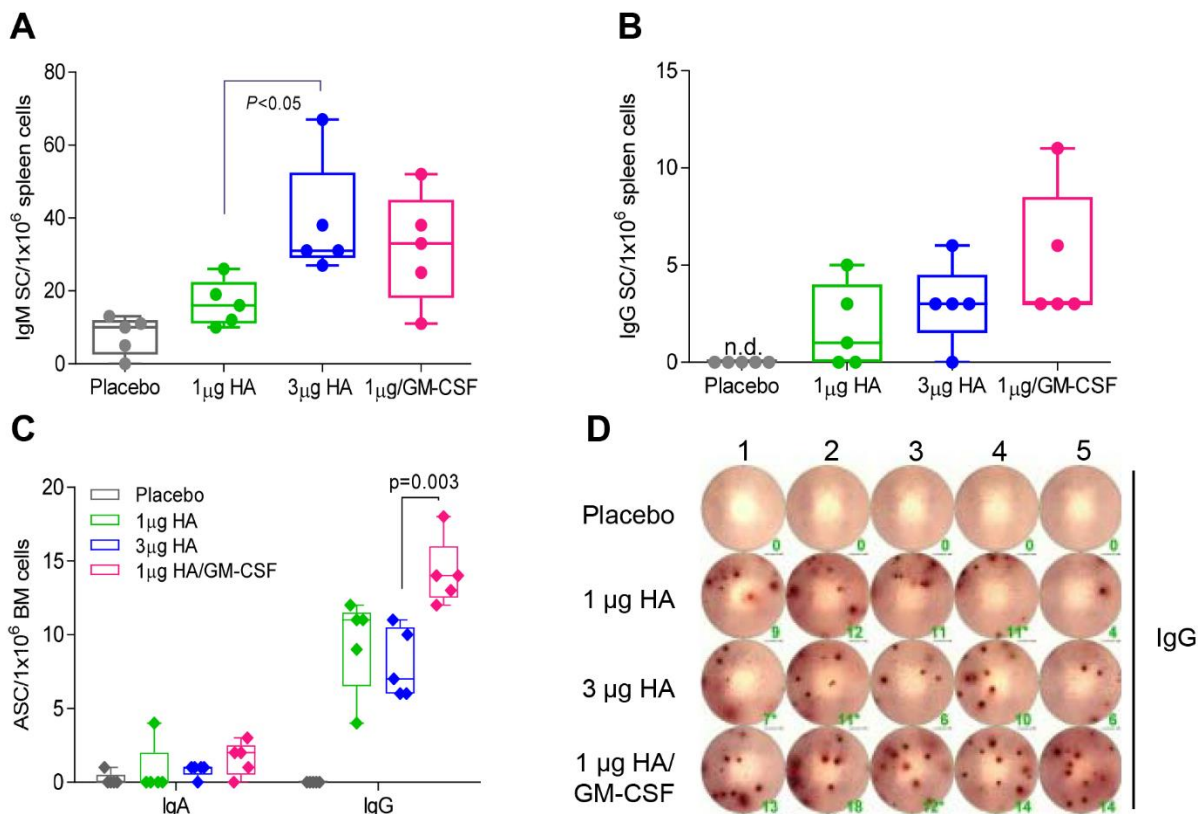


Fig. 8. Inclusion of GM-CSF enhanced activation of B cells in spleen and bone marrow.

Lymphocytes were isolated from the spleen 14 days post-MN vaccination to enumerate vaccine-specific ASCs. (A) IgM-secreting cells and (B) IgG-secreting cells were measured in ELISpot plates coated with 200 ng vaccine/well and incubated for 16 hours post isolation. (C, D) Bone marrow (BM) was harvested from mice 60 days post-MN vaccination to quantify vaccine-specific IgG SCs. All ASCs were enumerated in ELISPOT plates coated with A/California/07/2009 recombinant protein and normalized per 1×10^6 lymphocytes or BM cells respectively.

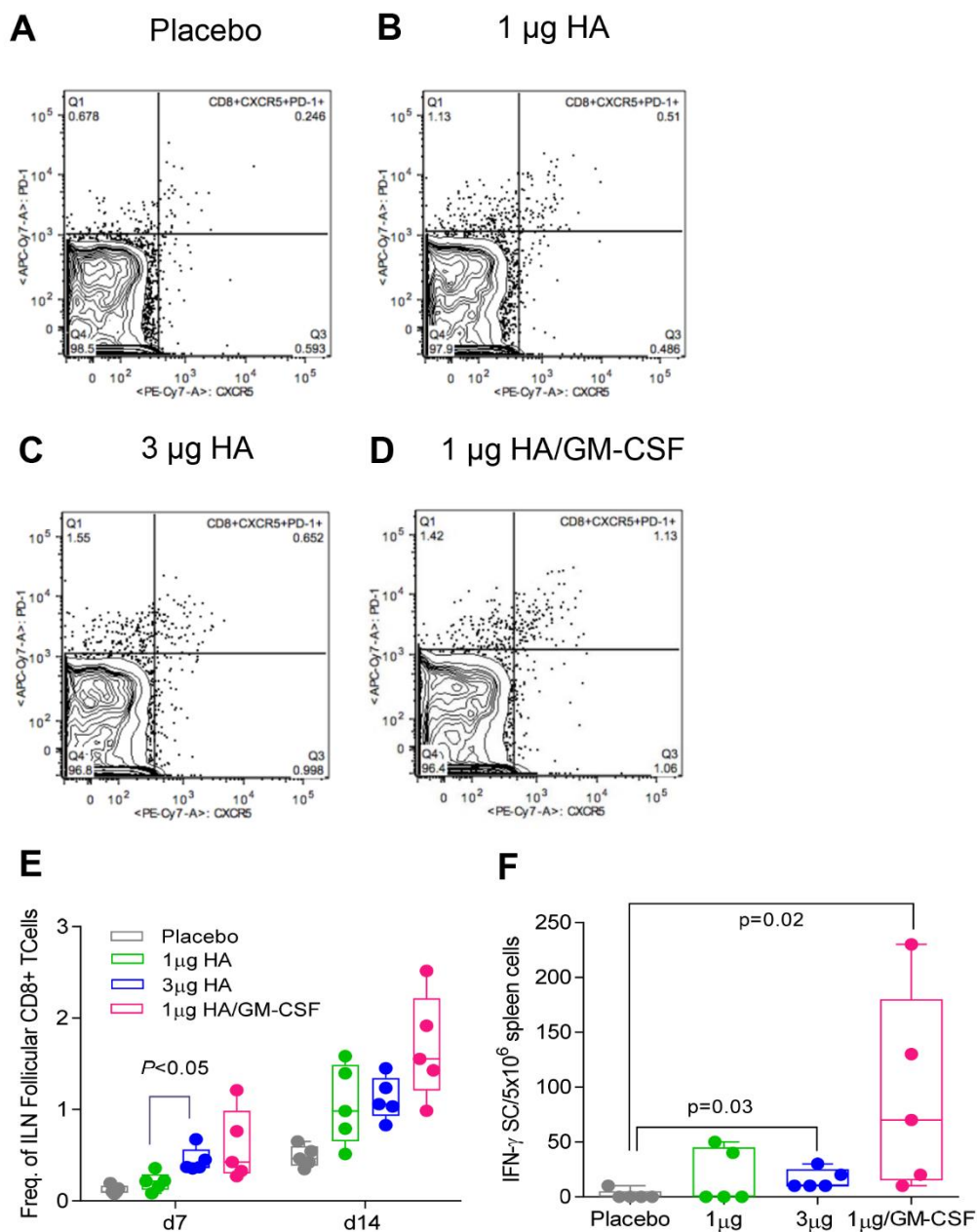


Fig 9. MN patch vaccination with GM-CSF increased CD8+ T cell responses in inguinal lymph nodes (ILN) and vaccine-specific IFN- γ responses in the spleen. Inguinal lymph nodes and spleens were harvested from mice 7 and 14 d.p.v. and measured for activation and vaccine-specific cytokine secretion. CD8+ follicular helper cells (CD8+CDXCR5+PD-1+) were determined for each sample, and representative images for (A) placebo, (B) 1 μ g

HA, and (D) 1 μg HA are shown. (E) Frequency of CD8⁺ follicular helper cells in ILN were quantified in FlowJo and plotted in GraphPad Prism 7. (E) Vaccine-specific IFN- γ were isolated from the spleen at day 7 and enumerated in ELISPOT plates following stimulation with A/Christchurch/16/2010 subunit vaccine. Values are expressed as mean \pm SEM and statistics were performed with Mann-Whitney test.

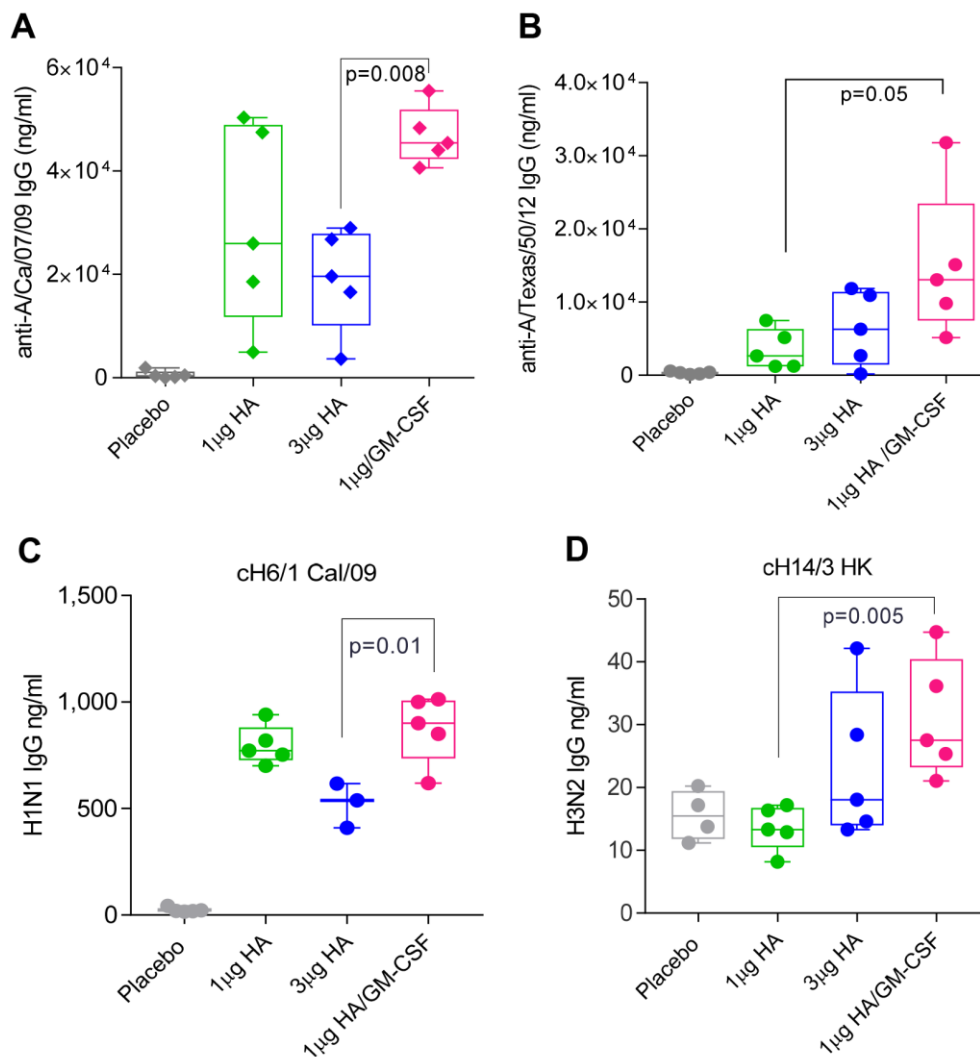


Fig. 10. GM-CSF adjuvanted MN patch immunization improved cross-reactive neutralization responses between homologous and heterologous viral strains. Serum was collected from mice 90 days post-A/Christchurch/16/2010 vaccination with dissolving MN. IgG reactivity with monovalent subunit vaccines for (A) H1N1 A/California/07/2009 and (B) H3N2 A/Texas/50/2012 was measured with ELISA. IgG reactivity with chimeric HA proteins was measured with ELISA against (C) H1 stalks (cH6/1 Cal/09) and (D) H3 stalks (cH14/3 HK). Statistics performed in Mann-Whitney test for comparison of 1 µg HA/GM-CSF vs. 1 µg HA groups.

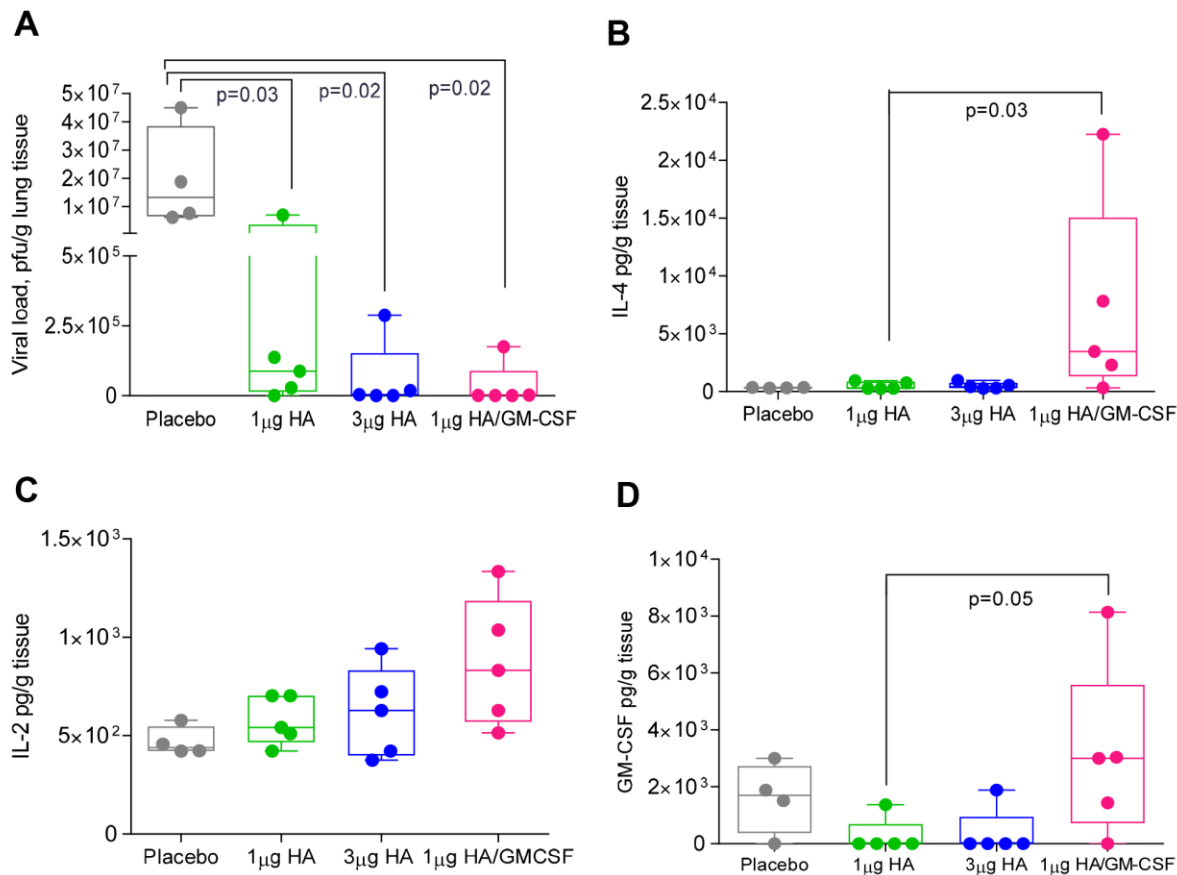
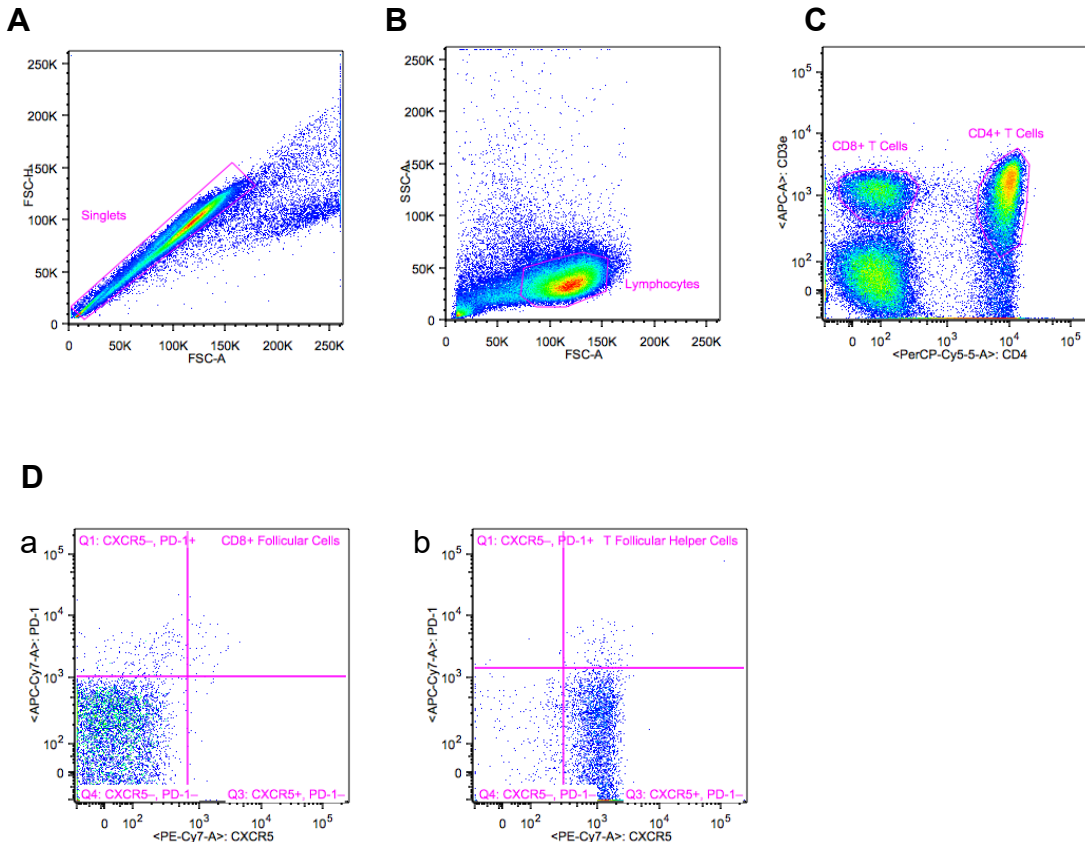
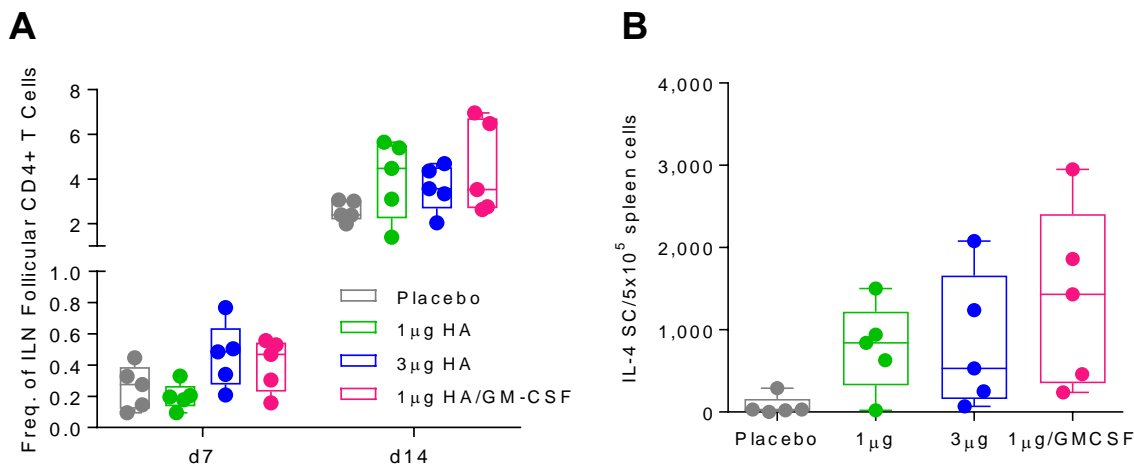


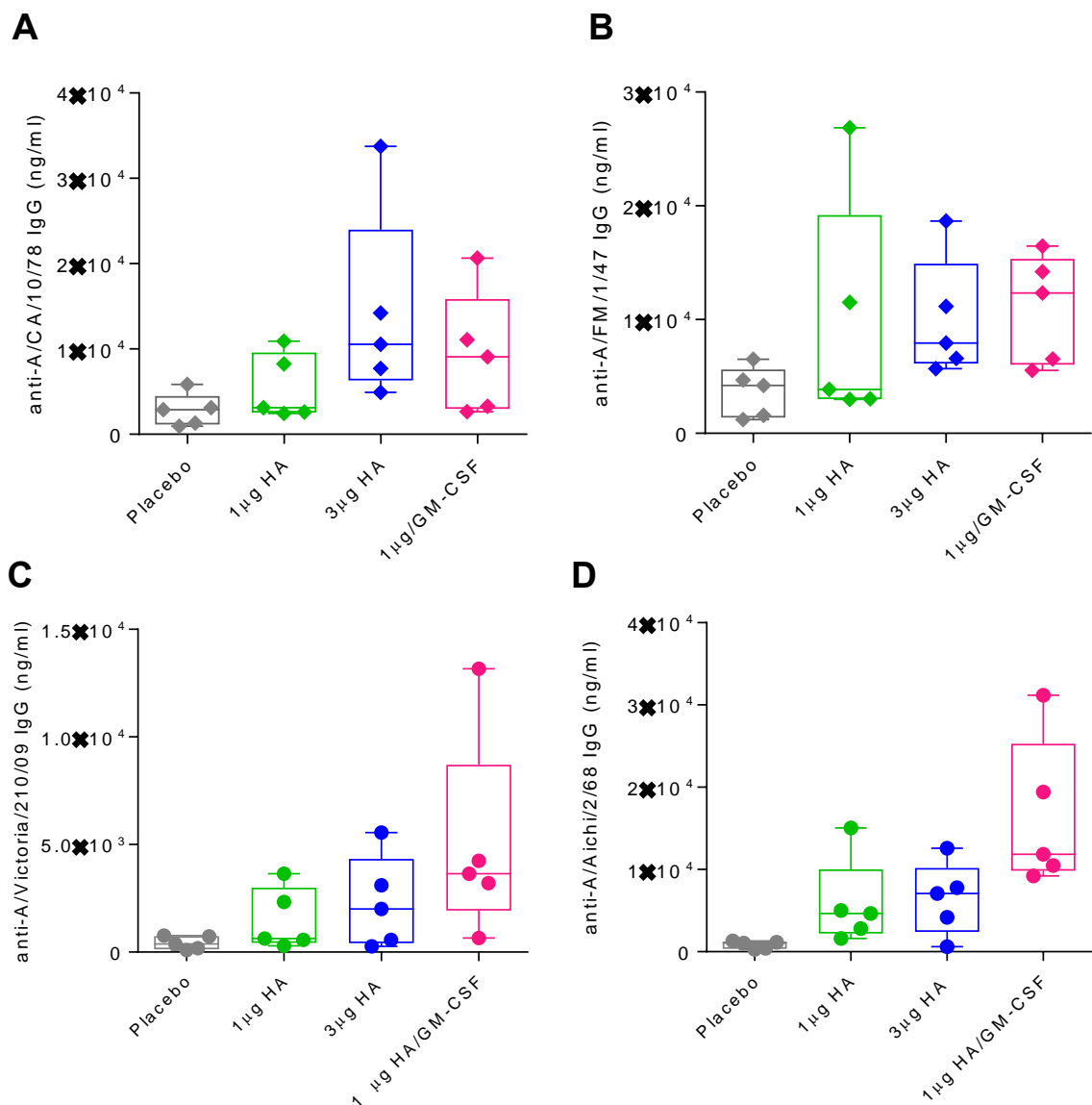
Fig. 11. Th1 cytokine responses to viral infection were increased in GM-CSF-adjuvanted MN vaccinated mice. Mice vaccinated with A/Christchurch/16/2010 MN were infected with 10xLD₅₀ mouse-adapted A/California/07/2009 virus 30 d.p.v. (A) Viral load (p.f.u.) was measured in lung lysates 4 days post-infection. Cytokine expression in lung lysates was quantified in a Bio-plex Pro Mouse Cytokine 8-plex assay. (B) IL-4 (C) IL-2 and (D) GM-CSF levels. Values are expressed as mean \pm SEM. Analysis of Mann-Whitney test between 1 μ g HA and 1 μ g HA/100 ng GM-CSF reached statistical significance of $p < 0.5$ in ELISPOT assays for IL-4 and GM-CSF secretion.



Suppl. Fig. 1. Gating strategies for flow cytometry. Lymphocytes were isolated from ILN 14 d.p.v. and analyzed for the frequency of follicular CD8⁺ and CD4⁺ T cells (Figure 9A and 9B, Suppl. Fig. 2A,B). Samples were acquired on a LSR II flow cytometer (BD Biosciences) and data were analyzed with FlowJo (Tree Star). Cells were gated for singlets (A) first and then lymphocytes (B). CD8⁺ follicular T cells were determined to be CD4⁻ (PerCP-Cy5.5⁻) CD3 ϵ ⁺ (APC⁺) (C) and CXCR5⁺ (PE-Cy7⁺) PD-1⁺ (APC-Cy7⁺) (Da). CD4⁺ follicular T cells were determined to be CD4⁺ (PerCP-Cy5.5⁺) CD3 ϵ ⁺ (APC⁺) (C) and CXCR5⁺ (PE-Cy7⁺) PD-1⁺ (APC-Cy7⁺) (Db).



Suppl. Fig. 2. Activation of T cells in inguinal lymph nodes (ILN) and spleen. Lymphocytes were isolated from the ILN and the spleen 7 and 14 days post-MN vaccination. Gating strategy for flow cytometry is described in Suppl. Figure 2 (A) CD4⁺ follicular cells (CD4⁺CXCR5⁺PD-1⁺) were quantified via flow cytometry, and (B) vaccine-specific IL-4-secreting cells were isolated from the spleen at day 7, and enumerated in ELISPOT plates following stimulation with A/Christchurch/16/2010 subunit vaccine. Values are expressed as mean \pm SEM.



Suppl. Fig. 3. Cross-reactive antibody titers against H1N1 and H3N2 viruses. Serum was collected from mice 90 days post-A/Christchurch/16/2010 vaccination with dissolving MN. IgG reactivity with monovalent subunit vaccines for (A) H1N1 A/California/10/1978 ($p=0.2$), (B) H1N1 A/FM/1/1947 ($p=0.3$), (C) H3N2 A/Victoria/210/2009 ($p=0.055$), and (D) H3N2 A/Aichi/2/1968 ($p=0.055$) was measured with ELISA. Statistics performed in Mann-Whitney test for comparison of 1 µg HA/GM-CSF vs. 1 µg HA groups.